SURFACTANT-MEDIATED SURFACE MODIFICATION OF MICROPARTICLES FOR PRESSURISED METERED DOSE INHALATION

EMMA LOUISE BEAUSANG

A thesis submitted in partial fulfilment of the requirements for the degree of Doctor of Philosophy

University of London School of Pharmacy
29-39 Brunswick Square
London
WC1N 1AX

2005

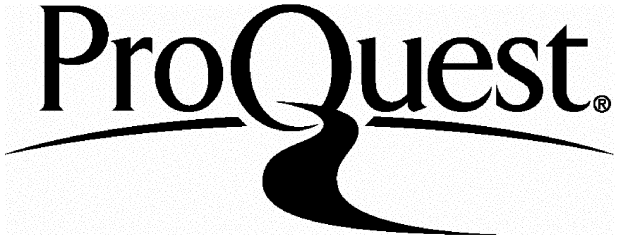

ABSTRACT

The necessary phase-out of CFC propellants and their replacement with HFA propellants has re-awakened an interest in the formulation science of pMDI suspension formulations, largely driven by the need to identify novel surfactants as a result of the altered physicochemical properties of HFA propellants with respect to CFCs. The aims of this thesis were to explore the validity of using surfactants with a low solubility in HFA propellants as stabilising agents in pMDI HFA suspension formulations, and in so doing to investigate the relationship between powder surface energy and suspension performance within these systems.

Adsorption of a range of non-ionic surfactants to the surface of a model hydrophilic drug, terbutaline sulphate (TS), was achieved and the performance of corresponding pMDI suspension formulations was investigated. Surfactant adsorption was found to improve pMDI suspension stability by reducing phase separation and particle aggregation. The improvement in suspension performance was linked to a reduction in both the dispersive and acidic components of powder surface energy following surfactant adsorption. Similar adsorption experiments were carried out using a model hydrophobic drug, budesonide. While surfactant adsorption to the drug surface succeeded in reducing powder surface energy values, the anticipated improvement in pMDI suspension performance was not observed. Surfactant adsorption did however reduce the amount of suspended material adhered to the container wall. The effect of surfactant adsorption to both drugs on pMDI suspension formulations over extended storage periods was investigated. Adsorption of a hydrophobic poloxamer surfactant to the surface of TS was seen to confer a limited protective effect against water-induced instability in pMDI suspension systems. In the case of budesonide, reduced adhesion to the container wall was seen in all surfactant-containing formulations when compared with controls. Attempts to correlate surface energy with adhesion were complicated by the necessary use of two separate methods for surface energy determination.

Work in this thesis has confirmed that surfactants with a low solubility in HFA propellants may be considered as potential stabilisers in pMDI suspension systems, and a greater understanding of the role played by surface energy in the performance of these systems has been achieved.

For my husband Matt,

ACKNOWLEDGEMENTS

I would firstly like to acknowledge my primary supervisor, Professor Graham Buckton for his encouragement and guidance over the course of this research. Dr. Steve Burns at AstraZeneca R&D Charnwood is owed thanks for his support as my industrial supervisor and indeed AstraZeneca are gratefully acknowledged for their financial support of this research. Throughout many trips to AstraZeneca labs over the course of my practical work I have received help and guidance from a number of Steve's colleagues and would like to thank Philippe Rogueda, Richard Burrell, Julian O'Brien and Steve Brown.

I would also like to thank you Dr. Simon Gaisford for kindly agreeing to proof-read the thesis despite not being involved in the project, and having a gaggle of PhD students of his own to worry about!

Thank you to the many willing bodies at the School of Pharmacy whose help has been much appreciated over the years – Keith, Lionel, John, Adrian and Rob.

The SEMs included in this thesis were taken by Dave Mc Carthy and Kate who I would both like to thank for creating the images, in addition to humouring me when I wanted to see how it was done.

I gratefully acknowledge the hard work of my undergraduate project student Maharanee Seetaram (Anoushka).

To Matt, whose constant support and encouragement have spurred on the completion of my practical work and the submission of this thesis. Throughout the past three years you have been my rock.

Finally, to my friends and colleagues on the third floor – the past four years would have been very dull indeed without the laughs (and beers). Thank you Abi, John, Ketan, Laurent, Ash, Brij, Amina and Dima.

TABLE OF CONTENTS

LIST OF TABLES

1 INTRODUCTION

2 MATERIALS AND METHODS

3 PREPARATION AND CHARACTERISATION OF TERBUTALINE SULPHATE – SURFACTANT MICROPARTICLES

4 PREPARATION AND CHARACTERISATION OF BUDESONIDE – SURFACTANT MICROPARTICLES

5 STABILITY OF TERBUTALINE SULPHATE – SURFACTANT PMDI FORMULATIONS IN THE PRESENCE OF WATER

6 ADHESION PHENOMENA IN BUDESONIDE PMDIS

LIST OF FIGURES

1 INTRODUCTION

2 MATERIALS AND METHODS

3 PREPARATION AND CHARACTERISATION OF TERBUTALINE SULPHATE – SURFACTANT MICROPARTICLES

4 PREPARATION AND CHARACTERISATION OF BUDESONIDE – SURFACTANT MICROPARTICLES

5 STABILITY OF TERBUTALINE SULPHATE – SURFACTANT PMDI FORMULATIONS IN THE PRESENCE OF WATER

6 ADHESION PHENOMENA IN BUDESONIDE PMDIS

LIST OF ABBREVIATIONS

γ	Surface tension
γ^{12}	Interfacial tension between two phases, 1 and 2
γ^{AB}	Combined Lewis-acid Lewis-base component of surface energy
γ^{D}/γ^{LW}	Dispersive component of surface energy
γ^{LV}	Interfacial tension between liquid and vapour
γ^{P}	Polar component of surface energy
γ^{SL}	Interfacial tension between solid and liquid
γ^{SV}	Interfacial tension between solid and vapour
γ^{+}	Lewis acid component of surface energy
γ^{-}	Lewis base component of surface energy
λ	Wavelength
θ	Contact angle
AN	Acceptor number (ICG analysis)
ANOVA	Analysis of variance
BDP	Beclometasone dipropionate
BP	British Pharmacopoeia
CFC	Chlorofluorocarbon
CMC	Critical micelle concentration
COAD	Chronic obstructive airways disease
DCA	Dynamic Contact Analyser
DCM	Dichloromethane
DN	Donor number (ICG analysis)
DLVO	Derjaguin, Landau, Verwey and Overbeek
DPI	Dry powder inhaler
DSC	Differential scanning calorimetry
FID	Flame ionisation detector
FPF	Fine particle fraction
HFA	Hydrofluoroalkane
HLB	Hydrophile-Lipophile balance
HPLC	High performance liquid chromatography
IGC	Inverse Gas Chromatography
IPAC	International Pharmaceutical Aerosol Consortium
K_A	Acidic component of surface energy (IGC analysis)
K_D	Basic component of surface energy (ICG analysis)
MMAD	Mass median aerodynamic diameter
NIR	Near infra-red
NIRS	Near infra-red spectroscopy
OSCAR	Optical suspension characterisation
PEG	Polyethylene glycol
PET	Polyethylene terephthalate
POEAE	Polyoxyethylene alkyl ether
PEO	Polyoxyethylene
pMDI	Pressurised metered dose inhaler
PMMA	Polymethyl methacrylate
PPO	Polyoxypropylene
PXRD	Powder x-ray diffraction
RH	Relative humidity
RMB	Reduction in mean backscattering

rpm	revolutions per minute
SEI	Surface energy interaction
SEM	Scanning electron microscopy
SNV 2^{nd} Der	Standard normal variate 2^{nd} derivative
SPF	Shake-pause-fire
TCD	Thermal conductivity detector
*T*g	Glass transition temperature
t_r	Probe retention time (IGG analysis)
TS	Terbutaline sulphate
UNEP	United Nations Environmental Program
UV	Ultraviolet
V_N	Retention volume (IGC analysis)
W_a	Work of adhesion
W_c	Work of cohesion

CHAPTER ONE

INTRODUCTION

1 INTRODUCTION

1.1 DRUG DELIVERY TO THE RESPIRATORY TRACT

1.1.1 RESPIRATORY DISEASE

Asthma and chronic obstructive airways disease (COAD) are two common chronic illnesses prevalent in today's population. Asthma is characterised by reversible airways obstruction and bronchial hyper-responsiveness. The incidence of asthma is increasing, manifested in the rising number of asthma-related general practitioner consultations and hospital admissions. Several factors may explain this increase, including air pollution, allergen exposure, tobacco smoke and diet (Boyter et al., 2000). Symptoms of asthma classically include shortness of breath, wheeze, cough and sleep disturbance resulting from airway inflammation, increased mucus production and reduced mucus clearance by the cilliary clearance mechanism (Gibbs & Portlock, 2002; Boyter et al, 2000). COAD, unlike asthma is characterised by irreversible airway obstruction. Two main conditions sit under the umbrella of COAD, chronic bronchitis and emphysema. Symptoms of these two conditions are known to differ, with bronchitic patients experiencing excess mucus production, wheeze, dyspnoea on exertion and a productive cough. In the case of emphysema, dyspnoea (shortness of breath) is present even at rest, and there is often minimal cough and mucus production. In reality, these two conditions are rarely observed in their purest form, and commonly patients may exhibit a mixture of signs and symptoms (Gibbs & Portlock, 2002). Mainstays of treatment for COAD and asthma are bronchodilator drugs that serve to maintain airway patency, and corticosteroid therapy to control any inflammatory response. In addition, antibiotic therapy, physiotherapy and oxygen therapy play a role in the management of an acute exacerbation.

1.1.2 STRUCTURE AND FUNCTION OF THE RESPIRATORY TRACT

In order to understand the physiology of respiratory disease, a brief overview of lung anatomy is necessary. The respiratory tract can be divided into an upper and a lower region. The upper region comprises the nose, nasal cavity, paranasal sinuses and pharynx, while the lower region consists of the larynx, trachea, bronchi, bronchioles and alveoli. Surface area greatly increases with successive airway generations. The

primary function of the respiratory tract is to facilitate ventilation. Thus air is carried from the atmosphere to the alveoli where gas exchange between the lungs and the circulatory system may then occur. As such, the respiratory tract consists of a respiratory portion and a conducting portion. The conducting portion allows the passage of air from the mouth or nose through the trachea and bronchi, as far as the terminal bronchioles. Here, the terminal bronchioles and the air exchange sacs or alveoli comprise the respiratory portion of the tract (Martini, 2002). The physiology of external respiration (the process of exchanging oxygen and carbon dioxide between the environment and the circulatory system) is made of up three processes. Pulmonary ventilation or breathing involves the physical movement of air into and out of the lungs. Gas diffusion describes the passage of gases across the alveolar membranes and capillary walls. Finally, oxygen (O_2) and carbon dioxide (CO_2) that have passed through these membranes are transported between alveolar capillaries and other body tissues. Control over external respiration is both local and central.

1.1.3 PARTICULATE ABSORPTION, METABOLISM AND CLEARANCE

The adult lung possesses between 200 and 600 million alveoli, roughly translating to an enormous 140 m^2 surface area available for absorption. Most compounds appear to be absorbed from this area by passive diffusion through alveolar epithelium and endothelium. The rate of absorption is in proportion to the partition coefficient of the absorbed particle at pH 7.4. Therefore, the rate-limiting step would appear to be absorption through a lipid-like membrane similar to that found in the gastrointestinal tract. However, the absorption of poorly lipid-soluble compounds occurs more rapidly than expected in the airways, suggesting the presence of aqueous pores in the alveolar cell membrane. Some compounds such as sodium cromoglicate, are known to be absorbed via carrier transport across the membrane (Gonda, 1990).

All liver enzymes involved in classic hepatic metabolism are found in lung tissue, but at lower concentrations. Enzymes present in the lower respiratory tract include cytochrome P-450 isoenzymes, flavin-containing mono-oxygenases, glutathione S-transferase and UDP-glucuronyl transferase. Despite the presence of an identical family of enzymes to that of the liver, pharmacokinetic studies have suggested that many compounds currently used in treatment of respiratory disease are not metabolised before absorption into the systemic circulation. This fact, coupled with

the evidence of a relatively lower concentration of enzymes and therefore a lower enzymatic activity when compared to the liver presents a real advantage of pulmonary delivery over traditional systemic administration (Gonda, 1990).

Clearance of unabsorbed particles in the respiratory tract is carried out by the muco-ciliary clearance mechanism. Under normal circumstances, increased mucus production in response to unpleasant stimuli serves as a defence mechanism. Cells lining the airways are coated with sticky mucus secreted by goblet cells and mucus glands. In the nasal cavity and in the lower respiratory tract, tiny hairs or cilia continuously moving serve to direct this mucus and any entrapped debris towards the pharynx, where it is swallowed and digested by the intestinal secretions. In contrast to this controlled response, in respiratory disease an increase in size of bronchial glands and goblet cells result in the production of thicker mucus. Increased mucus viscosity affects transport and can restrict ciliary clearance, forming a plug of mucus in the airway. This is coupled with the fact that mucus clearance is also reduced in the presence of airway inflammation (Martini, 2002). Patients with COAD are therefore very susceptible to opportunistic airborne bacteria or viruses and infection often develops. At the level of the bronchioles and alveoli the absence of cilia excludes the possibility of clearance by the mucus escalator; however any foreign body may be engulfed by alveolar macrophages which then migrate to the ciliated region (Gonda, 1990).

1.1.4 DRUG DELIVERY TO THE RESPIRATORY TRACT

As mentioned above, medicines currently licensed for the treatment of respiratory disease fall into two major categories. The bronchodilating drugs include the β2 agonists such as salbutamol and terbutaline, in addition to anticholinergic drugs or muscarinic agonists such as ipratropium bromide. Several corticosteroid drugs are used in the treatment of both asthma and COAD, including budesonide, beclometasone dipropionate and fluticasone. Delivery of these various drugs is primarily via the pulmonary route. Several reasons support local administration. Firstly, a more rapid onset of action is observed. In addition, the avoidance of systemic metabolism allows a lower overall dose to be administered to the patient, while providing a high concentration of drug in the airways. Thus a lower dose of drug may be administered to achieve the same therapeutic effect, limiting the

possibility of systemic side effects (Carveth & Kanner, 1999). Delivery of drugs to the target areas of the respiratory tract is not straightforward however. While local administration is relatively simple in some conditions such as skin disorders, several factors hinder efforts to deliver drugs to the deep lung, essential in the treatment of asthma and COAD. Drugs are delivered to the respiratory tract in the form of an aerosol. The serial branching of lung anatomy makes for a tortuous route from oropharynx to alveoli, and therefore achieving aerosol penetration to the deep lung is very difficult.

1.1.5 PARTICLE DEPOSITION IN THE RESPIRATORY TRACT

It has been estimated that less than 30 % of an emitted dose from either a pressurised metered dose inhaler (pMDI) or dry powder inhaler (DPI) reaches the lung, with the remainder impacting on the oro-pharynx (Hickey & Dunbar, 1997). The amount of aerosol produced by a device, the ventilation pattern of the patient and airway anatomy and geometry all affect the deposition pattern of an inhaled aerosol in the respiratory tract. Taking these factors into consideration during formulation and device design, efforts can be made to improve or optimise deposition and absorption of an emitted dose. The amount of aerosol produced, and the particle characteristics are determined by the both the device and the formulation being aerosolised. Particle characteristics can also change on the passage through the respiratory tract due to temperature and humidity effects. Particles for inhalation are commonly described by their mass median aerodynamic diameter (MMAD). This statistical measurement of the aerodynamic particle size represents the diameter around which the mass of the particles is equally distributed (Smyth, 2003). Measurement of the MMAD of a formulation is usually conducted using inertial impaction particle sizing techniques such as cascade impaction or multi-stage liquid impingement. In broad terms, the smaller the inhaled particle, the further it will travel into the lung. An optimal particle size for inhalation is generally agreed to be between 1 and 5 μm. Particles greater than 5 μm will tend to impact on the back of the throat and be swallowed, while particles smaller than 1 μm may be exhaled. The breathing pattern of the patient will also influence the amount of an inhaled dose reaching the target peripheral airways. An increased volume of respiration will carry particles further into the lungs towards the peripheral airways. As a result, patients are counselled to

take a deep breath when inhaling a metered dose. Inspiratory flow rate also affects deposition, with a flow rate of about 0.5 L/s required for optimal deposition of liquid aerosols, and a slightly higher flow rate for dry powder aerosols. However, too fast a flow rate will result in an increased proportion of the dose impacting on the throat. The act of breath-holding at the end of the inspiration will encourage particles to deposit. As previously discussed, airway morphology is predisposed to the impaction of particles on the back of the throat following inhalation. In addition, delivery of particles to the peripheral airways is more difficult in narrower airways such as those found in patients with COAD. The presence of an artificial airway as in the case of an endotracheal tube also reduces the delivery of aerosols to the lower respiratory tract (Aerosol Consensus Statement, 1991).

Particle deposition in the respiratory tract occurs by one of three primary mechanisms. The first of these mechanisms is inertial impaction. This describes the process of a particle with its own momentum (a product of its mass and velocity in the inspired air flow) impacting on an obstacle such as the back of the throat. The air-flow will change direction on approaching such an obstacle but the inertial force of the particle will carry it along the original trajectory resulting in impaction and deposition. Deposition by inertial impaction occurs at the pharynx (the narrow laryngeal opening into the trachea) and at the subsequent bifurcations in the upper and lower airways. Sedimentation, another deposition mechanism, occurs when the resident time of a particle in the airways is relatively long e.g. as a result of breath-holding. Gravitational forces will be responsible for the deposition of particles of a suitable mass by sedimentation. As particles of less than 3 μm are likely to deposit in this manner, sedimentation is thought to be of importance in the lower airways. Particles smaller than 0.5 μm do not have adequate mass to deposit by sedimentation. In this case, diffusion involving random Brownian motion is thought to be the significant deposition mechanism (Martonen, 1996). The proportion of deposition occurring by diffusion increases as particle size decreases. Breath-holding can enhance deposition by sedimentation and diffusion mechanisms. Particles may also deposit by lesser mechanisms such as interception and electrostatic attraction (Gonda, 1990). By understanding deposition mechanisms in addition to factors influencing deposition, formulators may endeavour to overcome challenges

presented by airway anatomy and target central or peripheral airways where drug absorption is desirable.

1.1.6 DEVICES DELIVERING AEROSOLS TO THE LUNG

Drugs are delivered to the lung in the form of an aerosol. Drug delivery devices must produce an aerosol of specific characteristics in order to successfully deliver a dose to the respiratory tract. Aerosol particle size should ideally be in the range 1-5 μm as discussed above. The device should produce reproducible drug dosing upon each actuation, consistently throughout its shelf life. Physical and chemical stability of the drug should also be preserved. Ideally, the device should be portable and should be relatively user-friendly with respect to the patient, with minimal training necessary (Dalby et al., 1996). Three such devices are commercially available. The pressurised metered dose inhaler (pMDI), dry powder inhaler (DPI) and nebuliser. Each device generates aerosolised drug by a different mechanism, and can also be differentiated from each other in terms of cost, portability and usability. A brief description of DPIs and nebulisers will follow, with pMDIs being considered in more detail.

DPIs deliver drug to the respiratory tract in an aerosol generated by the force of the patient's own inspiratory flow, and as such they are said to be breath-actuated. In general, DPIs require a slightly higher inspiratory flow rate when compared to pMDIs, with flow rates of 1-2 L/s being optimal (Aerosol Consensus Statement, 1991). DPIs have advantages over the classic pMDI device. The problematic actuation and inhalation co-ordination required of the patient when using a pMDI is not necessary as a consequence of breath-actuation, and the absence of propellant provides a more stable formulation. The formulation of DPI devices is not without its problems however. Achievement of uniform dosing upon each actuation is difficult, and older devices no longer commercially available relied on the puncturing of individual hard gelatin capsules containing the powder. One example of such a device was the Rotahaler® (GlaxoSmithKline). Devices currently commercially available include that of a powder reservoir away from which a dose is channelled and aerosolised upon actuation (e.g Turbohaler®, AstraZeneca) in addition to those employing a disk containing several blisters of premetered formulation, one of which is punctured upon each actuation (e.g. Accuhaler®, Allen & Hanbury) (British

National Formulary 49, 2005). DPI formulation is also complicated by powder flow, essential to allow uniform dosing and good lung deposition. Respirable particles, by virtue of their small surface area, are very cohesive. In an effort to combat this, lactose or another excipient powder is added to some DPI formulations to improve powder flow. Drug attaches to larger lactose carrier molecules during formulation and is liberated from this complex during actuation of the device. Despite the obvious advantage of breath-actuation, DPIs are considerably less cost-effective when compared to pMDIs and as such are generally only used in cases where patients have difficulty co-ordinating inhalation and actuation of pMDIs or where cost is not a concern.

Nebulisers are the least efficient of devices delivering agents to the lung. Due to inhalation through tidal breathing, it is estimated that only 2-10 % of the dose contained in the nebuliser will deposit in the lung (Aerosol Consensus Statement, 1991). Both solution and suspension formulations are used in these devices. Two types of nebuliser are currently available, air-jet and ultrasonic. Operation of an air-jet nebuliser requires an external gas supply, usually compressed air or oxygen, which is the driving force for liquid atomisation. Both single and multiple-use air-jet nebulisers are available. Conversely, ultrasonic nebulisers do not require such a gas supply. Respiratory solution or suspension is atomised by means of a piezoelectric crystal transducer. An alternating current is applied to the crystal, causing a vibration which when amplified and transferred to the liquid reservoir, causes the generation of aerosolised droplets. Nebuliser performance (both amount aerosolised per unit time and particle-size distribution) is known to be highly variable, depending on device design characteristics. However, advantages do exist over pMDIs and DPIs. In particular, nebulisers offer easy administration and a capability to aerosolise large volumes. A flow of 15-20 ml/h is common for air-jet nebulisers with higher values reported for ultrasonic devices. As a result, nebulised therapy is still first line treatment for acute asthma or COAD where a large amount of medication can be delivered to the lung and the issue of variability is less crucial (Carveth & Kanner, 1999). In addition to classic treatment for asthma and COAD, nebulisers are increasingly used in the treatment of other conditions, in particular the administration of the mucolytic rhDNase (Pulmozyme®, Roche) to patients with cystic fibrosis (Dalby et al., 1996).

1.2 METERED DOSE INHALERS

1.2.1 OVERVIEW OF PRESSURISED METERED DOSE INHALERS

The cheapest device currently available to deliver a pharmacologically active agent to the lung is the pMDI. These devices have been the mainstay of inhalation therapy since their introduction to the market by Riker Laboratories in the 1950s (McDonald & Martin, 2000). In the UK alone, 39 million pMDIs were used in 1999 (Department of the Environment, Transport and the Regions). However, in order to achieve optimal deposition from these devices, patients must perfect their administration technique. This technique must include a co-ordinated actuation and slow inhalation (0.5-0.75 L/s), a deep breath approaching inspiratory capacity inhalation and finally, at least a 4 second breath-hold. As a result, deposition from these devices is highly variable from patient to patient, and optimal deposition is not always achieved. Anything between 5-25 % of the labelled dose may deposit in the peripheral regions of the lung. In addition to this disadvantage, problems associated with pMDIs include variation in dose (dependent on shaking, priming, actuation time and can content), a cold feeling on the back of the throat (cold-freon effect) due to the evaporation of the propellant and the absence of a dose indicator, leaving patients unsure as to when the inhaler will empty (Keller, 1999).

1.2.2 MECHANICS OF AEROSOL GENERATION

A pMDI consists of five principal components: drug, surfactant or other excipient, propellant, metering valve and actuator. Each of these contributes to the mechanics of particle formation following actuation of the pMDI. A dose is stored within the metering chamber of the valve, and depression of the valve stem by the actuator releases the dose from the metering chamber to the atmosphere. The vapour pressure of the volatile propellant equilibrates with atmospheric pressure, resulting in rapid propulsion of the contents of the metering chamber through the actuator orifice along with evaporation of the propellant. Rapid evaporation of the volatile propellant on contact with the atmosphere gives rise to a cloud of the remaining micronised drug particles primed for deposition in the lung. A schematic of aerosol generation from a pMDI formulation is shown in Figure 1.1.

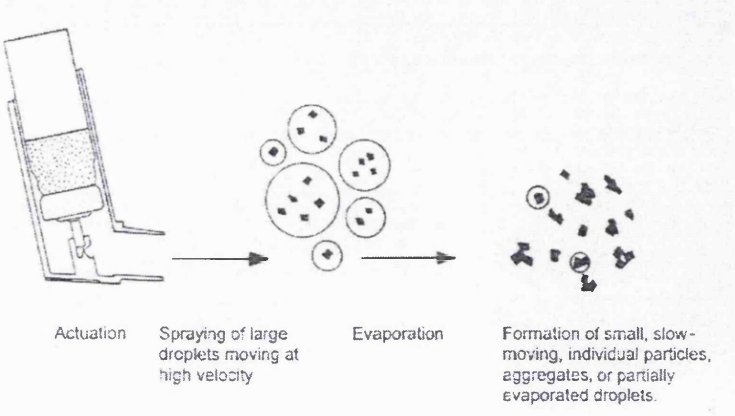

Figure 1.1 Aerosol generation from a pMDI (reproduced from Hickey and Evans, 1996)

Performance and efficacy of pMDIs is linked to the size of aerosol droplets, and the distribution and pattern of the plume formed as a result of inhaler actuation (Hickey & Evans, 1996).

1.2.3 FORMULATION CONSIDERATIONS

The presence of propellant in pMDI formulations serves as an energy source to expel the formulation from the valve in the form of rapidly evaporating droplets, in addition to providing a dispersion medium for the drug substance and other excipients. Historically, propellants employed in pMDI formulations were chlorofluorocarbon (CFC) propellants, the three most widely used being trichlorofluoromethane (CFC-11), dichlorofluoromethane (CFC-12) and 1,2-dichlorotetrafluoromethane (CFC-114). Choice of these propellants was based on their low pulmonary toxicity, high chemical stability and purity and compatibility with commonly used packaging materials, in addition to being non-flammable. These three propellants were commonly mixed to produce optimal conditions of vapour pressure, liquid density and solvency within the formulation. The effect of vapour pressure of the propellant or propellant blend on the size and exit velocity of the emitted spray in addition to the rate of propellant evaporation was first described by Polli et al., (1969). High vapour pressures produce faster exit velocities which in turn may result in a greater proportion of emitted dose depositing on the back of the throat. However, high-pressure systems also result in smaller droplets that evaporate

faster and these may penetrate deeper into the peripheral lung. Propellant density is also important in the context of the physical stability of a suspension formulation, and blending propellants of differing densities may improve suspension characteristics by creating a medium with a density approaching that of the disperse phase. Blending propellants is also useful for manipulating solvency properties of the system for both the drug substance (in the case of solution formulations) and surfactant or other excipients (Dalby et al., 1996). In recent years, CFC propellants have fallen out of favour due to their destructive effect on the earth's ozone layer. Novel hydrofluoroalkane (HFA) propellants have been chosen as replacements for use in pMDI formulations, but due to differences in several fundamental physicochemical properties, reformulation of pMDIs has proven more than challenging. This problem will be discussed in more detail in Section 1.2.5.

Drug is present in pMDI formulations in the form of a suspension or solution in propellant depending on the solubility of the active substance in the propellant-excipient mixture. The more common suspension formulations have the advantage of chemical stability, and the ability to deliver a greater mass per unit volume than solution formulations as these are limited by the maximum solubility of drug in propellant. However, suspension formulations must be carefully designed to maximise physical stability throughout shelf-life, with crystal growth, solvate formation and polymorph interconversion all possible manifestations of the physical instabilities that may befall suspended particles (Byron, 1992). The method used to micronise drug particles is an important factor to consider in the context of stability. Almost all milling techniques used to reduce particle size can cause disruption of crystalline material giving rise to amorphous regions (Vervaet & Byron, 1999). Methylprednisolone has been shown to have a higher amorphous content after micronisation with consequent problems of crystal growth in a model pMDI formulation (Phillips & Byron, 1994). Suspension stability is also influenced by the tendency for the suspended particles to aggregate and either sediment or cream in relation to density differences between disperse and continuous phases. A suspension of drug particles that do not remain evenly dispersed over the period of time between a patient shaking and actuating an inhaler can lead to problems of poor dose reproducibility and reduction in fine particle fraction (Hallworth, 1987). Scintigraphy studies of solution formulations have shown greater lung deposition

when compared to suspension formulations in both healthy and asthmatic patients (Sanders et al., 1997). However this must be balanced against the problem of chemical instability of drugs formulated in solutions (Soine et al., 1992). Qvar® (IVAX) is a device currently available consisting of a solution of beclometasone diproprionate in HFA 134a and ethanol.

The presence of a surfactant or other excipient is also an important component of a pMDI formulation. As previously mentioned, physical and chemical stability are crucial to pMDI performance and inclusion of a surfactant or co-solvent may improve suspension characteristics. Surfactants are currently employed in suspension formulations to prevent a multitude of physical instabilities including prevention of irreversible caking, minimising drug particle adhesion to container walls and valve components and slowing overly rapid separation between solid and liquid phases (Vervaet & Byron, 1999). The mechanism of action of surfactant stabilisation of pMDI systems will be described in greater details in a later section. Historically, the low HLB number surfactants oleic acid, lecithin and sorbitan trioleate were used in suspension pMDI formulations. Solubilities of these surfactants in CFC propellants ranged from 0.1 – 2.0 % w/v, however their solubility in HFA propellants is much reduced at 0.005 – 0.02 % w/v (Byron et al., 1994). Therefore following the switch to non-CFC propellants, the search for new surfactants is ongoing.

While it is generally assumed that surfactants must be soluble in a propellant in order to provide suspension stability, Byron et al showed that pre-coating albuterol with oleic acid prior to suspension in HFA 134a was efficient in retarding creaming rate of the suspension formulation over 30 seconds (1994). The creaming rate was highly dependant on the surfactant/drug ratio. Columbano investigated the application of alkylpolyglycoside surfactants as suspension stabilisers in HFA formulations of both salbutamol and BDP (2000). Again, these surfactants are insoluble in HFA propellants and are non-ionic in nature. Results from suspension stability testing in this work were encouraging in the case of the hydrophobic drug BDP. These results suggest that surfactant solubility in a propellant may not need to be high in order to stabilise a pMDI suspension. In fact, a patent application filed as early as 1990 protected formulations comprising any non-perfluorinated surfactants with a

"substantial insolubility" in propellants. Data published in support of the application showed decreased deposition on container surfaces for suspension pMDI formulations containing an appropriate surfactant. However, this effect was only apparently in formulations where the drug had been precoated with surfactant prior to mixing with propellant (Riker Laboratories Inc., 1990). In light of these data, the work of this thesis will concentrate on the use of surfactants possessing a similarly low solubility in HFA propellants.

1.2.4 PACKAGING CONSIDERATIONS

In addition to the above formulation considerations, pMDI packaging comprising the container, metering valve and actuator must also be considered. Containers for suspension formulations are typically packaged in aluminium canisters on an industrial scale. In the case of solution formulations, while some are contained in anodised aluminium canisters, most are packaged in plastic-coated glass bottles. Containers are manufactured to withstand an internal pressure of up to 180 psig (Dalby et al., 1996). The metering valve functions to hold a measured dose of formulation, typically a volume of between 25-100 μl, and deliver it through the actuator orifice. Emitted volumes must be consistently accurate to allow dose reproducibility. The volume of the metering chamber and the concentration of the drug substance contained in the formulation determine the emitted dose from the valve. Operation of the valve occurs when the valve stem is pressed into the body of the valve by depressing the actuator, resulting in release of metering chamber contents through the actuator orifice. When pressure on the stem is released, an internal spring returns the stem to its rest position and the metering chamber refills through a channel from the reservoir. Metering valves are crimped onto the neck of the aluminium can either before or after filling of the formulation, depending on fill method used. The seal at the site of crimping, in addition to elastomeric seals found internally in the valve, prevent leakage of the canister contents and the ingress of moisture (McDonald & Martin, 2000). A schematic of a typical metering valve is shown in Figure 1.2.

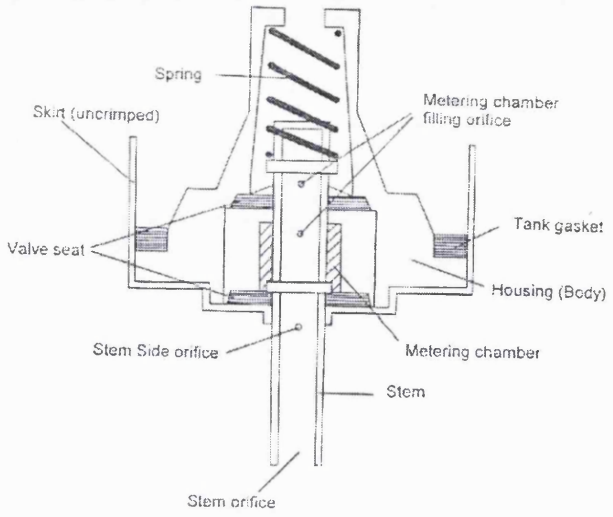

Figure 1.2 Metering valve (reproduced from Hickey & Evans, 1996)

Solvency properties of propellants are known to affect elastomeric valve components by affecting the degree of swelling or shrinkage and can therefore impair valve function as a barrier to moisture ingress, release of volatile components and reproducible dosing (Tiwari, 1998). The actuator of a pMDI functions to make depression of the valve easier, to direct the spray into the patient's mouth and to provide the orifice through which the metering valve discharges its spray. The orifice size, in addition to the volume of the metering chamber, dictates the volume and rate of emission of the aerosol formulation. Previously published work in this field has provided observations that high-pressure formulations (determined by vapour pressure of the propellant) exit small orifices faster. Subsequently, these formulations may either break into smaller droplets clouds, or may deposit on the actuator mouthpiece to a greater extent as a result of an increased tendency to impaction. Smaller orifice diameters and/or longer nozzle paths in the actuator can also cause the production of smaller droplets and/or de-aggregation of suspended material during the high speed passage of drug formulation through the nozzle (Vervaet & Byron, 1999). Therefore components other than those contained in the formulation also play an important role in the performance of a pMDI inhaler. Effects of valve and actuator can be particular to individual formulations however, and success of one valve in a particular pMDI formulation should not imply success with another (Dalby et al., 1996).

1.2.5 THE PROPELLANT ISSUE

A landmark document entitled the Montreal Protocol on Substances that Deplete the Ozone Layer was opened for signature on 16th September 1987 and entered into force in January 1989 (Montreal Protocol, 1989). The document published by the United Nations Environmental Program (UNEP) described global concerns surrounding the depletion or modification of the earth's ozone layer caused by emissions of certain substances, and the resulting adverse effects on human health, environment and climate. Aware that measures taken to protect the ozone layer should be based on relevant scientific knowledge, signatories were determined to protect it by taking precautionary measures to control and ultimately eliminate global emissions of harmful substances. Technical and economic factors were considered in addition to the needs of developing countries. The document described several substances harmful to the ozone layer and set realistic targets for reduction and eventual elimination of emissions produced from these substances. The propellants conventionally used in pMDI formulations were among those substances included in the protocol. The chemical structures of the CFC propellants are shown in Figure 1.3.

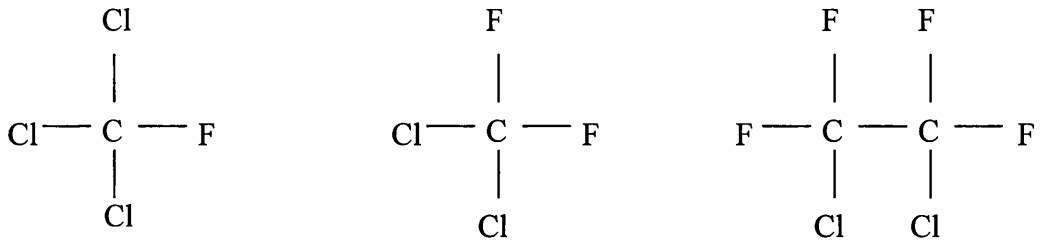

CFC-11 **CFC-12** **CFC-114**

Figure 1.3 Chemical structures of the CFC propellants

CFCs contribute to both the depletion of the ozone layer and to the greenhouse effect on global temperature. Depletion of the ozone layer occurs through an unbalancing of the stratospheric ozone formation and depletion equilibrium. In the absence of CFCs, ozone is broken down to molecular oxygen plus a free radical with the absorbance of ultraviolet B (UVB) radiation. Free radicals can then join together to yield molecular oxygen, or combine with molecular oxygen itself, thereby regenerating ozone. Chlorine atoms in CFCs are released following degradation by

UV radiation high in the upper atmosphere. These catalyse the breakdown of ozone to molecular oxygen without the formation of free radicals or the absorbance of UV radiation. Thus, ozone cannot be regenerated and more UV radiation is transmitted to the surface of the earth. The Montreal Protocol allowed certain "essential use" exemptions from targeted emission reductions in the case of substances necessary for health, where there is no technically and economically feasible alternative available. The use of CFCs in pMDI formulations has been granted such an exemption. Exemptions are reviewed every two years by the Technology and Economic Assessment Panel (TEAP) of the UNEP, with CFC use in pMDIs being reviewed annually (McDonald & Martin, 2000). In anticipation of reduced availability of CFCs and therefore increased production costs, the pharmaceutical industry has moved towards replacement propellants in pMDI formulations. Several alternatives were initially investigated including dimethyl ether (DME) and the low molecular weight hydrocarbons propane and butane. However, these candidate propellants are potentially flammable and more reactive than CFCs and also possess particularly low densities (Gupta & Adjei, 1997). A further two propellants have emerged as the lead candidates for CFC replacement. Both molecules are hydroflouroalkanes (HFAs), and thus lack the damaging chlorine atoms of the CFCs. The structures of tetrafluoroethane (HFA 134a) and heptafluoropropane (HFA 227) are shown in Figure 1.4.

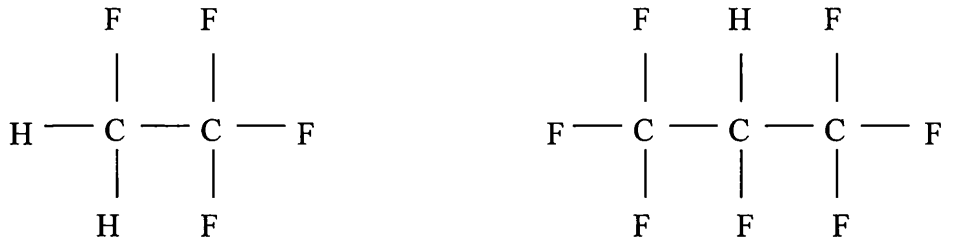

HFA 134a **HFA 227**

Figure 1.4 Chemical structures of HFA propellants

Both are non-flammable, non-ozone depleting, chemically stable propellants with vapour pressures suitable for pMDI use (McDonald & Martin, 2000). While HFAs do contribute to the greenhouse effect, it is to a lesser extent than CFCs and it was

estimated that emissions from HFA pMDIs would contribute less than 0.1 % of total global greenhouse gases by 2005 (International Pharmaceutical Aerosol Consortium (IPAC), 1997). Despite the formulation challenges that this transition has introduced, a more recent document by IPAC submitted to the United Nations Framework Convention on Climate Change stated that patient transition away from CFC MDIs will be almost complete in the EU by 2005, and in all other developed countries by 2008 (IPAC, 2002). Table 1.1 describes the differences in ozone depletion and global warming potential in addition to atmospheric life between the old and new propellants.

Table 1.1 Atmospheric properties of propellants. Ozone depletion potential is relative to CFC 11, which is given a value of unity (Smith, 1995).

Propellant	Ozone Depletion Potential	Atmospheric Life (years)	Global Warming Potential
CFC 11	1	60	1
CFC 12	1	125	3
CFC 114	0.7	200	3.9
HFA 134a	Zero	16	0.3
HFA 227	Zero	33	0.7

The overall performance of a pMDI is dependent on the interrelated effects of individual formulation components. This is coupled with the fact that regulatory authorities in both Europe and North America demand that new formulations deliver drug aerosols that are more reproducible in terms of delivered dose and particle size distribution than those emitted by the older dosage forms (Vervaet & Byron, 1999). Therefore it is clear how a fundamental change such as replacement of the propellant can alter previously successful formulations and present re-formulation difficulties to the pharmaceutical industry. HFA propellants differ from CFCs in respect to their boiling points, density, and solvency. The chemical structures of the two HFA propellants in question contain either one (HFA 227) or two (HFA 134a) small asymmetrical hydrogen atoms and as such are not completely halogenated in contrast to CFCs. As the fluorine-containing mantel surrounding the carbon atoms in HFAs is more electronegative than that of the CFCs, a distinct dipole is formed on the hydrogen-carbon bonds. As a result, HFA propellants are more polar in nature when

compared with CFCs. This increased polarity is manifested in the reduced solvency of HFA propellants for hydrophobic surfactants traditionally used in CFC pMDI formulations (Blondino & Byron, 1998; Byron et al., 1994). Partial solubility of suspended drug substance in the propellant may result in crystal growth with associated physical instability and unacceptable product performance (McDonald & Martin, 2000). Efforts have been made to define the characteristics necessary for dissolution of both excipients and drug in HFA propellants. Solutes with a low computed Log P value are suggested to be more soluble in these propellants (Dickinson et al., 2000). New surfactants that are more soluble in HFA are under investigation including polyethylene glycol (PEG), propoxylated PEG and perfluoroalkonic acids (Dalby et al., 1996). Oligolactic acids (OLA) surfactants have been examined as possible excipients in HFA formulation by 3M Healthcare. These are soluble in the new propellants and appear to provide good suspension stability (Stefely et al., 2000). However formulations containing these surfactants will only be available following demonstration of safety in chronic respiratory administration. Altered solvency properties are also important when considering the effect of propellant on valve elastomer components. Components developed for use in CFC pMDI systems will understandably react differently in the presence of HFAs, and it is reasonable to expect inadequate metering valve performance when old is combined with new. Smith describes reduced efficiency of such a system in the case of HFA 134a (1995). The performance of the standard CFC valve, observed by measuring weight per actuation, decreased over the lifetime of the device, and in the case of the last 10-20 actuations, only approximately 20-30% of the target weight per actuation was achieved. Compromised valve elastomer components previously compatible with CFC propellants may also lead to water ingress. Indeed, the compatibility of elastomeric components varies even between HFA propellants, with leaking through nitrile elastomers in HFA 134a systems ten times greater than that observed in HFA 227 systems (Schultz et al., 1994). HFA systems have a higher capacity for water than CFCs due to their increased polarity (Williams & Tcherevatchenkoff, 1997). As the addition of water to a formulation may cause hydrolysis of susceptible drugs and reduction of the system vapour pressure, elastomeric seals are crucial in maintaining a barrier to water ingress (Atkins et al., 1992). Several developments in the formulation of elastomers have resulted in improved compatibility of these components in HFA systems (McDonald & Martin, 2000).

As previously mentioned, HFA propellants also differ from CFCs with respect to their boiling point and vapour pressures. Table 1.2 presents data pertaining to both CFC and HFA propellants clearly indicating the differences.

Table 1.2 Properties of old and new propellants (Meakin et al., 2000)

Property	CFC			HFA	
	11	12	114	134a	227
Boiling Point, °C	24	-30	4	-26	-16
Vapour Pressure, 20°C, kPa	89	566	182	572	390
Dipole Moment	0.45	0.51	0.58	2.1	1.2
Dielectic constant	2.3	2.1	2.2	9.5	4.1

In the past, blends of CFC propellants have enabled formulators to manipulate these properties, with the result of increased flexibility during the formulation process. Propellant blends of HFA 134a and HFA 227 have been investigated; however as yet no commercially available product consists of such a blend (Smyth, 2003). In particular, the low boiling points of the HFA propellants create practical problems during manufacture due to the evaporation of these volatile liquids on exposure to room temperature. The preparation or filling of pMDIs is generally by one of two conventional methods, that of cold-filling or pressure-filling. The cold-filling method requires the propellant to be maintained at a temperature approximately 20 °C below its boiling point. Once filled into open canisters, the metering valve is then crimped on the top of the can to provide a pressure seal. Pressure filling on the other hand requires the propellants to be kept at a temperature between 10-20 °C and under pressure. This necessitates specific equipment to withstand the required pressure (Smith, 1995). By blending CFC propellants, filling of pMDIs at room temperature and atmospheric pressure was possible; however the absence of an HFA propellant equivalent to CFC 11 in boiling point precludes this possibility. The vapour pressure of a pMDI system is an important consideration when targeting peripheral lung deposition, and as previously mentioned, higher vapour pressure may result in smaller, more respirable aerosols but at the cost of increased oro-pharyngeal deposition due to increased spray velocity. The variation in vapour pressure of CFCs allowed for manipulation of overall system vapour pressure through the use of propellant blends. In contrast, the two HFA propellants are relatively similar in

vapour pressure, and so another option for formulation flexibility is removed. Despite a narrower margin for manipulation of propellant properties, efforts have been made to optimise density and vapour pressure of HFA systems. Williams & Liu showed increased physical stability of a triamcinolone acetonide formulation when the density of the propellant blend approached that of the density of the suspended drug particles (1998). MMAD was also decreased by using propellant blends of a higher vapour pressure.

As a result of new challenges to the formulation of pMDI systems, the pharmaceutical industry has invested substantial time and effort into overcoming these obstacles. Airomir™, the first marketed non-CFC pMDI was developed by 3M Healthcare. This formulation contains salbutamol sulphate suspended in HFA 134a with a surfactant and a small amount of the co-solvent ethanol (June, 1997). Qvar® was subsequently developed by the same company (now marketed by IVAX Pharmaceuticals). This pMDI contains BDP in a solution formulation with HFA 134a (Donnell, 2001). Both formulations are claimed to have improved performance over traditional CFC formulations of the same drugs, with Qvar® requiring only half the previously advised dose due to increased fine particle fraction. Clinical studies have investigated the efficiency of new formulations in the patient. A comparison between a CFC and an HFA pMDI formulation of fluticasone proprionate showed an equivalent dose proportionality effect on drug plasma concentrations after 24 hours (Kunka et al., 2000). Equivalence between a CFC and an HFA formulation was also observed in the case of salbutamol, where median use, peak expiratory flow rate and forced expiratory volume in 1 second (FEV_1) were measured in asthmatic patients (Baumgarten et al., 2000).

Aerosol delivery systems are under continuing development as the need for accurate and efficient delivery systems increases, both in terms of the portfolio of drugs delivered via the pulmonary route and the devices used to achieve this delivery. Attention is now focussed on the local delivery on various biotechnology-derived products such as prostaglandin E (PGE) VI, interleukins and oligonucleotides (Dalby & Smyth, 2003). In addition, various new devices are under development including several single-breath liquid systems. One such system is the AeroDose (Aerogen, USA), comprising a hand-held vibrating orifice array system (DeYoung, 1998).

Electrohydrodynamic sprays are also under investigation, whereby a charge is applied to a liquid stream, causing the atomisation of droplets (Batelle Pulmonary Therapeutics, USA) (Ding et al., 2002). Understanding the science underlying the pulmonary delivery of aerosols will therefore continue to be of great importance in order to achieve the desired therapeutic results.

1.3 INTERFACIAL PHENOMENA

The term "interfacial phenomena" is given to the behaviour of molecules situated at an interface between two phases within a system, a pharmaceutical system in the context of this work. A review of pMDI suspension formulations conducted in Section 1.2 has clearly indicated the complex nature of such systems, arising from the presence of multiple constituents. In turn, multiple interfaces exist within pMDI suspension systems e.g. drug-propellant, drug-container, propellant-container, propellant-valve etc. Interactions between the different phases are a consequence of long-range van der Waals attractive forces and are physical rather than chemical in nature. As such, interfacial forces are much weaker than chemical or covalent bonds (< 40 kJ/mol compared with 300-700 kJ/mol) but exert a greater influence over larger intermolecular distances. An understanding of interfacial phenomena is therefore essential in order to understand in turn the behaviour of such systems.

1.3.1 SURFACE TENSION

Surface tension describes the net inward force of attraction imposed on molecules of a liquid situated at a liquid/vapour interface. Molecules positioned within the bulk of a liquid are surrounded by other molecules and as such are subject to attractive forces in all directions from neighbouring molecules. However, molecules at the surface, by virtue of their position, are not subjected to the same attractive forces. While molecules of vapour do interact with surface molecules, the interaction is weak in comparison to the attractive forces of molecules in the bulk. Surface tension acts downwards in a direction perpendicular to the liquid/vapour interface, and so causes the surface to contract. Contraction of the surface is spontaneous and is accompanied by a decrease in free energy. As such, surface free energy of the liquid is described as the work w, required to increase the surface area A by 1 m^2 (Equation 1.1).

$$w = \gamma \Delta A \qquad \text{(Equation 1.1)}$$

In the case of liquids, surface free energy is numerically equivalent to surface tension (γ). The surface tension of a liquid may be altered by changing the vapour phase against which it is measured in addition to altering the temperature of the system.

The presence of impurities within the liquid under investigation will also influence the surface tension, in the same way as the inclusion of a surface active molecule. This phenomenon will be discussed in greater detail in Section 1.4.2. Figure 1.5 describes the imbalance of surface forces giving rise to surface tension.

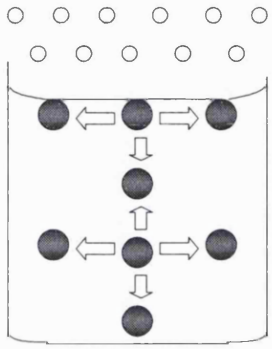

Figure 1.5 The imbalance of forces at the liquid/vapour interface giving rise to surface tension

Several methods of measuring surface tension exist, including the Wilhelmy plate method, the ring method, drop weight and drop volume method and capillary rise method (Fell, 2002). The Wilhelmy plate method has been used to measure surface tension in work reported in this thesis. This has been conducted using a Dynamic Contact Analyser (DCA) (Cahn, US) and is described in full in Chapter Two, Section 2.2.9.

1.3.2 CONTACT ANGLE AND SURFACE FREE ENERGY

The contact angle formed by a liquid on a solid has been defined as the angle formed between the tangent drawn at the interface between the liquid droplet, solid and vapour and is described in Figure 1.6 (Buckton, 1995a). This angle is the consequence of three interfacial forces arising from the solid-liquid interface (γ_{SL}), the solid-vapour interface (γ_{SV}) and the liquid-vapour interface (γ_{LV}).

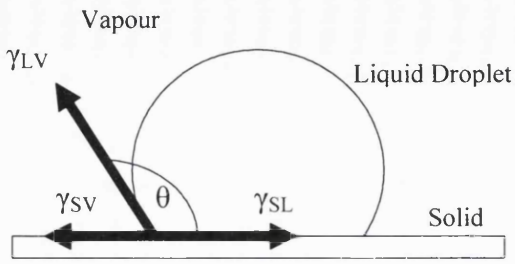

Figure 1.6 The three interfacial forces acting on a droplet of liquid, with the contact angle marked as θ

Young's equation relates these three interfacial forces to the contact angle, θ (Equation 1.2). In this way, contact angle may be related to the surface tension of a liquid, or the surface energy of a solid.

$$\gamma_{LV} Cos\theta = \gamma_{SV} - \gamma_{SL} \qquad \text{(Equation 1.2)}$$

The measurement of contact angle values for a liquid on a solid provides an indication of the ability of the liquid to wet the solid. A contact angle of 0 ° corresponds to total spreading of the liquid over the solid surface, whereas a contact angle of 180 ° is observed in systems where no wetting will occur. A critical value for contact angles is believed to be 90 °, below which wetting will occur to a reasonable extent, and above which wetting is poor. Young's equation describes an "ideal" solid, i.e. one that is rigid, flat and chemically homogenous. Under these conditions, one unique contact angle formed by the liquid on the solid may be measured (Good, 1993). In reality, as is so often the case in pharmaceutical systems, ideal conditions are not met. The complex nature of solid surfaces gives rise to two different values for the advancing and receding contact angles known as hysteresis. Contact angle measurement of a liquid on a flat solid surface is therefore straightforward. Dynamic contact angle analysis (DCA) has also been used for this purpose in work presented here. The measurement of contact angles on pharmaceutical powders is more complicated. While several methods including the sessile drop method, liquid penetration and dynamic contact angle analysis may be

used, at least two of these methods require the compression of the powder into a flat disk or wafer prior to analysis. Compression of the powder may corrupt the solid surface and in turn produce a result that is not representative of the starting material (Buckton, 1993). In practice, powder surface energy is increasingly measured using inverse gas chromatography (IGC), a technique allowing measurements to be taken on unadulterated samples. A description of IGC may be found in Chapter Two, Section 2.2.4.

1.3.3 COMPONENTS OF SURFACE FREE ENERGY

Surface tension and surface energy may be expressed as the sum of their component intermolecular forces. Fowkes first described the simplified subdivision of surface tension and surface energy into dispersive (γ^D) and polar (γ^P) interactions (1963). Fowkes then further described the interaction between two phases of a system as being equal to the geometric mean of the two components, his work culminating in Fowkes' Geometric Mean Equation (Equation 1.3).

$$\gamma_{12} = \gamma_1 + \gamma_2 - 2(\gamma_1^D \cdot \gamma_2^D)^{0.5} - 2(\gamma_1^P \cdot \gamma_2^P)^{0.5} \qquad \text{(Equation 1.3)}$$

Wu further developed the work of Fowkes, using a harmonic mean rather than a geometric mean to describe interfacial interactions (Equation 1.4). The use of Wu's harmonic mean equation was found to produce a better agreement between experimental and calculated values of interfacial energy for low energy systems such as organic liquids (Wu, 1971).

$$\gamma_{12} = \gamma_1 + \gamma_2 - 4\left(\frac{\gamma_1^D \cdot \gamma_2^D}{\gamma_1^D + \gamma_2^D}\right) - 4\left(\frac{\gamma_1^P \cdot \gamma_2^P}{\gamma_1^P + \gamma_2^P}\right) \qquad \text{(Equation 1.4)}$$

Several methods of calculating surface energy parameters in terms of their dispersive and polar components were subsequently described including the Neumann equation of state and the Wu equation of state (Neumann et al., 1974; Wu, 1979). However, attentions have since shifted from this more conservative approach to surface energy components in favour of a theory developed in the combined works of van Oss.

Van Oss developed an extension of the geometric and harmonic mean approach to surface energy components, describing surface energy interactions in terms of Lifshitz van der Waals (γ^{LW}) or apolar forces, and polar forces (van Oss et al., 1987). Apolar forces were described as comprising London dispersive forces, Keesom orientation forces and Debye induction forces. The polar forces in question are hydrogen-bonding interactions and were described by van Oss as (Lewis) acid-base (γ^{AB}) or electron-acceptor – electron-donor interactions (γ^{+} and γ^{-} interactions respectively). The contributions of γ^{LW} and γ^{AB} interactions towards the total surface tension of a liquid or the total surface energy of a solid *i*, are additive and the relationship is described in Equation 1.5.

$$\gamma_i^{TOT} = \gamma_i^{LW} + \gamma_i^{AB} \qquad \text{(Equation 1.5)}$$

However, the contributions of the individual γ^{+} and γ^{-} components to the overall γ^{AB} parameter are not additive. Therefore to correctly describe the relationship between these parameters, Equation 1.6 is used which expresses γ^{AB} as the geometric mean of its two constituent parameters.

$$\gamma_i^{AB} = 2\sqrt{\gamma_i^{+} \cdot \gamma_i^{-}} \qquad \text{(Equation 1.6)}$$

Lewis acid and Lewis base values for a large number of liquids are not equal, and indeed it is common for materials to be predominantly electron accepting or electron donating (with either γ^{+} or γ^{-} equal to zero), otherwise known as monopolar. Equation 1.6 in turn states that for such materials, γ^{AB} will equal zero. Monopolar materials will consequently have a total surface energy equal only to the apolar interaction γ^{LW}.

Under the conditions defined in the van Oss theory of surface tension and surface energy components, the interaction between two phases 1 and 2 due exclusively to γ^{LW} apolar forces when combined with the Young equation is described by Equation 1.7.

$$\gamma_1^{LW}(1 + Cos\theta) = 2\left(\gamma_1^{LW} \cdot \gamma_2^{LW}\right)^{0.5} \qquad \text{(Equation 1.7)}$$

The interaction between polar forces at an interface is unsurprisingly more complicated given that two separate polar forces contribute to the overall acid-base interaction, and is described by Equation 1.8.

$$\gamma_{12}^{AB} = 2\left(\sqrt{\gamma_1^+ \cdot \gamma_1^-} + \sqrt{\gamma_2^+ \cdot \gamma_2^-} - \sqrt{\gamma_1^+ \cdot \gamma_2^-} - \sqrt{\gamma_1^- \cdot \gamma_2^+}\right) \quad \text{(Equation 1.8)}$$

Apolar and polar interactions contributing to the total interfacial tension can be combined with Young's equation to give Equation 1.9.

$$\gamma_1(1+Cos\theta) = 2\left[\left(\gamma_1^{LW} \cdot \gamma_2^{LW}\right)^{0.5} + \left(\gamma_1^+ \cdot \gamma_2^-\right)^{0.5} + \left(\gamma_2^+ \cdot \gamma_1^-\right)^{0.5}\right] \quad \text{(Equation 1.9)}$$

Equation 1.9 may be used to calculate individual surface energy components of uncharacterised liquids or solids providing contact angle data of three fully characterised liquids on the solid under investigation (or surface tension data in the case of a liquid under investigation) are known. A series of simultaneous equations may then be solved for the three unknown surface energy parameters of γ^{LW}, γ^+ and γ^- of the material under investigation (van Oss et al., 1988). The principles governing the calculation of unknown surface energy parameters have been applied in this thesis to characterise both a model HFA propellant (Chapter Three, Section 3.12.3) and various pMDI container wall materials (Chapter Six, Section 6.3.4).

1.3.4 APPLICATIONS OF SURFACE ENERGY INVESTIGATIONS

Elucidation of surface energy and interfacial interaction parameter data for materials provides useful information pertaining to the behaviour of pharmaceutical solids and liquids. A description of the relationship between contact angle data and the ability of a liquid to wet a solid has been previously described in Section 1.3.2. Additional physicochemical characteristics of pharmaceutical systems that may be predicted using surface energy data are cohesion and adhesion. Cohesion describes the interaction between two molecules of the same solid and is equivalent to twice the apolar component of the solid surface energy. Work of cohesion (W_c) may be calculated using Equation 1.10. Cohesive forces are of particular relevance in pharmaceutical systems containing microparticles which possess a high surface energy by virtue of their small particle size. Cohesion in suspension pMDI systems

is observed in the aggregation of suspended particles within the disperse phase and can have implications for re-suspension (Parsons et al., 1992).

$$W_c = 2\gamma^D \qquad \text{(Equation 1.10)}$$

The adhesion of one solid on another may also be described in terms of surface energy parameters, corresponding to the sum of the individual total surface energies for each solid minus the interfacial energy between the two solids (Equation 1.11). The total interfacial energy between the two phases may be calculated using Equation 1.12. A comparison of the works of cohesion and adhesion within pharmaceutical systems may serve to predict the behaviour of particles within the system in terms of the most likely interactions (Buckton & Chandaria, 1993). Work of adhesion parameters for various formulations have been calculated in Chapter Six of this thesis, in an investigation of the relationship between powder surface energy and microparticle adhesion to the container wall in pMDI suspension formulations (Section 6.3.5).

$$W_a = {\gamma_1}^{TOT} + {\gamma_2}^{TOT} - {\gamma_{12}}^{TOT} \qquad \text{(Equation 1.11)}$$

$${\gamma_{12}}^{TOT} = \left(\sqrt{{\gamma_1}^{LW}} - \sqrt{{\gamma_2}^{LW}}\right)^2 + 2\left(\sqrt{\gamma_1^+ \cdot \gamma_1^-} + \sqrt{\gamma_2^+ \cdot \gamma_2^-} - \sqrt{\gamma_1^+ \cdot \gamma_2^-} - \sqrt{\gamma_1^- \cdot \gamma_2^+}\right)$$

(Equation 1.12)

As such the investigation of surface energy and interfacial parameters of powders present in pharmaceutical systems may provide an insight into the behaviour of such systems in terms of their physicochemical properties.

1.4 SURFACTANTS

1.4.1 CLASSIFICATION OF SURFACTANTS

Surfactant molecules are characterised by their possession of two chemical moieties, both a hydrophilic (water-liking) and hydrophobic (water-hating) region, and are therefore referred to as amphiphilic molecules. The typical structure of a surfactant molecule is depicted in Figure 1.7. Hydrophilic regions are commonly composed of an ionisable, polar or water soluble group, while the hydrophobic portion is usually made up of a saturated or unsaturated hydrocarbon chain. By nature of their distinct structure, surfactant molecules orientate themselves preferentially at the interface between two phases in a system, be it liquid/vapour, liquid/liquid, or liquid/solid interfaces. Adsorption of an ordered layer of surfactant molecules at a surface or interface results in a decrease in surface or interfacial tension. As the concentration of surfactant molecules in a solution increases, they will tend to self-associate to form spherical structures known as micelles. Types of surfactant are largely defined by the nature of the hydrophilic group, and can be anionic (possessing a negatively charged polar head group), cationic (possessing a positively charged polar head group), ampholytic (behaving either as ionic or non-ionic surfactants depending on pH) or non-ionic.

Non-ionic surfactants have the advantage of low toxicity and are also compatible with other surfactants. There are two common types of non-ionic surfactant, fatty acids and fatty acid alcohol ethoxylates. Both contain a polyether polar head group produced by the polymerisation of ethylene oxide. Oleic acid, lecithin and sorbitan triethanoleate, the surfactants of choice used in CFC pMDI formulations are among the non-ionic surfactants. Non-ionic surfactants may be further classified in terms of their hydrophile-lipophile balance (HLB) number assigned according to the overall polarity of the molecule, in direct proportion to the number of ethylene oxide units. An HLB value of 6 or below is synonymous with hydrophobicity while a value between 8 and 30 is common to hydrophilic surfactants. HLB numbers provide an indication as to the possible applications of a particular surfactant with values of 3-6 indicating an ability to emulsify water-in-oil emulsions, and values 7-9 indicating wetting ability for example.

Figure 1.7 Amphiphilic nature of a surfactant molecule

1.4.2 PHYSICOCHEMICAL PROPERTIES OF SURFACTANTS

One of the most important properties of surfactant molecules is their ability to migrate to a surface or an interface and decrease the surface or interfacial tension when present in a dilute solution. Surfactant molecules orientate themselves at a surface or an interface in order that the hydrophobic chain moiety projects out of an aqueous solution thus achieving a state of minimum free energy. This causes displacement of some water molecules from the surface, to be replaced by surfactant molecules. The reduction in surface tension subsequently achieved by surfactant molecules is attributable to the reduced interaction between water and surfactant molecules over that between two water molecules at the surface. In the presence of an increasing concentration of surfactant molecules, behaviour of the surface active agent deviates from this ideal. Surfactants are known to self-associate into spherical structures known as micelles at a defined "critical micelle concentration" (CMC). The position of surfactant molecules in a micelle is orientated so that the polar headgroups are exposed to the aqueous solution, protecting the hydrophobic chains within the centre of the structure. Changes in physical properties of the solution such as osmotic pressure, turbidity and electrical conductance may also be observed once the concentration of surfactant has exceeded that of the CMC. CMC values are unique to individual surfactants in an aqueous solution. A further increase in concentration above the CMC may result in the formation of non-spherical micelles resulting from micelle growth in one or two dimensions giving rise to prolate (cigar-shape) or oblate (disc-shape) micelles. At concentrations substantially greater than the CMC, the increased density of the system caused by the large concentration of surfactant molecules may result in the formation of liquid crystalline phases. These commonly take the form of a cubic, hexagonal or lamellar shape. Surfactants may also be characterised by a "cloud point", a critical temperature above which a solution of surfactant molecules will become turbid, even at a low concentration. The phenomenon is reversible upon cooling of the solution below the critical

temperature. Finally the Krafft point, another phenomenon observed in aqueous solutions of surfactant, describes the temperature above which increasing concentrations of surfactant will be soluble in the aqueous phase despite the solution concentration exceeding the CMC.

Surfactants are used in a wide range of other applications in both pharmaceutical and other industries. Surfactants can be used as wetting agents to aid the spreading of liquid over a surface. This occurs through both lowering of the interfacial tension and adsorption to the surface of the phase to be wetted. Detergency is another surfactant property exploited by these industries, whereby the presence of surfactant in a solution can increase the solubility of an organic material in an aqueous medium. The ability of surfactants to form structures such as micelles has been particularly exploited in the pharmaceutical industry. The phenomenon allows non-polar solutes to be incorporated at the centre of a micelle and thus protect them from the aqueous medium. Stabilisation of emulsion formulations is also possible. Emulsions are known to be immiscible systems, and are therefore thermodynamically unstable. Dispersed drops will aggregate rapidly and eventually the two phases will separate completely in order to achieve the lowest possible interfacial contact. The addition of a surfactant to such a system can retard phase separation of the immiscible components by lowering the interfacial tension. Further applications of surfactants include their use as foaming or de-foaming agents (reviewed by Buckton, 1995a).

1.4.3 ADSORPTION AT A SOLID/LIQUID INTERFACE

The process of adsorption describes the accumulation of a substance at an interface. It is a surface process, distinct from absorption in that penetration of one component through the other does not occur. There are two types of adsorption, physical and chemical. Physical adsorption occurs through weak van der Waals attractive forces, whereas chemisorption involves an ion exchange between the two phases (reviewed by Florence & Attwood, 1998). The adsorption of a surfactant at the boundary between two phases is a property often used in the pharmaceutical and cosmetic industries. In the context of this work, the ability of surfactants to stabilise suspensions by adsorbing to a surface is most relevant. Conventional analysis of surfactant adsorption mechanisms in aqueous solutions involves the use of adsorption isotherms, whereby the amount of surfactant adsorbed is considered in

relation to the equilibrium concentration of surfactant. The shape of the adsorption isotherm may vary. The isotherm shape for adsorption at the solid/liquid interface generally follows one of two classifications, the Langmuir or the Freundlich isotherm (shown in Figures 1.8 and 1.9). Interpretation of adsorption isotherms is achieved through the use of equations derived from the study of adsorption of gases on solids, with the Langmuir and Freundlich equations being most commonly used. Adsorption of surfactant molecules at the solid/liquid interface occurs through several intermolecular forces including electrostatic interactions, van der Waals attractive forces, and hydrophobic interactions (Myers, 1988).

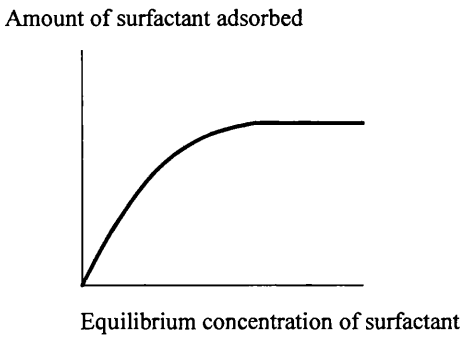

Figure 1.8 Langmuir isotherm

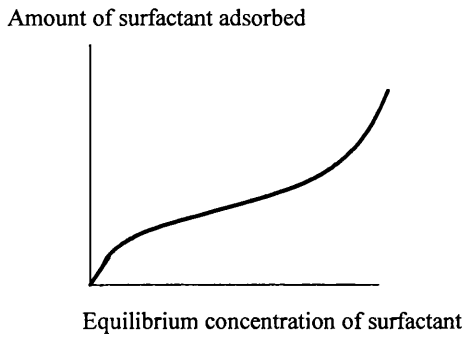

Figure 1.9 Freundlich isotherm

Adsorption of surfactants to the surface of a solid is greatly influenced by the nature of the solid in question. Adsorption of surfactants to the surface of non-polar solids is due primarily to dispersive interactions, while adsorption to polar solids may result from dipolar interactions, hydrogen bonding and acid-base interactions in addition to dispersive interactions. The orientation of surfactant molecules is also influenced by the nature of the solid as one would expect. Adsorption on hydrophobic solids in aqueous solution will be such that the hydrophobic surfactant groups are associated with the solid surface, while the hydrophilic groups extend into the aqueous solution. The orientation of the surfactant molecule may also alter as increasing amounts of surfactant are adsorbed on the solid, with molecules initially taking up a "train" shape on the solid surface. Surfactant molecules are subsequently required to condense to allow adsorption of further molecules and will be orientated perpendicular to the solid surface in close assembly (Myers, 1988). The adsorption of surfactant to the surface of dispersed particles may in turn act to confer stabilising

properties on the dispersion, retarding separation of the disperse and continuous phases. The stabilisation of suspension pMDI systems resulting from the addition of a surfactant is discussed in Section 1.4.4.

1.4.4 SURFACTANT STABILISATION OF pMDI SUSPENSION FORMULATIONS

Suspension stability in pharmaceutical systems is conventionally described by the DLVO theory, developed by Derjaguin and Landau, and Verwey and Overbeek. This theory states that a stable redispersable suspension can be formed via controlled aggregation or flocculation (Ranucci et al., 1990). Understood in this theory is that deflocculated suspensions are unstable and will flocculate irreversibly over time, forming a hard cake after complete sedimentation or creaming. The fate of a dispersed particle in suspension may be predicted using Stoke's Law whereby sedimentation velocity is influenced by the particle radius, the density difference between the disperse and continuous phases, the viscosity of the continuous phase and the acceleration of the dispersed particle under gravity. Van der Waals attractive forces are responsible for the permanent aggregation between sedimented or creamed drug particles. Controlled flocculation on the other hand, occurs when interparticulate distances are large enough to result in reduced van der Waals forces. A suspension forming flocs in this manner will separate over time, but will have a large sedimentation volume and should be much easier to redisperse on shaking.

While well defined, the DLVO theory was founded in aqueous media and therefore the application of such a theory to the non-aqueous media of pMDI propellants is controversial. Due to the non-aqueous nature of HFA propellants, ion concentration in pMDI formulations is very low, and as a result electronic repulsive forces are likely to be negligible. Assuming the interparticulate distances in pMDI suspension formulations exceed the range of van der Waal's electronic forces, the only remaining repulsive force between particles is provided by steric forces introduced following the addition of a surfactant to the formulation. By virtue of its preferred orientation between the solid/liquid interface and projection of the molecule tail into the media, adsorption of a surfactant to the surface of a suspended particle will thus increase the separation distance between suspended particles. Thus, manipulation of steric forces is the theoretical key to stabilising a suspension pMDI (Vervaet & Byron, 1999). This manipulation can be achieved by varying the type and

concentration of surfactant, however only experimentation allows the formulator to determine the efficiency of a surfactant in a particular formulation. Regardless of surfactant stabilisation, suspensions will inevitably separate over time if there is a difference in density between the disperse and continuous phases.

1.4.5 BLOCK CO-POLYMER SURFACTANTS

Synthetically derived, block co-polymer or poloxamer surfactants are made up of an a-b-a structure. The "a" block is polyethylene oxide (PEO), a hydrophilic polymer while the "b" block is polypropylene oxide (PPO), a hydrophobe. The inverse of this assembly is also possible, with two hydrophobic POP groups on either end of a hydrophilic POE group. The structure of a poloxmer molecule is shown in Figure 1.10. The size of both regions can be varied to alter the overall molecular weight, and proportion of hydrophile to hydrophobe. This in turn allows manipulation of poloxamer properties.

$$HO(CH_2.CH_2.O)_a\text{-}(CH_2.CH(CH_3)O)_b\text{-}(CH_2.CH_2.O)_aH$$

PEO **PPO** **PEO**

Figure 1.10 Typical structure of a poloxamer surfactant

The nomenclature of poloxamer surfactants follows two conventions. The first and more generic of the classifications is based on a three digit number, and corresponds to the hydrophile/hydrophobe balance of the poloxamer. The first two digits when multiplied by 100 relate to the approximate molecular weight of the hydrophobe. The last digit when multiplied by 10 gives the approximate content of the hydrophile, expressed as a percentage of the total molecular weight. It follows that poloxamer 188 is made up of approximately 80 % PEO, with the molecular weight of PPO equalling approximately 1,880. In fact, the true molecular weight of the hydrophobe in this surfactant is equal to 1,740 (Buckton, 1995a). Pluronic® surfactants, manufactured by BASF follow a slightly different nomenclature, with each number preceded by a letter corresponding to physical state at room temperature. Therefore those prefixed with "F" are flakes, "L" are liquids and the letter "P" describes an intermediary state (Ali, 2000).

Historically, it was thought that poloxamer surfactants did not aggregate in a conventional manner to form micelles in response to increasing concentration in aqueous solution. However, this has now been shown to be the case. Work published by Linse showed transition from a monomeric solution to a solution containing spherical aggregates following either increasing surfactant concentration or increasing temperature (1993). At even higher concentrations, infinitely long rod-like aggregates were present, and eventually the system separated into two phases. Work using dye solubilisation techniques to investigate the CMC revealed it to be dependant on temperature and the size of the PEO headgroup, with micelle formation attributable to the hydrophobic portion of the surfactant (Alexandridis et al., 1994). Adsorption of poloxamers to a hydrophobic surface is believed to be irreversible, as the PPO group binds to the surface in a loop and chain structure. As such it is unlikely that all bonds will break simultaneously. The hydrophilic PEO chains then project up to 15 nm from the solid surface (Rudt & Muller, 1993). Work published by Carthew et al., investigated the adsorption of P338 and P188 onto a model hydrophobic drug from solutions of varying concentrations and at different temperatures. Adsorption was shown to fall, then increase and finally fall again as temperature was increased. This was attributed to a phase transition in the poloxamer solution at specific temperatures (1995). A further study by the same authors found surface hydrophobicity to be greatly influenced by the amount of poloxamer adsorbed, however coating layer thickness was essentially unchanged by the temperature of adsorption (1997).

1.4.6 POLYOXYETHYLENE ALKYL ETHER SURFACTANTS

Polyoxyethylene alkyl ether surfactants comprise another group of synthetic non-ionic polymer surfactants, consisting of an alkyl chain of a certain length, joined to the hydrophilic head group containing a certain number of oxyethylene units. The structure of these surfactants is represented by C_aEO_b, where *a* is the number of carbon units in the alkyl chain, and *b* the number of ethylene oxide units (Buckton et al., 1994). The alkyl chain may consist of several apolar moieties including alcohols, fatty acids or amides (Berthod et al., 2001). They have been shown to form several liquid crystalline structures in high concentration (Mitchell et al., 1983). This phenomenon may form the basis of cream or ointment formulations for transdermal drug delivery. At low concentrations in a mixture with cholesterol, these surfactants

have been shown to form vesicles suggesting an application as potential drug delivery systems (Hofland et al., 1989). Solubilisation capabilities of this group of surfactants have also been assessed, and investigation into the effect of lengthening the alkyl chain length showed maximum solubilisation at a chain length of 16 carbon units (Elworthy & Patel, 1982).

1.5 AIMS OF THE PHD

The need for alternative surfactants for inclusion in HFA pMDI suspension formulations resulting from the altered solvency properties of these propellants when compared with their predecessor CFC propellants has been discussed at length in the introduction to this thesis. It is generally assumed that surfactants must be soluble in a propellant in order to provide suspension stability. However, the work of several authors has suggested that surfactant solubility in a propellant may not need to be high in order to stabilise a pMDI suspension. The relationship between the behaviour of such complex suspension pMDI formulations and surface energy is not clearly understood. In light of these facts, the aims of this thesis are:

- To explore the use of alternative surfactants possessing a low solubility in HFA propellants as stabilising agents in pMDI HFA suspension formulations.

- To further elucidate the relationship between powder surface energy and suspension performance of pMDI suspension formulations in HFA propellants by modifying powder surface energy of the model hydrophilic drug terbutaline sulphate and the model hydrophobic drug budesonide through the adsorption of alternative surfactants to the drug surface.

The individual aims and objectives of each chapter are clearly defined at the beginning of each chapter.

CHAPTER TWO

MATERIALS AND METHODS

2 MATERIALS AND METHODS

2.1 MATERIALS

2.1.1 BUDESONIDE

Budesonide (16α,17-[(1*RS*)-Butylidenebis(oxy)]-11β,21-dihydroxypregna-1,4-diene-3,20-dione) was obtained from AstraZeneca (Charnwood, UK) in a micronised form (batch 4462L.). Budesonide is one of a number of therapeutic corticosteroids currently used in the treatment and prevention of respiratory diseases by reducing airway hyper-responsiveness and the bronchial mucosal inflammation reaction (BNF 49, 2005). As such it is commonly prescribed for patients suffering from both asthma and chronic obstructive airways disease (COAD). Due to its steroid ring structure, the drug is hydrophobic and practically insoluble in water. It is a white or almost white crystalline powder freely soluble in dichloromethane, and sparingly soluble in alcohol (BP, 2003). The chemical structure of the budesonide molecule is shown in Figure 2.1.

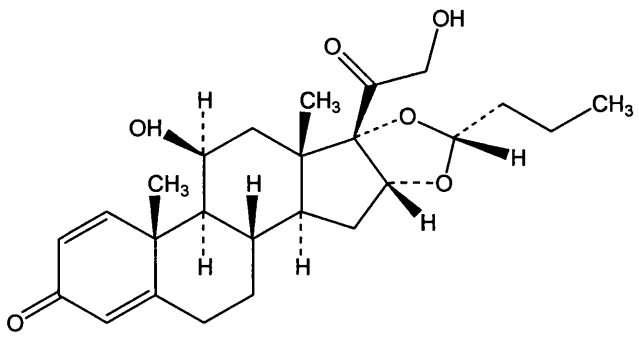

Figure 2.1 Chemical structure of the budesonide molecule

2.1.2 TERBUTALINE SULPHATE

Terbutaline sulphate (TS) (bis[(1*RS*)-1-(3,5-dihydroxyphenyl)-2-[1,1-dimethylethyl)amino]ethanol] sulphate) was also obtained from AstraZeneca (Charnwood, UK) in micronised form. As a bronchodilator drug similar to salbutamol, TS is used to treat bronchoconstriction associated with asthma and

COAD in addition to other respiratory conditions. TS also exists as a white crystalline powder, freely soluble in water, and only slightly soluble in alcohol (BP, 2003). Polymorphism of TS has been observed, with two crystal forms identified, A and B. Polymorphic form may be clearly identified from x-ray powder diffraction patterns (Ahuja and Ashman, 1991). The chemical structure of TS is shown in Figure 2.2.

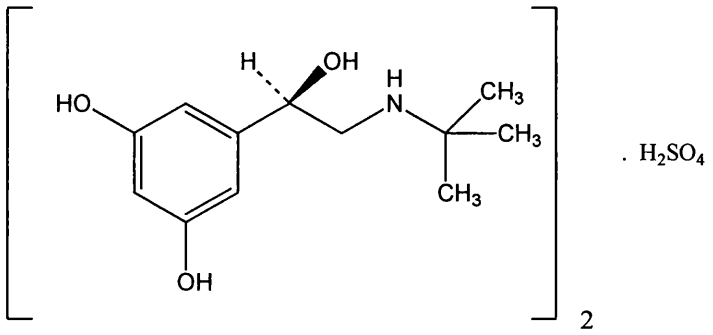

Figure 2.2 Chemical structure of the terbutaline sulphate molecule

2.1.3 SURFACTANTS

A description of the nature of polyoxyethylene-polyoxypropylene block co-polymers in addition to polyoxyethylene alkyl ether surfactants may be found in Chapter One. All surfactants used in these studies were gratefully received as donations from the manufacturers BASF, Uniqema, Condea and Sasol; a list of which may be seen in Table 2.1. Surfactants were used as received from manufacturers, and no further purification step was performed on receipt. Where possible, certificates of analysis were obtained from the supplier to ensure compliance with a specification.

2.1.4 HYDROFLUOROALKANE PROPELLANTS

A description of the nature of hydrofluoroalkane propellants (HFA) propellants may be found in Chapter One. HFA propellants 227 and 134a used in these studies were purchased from Solvay Fluor Derivative (Germany). So called "model propellant" – 2H 3H Decafluoropentane (Apollo Scientific, Lot 9956) – was obtained though AstraZeneca (Charnwood, UK).

In addition to listing details of surfactants used, Table 2.1 lists sources and batch numbers for other important materials used in these studies.

Table 2.1 Source of materials used in this research

Material	Supplier	Batch Number
Synperonic® F127	Uniqema	2804BK0518
Synperonic® F108	Uniqema	2205BS0562
Synperonic® L31	Uniqema	1204B00207
Pluronic® F38	BASF	WPTW-515B
Pluronic® L101	BASF	WPOX-519B
Pluronic® L121	BASF	WPBT-512B
Pluronic R® 31R1	BASF	WPDX-507B
Pluronic R® 10R5	BASF	WPAV-554B
Biodac 39, $C_{10}EO_3$	Condea	991028
Biodac 59, $C_{10}EO_5$	Condea	000626
Novel II $C_{12\text{-}16}EO_3$	Condea	0807-1
Novel II $C_{12\text{-}16}EO_7$	Condea	0807-2
Marlipal MG, $C_{12}EO_7$	Sasol	3083
Oleic Acid	PROLABO	L071
Span 20	Sigma	12H1331
Span 85	Sigma	39H0149
1-Bromonaphthalene	Fisher	0416672
Diiodomethane	Acros Organics	A017498001
Ethylene glycol	Sigma	032K0024
Repelcote	BDH	F60381
Sigmacote	Sigma	102K4385
PMMA	Aldrich	18226-3
Iodine	BDH	B826914113
Potassium iodide	BDH	B755157120

2.2 METHODS

2.2.1 PARTICLE SIZE ANALYSIS BY LASER LIGHT SCATTERING

2.2.1.1 INTRODUCTION

Several methods may be used to measure particle size. Among these are sedimentation rate, and sieving. The principle behind measurement of particle size by laser light diffraction is rooted in the variation of patterns of light intensity observed with different angles of diffraction. As such, light scattered by particles is measured by detectors which record an electric current proportional to the intensity of the scattered light falling on them. From the measurement, a range of particle sizes describing the sample in question will be calculated using a mathematical model to give a distribution of particle volume.

The algorithm used in laser light scattering to translate light scattering intensity to particle volume diameter involves the idea of an "equivalent sphere". An equivalent sphere is a sphere that can be described by a single linear dimension, the diameter or radius and so is a sphere equal to the particle to be measured in terms of the physical parameter that is being measured. Laser light scattering, being volume based, allows the equivalent sphere to be a sphere occupying the same volume of the particle to be measured. In other words, a sphere which when measured would produce the same scattering intensities as the particle. One important property of particles to be analysed is the refractive index (RI) of their component parts, in addition to that of the dispersing medium with reference to air. This refers to the ratio of the sine of an angle of incidence to the sine of an angle of refraction of a beam of light that passes from air into the substance (BP, 2003).

2.2.1.2 EXPERIMENTAL

A Mastersizer S (Malvern Instruments, Malvern, UK) was used for all laser light scattering measurements in this work. Light is supplied by a low power Helium-Neon laser. Light shines from the source, through two lenses which expand the beam, and a spatial filter that improves the beam's quality. The analyser beam is then presented with particles to be analysed using the sample measurement cell provided. Light diffracted by sample particles is then passed through a range lens of

focal length 300 mm, allowing measurement of particle size over the range 0.5 – 900 μm. As this lens operates at its focal position with respect to the detector, it acts as a Fourier transform lens. Scattered light is then detected by a multi-element detector, known as the "diode". Finally, data are transferred to software attached to the instrument for calculation of relative volume distribution (Malvern Diffraction Training Manual).

Sample preparation prior to particle size analysis is an important step to ensure scattered light is the result of interruption of laser light by discreet particles and not large agglomerates. In this work, particles to be analysed were suspended in a non-solvent to a concentration of approximately 0.025 % w/v. A number of drops of polyoxyethylene sorbitan monolaureate (Tween 20, Sigma) were then added and the suspension was sonicated for 1 minute to ensure adequate dispersion. Sample dispersions were then added dropwise to the measurement cell to reach a light obscuration value of between 13 and 20 %. In the case of budesonide samples, the non-solvent employed was purified water, whereas for terbutaline sulphate samples, chloroform was used. Appropriate values for the density and refractive index of the material under investigation were input, provided in Table 2.2. Measurements for each sample were carried out a total of five times, and results expressed as median volume diameter ± standard deviation, in addition to SPAN of particle size distribution (Equation 2.1), calculated by dividing the RANGE of particle volume (Equation 2.2) by volume median diameter (Elversson et al., 2003).

Table 2.2 Values for density and refractive index of budesonide and TS (All data produced in-house at AstraZeneca R&D Charnwood, UK)

	Density (g/ml)	**Refractive Index**
Budesonide	1.322	1.6
Terbutaline Sulphate	1.349	1.6

$$\textbf{SPAN} = \frac{\text{RANGE}}{\text{D(v,0.5)}} \qquad \text{(Equation 2.1)}$$

$$\textbf{RANGE} = \text{D(v, 0.9)} - \text{D(v, 0.1)} \qquad \text{(Equation 2.2)}$$

2.2.2 POWDER X-RAY DIFFRACTION

2.2.2.1 INTRODUCTION

Powder x-ray diffraction (PXRD) is a useful tool for investigation of solid-state characteristics. The structure of a crystalline material is such that it readily diffracts x-rays giving rise to a characteristic "pattern" specific to that material. Such a pattern will consist of a series of peaks, the position of which correspond to the periodic spacing of atoms in the solid state. Thus a fingerprint is provided that in turn may be used in product identification for example in the differentiation between possible polymorphic forms. Regions of disorder or amorphous material often result from processing-induced disruption of crystal structures. In contrast to the long-range three-dimensional order of molecules within a crystalline material, a disordered solid will cause an irregular diffraction of x-rays when compared with the crystalline state, resulting in the easily identifiable "halo" pattern attributable to amorphous materials. Diffraction of x-rays was first interpreted by Bragg, giving rise to the Bragg equation (Equation 2.3).

$$n\lambda = 2d \sin \theta \qquad \text{(Equation 2.3)}$$

Bragg explained the diffraction of radiation in terms of diffracted beams behaving as though reflected from planes existing throughout the crystal lattice. Briefly, the Bragg equation states that an integer multiplied by the wavelength (λ) of the radiation will equal twice the distance between planes (d) multiplied by the sine of the angle of incidence (the angle at the point of diffraction, θ), (Bryn, 1999). In addition to its use in product identification, PXRD may also be used to quantify levels of amorphous content. However, as this technique measures diffraction of x-rays by the bulk material, the limits of detection of amorphous material are generally accepted to be 5-10 % (Saleki-Gerhardt et al., 1994). Nevertheless, PXRD is long established as a convenient and simple method to distinguish between different polymorphic drug forms, in addition to identifying the presence of significant levels of amorphous material.

2.2.2.2 EXPERIMENTAL

A Philips PW3710 X-Ray Powder Diffractometer (Philips, Cambridge, UK) was used in this work. Within this apparatus, a copper anode inside the x-ray tube is bombarbed by electrons under high potential, resulting in the production of x-rays which then pass out of the tube through a beryllium window. A series of divergence slits within the goniometer then focus the diverging x-ray beam onto the flat surface of the sample. X-rays diffracted by the sample at the angle of incidence converge approximately to a straight line, and it is here that the receiving slit is situated. Before reaching the detector, the x-ray beam must pass through the receiving slit, in addition to a second parallel slit system, a scatter slit and a monochromator. The detector then delivers an output of intensity versus scan angle 2θ. In this work, approximately 50 mg of sample was loaded onto a sample holder and compressed to give a smooth surface of powder to a thickness of 2 mm. All measurements were taken at 45 kV and 30 mA. Samples were scanned over the range 5-30 °2θ, at a scan rate of 0.005 °2θ/s with a time per step of 4 seconds.

2.2.3 SCANNING ELECTRON MICROSCOPY

2.2.3.1 INTRODUCTION

Scanning Electron Microscopy (SEM) is a technique used to image the surface of very small particles. A fine beam of medium-energy electrons is used to scan the sample in a series of parallel tracks, interacting with the sample and giving rise to signal responses. These are measured and then displayed to provide an image of the sample. Images of almost three-dimensional quality may be produced as a result of the depth of field employed by the apparatus. Particles as small as 1 μm in diameter may be visualised, and therefore this technique is useful in the study of pharmaceutical powders.

2.2.3.2 EXPERIMENTAL

A small amount of the sample to be analysed is mounted onto an adhesive carbon disc attached to an SEM stub. In turn, this stub is coated with an extremely fine film of gold using a sputter coater at 30 mA (Emitech K550 Sputter Coater, Emitech, UK). Micrographs were produced using a Philips XL30 Scanning Electron

Microscope (Philips, Eindhoven, Netherlands) at the voltage displayed on individual micrographs.

2.2.4 INVERSE GAS CHROMATOGRAPHY

2.2.4.1 INTRODUCTION

Inverse gas chromatography (IGC) is increasingly used to assess the surface energy components of pharmaceutical powders. Unlike contact angle measurements, which require sample powder to be compressed to form a flat surface, and so may result in changes in the very properties under investigation, IGC allows powder samples to be measured without corrupting the solid surface giving rise to a more representative interpretation of surface characteristics. An inverted application of conventional gas chromatography, IGC involves the probing of an unknown, stationary powder surface by injecting liquids or vapours of known characterised adsorbates or probes through a glass column packed with the sample powder. Probes are carried through the column by a carrier gas, helium. In addition to providing information about the different components of powder surface energy, IGC may be used to investigate the distribution of surface energy across a powder surface in addition to powder surface area. In the pharmaceutical industry, IGC has found a role in the investigation of batch to batch variations of pharmaceutical products (Buckton, 1995b).

2.2.4.2 IGC AT INFINITE DILUTION

The essential experimental parameter measured in IGC is the net retention volume (V_N). This refers to the net volume of carrier gas required to elute the probe, and relates to the partitioning of the adsorbate between the mobile and stationary phases (Ticehurst et al., 1994). Probes are required to be injected through the column at infinite dilution, a term which refers to the very small quantity of vapour required to achieve substantially less than monolayer molecular coverage of the powder surface. The rationale behind this requirement is the knowledge that retention time is reduced following injection of increasingly larger quantities of probe vapour. This is believed to be the result of probe interaction with surface sites of lower energy. At infinite dilution however, V_N is independent of the magnitude of probe injection, and the elution peak that results is essentially Gaussian (Grimsey et al., 2002).

2.2.4.3 MEASUREMENT OF DISPERSIVE SURFACE ENERGY

Calculation of dispersive surface energy relies on relating V_N to the standard free energy of adsorption of the probe, ΔG_A, which can be obtained using Equation 2.4.

$$-\Delta G_A = -RT(\ln K \cdot p_{sg}/p) \qquad \text{(Equation 2.4)}$$

K refers to the partition coefficient of the probe between the carrier gas and the powder surface, R is the universal gas constant, T is the absolute temperature and p_{sg} and p are standard vapour state and pressure respectively (De Boer, 1968).

Once ΔG_A has been obtained, it may be related to V_N using Equation 2.5.

$$-\Delta G_A = RT\ln V_N + C \qquad \text{(Equation 2.5)}$$

Here, C is a constant, dependent on powder surface area in addition to the standard state values defined by De Boer. The free energy of adsorption of the probe ($-\Delta G_A$) can be related to the work of adhesion (W_A) of the probe on the powder surface as a first approximation according to Equation 2.6.

$$-\Delta G_A = N_a W_A + C \qquad \text{(Equation 2.6)}$$

In this equation, N is Avogadro's number while the surface area of the probe molecule is denoted by a. Using theory described by Fowkes (1964) which expressed W_A of non polar probes in terms of their surface energy shown in Equation 2.7, and combining Equations 2.5 and 2.6, a final equation expressing dispersive components of surface energy is obtained (Equation 2.8).

$$W_A = 2(\gamma_l^d \cdot \gamma_s^d)^{1/2} \qquad \text{(Equation 2.7)}$$

$$RT\ln V_N = a \cdot (\gamma_l^d)^{1/2} \cdot 2N \cdot (\gamma_s^d)^{1/2} + C \qquad \text{(Equation 2.8)}$$

The dispersive components of the surface free energies of the liquid probe and the solid powder are described by γ_l^d and γ_s^d respectively. Should a plot of $RT\ln V_N$ (free energy of adsorption of probe) versus values for dispersive components of surface free energy of the alkane probes be constructed, a straight line would be obtained. This is expected when it is considered that alkanes are non-polar molecules and thus interact with other surfaces by dispersive forces only. An example of such a plot is shown in Figure 2.3.

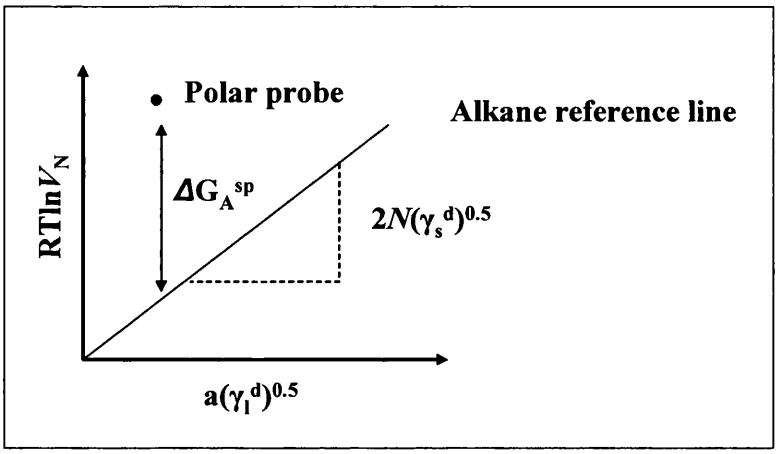

Figure 2.3 Determination of dispersive component of surface free energy

As can be seen in the above figure, the slope of the alkane reference line is equal to $2N(\gamma_s^d)^{0.5}$, and so the dispersive component of solid surface free energy may be deduced.

2.2.4.4 MEASUREMENT OF SPECIFIC POLAR INTERACTIONS

Injection of polar probes in addition to non-polar alkanes allows determination of specific polar interactions. A polar probe injected onto a non-polar surface will interact with the surface through dispersive forces alone. However, in the case of a polar surface, the probe will interact through a combination of dispersive and specific interactions. Specific interactions are those forces which occur over and above dispersive interactions, and may consist of several possible forces; dipolar, hydrogen-bond type, acid-base, metallic, magnetic and hydrophobic interactions (Papirer and Balard, 1999). Using the same plot as seen in Figure 2.3, an estimation of the specific interaction of a polar probe ($-\Delta G_A^{sp}$) can be obtained from the

displacement of the polar probe above the alkane reference line. In addition to plotting $RT\ln V_N$ vs. $a(\gamma_l^d)^{0.5}$, various physical properties may be used including boiling point, dispersive component of the heat of vaporisation of the probes and log of the saturation vapour pressure of the solutes.

Theory developed in the 1970s dictated that specific interactions constitute primarily acid – base interactions, or electron donor – electron acceptor interactions (Gutmann, 1978; Drago et al., 1971). Gutmann (1978) derived numbers to describe the electron donor or base (DN), and electron acceptor or acid (AN) properties of certain liquids. However, some modifications were proposed by Riddle and Fowkes (1989) who considered that a portion of the electron acceptor value was attributable to dispersive forces which had not been taken into consideration by Gutmann. As such a modified electron acceptor number was introduced AN*, representing purely polar interaction forces.

Once DN and AN* are known, the specific interaction of the probe with the powder surface ($-\Delta G_A^{sp}$) obtained from the plot in Figure 2.3 may be used to calculate the acid (K_A) and base (K_D) parameters of the solid surface using Equation 2.9.

$$-\Delta G_A^{sp} = K_A \cdot DN + K_D \cdot AN^* \qquad \text{(Equation 2.9)}$$

The resulting parameters provide information about the specific interactions of the surface with the polar probe. Measuring the $-\Delta G_A^{sp}$ for several polar probe vapours and rearranging Equation 2.9 allows the construction of a straight line plot of $\Delta G_A^{sp}/AN^*$ vs. DN/AN^*. From this plot values for K_A and K_D may be obtained where K_A is equal to the gradient of the line, and K_D to the intercept with the y axis.

2.2.4.5 EXPERIMENTAL

2.2.4.5.1 APPARATUS

Experiments in this work were carried out using an inverse gas chromatograph (Surface Measurement Systems Ltd., UK). This apparatus is based on the Agilent 6890 Gas Chromatograph (using the oven, detectors and valve system), and is attached to a purpose-built flow control system consisting of 6 flow controllers (MKS Instruments) responsible for regulating gas flow. In this way the flow of dry carrier gas (helium), in addition to separate helium flows saturated with water vapour and organic solvent vapours may be controlled to produce correct ratios of reference and elutant gas mixtures. Elution or "pulse" experiments were carried out in all cases during this work. As such, an automatic injection valve introduced 250 μl of each probe into the reference gas flow which was then carried through the sample column to the detectors.

The detectors attached to the gas chromatography apparatus are the thermal conductivity detector (TCD) and the flame ionisation detector (FID). The TCD is responsible for measuring the difference in heat capacity between the helium and organic vapour exiting the column compared with a pure helium flow. The FID burns any vapour exiting the column in a mixture of hydrogen and air. Any organic molecules present will ionise in the flame, and the resulting electrical current is measured. Sample columns are contained in an oven that can be maintained at between room temperature and 390 K. Chemometric software (Hewlett Packard) integrated with the purpose-written iGC Controller software (Surface Measurement Systems Ltd., UK) was used to operate the IGC remotely from a computer. Data analysis was carried out in Microsoft Excel using dedicated software analysis macros written by Surface Measurement Systems Ltd. A photograph of the assembled parts may be seen in Figure 2.4.

Figure 2.4 Photograph of IGC apparatus

2.2.4.5.2 Sample preparation

Glass columns were used to pack powders under investigation. These columns were cut to approximately 300 mm in length, and possessed an internal diameter of 3 mm. The column interior was treated before packing in order to render the glass surface inert and prevent sample powder interacting with the column. Using a method described by Mohammed and Fell (1982), columns were treated with Repelcote (BDH) and then washed thoroughly with absolute alcohol and purified water. Once treated, columns were packed with between 150 and 300 mg of sample powder. Using an automated tapping apparatus, powder was ensured to be evenly distributed throughout the column preventing the formation of any void space. Silanated glass wool (Chrompack) was used to plug both ends of the column.

2.2.4.5.3 Experimental protocol

Surface energies of powders under investigation were determined using injections of 0.04 % v/v of vapour probes. Methane was used as the non-reactive reference probe. Five alkane probes of increasing carbon chain length were used to obtain dispersive components of surface energy – hexane, heptane, octane, nonane and decane. In the case of specific interaction determinations, four polar probes were used – acetone, chloroform, ethanol and ethyl acetate. All probes were of HPLC grade. All columns were subjected to three repeats of a protocol involving injection of all probes and methane (10 injections in all). Both vapour solute bottles and sample columns were

maintained at a temperature of 303 K. Carrier gas flow rate was maintained at 10 ml/min provided probe retention time and pressure drop along the column were satisfactory.

2.2.5 FILLING OF pMDI SAMPLES

2.2.5.1 COLD FILLING

2.2.5.1.1 INTRODUCTION

Allowing filling of propellant into pMDI vials through cooling to below its boiling point and therefore permitting the pouring of liquid propellant, this method is a relatively straightforward and inexpensive means of preparing pMDI samples. However certain disadvantages are associated with cold filling, namely the need to use an open system which can lead to condensation of moisture on equipment surfaces and absorption into the pMDI, in addition to potential propellant loss as the cold propellant comes into contact with the "hot" vial (Smith, 1995).

2.2.5.1.2 EXPERIMENTAL

Cold filling was carried out using apparatus donated by AstraZeneca (Charnwood, UK). Propellant was released from the gas cylinder through a metal hose and directed through this hose coiled several times around the inside surface of a hollow reservoir vessel, the core of which was packed with dry ice. In this way propellant was cooled to a temperature below its boiling point and could be dispensed through a tap at the bottom of the vessel. A known volume of propellant was added to open, clear 15 ml polyethylene terephthalate (PET) vials (Precise Plastics, UK) pre-loaded with microparticles. Finally, a metering valve was crimped around the collar of the vial using a 3000B manual bottle crimper (AeroTech Laboratories, USA).

2.2.5.2 PRESSURE FILLING

2.2.5.2.1 INTRODUCTION

In contrast to cold-filling, pressure-filling maintains propellant in its liquid form by storage under the required pressure supplied in the form of nitrogen gas. As such, appropriately reinforced containment apparatus is needed. Also in contrast to cold-filling, valves are crimped onto pMDI containers prior to filling, and so propellant is filled through a depressed valve into a closed system. Pressure filling allows more accurate aliquots of propellant to be dispensed when compared with cold filling and this combined with the fact that it constitutes a closed system dictates it is the preferred method of the two. However, the particular apparatus required in addition to the increased safety requirements necessitated by the pressurised nature of the system contribute to a significantly more expensive initial set up and on-going operation of the apparatus.

2.2.5.2.2 EXPERIMENTAL

The majority of pressure filling employed in preparation of pMDI samples throughout this work was carried out at the School of Pharmacy using a pressure burette (AeroTech Laboratories, USA). Liquid propellant was released from the cylinder and allowed to fill the burette through a valve at the lower end of the glass reservoir. Once full, nitrogen gas was released and directed over the stored liquid propellant preventing evaporation. Depending on whether HFA 227 or HFA 134a were present, pressure in the burette was maintained at 4 bar and 5 bar respectively, consistent with the discreet differences in propellant vapour pressure. Propellant was filled into identical PET pMDI vials as mentioned above, through a continuous valve.

Preparation of pMDI samples for a study examining shake-pause-fire testing of terbutaline sulphate formulations detailed in Chapter Three, Section 3.8 was carried out at AstraZeneca (Charnwood, UK). A larger scale diaphragm operated pMDI pressure filling apparatus supplied by DH Industries (UK) was used in this work. This apparatus consists of a large volume reservoir of liquid propellant, filled using a pneumatic pump. Propellant is siphoned from the reservoir to the filling system, and dispensed into pMDI vials one at a time. Metered volume of propellant may be

altered to allow addition of up to 20 ml of propellant to each vial. As in pressure-filling carried out using a burette, valves are crimped onto vials prior to filling. This larger scale equipment has the advantage of allowing the use of metered valves. In this study, 50 µl metering valves (Valois, France) were crimped onto 11.5 ml perflouroalkane (PFA) coated aluminium canisters using an automatic crimper operated by compressed air (Pamasol P2002 Crimper, Pamasol, Switzerland).

2.2.6 OSCAR

2.2.6.1 INTRODUCTION

OSCAR (Optical Suspension Characterisation) was originally described by Jinks (1995). This apparatus is designed to measure change in light transmission with time through an upper and lower region of a pre-agitated pMDI sample contained in a transparent polyethylene terephthalate (PET) vial (Figure 2.5). A stable suspension will result in occlusion of the infra-red beam, and therefore the transmitted signal at both detection points will be low. Conversely, a suspension that has separated as a result of either creaming or sedimentation, will give rise to increasing light transmission at the lower or higher photodetector respectively (Brindley, 1999). Small local changes in light intensity are also detected, and can give rise to signal fluctuation representative of flocculation. Correlation between results obtained from the OSCAR apparatus and a commonly used analytical method (shake-pause-fire) for investigating suspension stability has previously been shown (Govind et al., 2000). Such analytical methods are often time-consuming and laborious, and therefore OSCAR has advantages over such methods in its simplicity, in addition to its non-invasive, non-destructive nature.

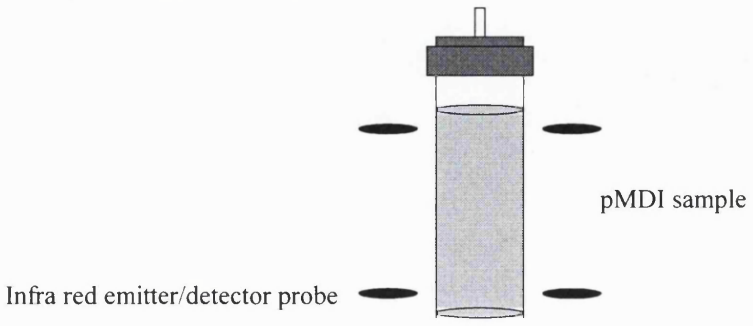

Figure 2.5 Schematic of OSCAR apparatus

2.2.6.2 EXPERIMENTAL

Calibration of photodetector sensitivity was carried out using commercially available Reagecon Turbidity NTU standards (Reagecon Diagnostics Ltd., Ireland) of similar opacity to the samples under investigation. Detector sensitivity was adjusted to obtain a reading of 5 volts, at both the upper and lower photodetector. The apparatus consists of a twin-headed test assembly, one head analysing dilute suspensions, and the other concentrated suspensions. Two matched pairs of infra-red emitter/detector probes are positioned at the upper and lower regions of the pMDI sample. Emitters employ infra-red light at a wavelength of 880 nm. These are height-adjustable to choose an optimal scanning position for each sample. A total of 1000 measurements are taken at each photodetector throughout the course of the experiment. The analogue voltage signal obtained is then converted to digital information and analysed by a computer giving a profile of light transmission through both regions of the suspension over time. Samples to be analysed were agitated prior to examination by immersion in an ultrasonic water bath for 1 minute. Vials were then immediately transferred to the test assembly and scanned over a period of three minutes.

2.2.7 TURBISCAN

2.2.7.1 INTRODUCTION

A similar principle to that described for OSCAR analysis is employed in the Turbiscan MA 2000 apparatus (Formulaction, France). Developed initially for the analysis of physical destabilisation of concentrated emulsions and suspensions, the instrument has recently been used to investigate stability of suspensions contained in pressurised systems, namely pMDI samples (Elson et al., 2003). Utilising the same principle of infra-red light detection as seen in the OSCAR apparatus, this instrument measures light transmitted through a sample. However, in contrast to the OSCAR apparatus, light back scattered by the sample is also measured. In addition, the Turbiscan instrument analyses the entire length of the sample, rather than at two discreet points as is the case with OSCAR. As such, the data obtained from Turbiscan MA 2000 can be used to construct a more comprehensive representation of suspension behaviour. A schematic of the Turbiscan apparatus is shown in Figure 2.6.

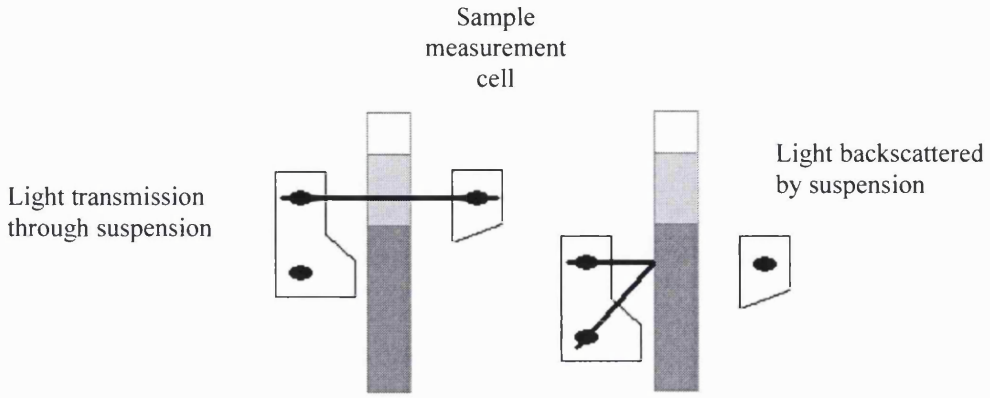

Figure 2.6 Schematic of Turbiscan apparatus (adapted from Formulaction)

2.2.7.2 EXPERIMENTAL

The apparatus itself is contained within a temperature controlled environment, maintained at 17 ° C. The reading head contained within the instrument is composed of a pulsed near-infrared light source at a wavelength of 850 nm, in addition to two synchronous detectors receiving light which passes through, and is reflected by, the sample. The reading head scans the length of the sample (up to a maximum of approximately 80 mm) and collects transmission and backscattering information every 40 μm. This analogue information is converted to a digital output using Turbisoft software provided with the apparatus and gives rise to a stability profile plotting transmitted and backscattered light flux as a percentage against sample height in mm at a given time. The apparatus is calibrated with a non-absorbing reflectance standard of polystyrene latex beads, and a transmittance standard of silicon oil (Mengual et al., 1999). The sample to be analysed is contained in a cylindrical glass measurement cell, which has been modified through the attachment of a pressurised head-set (manufactured in-house at AstraZeneca R&D Charnwood, UK) preventing evaporation of volatile propellant systems. A vacuum is applied to the Turbiscan measurement cell, allowing the transfer of samples to be analysed from their pressurised container, through a valve contained in the head set, into the glass measurement cell. All pMDI suspension samples analysed using this instrument were agitated prior to scanning in an ultrasonic bath for 1 minute. The measurement cell was then placed within the instrument, and scans carried out at defined intervals over a three minute period. The scanning protocol adopted during these studies was

as follows: a total of five scans were taken at t=0 min, t=0.5 min, t=1 min, t=2 min and finally at t=3 min. Each sample was scanned twice.

2.2.8 SPRAY DRYING

2.2.8.1 INTRODUCTION

The process of producing small droplets by liquid atomisation, followed in turn by drying of these droplets into individual particles using a drying gas is known as spray drying. Advantages of spray drying are many, and include the ease of continuous operation, production of particles of consistent quality and its suitability for use with both heat-sensitive and heat-resistant materials. One disadvantage associated with this technology is the significant cost involved with system set-up, in addition to the relatively low yields that spray-drying frequently produces (Wendel & Celik, 1997). Despite this, spray drying has become a commonly adopted process across most major industries. Examples of spray dried material found in the home include household cleaning products, foodstuffs such as instant coffee and powdered milk in addition to components of paint. In the pharmaceutical industry, spray drying is widely employed in formulation of many medicines, for example paracetamol tablets formed by the pressing of a spray dried powder (Masters, 2002).

Several steps are involved in the process of spray drying. Initially, a liquid feed (which may be a solution, suspension or emulsion) is atomised into a spray of spherical droplets, which is then exposed to a drying medium, usually air, causing moisture to evaporate from the droplets. The direction of air flow relative to the stream of atomised droplets dictates the type of equipment used. In co-current models, the flow of compressed air and atomised feed travels in the same direction; as opposed to in opposite directions seen in counter-current models. Models employing a mixture of the two principles are also available. Following particle drying, spray dried product is separated from air flow and collected, using a cyclone. Exhaust air is filtered in order to maximise yield, in addition to providing environmental protection.

Control over several experimental parameters provides scope for particle engineering allowing the production of materials of varying physicochemical characteristics.

Examples of variable parameters include concentration of feed solution/suspension, inlet and outlet air temperatures, as well as feed flow rate and air flow. In turn, manipulation of these parameters can result in varied yield, particle size, morphology and density, component concentration and product bioavailability (Wendel and Celik, 1997).

Maa et al., (1997) found particle morphology to be closely linked to drying rate, with fast drying resulting in crust formation leading to collapse, and subsequently aspheroid particles. This work also noted that surfactants added to spray drying mixtures are likely to occupy the droplet surface, driven by their attraction to air/liquid interfaces. Thus, the layer of surfactant may decrease the internal motions and surface turbulence leading to formation of a smoother particle surface at the end of the spray-drying process. Findings from several studies suggest certain consistent outcomes following manipulation of spray dryer parameters, for example the evidence of increased yield following a low feed flow rate, whereas a high flow rate is linked to increased particle size, in addition to a higher residual moisture content of the final particle (Billon et al., 2000; Esposito et al., 2000).

2.2.8.2 EXPERIMENTAL

The spray-drying apparatus used in this work, a Buchi Mini Spray Dryer 191 (Buchi, Switzerland), is an example of a small scale system used to produce experimental batches of spray dried product. A schematic of this model is shown overleaf in Figure 2.7. This apparatus employs a co-current flow system using compressed air as a drying medium for a liquid feed introduced to the drying medium by way of a peristaltic pump. Parameters that may be manipulated on this model include feed flow rate, inlet air temperature, air flow and aspirator speed. Outlet temperature may not be independently varied, and is therefore linked to inlet temperature and feed flow rate, with an increased outlet temperature resulting from either an increase in inlet temperature or a reduction in feed flow rate.

Development of the parameters employed in this study to produce spray dried budesonide-surfactant particles is described fully in the experimental protocols and results of Chapter Four.

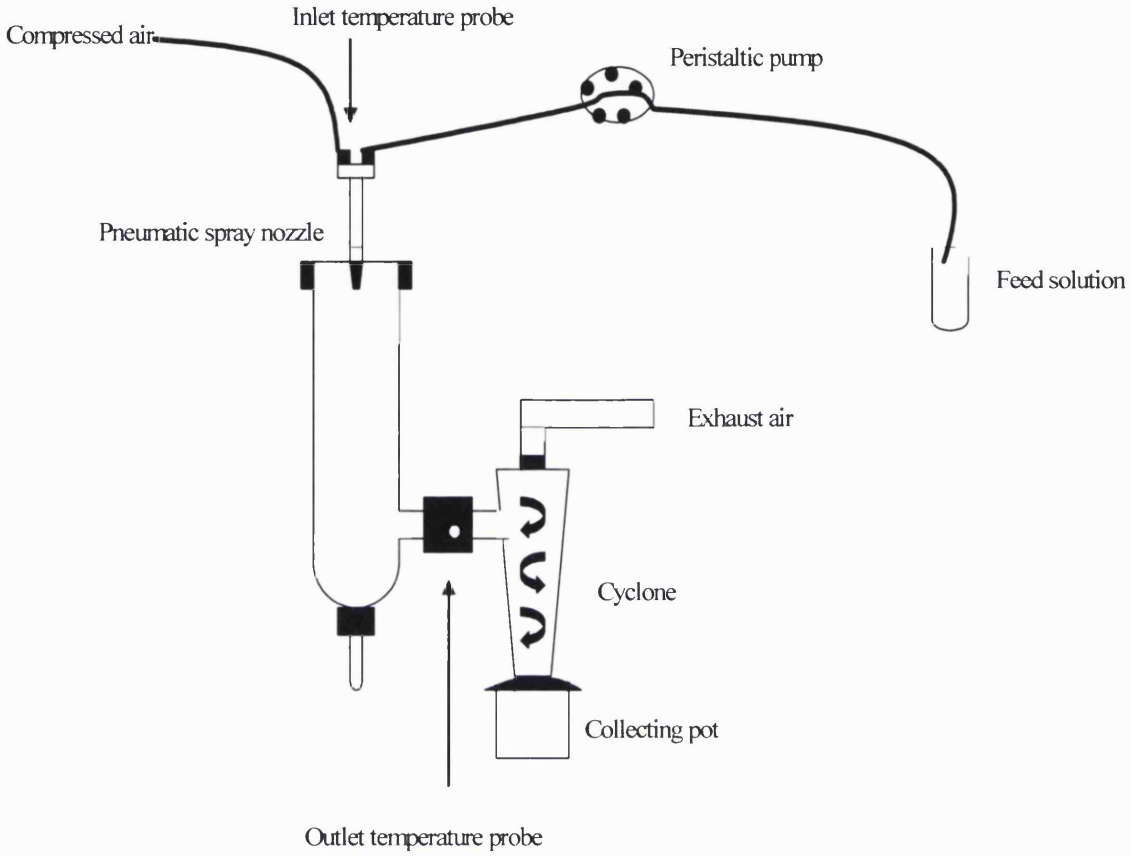

Figure 2.7 Schematic of Buchi Mini Spray Dryer 191

2.2.9 SURFACE TENSION AND DYNAMIC CONTACT ANGLE MEASUREMENTS

2.2.9.1 INTRODUCTION

One commonly used technique to measure liquid surface tension and the contact angle formed on solid surfaces is that of the Wilhelmy plate. In the attachment method, a thin glass plate is held above the test liquid at the beginning of an experiment. The test liquid is then raised to meet the plate at a set rate to the point where the plate has been immersed in the liquid. The liquid is then lowered away from the plate causing the plate to exit the liquid. The force registered by a balance at the point when the plate is wetted by the liquid, divided by the perimeter of the plate surface in contact with the liquid is equal to the liquid surface tension. Using

this surface tension value in future experiments, the value of a contact angle formed by a liquid on the surface of the plate may be calculated. Force measured upon immersion and emersion of the plate gives an advancing and receding contact angle respectively, being equal to cos θ, where θ is the contact angle (Good, 1993). For a smooth, flat and homogenous surface, advancing and receding angles should be equal. Any deviation from this is known as contact angle hysteresis and may be attributable to either contaminants on the plate or an interaction between the liquid and plate surface upon immersion, altering the plate surface.

2.2.9.2 EXPERIMENTAL

All surface tension and contact angle measurements made in these studies were performed on a Dynamic Contact Analyser (DCA; Cahn DCA-312, Cahn Instruments USA), an apparatus based on the Wilhelmy plate technique. The apparatus consists of an in-line stirrup gripping a thin glass slide suspended from an electro-balance over a motorised platform housing a beaker containing the test liquid. A water circulator (Gallenkamp) maintains system temperature at 25 °C. Platform height is controlled by a computer, and is elevated and lowered to a depth of 5 mm as directed to facilitate immersion and emersion of the slide in and out of the test liquid. Platform speed is programmed at 151.7 μm/s. As such, the DCA apparatus utilises the attachment method of the Wilhelmy plate technique. Force data were collected at regular intervals as a function of platform height, and the resulting force-depth isotherms were used to calculate liquid surface tension. Equation 2.10 describes the equation used by integrated software to calculate surface tension and contact angle values. Here F corresponds to the sample force at zero immersion depth, measured by the balance (mg), p is equal to the perimeter of the glass slide (cm), and Cos θ, as mentioned previously, is the contact angle between the glass slide and the liquid. Finally 0.981 is a conversion factor to allow calculation of results in dynes (Cahn DCA 213 Manual).

$$F = \frac{\gamma_{LV} \times p \times \mathrm{Cos}\theta}{0.981} \qquad \text{(Equation 2.10)}$$

In all experiments carried out, glass slides (BDH, 22X22 μm) were initially cleaned of oily deposits by suspending in a Bunsen flame. Surface tension and contact angle

measurements were calculated as the average of five determinations. Receding contact angle data were used in calculation of surface tension values, whereas in the case of contact angle determinations, advancing contact angle data was used.

2.2.10 NEAR INFRA-RED SPECTROSCOPY

2.2.10.1 INTRODUCTION

Near infra-red spectroscopy (NIRS) is often used as an identification tool to recognise organic structures. The spectra which are obtained cover the approximate wavelength region of 780 nm to 2500 nm, or from the red end of the visible region, to the beginning of the mid infra-red (IR) region. Absorbencies detected in spectra are associated with molecular vibrations caused by chemical bonds bending or stretching, and in the case of NIRS are restricted to C-H, N-H, O-H and S-H resonances. While the majority of molecular vibrations show a fundamental frequency in the mid IR region, first and second overtones of these vibrations are observed as absorbencies in the NIR region. It is these overtones that provide the basis of NIRS as an analytical technique. The analysis of spectra is based on the absorbance peak wavelength and amplitude with specific resonances occurring at known wavelengths (e.g. the O-H bond of water produces a characteristic absorbance peak at between 1900 and 1940 nm, the precise wavelength relating to the nature of the water). Advantages of this technique are its rapid and non-destructive nature, with no sample preparation generally required. NIR spectra may contain information about the physical properties of a sample, including particle size, compaction density and the presence of different polymorphs. Mathematical treatment of spectral data by obtaining the second derivative may minimise influence of these properties in the pursuit of sample comparison or identification (Jee, 2003). In addition to its use as a qualitative method, NIRS may also be used to quantify individual components in a mixture. Extensive calibration studies are necessary to facilitate use of NIRS in quantitative analysis.

2.2.10.2 EXPERIMENTAL

All NIR spectra obtained in these studies were taken using a Random Content Sampler (FOSS NIRSystems, Denmark). A tungsten-halogen lamp contained within this instrument provides an energy source which directs a light through a holographic grating. This produces the required wavelength range of 1100 to 2500 nm. Upon contact with a sample, light is diffusely reflected and subsequently measured by a lead sulphide detector. System suitability tests were carried out prior to each use of the instrument, assessing levels of photometric noise and wavelength accuracy. The instrument was programmed to make a total of 64 measurements between 1100-2500 nm. A reference spectrum was obtained using a white reflective ceramic tile standard. Radiation reflected by the sample was then measured as a function of wavelength and with respect to reflectance of the standard. Spectra were analysed using Vision software 2.20 (FOSS NIRSystems, Denmark).

CHAPTER THREE

PREPARATION AND CHARACTERISATION OF TERBUTALINE SULPHATE – SURFACTANT MICROPARTICLES

3 PREPARATION AND CHARACTERISATION OF TERBUTALINE SULPHATE – SURFACTANT MICROPARTICLES

PART A: PARTICLE ENGINEERING

3.1 INTRODUCTION

A full description of challenges presented to the pharmaceutical industry as a result of the need to substitute HFA propellants for CFCs has been detailed in Chapter One. The challenge of most relevance to this research is the failure of surfactants of choice in CFC formulations (e.g. oleic acid, span 85 and lecithin) to dissolve in HFA propellants. Searches for alternate surfactants with a high solubility in HFAs have produced suggested alternatives such as oligolactic acid based excipients, exhibiting solubilities of up to more than 5 % w/w in both HFA 227 and HFA 134a (Stefely et al., 2000). Other compounds including various fluorinated acids have been screened as potential pMDI suspension stabilisers, and while these compounds have been shown to dissolve in HFAs their efficiency as suspending agents has yet to be assessed (Dickinson et al., 2000). However, the intention of this research is to explore the possibility of using surfactants with a low solubility in HFA propellants as pMDI suspension stabilisers. As such, a range of surfactants has been examined here as potential stabilisers. Surfactant solubility in HFA propellants has been investigated to ensure a reasoned selection of surfactants based on their low solubility in these propellants. In turn, selected surfactants have been adsorbed onto the surface of a model hydrophilic drug terbutaline sulphate (TS). Effect of surfactant adsorption on powder properties has then been examined using a number of characterisation techniques. In this way it is hoped to modify the drug surface sufficiently in order to confer stabilising properties on a suspension of drug-surfactant microparticles in HFA, without compromising microparticle properties essential in inhalation formulation such as particle size.

3.2 EXPERIMENTAL PROTOCOL

3.2.1 SURFACTANT SOLUBILITY TESTS IN HFA PROPELLANTS

In order to investigate the solubility of surfactants to be employed in this research in HFA propellants, a visual assessment of solubility in both HFA 134a and HFA 227 was carried out. As such, an increasing mass of each surfactant was added to transparent PET vials (Precise Plastics, UK) prior to filling with a known mass of propellant. Propellant was transferred to sample vials through continuous valves (Valois) by pressure-filling, previously described in Chapter Two. Initial tests were carried out at a system concentration of 0.01 % w/w. Samples were visually assessed under magnification for surfactant dissolution in the propellant phase, deemed to have occurred when no evidence of two separate phases was visible. In the case of surfactant dissolution, further samples were prepared containing an increased concentration of surfactant. This process was repeated until the system concentration was such that two separate phases of surfactant and propellant were evident. To confirm suspected phase separation, a final sample was prepared at a higher surfactant concentration to ensure the limit of surfactant solubility had been estimated correctly.

A range of hydrophilic and hydrophobic non-ionic surfactants were used in the experiments described in this Chapter. A list of these surfactants may be found in Chapter Two, Table 2.1. For convenience, the names of some surfactants have been shortened when referred to in the results sections of this and subsequent chapters. Accordingly, the surfactants Biodac 39, Biodac 59, Novel II $C_{12\text{-}16}EO_3$, Novel II $C_{12\text{-}16}$ EO_7 and Marlipal MG $C_{12}EO_7$ listed in Table 2.1 will hereafter be referred to as B39, B59, 1216CO3, 1216CO7 and MMG.

3.2.2 ADSORPTION OF SURFACTANTS ONTO MICRONISED TERBUTALINE SULPHATE

Surfactant adsorption on to the surface of micronised TS was carried out according to methods previously described by Carthew (1999) and Columbano (2001), whereby micronised drug was incubated with a surfactant solution in a solvent that was in fact a non-solvent for the drug in question. In line with these protocols, 0.2 g of micronised TS was incubated with a surfactant solution in dichloromethane. Surfactant solutions in dichloromethane were prepared at a concentration of 200

mg/L. Incubation was carried out in a shaking water bath (Grant), maintained at a temperature of 25 °C for a period of three hours. Drug-surfactant particles were subsequently recovered following filtration under vacuum using a Buchner funnel, and filter paper size No. 2 (Whatman). Filter papers were then allowed to dry naturally at room temperature overnight, and drug-surfactant particles collected the following day.

3.2.3 POLOXAMER ADSORPTION ULTRA VIOLET SPECTROSCOPY ASSAY

In the case of poloxamer surfactants, an attempt was made to assess the amount of surfactant adsorbing on to the drug surface. The protocol described by Baleaux (1972) was adopted, with some modification. The original publication describes preparation of an aqueous indicator solution consisting of 1 g of iodine, in addition to 2 g of potassium iodide made up to 100 ml volume with purified water. Surfactant solutions are prepared at decreasing concentrations, 10 ml of which is added to 0.25 ml of indicator solution. Absorbance in the visible region at 500 nm was then measured in order to construct concentration calibration curves from which unknown concentrations may be subsequently deduced. Accordingly, in this research an indicator solution was prepared containing the prescribed masses of iodine and potassium iodide, but substituting dichloromethane for purified water. It was intended to construct calibration curves in dichloromethane, representative of the experimental conditions imposed in surfactant adsorption to TS. However, due to incomplete dissolution of potassium iodide in dichloromethane this proved impossible. Instead, an attempt was made to assay previously prepared TS-surfactant particles for their poloxamer content by dissolving particles in purified water at a known concentration and subsequently assaying according to the Baleaux protocol. As such, surfactant concentration would be assessed against calibration curves for poloxamer concentration in purified water. Unfortunately this also proved impossible, as it was discovered that the presence of TS corrupted the colour of the indicator solution and so rendered it useless. It was consequently decided to search for an alternate method of assessing the extent of surfactant adsorption.

3.2.4 TERBUTALINE SULPHATE ULTRA VIOLET SPECTROSCOPY ASSAY

A further attempt was made to assess the mass of surfactant adsorbing on to the surface of TS, indirectly in this case, by assaying for TS concentration. Following a

UV assay for TS previously described by Ahuja and Ashman (1991) where TS in 0.1 N HCl exhibited a maximum absorbance at 276 nm, a calibration curve for TS concentration in 0.1 N HCl was constructed. Solutions of TS were prepared at decreasing concentrations of 0.01%, 0.008%, 0.006%, 0.004%, and 0.002 % w/w. Absorbance was measured at 276 nm in an Ultrospec 2000 UV/VIS Spectrophotometer (Pharmacia Biotech, UK). All measurements were repeated three times. Subsequent to construction of a calibration curve, a known mass of TS-surfactant particles was dissolved in 0.1 N HCl and assayed for their TS content.

3.2.5 PARTICLE MORPHOLOGY INVESTIGATION BY SCANNING ELECTRON MICROSCOPY

Morphology of drug-surfactant particles was assessed by SEM according to the method detailed in Chapter Two. In this way it was hoped to identify any changes in particle morphology resulting from surfactant adsorption or the adsorption process.

3.2.6 PARTICLE SIZE ANALYSIS BY LASER LIGHT SCATTERING

Particle size of micronised TS in addition to TS-surfactant particles was examined by laser light scattering in order to investigate the effect of surfactant adsorption on particle size. Chloroform was employed as the non-solvent in which particle size was assessed. Suspensions of TS particles were prepared at an approximate concentration of 0.005 % w/v. Suspensions were sonicated and particle size measured until further sonication failed to reduce particle size. In this way, it was ensured that primary particle size was measured, and not that of any aggregates.

3.2.7 PHYSICAL STATE INVESTIGATION BY POWDER X-RAY DIFFRACTION

Drug-surfactant particles were analysed by PXRD in order to assess whether the adsorption of surfactant or the adsorption process itself altered the physical state of micronised TS. Powder samples were scanned according to the protocol described in Chapter Two.

3.2.8 SURFACE ENERGY ANALYSIS BY INVERSE GAS CHROMATOGRAPHY

As a final characterisation of drug-surfactant particles, effect of adsorption of surfactant on to the surface of micronised TS on powder surface energy was assessed by IGC. This technique has been previously described in Chapter Two.

3.3 RESULTS AND DISCUSSION

3.3.1 SURFACTANT SOLUBILITY IN HFA PROPELLANTS

The following two tables describe the solubility of surfactants used in this research in HFA propellants 134a (Table 3.1) and 227 (Table 3.2). Evidence of dissolution at a particular concentration is marked with a "+", whereas a "–" indicates insolubility. Some surfactants are listed according to their abbreviated names, a full description of which may be found in Chapter Two.

Table 3.1 Surfactant solubility at increasing concentrations in HFA 134a, with observed solubility marked as "+", and insolubility as "–".

Surfactant	0.01 % w/w	0.02 % w/w	0.05 % w/w	0.08 % w/w	0.1 % w/w
F127	—	—	—	—	—
F108	—	—	—	—	—
L31	+	+	—	—	—
31R1	+	+	—	—	—
L101	+	—	—	—	—
L121	+	—	—	—	—
B39	+	+	+	—	—
B59	+	—	—	—	—
1216CO-3	+	+	+	—	—
1216CO-7	+	—	—	—	—
MMG	+	+	+	—	—
Span 20	—	—	—	—	—
Span 85	+	—	—	—	—
Oleic Acid	—	—	—	—	—

Table 3.2 Surfactant solubility at increasing concentrations in HFA 227

Surfactant	0.01 % w/w	0.02 % w/w	0.05 % w/w	0.08 % w/w	0.1 % w/w
F127	—	—	—	—	—
F108	—	—	—	—	—
L31	+	+	—	—	—
31R1	+	+	+	—	—
L101	+	+	—	—	—
L121	+	+	—	—	—
B39	+	+	+	—	—
B59	+	—	—	—	—
1216CO-3	+	+	+	—	—
1216CO-7	+	—	—	—	—
MMG	+	+	—	—	—
Span 20	—	—	—	—	—
Span 85	—	—	—	—	—
Oleic Acid	+	—	—	—	—

Results from solubility tests have been collated and presented as limits of surfactant solubility in both propellants. These may be observed in Table 3.3.

Table 3.3 Summary of findings of surfactant solubility tests in both propellants

Surfactant	Solubility in HFA 134a (% w/w)	Solubility in HFA 227 (% w/w)
F127	< 0.01	< 0.01
F108	< 0.01	< 0.01
L31	< 0.08	< 0.08
31R1	< 0.08	< 0.08
L101	< 0.05	< 0.05
L121	< 0.05	< 0.05
B39	< 0.08	< 0.08
B59	< 0.02	< 0.02
1216CO-3	< 0.08	< 0.08
1216CO-7	< 0.05	< 0.08
MMG	< 0.08	< 0.08
Span 20	< 0.01	< 0.01
Span 85	< 0.02	< 0.01
Oleic Acid	< 0.01	< 0.02

The above results from solubility assessments confirm that surfactants selected for use in this research do indeed exhibit a low solubility in both HFA propellants. Conventional surfactants in CFC propellants, such as oleic acid and Span 85 have been shown previously to be miscible in all proportions with CFC-11, CFC-12 and CFC-114 (Blondino and Byron, 1998). In contrast, the evidence in Table 3.3 of an upper limit of solubility equalling 0.08 % w/w surfactant concentration in HFAs for the surfactants examined here constitutes a major difference in excipient solubility compared with conventional CFC pMDI formulations.

3.3.2 UV ASSAY CALIBRATION CURVE FOR TERBUTALINE SULPHATE CONCENTRATION IN 0.1 N HCL

A calibration curve plotting TS concentration in 0.1 N HCl versus UV absorbance at 276 nm may be seen in Figure 3.1. The magnitude of standard deviation values was such that they were indistinguishable on the axes scale employed.

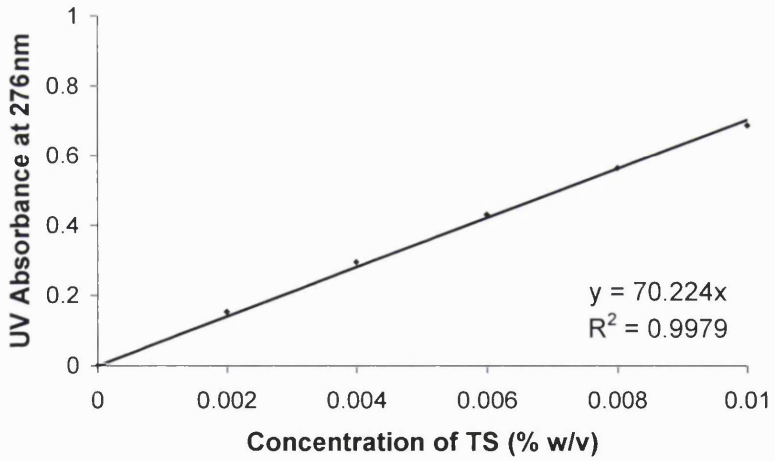

Figure 3.1 UV assay calibration curve for TS concentration in 0.1 N HCl

Attempts to deduce the mass of surfactant present in TS-surfactant microparticles by assaying for TS in these microparticles followed by subtraction from an expected absorbance taken from the calibration curve in Figure 3.1 proved difficult. Absorbance values for TS-surfactant microparticles were found to be consistently similar to those expected from the calibration curve, across the range of surfactant formulations investigated. Results for UV absorbances of prepared formulations are consequently not shown. As such, two possibilities emerged. Firstly, that no

surfactant adsorption had taken place over the three hour period of incubation imposed on micronised TS, resulting in the identical UV absorbances measured for TS-surfactant microparticles. Secondly, it is possible that the level of surfactant adsorbed on to the drug surface is outside the limit of detection of this method. The UV/Vis spectrophotometer employed in these measurements provided absorbance values to three decimal places, and therefore would not be sensitive enough to detect differences in TS mass accurately at the level of milligrams. Results previously published by Carthew (1999), Ali (2000) and Columbano (2000) confirm the possibility of very small masses of surfactant adsorbing on to a drug surface, sufficient to alter surface properties. Adsorption studies of various poloxamer surfactants onto the surface of the two hydrophobic drugs ibuprofen and ketoprofen revealed the extent of adsorption from an aqueous surfactant solution at a similar concentration to that used in this work to be in the range of 5-10 mg/g. Experiments were conducted at increasing temperatures, including 25 °C, but incubation was allowed to continue overnight, rather than the three hour period adopted in this study (Ali, 2000). Similar work involving the adsorption of poloxamer surfactants to the surface of the hydrophobic drug atovaquone found adsorption to be in the region of 3 mg/g when 0.2 g of drug was incubated with 20ml of a solution of the poloxamer surfactant F108 at a concentration of 120 mg/L (Carthew, 1996). However, both adorption experiments described above were conducted in aqueous systems, and involved adsorption to a hydrophobic surface. The application of conclusions drawn from the studies of Carthew and Ali to adsorption studies undertaken here is therefore questionable. Surfactant behaviour in organic solvents is not well understood, the volatility of such systems complicating the measurement of small concentration changes. In a similar adsorption protocol to that described in this work, Columbano (2000) investigated the adsorption of an alkylpolyglycoside surfactant to the surface of the hydrophilic drug salbutamol sulphate from a solution in dichloromethane. While the amount of surfactant adsorbed to the drug surface was not measured, a three hour period of incubation with surfactant was sufficient to result in a modification to drug surface energy when compared with a control.

Despite the significant differences in system parameters between the previously published work described above and studies recorded here, the supposition that despite the lack of reduction in UV absorbance for TS-surfactant microparticles,

some surfactant adsorption may have taken place is permitted. Due to time constraints, further attempts to measure the mass of surfactant adsorbed on to the surface of TS directly were not pursued. It was instead hoped that further characterisation of TS-surfactant particles would provide indirect evidence of successful surfactant adsorption by revealing characteristic changes in physical properties such as powder surface energy.

Adsorption of non-ionic surfactant species at various interfaces has been extensively studied. Of particular relevance to this work, the adsorption characteristics of PEO-PPO-PEO block copolymer surfactants in aqueous systems has been investigated by several groups giving rise to a sound theory of the mechanics of surfactant adsorption. Studies on the adsorption characteristics of poloxamers on polystyrene latex suggested the surfactant molecule associating with a substrate surface in a combination of loops or chains (Kayes and Rawlins, 1979). Further work supported this hypothesis and described adsorption in terms of thin POP loops or trains attached to the substrate surface, with longer POE chains extending from the surface (Baker and Berg, 1988). Numerous attempts to measure critical micelle concentrations (CMC) for poloxamer surfactants have also been carried out. While it was initially unclear whether these molecules aggregated in a conventional manner to form micelles, several studies have since published CMC data for a range of poloxamer molecules (e.g. Alexandridis et al., (1994)). The concentration of surfactant solutions employed in this work of 0.02 % w/v may be compared with published data in Table 3.4. Of interest are the values pertaining to F108 and F127, both of which have been used in this research. Values for other poloxamers have been shown to demonstrate the breadth of CMCs for these polymers. CMC values listed were obtained at 25 °C, therefore mimicking temperature conditions imposed in this work. Even considering the existence of such a broad spectrum of CMCs, it is clear that the lowest CMC value reported is in fact higher than the surfactant concentration used in adsorption studies on TS in this work. As such, it has been assumed that at the surfactant concentration of 0.02 % w/v used in this research, no aggregates of poloxamer molecules are present, and surfactants exist as monomers in solution.

Table 3.4 CMC values for some poloxamer surfactants (Alexandridis et al., 1994)

Polymer	CMC at 25 °C (% w/v)
P84	2.6
P85	4.0
P103	0.07
P104	0.3
P105	0.3
P123	0.03
F108	**4.5**
F127	**0.7**

3.3.3 PARTICLE MORPHOLOGY INVESTIGATIONS BY SEM

Some results from particle morphology investigations are shown in the following figures. It can be observed from Figures 3.6 and 3.7 that the incubation period necessary for surfactant adsorption has not altered the morphology of micronised TS. The powder has retained an irregular shape with an apparently rough surface. The powder also appears to be substantially aggregated; however primary particle size is seen to be within the limits of that prescribed for inhaled drug delivery of 2-5 μm (Aersol Consensus Statement, 1991). Subsequent figures reveal the morphology of TS-surfactant microparticles following the adsorption process and particle recovery. Making the assumption that surfactant adsorption has indeed taken place, again it seems that microparticle morphology and size have not been affected.

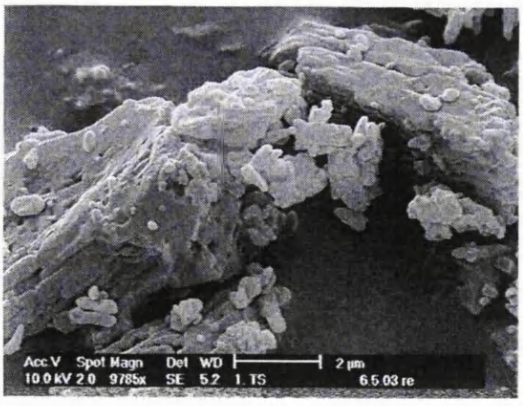

Figure 3.2 SEM of micronised TS

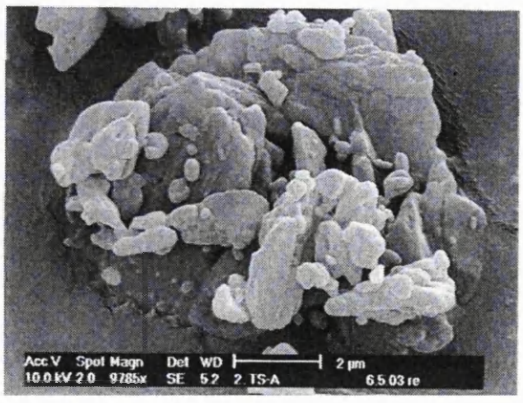

Figure 3.3 SEM of micronised TS control

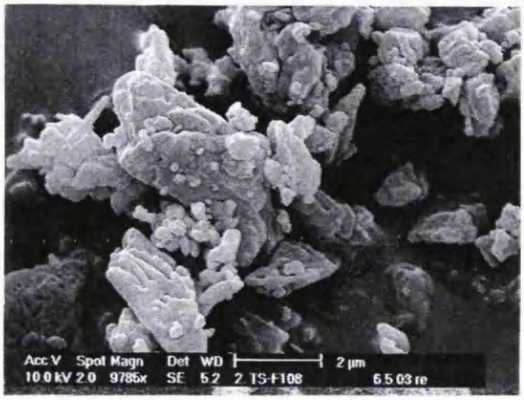

Figure 3.4 SEM of TS following adsoption of the poloxamer surfactant F108

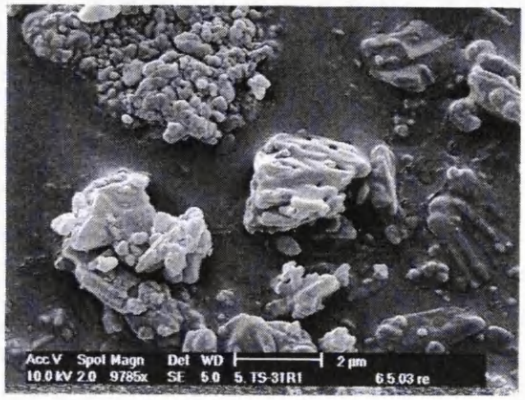

Figure 3.5 SEM of TS following adsorption of the poloxamer surfactant 31R1

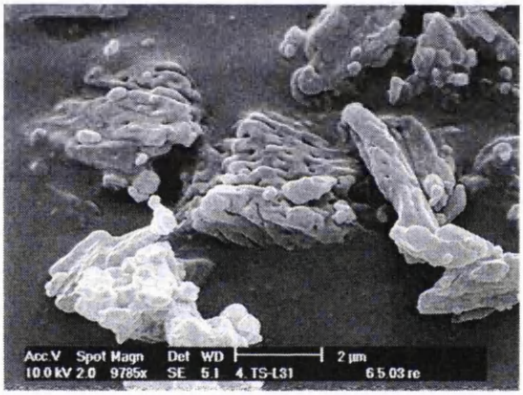

Figure 3.6 SEM of TS following adsorption of the poloxamer surfactant L31

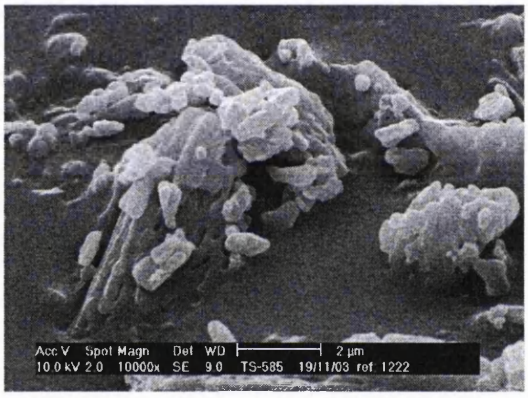

Figure 3.7 SEM of TS following adsorption of the surfactant Span 85

One exception can be identified in Figure 3.5. This SEM shows the surface of TS-31R1 microparticles. It appears from the micrograph that some areas of powder surface have altered from irregular polydisperse aggregates to a mass of small particles, resembling an aggregate with a grainy texture. This was the only formulation to show an alteration in surface appearance following surfactant adsorption. The nature of the particular surfactant contained in this formulation is slightly different to others employed in this research in that it is a reverse poloxamer, and therefore possesses two hydrophobic moieties on either side of a hydrophilic core. It is unlikely that this would result in the observed alteration in morphology which can be more likely ascribed to a rogue contaminant in the batch of TS tested,

or corruption of the sample prepared for SEM analysis. However, analysis of this sample was not repeated and so this cannot be confirmed.

3.3.4 PARTICLE SIZE ANALYSIS BY LASER LIGHT SCATTERING

Table 3.5 contains results from particle size analysis by laser light scattering of all TS-surfactant formulations prepared. Span of microparticles has been previously defined in Chapter Two and gives an indication of the particle size distribution within the powder bulk. Initial particle size of micronised TS was found to be 5.07 (±0.57) μm in diameter, somewhat unexpected as a batch of micronised material for inhalation would more usually possess a mean volume diameter of 2-3 μm. Considering the initial size of drug material, adsorption of surfactant or the adsorption process does not appear to have increased particle size, with all formulations exhibiting a similar size to the parent particle following the adsorption process. Studies conducted into the adsorption characteristics of poloxamer molecules have measured adsorbed layer thickness on substrate molecules. Results have shown that the adsorption of poloxamers increases particle radius by up to 20 nm in length (Baker and Berg, 1988; Kostarelos et al., 1998). Given that the sensitivity of the apparatus used here is limited to micrometer-sized particles, it is therefore unsurprising that mean volume diameter of TS-surfactant microparticles is not seen to have changed following the adsorption process.

Table 3.5 Particle size analysis by laser light scattering

Formulation	Mean Volume Diameter (µm ± SD, n=5)	Span (co-efficient of spread)
Micronised TS	5.07 (0.57)	2.09
TS Control	5.72 (0.57)	3.68
TS-F127	5.30 (0.14)	2.45
TS-F108	5.56 (0.75)	6.23
TS-L31	5.57 (0.41)	3.43
TS-L101	5.82 (0.52)	4.03
TS-L121	5.31 (0.34)	3.97
TS-31R1	5.07 (0.20)	2.29
TS-B39	4.89 (0.54)	4.45
TS-B59	5.41 (0.48)	3.07
TS-1216CO3	5.23 (0.65)	2.89
TS-1216CO7	5.91 (0.54)	4.01
TS-MMG	5.45 (0.41)	3.65
TS-Span 20	4.91 (0.63)	4.21
TS-Span 85	5.91 (0.32)	3.71
TS-Oleic Acid	5.11 (0.45)	2.67

3.3.5 PHYSICAL STATE INVESTIGATION BY POWDER X-RAY DIFFRACTION

Results from PXRD studies revealed the micronised TS used in this work to have a crystalline structure. Figure 3.8 shows patterns for micronised TS in addition to a TS control and it can be seen that the adsorption process has not altered the drug physical form present.

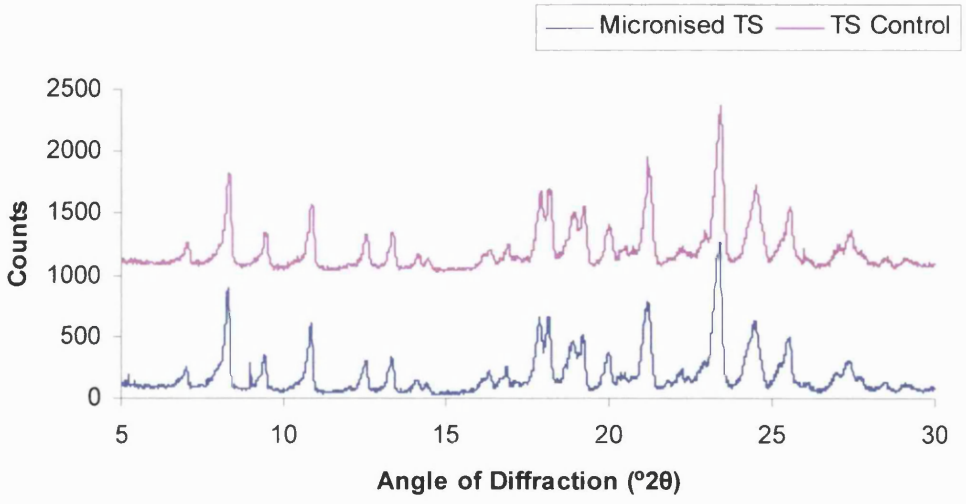

Figure 3.8 X-ray diffraction pattern comparing original micronised TS with TS following incubation in DCM

It is clear from the x-ray diffraction patterns observed in Figure 3.8, that the crystal structure of TS remains unaltered by the incubation technique used to adsorb surfactant on to the drug surface. Retained crystallinity may be considered an advantage in the preparation of future pMDI suspension formulations. The propensity of amorphous structures to behave unpredictably in formulations has been well documented. Areas of disorder are known to exist in a higher energy state and are thus thermodynamically unstable. Amorphous regions tend to incorporate molecules of water within their disordered molecular structure, which may cause both chemical and physical transitions to occur. However, the limit of detection of amorphous content using PXRD is generally accepted to be 5 %. As such, the possibility that small regions of amorphous material are present within the TS samples examined cannot be ruled out. What is clear is that the process of incubation of micronised TS in DCM has not altered crystalline structure. Two polymorphic forms of TS are known to exist, forms A and B (Ahuja and Ashman, 1991). Investigation of peak position in samples shown in Figure 3.8 against that described by Ahuja and Ashman revealed a structure closest to the B form, however an exact match was not obtained. This is likely due to the fact that the process involved in TS manufacture produces a sample containing both polymorphic forms of TS crystal structure.

X-ray patterns for TS-surfactant formulations all exhibited an identical pattern to that of micronised TS. As such, surfactant adsorption would not appear to have altered the physical form of the substrate molecule. Patterns for all TS-surfactant formulations obtained by PXRD were identical. Some of these may be seen in Figure 3.9.

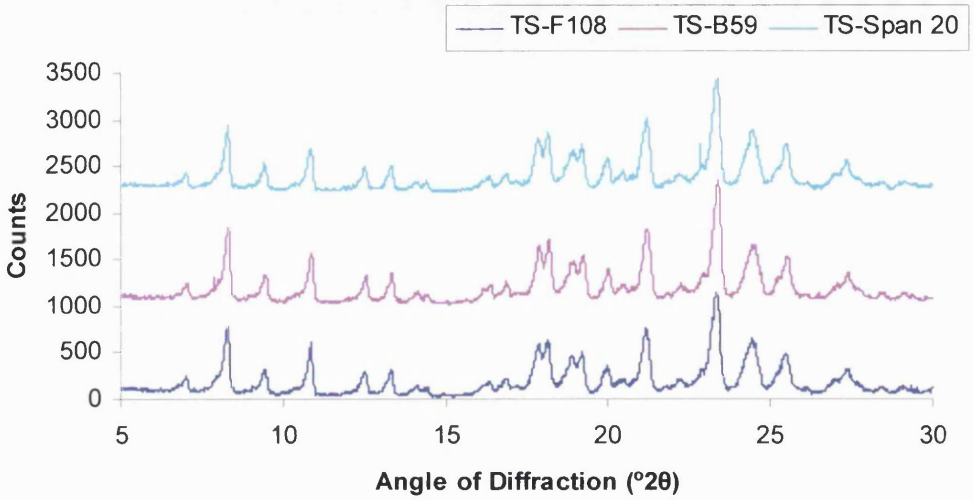

Figure 3.9 X-ray diffraction pattern for various TS-surfactant formulations

3.3.6 SUFACE ENERGY ANALYSIS BY INVERSE GAS CHROMATOGRAPHY

As discussed in Chapter Two, powder surface energy components may be deduced in part from a plot of $RT\ln V_N$ vs. $a(\gamma_l^d)^{0.5}$. Figure 3.10 shows such a plot for a sample of micronised TS prior to any manipulation. As expected, dispersive components of surface energy for alkane probes form a straight line, from which the dispersive component of powder surface energy may be deduced. Also in line with expectation is the location of polar probe data points, above the alkane line. The distance of each point from the alkane line corresponds to the specific free energy of adsorption of the polar probe on the powder surface (ΔG_A^{sp}).

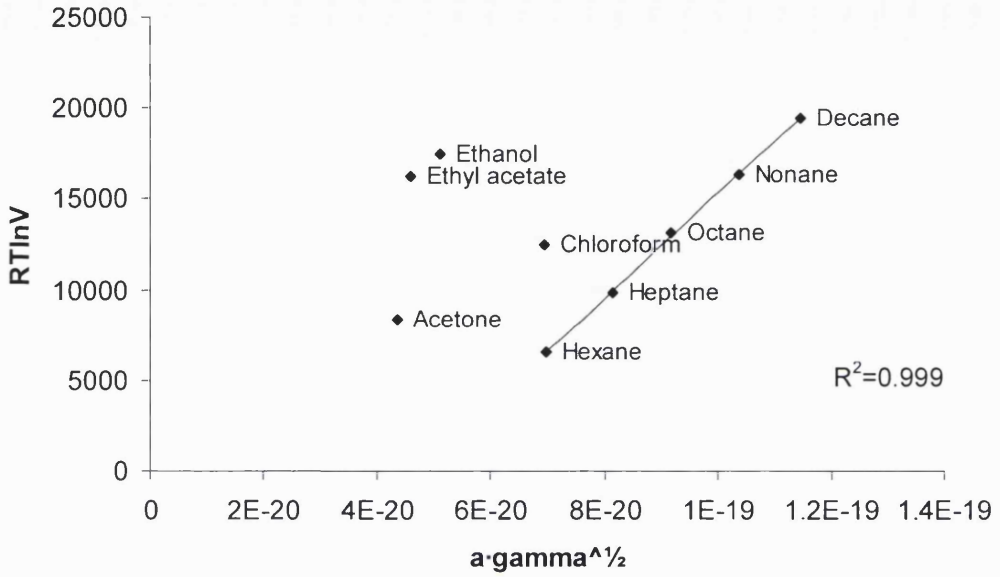

Figure 3.10 Plot of RTlnV vs. $a(\gamma_l^d)^{0.5}$ for micronised TS

Specific free energies of adsorption, or displacement of polar probes from the alkane line are shown in Table 3.6.

Table 3.6 Specific free energies of adsorption of polar probes for micronised TS

Probe Molecule	**ΔG_A^{sp} (mJ/m^2, n=3 ± SD)**
Acetone	9227.72 (17.59)
Chloroform	5967.58 (23.24)
Ethanol	16204.58 (31.37)
Ethyl acetate	16438.32 (29.22)

Using the values in Table 3.6, and reference values for AN* and DN of polar probe molecules in question, Equation 2.9 (Chapter Two) was used to calculate K_A and K_D, the acid-base components of powder surface energy for micronised TS, listed in Table 3.7.

Table 3.7 Acid-base components of powder surface energy for micronised TS

	K_A	**K_D**	**K_D/K_A**
Micronised TS	200.31 (0.32)	26.76 (0.41)	0.133

Powder surface energy components of all formulations were calculated similarly to that of micronised TS. All values are expressed as the mean of three determinations, plus or minus a standard deviation. Table 3.8 contains surface energy results for all formulations tested.

Table 3.8 Powder surface energy results for all TS formulations

Formulation	γ^d (mJ/m^2)	K_A	K_D	K_D/K_A
Micronised TS	56.6 (0.2)	200.3 (0.3)	26.8 (0.4)	0.13
Control TS	54.0 (0.2)	189.0 (0.2)	18.9 (1.0)	0.10
TS-F108	39.3 (0.1)	125.9 (0.2)	30.8 (0.4)	0.25
TS-F127	38.9 (0.1)	127.6 (0.2)	31.2 (0.2)	0.24
TS-L31	40.1 (0.1)	139.0 (0.2)	26.7 (0.6)	0.19
TS-31R1	37.7 (0.1)	126.8 (0.1)	29.7 (0.9)	0.23
TS-B39	40.4 (0.1)	139.0 (0.2)	12.9 (0.4)	0.09
TS-B59	40.6 (0.2)	141.8 (0.4)	20.6 (0.2)	0.15
TS-MMG	39.9 (0.1)	136.1 (0.3)	23.9 (0.2)	0.18
TS-L121	32.0 (0.6)	97.1 (1.6)	43.6 (0.5)	0.45
TS-L101	33.0 (1.5)	94.5 (0.9)	44.2 (0.4)	0.47
TS-Span 20	39.4 (0.7)	115.2 (1.2)	-11.9 (0.1)	-0.10
TS-Span 85	41.3 (0.2)	164.9 (0.4)	-7.3 (0.1)	-0.04
TS-Oleic Acid	39.4 (0.2)	163.5 (0.5)	-15.4 (0.8)	-0.09

Results from IGC analysis provide an interesting insight into the hitherto uncertainty surrounding the adsorption of polymer to the surface of micronised drug. Repeated attempts to assess the extent of polymer adsorption proved unsuccessful. Coupled with results from TS-surfactant microparticle characterisation that failed to show any alteration in microparticle size, morphology or physical form, proof of successful adsorption of polymer to the drug surface has not been presented. However, results from IGC analysis show a marked alteration in drug surface properties following adsorption of all polymers investigated. Considering firstly the dispersive component of powder surface energy (γ^d), polymer adsorption has resulted in a noticeable decrease in values, to varying extents depending on the polymer concerned. While γ^d for micronised TS is found to be 56.6 mJ/m^2, values for TS-surfactant formulations vary from 41.3 mJ/m^2 for TS-Span 85, to as low as 32.0 mJ/m^2 for TS-L101. It would appear that the process of incubation is to a small extent responsible for the observed decrease in surface energy components; given a value for TS control is seen as 54.0 mJ/m^2. The acid component of powder surface

energy (K_A) is also observed to have been universally decreased following adsorption of surfactant to the drug surface. Again, a slight decrease must be ascribed to the incubation process. The extent of modification to the K_A value once again varies according to polymer used. In contrast, no pattern in alteration to the base component of powder surface energy (K_D) is apparent. Values in Table 3.8 for K_D alternatively increase and decrease according to the polymer adsorbed on to the drug surface.

Overall, results from IGC analysis suggest the surface of TS has become less polar following surfactant adsorption with a reduction in both the dispersive and acid component of surface energy. Clues as to the orientation of the surfactant molecule on the drug surface may be gleaned from these findings. Considering the hydrophilic nature of TS in addition to the non-polar medium of DCM, it may be assumed that the more hydrophilic polythethylene oxide (PEO) chains contained in the various surfactants employed here will adsorb preferentially to the drug surface. Work conducted by Kronberg et al., (1981) and Killman et al., (1998) comparing the adsorption characteristics of some poloxamer surfactants on both hydrophobic and hydrophilic surfaces would seem to support this theory. Yet again however, these studies were conducted in aqueous media and also on "ideal" surfaces (i.e. not drug surfaces) and as such conclusions drawn may not be wholly applied to investigations reported here. The possibility of the formation of a bilayer of adsorbed surfactant on a hydrophilic surface was also discussed in work by Killman et al., in addition to work by Malmsten et al., (1992). Examination of the structure of the TS molecule in light of these theories regarding surfactant orientation at the drug surface reveals a possible explanation for the reduced polarity described by results obtained from IGC. It may be suggested that hydrogen bonding between hydrogen atoms and hydroxyl groups on both the drug surface and PEO chains of the polymers used serves to mask the projecting hydroxyl groups of the TS molecule, thus reducing surface polarity. Furthermore the preferential adsorption of PEO chains to the drug surface allows polypropylene oxide (PPO) groups to orient themselves outermost, contributing to the reduced surface polarity.

In terms of the anticipated effect that the observed modification to powder surface energy may have on suspension performance in a pMDI formulation, a decrease in γ^d is generally found to be consistent with an improvement in performance. Microparticles for inhalation, by virtue of their very small surface area, possess highly energetic surfaces giving rise to an inherent instability, as microparticles seek to aggregate or adhere to container surfaces in an effort to minimise the total surface free energy (Parsons et al., 1992). As such, any reduction in microparticle surface energy may be expected to improve pMDI suspension stability. Alteration in acid-base components may also be considered in terms of a possible effect on suspension performance. In particular, the reduction in K_A observed in all surfactant-containing formulations suggests a significant alteration in the surface nature of TS microparticles, specifically a reduction in the acidic nature of the microparticle surface. Such a change indicates a reduction in the polarity of the surface. In this case, a strongly acidic microparticle surface has been modified to one that will interact less with basic surfaces. Despite the reduction in K_A however, all microparticle surfaces remain predominantly acidic, with K_D/K_A values of less than 1. Surface acidity is markedly reduced to as much as half its original magnitude in some formulations (TS-L101, TS-L121, TS-Span 20). Of note is the hydrophobic nature of the surfactants in question, a factor which may be responsible for the significant reduction in K_A values for these three formulations. However, Span 85 and oleic acid are also hydrophobic in nature, but do not display a similar reduction in K_A values, preventing any conclusive interpretation of the data. The relevance of all powder surface energy modifications observed here in terms of pMDI suspension performance will be investigated further in Part C of this chapter.

Contrary to expectation, a number of K_D values listed in Table 3.8 are seen to be negative. Calculation of a negative value results from the position of polar probe molecules below that of the alkane line in a plot such as that seen in Figure 3.10. As such, distance from the polar probe molecule to the alkane line (the specific energy of adsorption, ΔG_A^{sp}) is measured as a negative value. It is unclear why the three formulations in question have shown an altered interaction with polar probe molecules such that retention volume is significantly altered compared to all other formulations. Alternate methods of data analysis may be employed in order to re-plot data such that K_D values are no longer deduced as being negative. These involve

plotting $RTlnV_N$ vs. a physicochemical property such as vapour pressure or boiling point of polar probe molecules (Chehimi & Pigois-Landureau, 1994). However, given that negative values were obtained for only three formulations, coupled with the fact that it would appear changes to K_D following surfactant adsorption do not follow any discernible pattern, re-analysis of these data was not carried out.

Observed reductions in powder surface energy appear to vary according to the polymer adsorbed on to the drug surface. In an effort to ascertain a link between surfactant structure and surface energy modification, both γ^d and K_A values for all formulations were plotted against polymer molecular weight, in addition to hydrophile – lipophile balance (HLB) ratio.

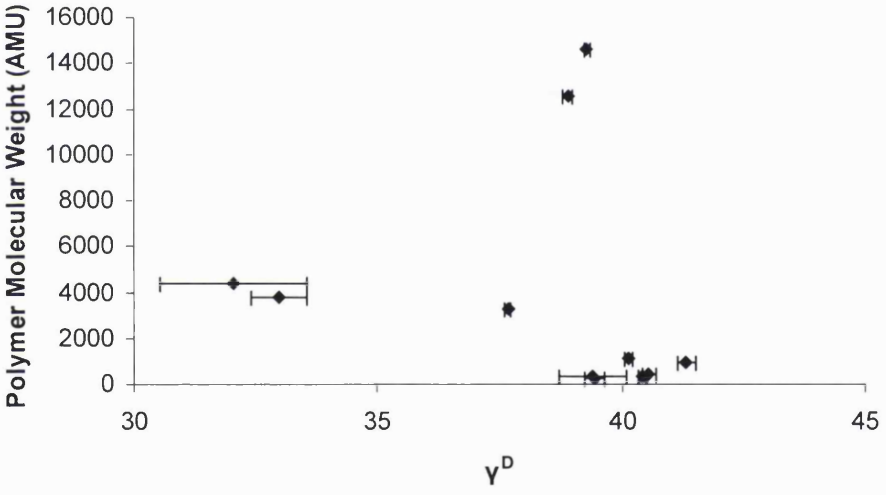

Figure 3.11 Relationship between γ^D and polymer molecular weight

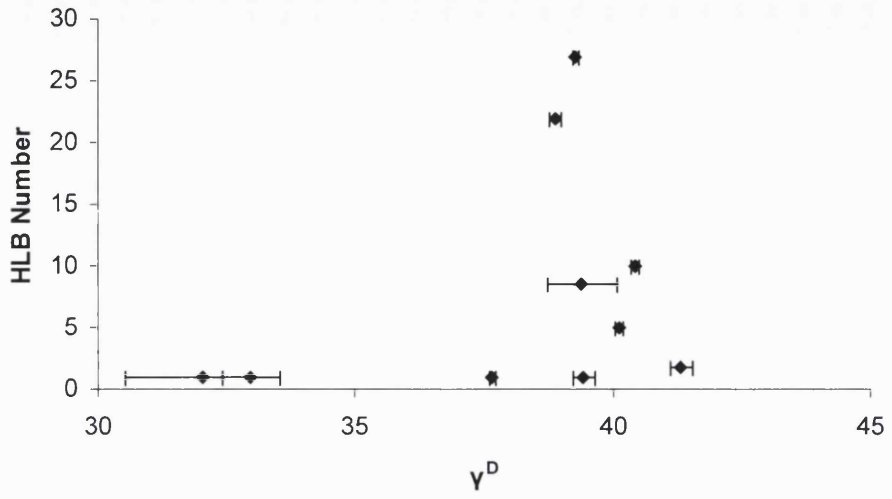

Figure 3.12 Relationship between γ^D and polymer HLB number

It is clear from Figures 3.11 and 3.12 that no correlation between polymer-induced dispersive surface energy modification and any single aspect of polymer structure may be found. Further attempts to investigate whether any correlations existed between polymer structure and Acid-Base components of powder surface energy (i.e K_A, K_D and K_D/K_A) also failed to find any discernible pattern. This is unfortunate, as the ability to predict how a particular surfactant may modify a drug surface following adsorption would prove a useful tool in formulation, precluding the need for time-consuming screening of a range surfactants.

3.4 SUMMARY AND CONCLUSIONS

Results from Part A have helped to construct a picture of modified TS microparticles prepared following surfactant adsorption. Several attempts to measure the amount of surfactant adsorption were unsuccessful. In addition, a range of materials characterisation techniques have shown microparticle size, morphology and physical form to remain unchanged. In contrast, powder surface energy was found to be markedly altered in formulations containing adsorbed surfactant. A reduction in both the dispersive component and acidic component of surface energy was seen, however alterations to the basic component of surface energy did not follow any discernible pattern. Attempts to discover a correlation between polymer structure and microparticle powder surface energy modification following adsorption proved inconclusive. Moving forward from these studies, the effect of surfactant-induced

microparticle surface modification on pMDI suspension performance will subsequently be investigated. It is hoped that the reduction in powder surface energy may confer stabilising properties on a formulation of TS-surfactant microparticles suspended in HFA propellants.

PART B: pMDI FORMULATION AND SUSPENSION STABILITY TESTING

3.5 INTRODUCTION

Part A of this chapter has provided an essential background to the formulation considerations involved in creating modified terbutaline sulphate microparticles. Successful modification of drug surface properties through the adsorption of a range of non-ionic surfactants has been demonstrated from surface energy analysis. Subsequent investigations into the effect of drug surface modification will focus on the corresponding alteration in suspension performance of a pMDI sample containing experimental formulations. Ultimately, this work aims to reveal the relationship between powder surface energy and pMDI suspension performance, in light of the observation that it is this physicochemical property alone that has been found to change following adsorption of surfactant. By preparing pMDI samples for all formulations and examining suspension performance using a number of techniques, this relationship will be explored.

3.6 COMPARISON OF TWO OPTICAL METHODS FOR ASSESSING pMDI SUSPENSION STABILITY

In order to determine the technique of choice for investigation of pMDI suspension formulation performance, two optical techniques were compared. The techniques in question were Optical Suspension Characterisation (OSCAR) and Turbiscan, both of which have been explained in full in Chapter Two. In this preliminary study, the behaviour of two formulations was examined: that of a TS control, and of TS-F127 surfactant microparticles. Suspension formulations were prepared at two concentrations, 0.15 % w/w and 0.3 % w/w in both HFA 227 and HFA 134a using a pressure burette (AeroTech Laboratories, US). In this way it was hoped that a broad range of suspension variables would be created, enabling a comprehensive comparison of the two techniques.

3.6.1 EXPERIMENTAL PROTOCOL

3.6.1.1 pMDI SUSPENSION PREPARATION OF TS-SURFACTANT PARTICLES IN HFA PROPELLANTS

Suspensions of micronised TS and TS- surfactant particles were prepared using a pressure burette as described in Chapter Two, Section 2.2.5.

3.6.1.2 OSCAR ANALYSIS

A description of the OSCAR apparatus may be found in Chapter Two, Section 2.2.6. Turbidity standards (Reagecon Diagnostics Ltd., Ireland) were used to calibrate the upper and lower photodetectors of the apparatus prior to use (Reagecon standard 4000 was used for suspensions filled at 0.3 % w/w, Reagecon standard 2000 used for suspensions filled at 0.15 % w/w). Photodetector positions were adjusted to 2.5 mm above the bottom of the sample vial, and 2 mm below the suspension meniscus. Samples were sonicated for 1 minute prior to analysis to ensure good dispersion of suspended material. Each pMDI sample was scanned for three minutes, with a total of 1000 measurements taken at each photodetector over this period. This scanning protocol was carried out twice on each pMDI sample.

3.6.1.3 TURBISCAN ANALYSIS

A description of the Turbiscan apparatus may be found in Chapter Two, Section 2.2.7. Samples previously scanned by OSCAR were transferred from PET vials to the Turbiscan measurement cell through a valve in the pressurised head attachment under vacuum. Formulations were again sonicated for 1 minute prior to analysis. The scanning protocol adopted for Turbiscan analysis was as follows: a total of five scans were taken over three minutes at t = 0 min, 0.5 min, 1 min, 2 min and finally 3 min. Each scan took measurements of the entire sample cell as previously described. Again, the scanning protocol was carried out twice on each pMDI sample.

3.6.1.4 DATA ANALYSIS

Data files generated by the OSCAR apparatus were analysed using Microsoft Excel in order to construct charts plotting light transmission through the sample over time at both the top and bottom of the pMDI suspension. In the case of files generated from Turbiscan analysis, charts were also constructed in Microsoft Excel plotting

backscattered light against the sample cell length for each time point. Light transmission through samples of both fill concentrations proved negligible and so these data were not considered. Using Turbisoft software included with the Turbiscan apparatus, mean backscattering values of the five scans over a defined range of the sample cell (30-40 mm) were obtained, which could then be plotted over time. As an additional treatment of Turbiscan data, variance of scans at t = 0.5 min, 1 min, 2 min and 3 min from an initial scan at t = 0 min was calculated, and standard deviation of this variance across the data range for each scan was determined. A standard deviation value for each scan was then plotted against time.

3.6.2 Results and Discussion

3.6.2.1 OSCAR analysis

Formulations containing micronised drug alone were seen to be unstable over the three minute scan period. Poor suspension performance was observed as a rapid creaming (in the case of HFA 227) or sedimentation (HFA 134a) rate. Instability of formulations containing drug alone was consistent, regardless of the fill concentration or propellant system examined. Figure 3.13 shows the OSCAR trace for such a formulation in HFA 134a, at a fill concentration of 0.3 % w/w.

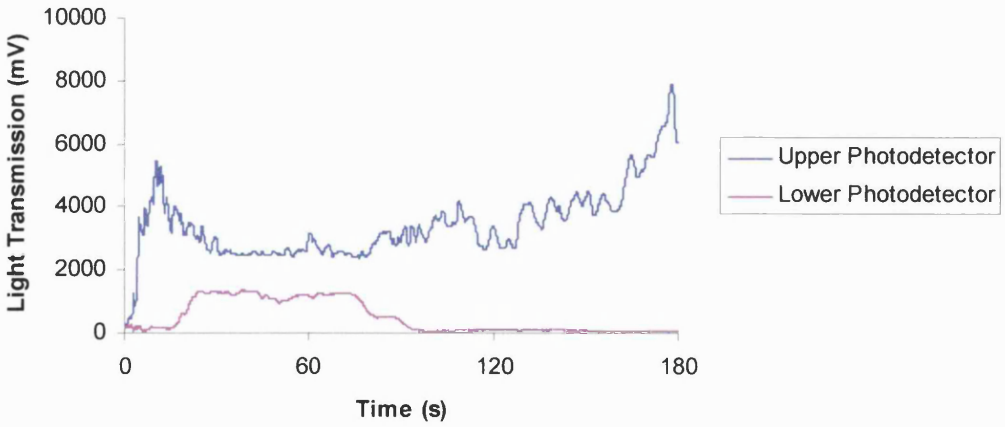

Figure 3.13 OSCAR result for a formulation containing TS control in HFA 134a (0.3 % w/w).

As expected, light transmission measured at the upper and lower photodetectors is equal in the initial stages of the scan period. However, rapid separation of the

suspension occurs almost immediately, with suspended material settling to the bottom of the sample vial. As such this suspension is seen to sediment, evident as an increase in light transmission at the upper photodetector with time. Also notable in Figure 3.13 is the flocculated nature of the suspension, observed in the fluctuation in measured light transmission. In the case of formulations containing surfactant, significant improvements in suspension stability were observed, specifically a reduced sedimentation or creaming rate in addition to reduced flocculation. Figure 3.14 shows the result for a formulation containing drug in addition to F127 in HFA 134a at a concentration of 0.30 % w/w. Similar to the previous figure, light transmission through the top and bottom of the suspension is initially equal. However, in the case of this formulation, there is little deviation from this initial light transmission throughout the course of the scan. Traces for the upper and lower photodetector are seen to be superimposed on one another, consistent with a stable, evenly dispersed suspension. The smooth profile observed indicates the absence of flocculation.

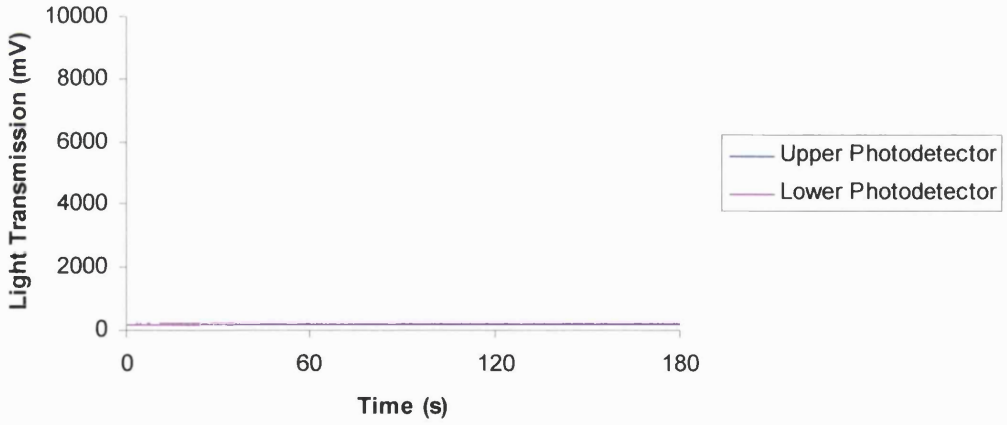

Figure 3.14 OSCAR trace for a formulation containing TS-F127 in HFA 134a (0.30 % w/w).

In summary, findings from OSCAR analysis clearly showed the stabilising influence of surfactant adsorption on pMDI suspension performance. A comparison between formulations of different fill concentrations or in different propellant systems was not possible however, due to the lack of an objective, comparative data analysis method.

3.6.2.2 TURBISCAN ANALYSIS

Results from Turbiscan experiments supported findings from OSCAR analysis, and confirmed that adsorption of surfactant to the drug surface had succeeded in improving pMDI suspension stability. Figure 3.15 shows the chart obtained from a Turbiscan experiment on the identical formulation to that represented in Figure 3.13, i.e. a formulation containing drug alone in HFA 134a. Each horizontal trace corresponds to a single scan of the entire sample cell, with the scan time recorded in the legend. Over the course of the three minute experiment, back scattering is observed to decrease across the majority of the sample length as the suspension clarifies, and in the case of this formulation in HFA 134a, forms a layer of sediment at the bottom of the sample cell. An isolated increase in backscattering over time can be seen in this region. Extensive flocculation can also be observed in this figure, with backscattering increasing at discreet points along the sample length corresponding to the presence of aggregated material. Data seen in Figure 3.15 over the regions 0-3.5 mm and 70-80 mm do not relate to the suspension, but rather to the morphology of the bottom region, in addition to the empty upper region of the sample cell. The return of this irrelevant information is unavoidable as turbiscan scans the entire length of the sample cell whether or not it contains material.

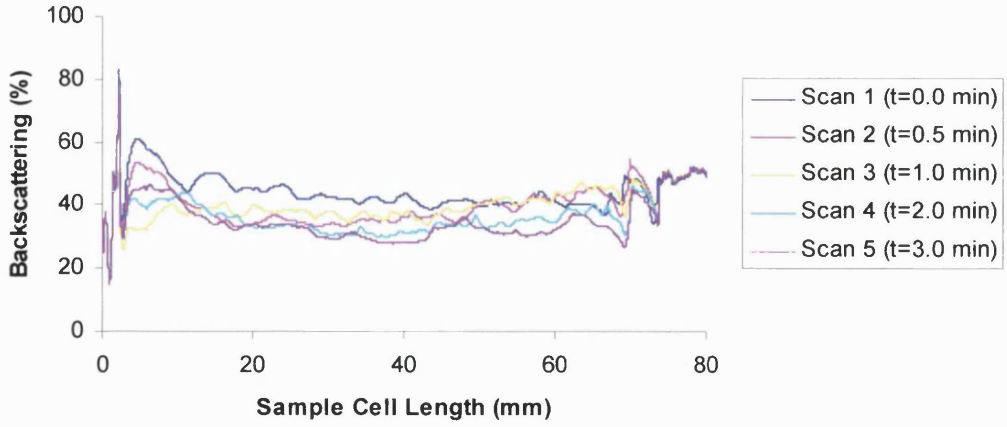

Figure 3.15 Turbiscan trace for a formulation containing TS control in HFA 134a (0.30 % w/w)

A representation of a stable suspension is shown in Figure 3.16. Again these data refer to the identical formulation shown in Figure 3.14 to allow a comparison with OSCAR analysis.

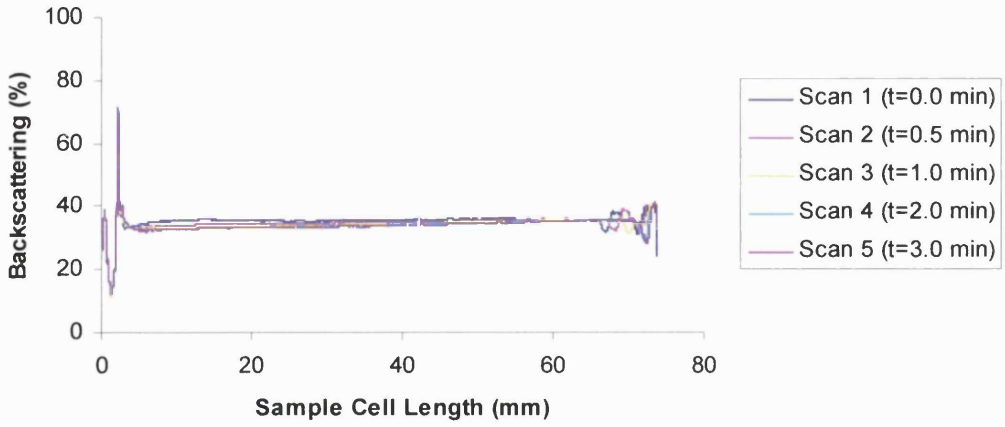

Figure 3.16 Turbiscan trace for a formulation containing TS-F127 in HFA 134a (0.15 % w/w)

Similar to the profile obtained from OSCAR analysis, traces in Figure 3.16 are superimposed on one another as light backscattered by the suspension remains almost constant. In the case of Turbiscan, this corresponds to little or no sedimentation occurring in this formulation over the course of the three minute examination. Again irrelevant information not pertaining to suspension behaviour is seen in the regions 0-3.7 mm and 70-80 mm.

As such, turbiscan analysis was consistent with OSCAR data in confirming that adsorption of surfactant to the drug surface succeeded in improving suspension behaviour over the three minute scan period. However, in addition to this information, data manipulation possible using the Turbisoft software allowed an objective comparison of all formulations. As previously described, mean backscattering values over the region 30-40 mm of the sample cell were obtained for each formulation. These data were then plotted as a function of time. By choosing close to the central region of the sample, a comparison between both sedimenting and creaming formulations is possible.

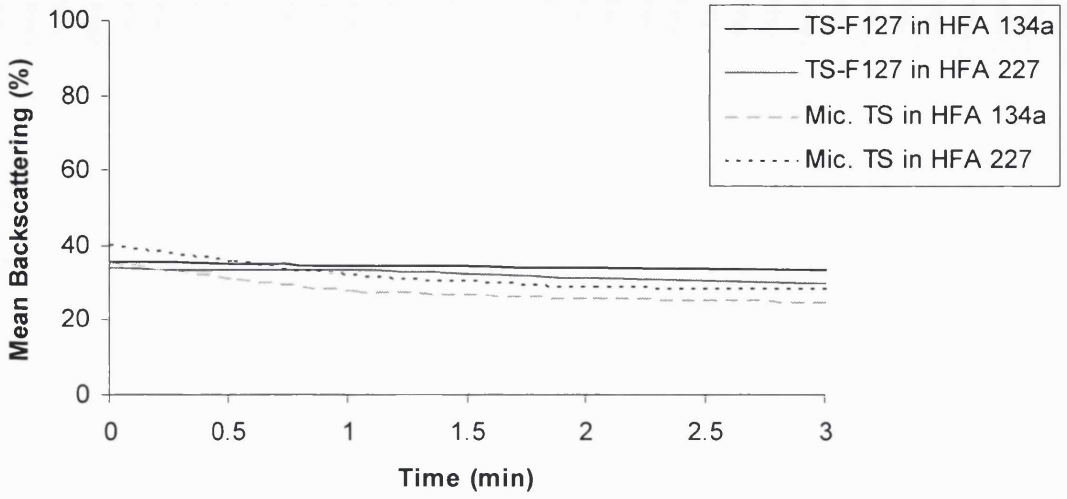

Figure 3.17 Mean backscattering data for all formulations of fill concentration 0.15 % w/w

Examining traces for the four formulations shown in Figure 3.17, the stabilising effect of surfactant adsorption is once more shown, as formulations containing surfactant present a flatter profile over three minutes. However, subtle differences between formulations may also be observed. It appears that surfactant adsorption is slightly more effective at improving suspension stability in the propellant HFA 134a when compared with HFA 227, as mean backscattering decreases by 1.86 (± 0.79) % in HFA 134a as opposed to 4.34 (± 1.36) % in HFA 227. This was all the more evident in formulations of fill concentrations 0.3 % w/w (Figure 3.18). In the case of these more concentrated formulations, mean backscattering of formulations containing surfactant decreased by 2.71 (± 1.32) % in HFA 134a, whereas it decreased by 13.21 (±1.78) % in HFA 227.

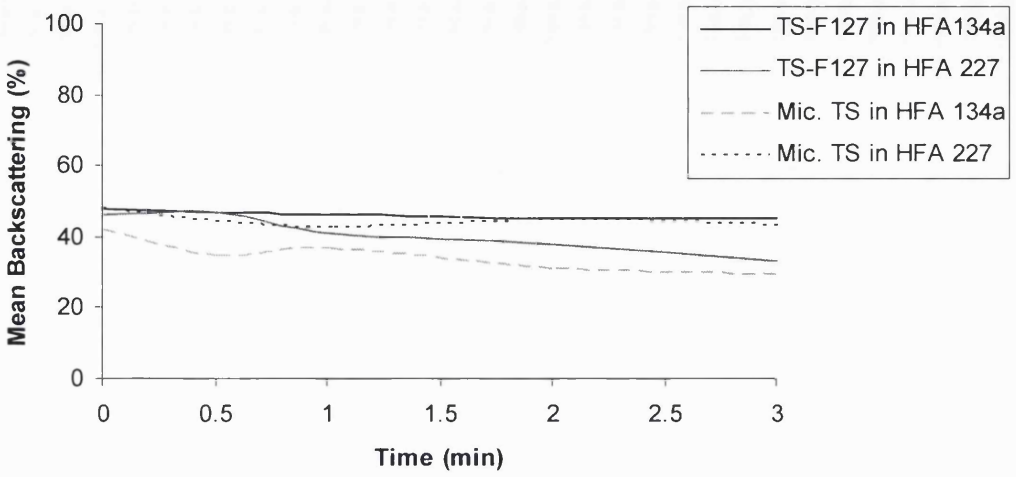

Figure 3.18 Mean backscattering data for all formulations of fill concentration 0.30 % w/w

The ability to calculate mean backscattering has therefore allowed greater insight into the extent of suspension stability conferred on various formulations by surfactant adsorption. Findings have suggested that a more favourable result will be seen in formulations suspended in HFA 134a rather than HFA 227, and in also in more dilute formulations.

As a final interpretation of data obtained from Turbiscan analysis, backscattering variance of all formulations was plotted against time according to the data analysis method previously described in Section 3.6.1.4 of this chapter. Figure 3.19 shows the results for all formulations in HFA 134a. A stable suspension should have little deviation in backscattering value across the length of the sample, as material remains suspended evenly. As expected, formulations containing surfactant are seen to have little change in standard deviation over the three minute scan period. In contrast, in the two uppermost traces in Figure 3.19, corresponding to formulations without surfactant, standard deviation is seen to vary. Fluctuation in these traces is suggestive of an unstable suspension, whether it is due to extensive flocculation, or a rapid separation rate.

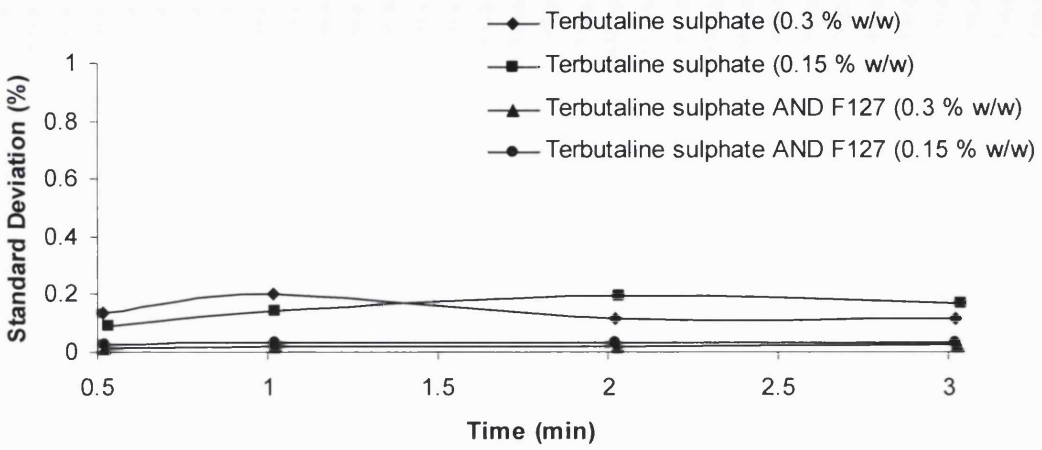

Figure 3.19 Backscattering variance for all formulations in HFA 134a

Figure 3.20 shows a similar chart to Figure 3.19, showing results for all formulations contained in HFA 227. These data would seem to support previous conclusions from data relating to mean backscattering, namely that surfactant adsorption had a greater stabilising effect on pMDI performance in HFA 134a when compared with HFA 227. Formulations containing surfactant are seen to have a lower standard deviation in backscattering variance across the sample cell when compared with formulations containing drug alone. However, standard deviations for all formulations in Figure 3.20 are seen to increase over the three minute scan period.

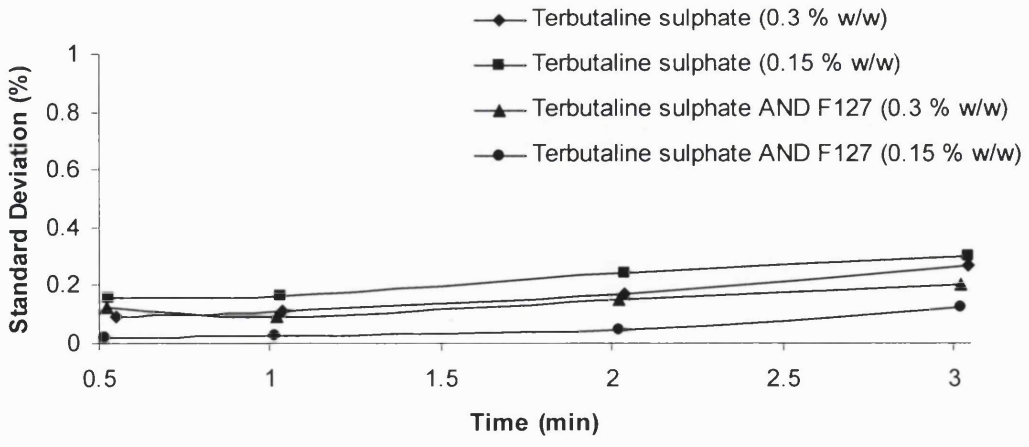

Figure 3.20 Backscattering variance for all formulations in HFA 227

Experiments carried out in this study have allowed a comprehensive comparison of the two optical methods for pMDI suspension characterisation in question. Data obtained from OSCAR analysis has shown this apparatus to be a convenient tool in the characterisation of pMDI suspension samples, clearly showing suspension separation, and flocculation behaviour. Experiments may be carried out rapidly and in quick succession in a non-invasive, non-destructive manner, as samples are scanned in their original container. As such, it is possible to scan the same sample repeatedly, after varying time points if so desired. However, data from OSCAR only correspond to suspension behaviour at the upper and lower regions of the sample vial, and therefore the formation of flocs within the area of suspension between the upper and lower photodetectors will not be identified. In addition, an objective comparison of suspension stability between different formulations is not possible.

Turbiscan analysis was also shown to be a valid method for characterising pMDI suspension behaviour. Separation of suspended material from the continuous propellant phase in addition to any floc formation was evident. In contrast to OSCAR, data obtained from Turbiscan represent the entire sample and so a complete picture of suspension performance can be constructed. Turbiscan also provides the advantage of measuring light backscattered by a formulation in addition to transmission, information which proved invaluable in this study as light transmitted through the suspensions investigated was negligible. The facility to obtain mean backscattering information over a defined zone of the sample was found to be very useful as a tool to objectively compare different formulations. This comparison allowed the identification of subtle differences in suspension stability which had not been possible using OSCAR analysis alone. Turbiscan therefore, would appear to be the preferred technique over OSCAR. However, certain disadvantages to this technique should be considered. Perhaps most notable is the required transfer of suspension samples into purpose-built glass measurement cells, the action of which may arguably alter suspension concentration slightly. In addition, suspension behaviour within a PET vial and within a glass cell may differ, due to the distinct surface energetics of container materials. However, to follow this argument to completion, PET vials are no more representative of commercial formulations than a glass measurement cell, as pMDIs are conventionally formulated for market sale in aluminium canisters. A secondary issue with regard to Turbiscan is the length of

time each individual scan of the sample cell will take, in this study observed to be approximately 22 seconds. At best, this will prevent repeat scans being taken sooner than 22 seconds after the initial scan at t = 0 minutes. At worst however, suspension stability at a particular time point may not be accurately represented if in the case of an unstable suspension, 22 seconds is long enough for significant further separation to have occurred. Despite these two points of concern however, on balance the results obtained from this study suggest that Turbiscan is indeed the preferred optical method for the characterisation of pMDI suspension performance, and was subsequently chosen to characterise all TS-surfactant pMDI suspension formulations.

3.7 SUSPENSION STABILITY OF TS-SURFACTANT MICROPARTICLE pMDI FORMULATIONS BY TURBISCAN ANALYSIS

3.7.1 EXPERIMENTAL PROTOCOL

3.7.1.1 PREPARATION OF TS-SURFACTANT MICROPARTICLE pMDI FORMULATIONS

TS-surfactant microparticle suspensions were prepared in both HFA 227 and HFA 134a. It was decided to formulate suspensions at a concentration of 0.2 % w/w in reference to a commercially available TS formulation in a CFC propellant system (Bricanyl®). Suspensions were formulated using a pressure burette as described previously.

3.7.1.2 SCANNING PROTOCOL IMPOSED ON TS-SURFACTANT pMDI SUSPENSION FORMULATIONS

Samples were scanned according to an identical protocol to that adopted in the preliminary study. As such, samples were sonicated for one minute, and then scanned five times over a period of three minutes. All samples were scanned three times. Results shown represent the mean of three scans.

3.7.2 RESULTS AND DISCUSSION

Initial investigations aimed to assess the performance of pMDI suspension formulations containing TS alone. Accordingly, the following results pertain to pMDI samples containing a TS control in both HFA propellants.

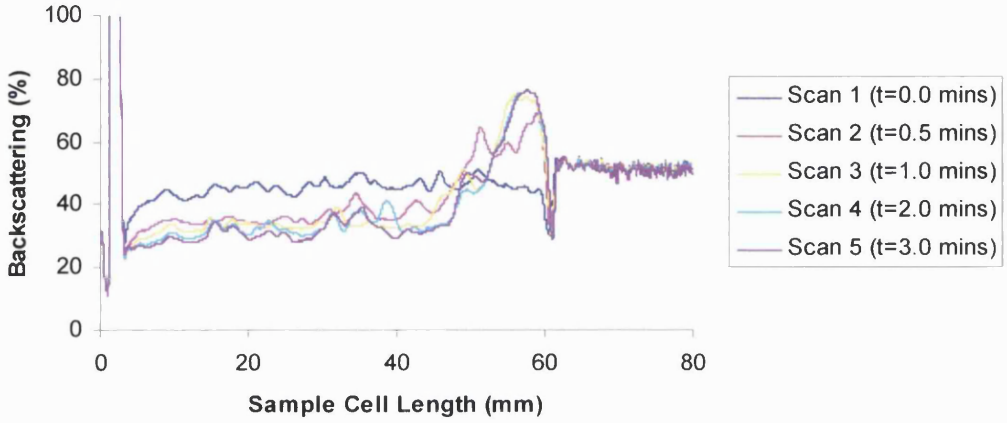

Figure 3.21 Turbiscan trace for formulations containing a TS control in HFA 227

Once again, pMDI suspension concentration was found to be above that enabling transmission data to be useful. As such, only backscattering data are considered here. The behaviour of the formulation seen in Figure 3.21 is in line with that expected of a sample in HFA 227. Due to density differences, dispersed material separated from the continuous phase will form a creamed layer above the suspension bulk. The formation of a creamed layer is easily observed as an increase in the backscattering signal in the upper regions of the sample cell. Also of note, backscattering signal is seen to decrease across the remainder of sample cell length over the three minute scan period. This reduction may be ascribed to clarification of the suspension bulk occurring simultaneously with creamed layer formation.

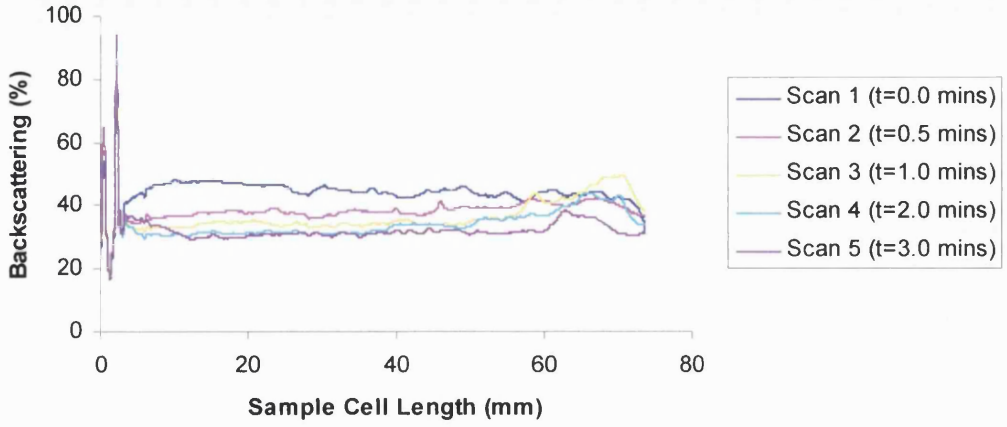

Figure 3.22 Turbiscan trace for formulations containing a TS control in HFA 134a

The interpretation of turbiscan data describing behaviour of a sample containing TS control in HFA 134a did not prove as straightforward. Figure 3.22 shows a similar reduction in backscattering signal over the three minute scan period, consistent with clarification of the suspension over time. However, in contrast to Figure 3.21 where a creamed layer is evident, the expected formation of a settled layer of suspended material in HFA 227 resulting from the altered difference in density between the two phases is not apparent in Figure 3.22. Despite a lack of experimental data to support it, sedimentation was visually observed to have occurred during the course of the experiment. A likely explanation is that the fluctuation in backscattering signal caused by the bottom meniscus of the glass measurement cell obscures the increase in backscattering expected. In the case of suspension of a TS control in both propellants, overall performance of pMDI samples may be interpreted as poor. The changes observed in backscattering signal suggest significant separation of dispersed particles from the continuous phase over the course of three minutes. In addition to suspension separation, the fluctuations observed in backscattering traces at a particular time point may correspond to the formation of flocs within the suspension system, giving rise to isolated increases in backscattering at discreet points along the sample cell length. Relating these findings to clinical performance of a pMDI formulation, separation occurring over this short time may result in a patient receiving either sub or supra-optimal dosing of medication, with the occurrence of the related problems of sub-therapeutic dosing or drug-induced side effects.

Analysis of pMDI suspension samples of formulations containing adsorbed surfactant gave rise to a range of backscattering profiles, with performances varying from that similar to control formulations to profiles indicative of improved suspension stability over the period of investigation. All formulations previously characterised in Part A of this chapter were investigated using the Turbiscan apparatus.

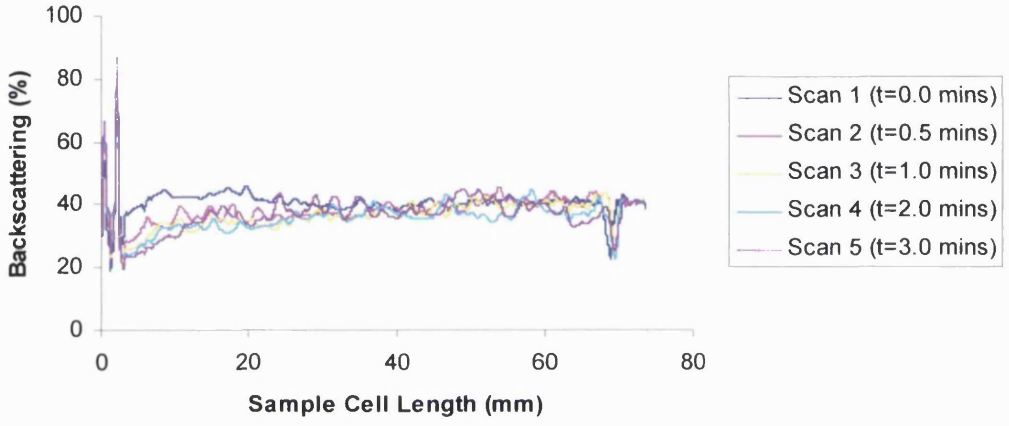

Figure 3.23 Turbiscan trace for formulations containing TS-F108 in HFA 227

Figure 3.23 shows a trace for TS-F108 in HFA 227. Behaviour of the suspension sample appears erratic across the entire length of the sample cell, even more so than that of the control formulation in an identical propellant system. Backscattering is observed to decrease over the three minute scan period, consistent with suspension clarification, however unlike the control formulation, the formation of a creamed layer is not as easily observed. Significant fluctuation in backscattering traces may also be observed, suggestive of extensive flocculation. While controlled flocculation may be desirable under the terms of the DLVO theory (discussed in Chapter One) in order to prevent the formation of an irreversible cake, extensive flocculation may be expected to contribute to suspension separation under the rules of Stoke's Law, whereby particle size is linked to sedimentation rate. The extent of flocculation may explain the lack of evidence of a creamed layer, as a large proportion of suspended material is contained in the suspension bulk, located within loose aggregates or flocs.

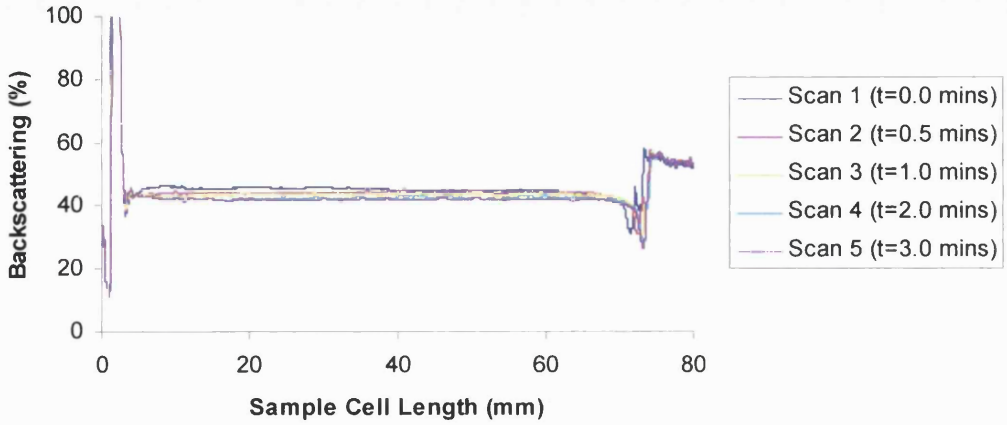

Figure 3.24 Turbiscan trace for a formulations containing TS-F108 in HFA 134a

Figure 3.24 shows the Turbiscan trace of a pMDI sample with favourable suspension behaviour when compared with the same formulation in HFA 227. While the backscattering signal is also seen to decrease over the period of investigation, it is to a lesser extent than that observed in Figure 3.21 and so the suspension appears to be separating at a slower rate in this alternative propellant. It would also appear that the extent to which flocculation is occurring in the system contained within HFA 134a is also reduced, as backscattering traces appear more level.

Examination of two further TS-surfactant containing formulations are seen in Figures 3.25 and 3.26. The profiles observed appear to suggest a substantial improvement in suspension performance over a control formulation in the same propellant. The backscattering signal may be seen to remain almost constant over the three minute scan period, with serial measurements detecting backscattering levels very similar to one another. No formation of a layer of sediment is evident, however the possibility of obscuration of the backscattering signal by the sample cell meniscus cannot be ruled out.

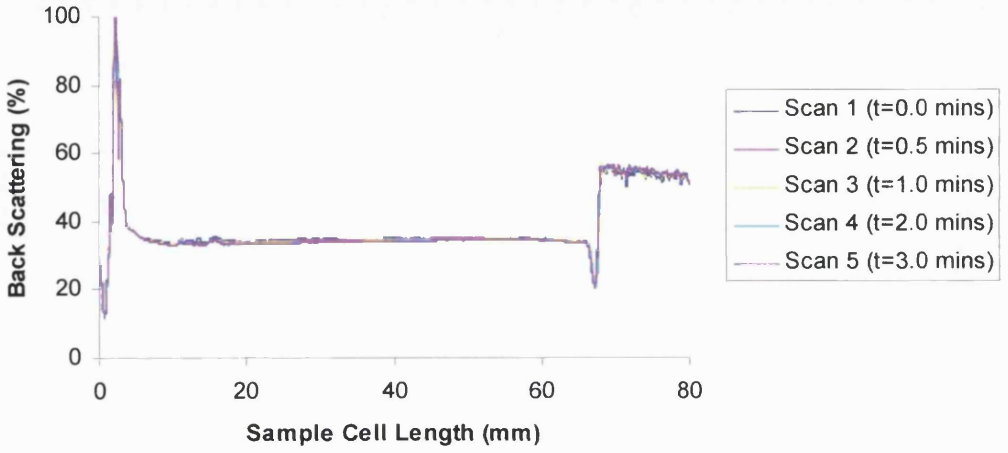

Figure 3.25 Turbiscan trace for a formulation containing TS-F127 in HFA 134a

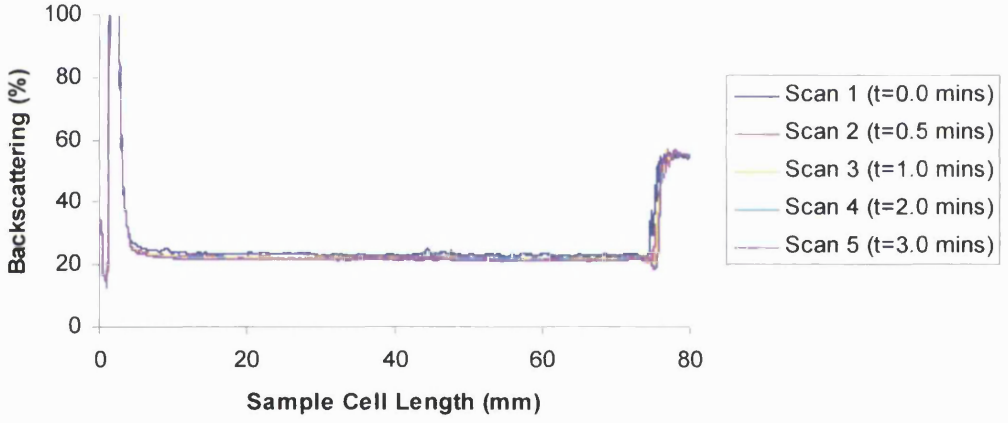

Figure 3.26 Turbiscan trace for a formulation containing TS-L121 in HFA 134a

The success achieved in conferring stabilising properties on a suspension of TS observed in the previous three figures was not true of all formulations tested. The Turbiscan trace observed in Figure 3.27 reveals the persistent instability of a formulation containing the adsorbed poloxamer surfactant L121. Again, the formation of a creamed layer of suspended material is clearly evident, together with fluctuations in the backscattering signal measured, indicative of flocculation. This is in sharp contrast to the trace obtained for an identical formulation, but in the alternative propellant HFA 134a (Figure 3.26).

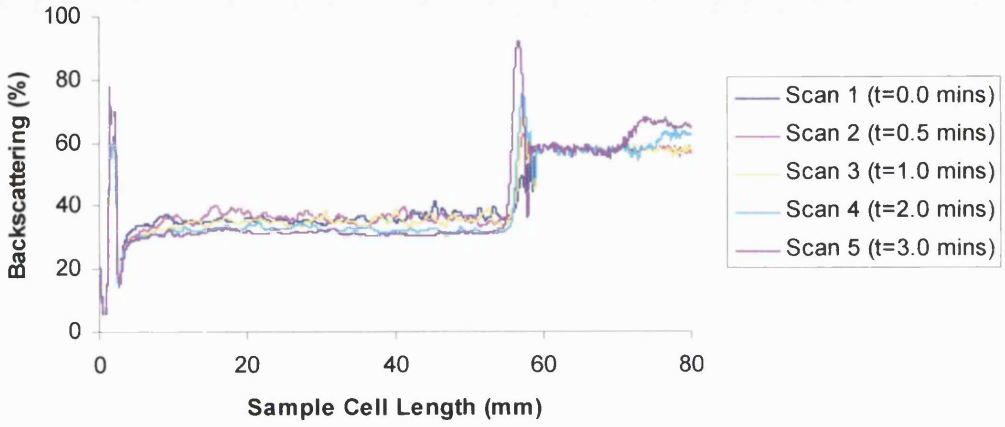

Figure 3.27 Turbiscan trace for a formulation containing TS-L121 in HFA 227

While traces obtained for individual formulations from Turbiscan experiments provide useful information pertaining to their suspension performance, they do not easily allow comparison of different formulations. As described previously in work comparing the OSCAR and Turbiscan techniques, calculation of mean backscattering over a defined zone of the sample cell length (30-40 mm) for each formulation examined allows an objective comparison between all formulations to be made. Plotting mean backscattering for all formulations over the three minute scan period allows a visual examination of the slope of all traces, thus giving a relative indication of suspension performance. Figures 3.28 and 3.29 present these results, with mean backscattering for a TS control denoted by a bold blue line.

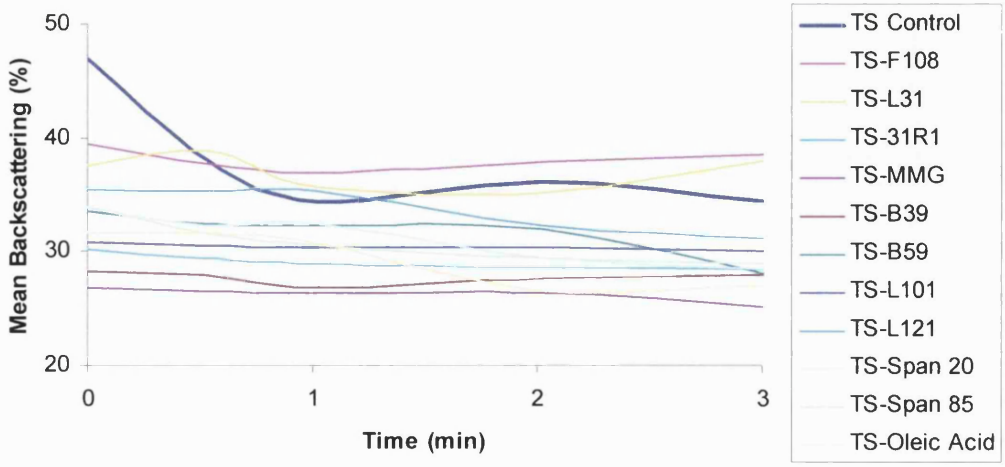

Figure 3.28 Mean backscattering across zone 30-40 mm of sample measurement cell for all formulations tested in HFA 227

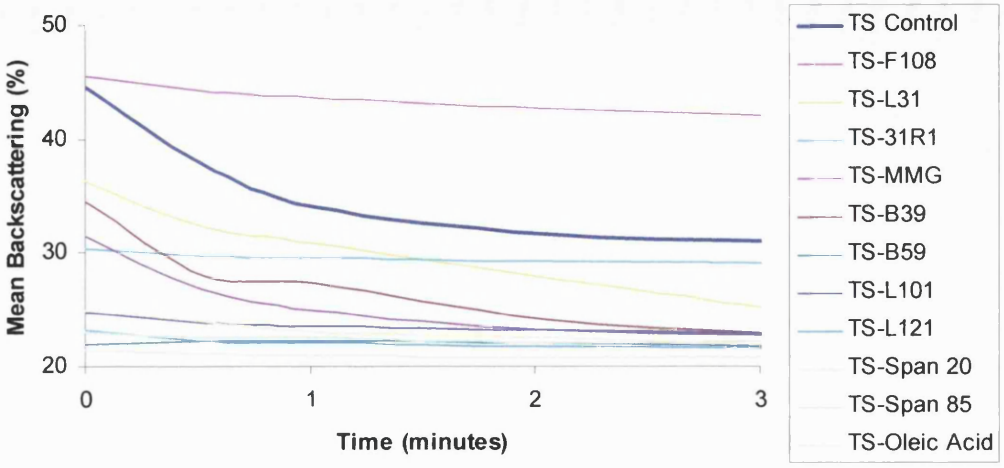

Figure 3.29 Mean backscattering across zone 30-40 mm of sample measurement cell for all formulations tested in HFA 134a

Examination of mean backscattering results supports findings initially taken from traces for individual formulations, confirming the instability of formulations containing TS alone. It is clear that a range of stabilities are achieved following adsorption of surfactants to the drug surface, in both propellant HFA 227 and 134a. Unexpectedly, baseline mean backscattering is not constant for all formulations. Considering particle size analysis had previously found all formulations to possess a similar volume mean diameter, light initially backscattered by each formulation would be expected to be identical, given that each formulation was subjected to an identical period of sonication to ensure good dispersion of the suspension. A possible explanation for this discrepancy is the reduced flocculation observed in some surfactant-containing formulations when compared with a TS control. The formation of large flocs within a formulation will give rise to an increase in backscattering as particle size increases, reducing the amount of light permitted to pass through the sample. As such, it may be suggested that formulations with lower values for baseline mean backscattering observed in Figures 3.28 and 3.29 contain particles still close to the primary particle size, whereas other formulations have already begun to flocculate extensively.

Data from Figures 3.28 and 3.29 were further used to construct charts plotting a reduction in mean backscattering for each formulation over the three minute scan period, in each HFA propellant. These results may be observed in Figures 3.30 and

3.31, where micronised TS has been shortened to MTS. Formulations exhibiting a small or negligible reduction in mean backscattering may be considered to show an improvement in suspension performance over a TS control formulation, seen to have the largest reduction in mean backscattering in both HFA propellants.

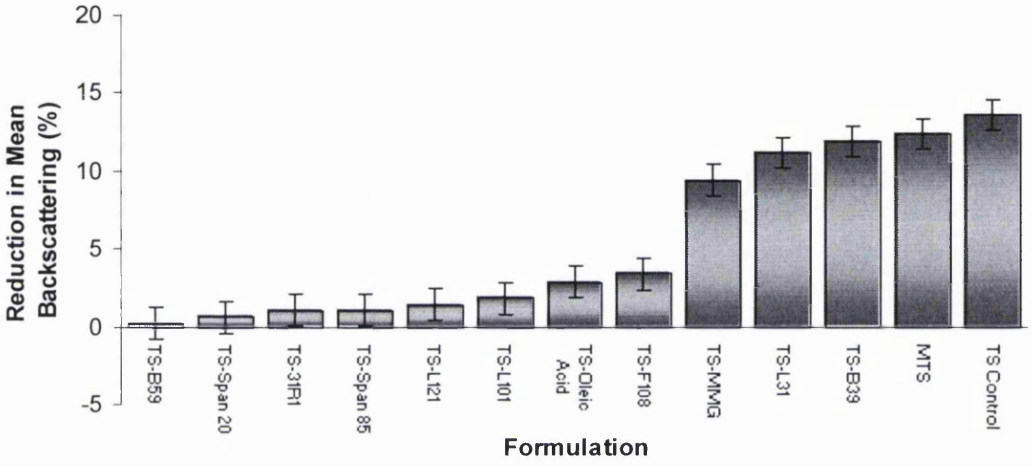

Figure 3.30 Reduction in mean backscattering for all formulations in HFA 134a

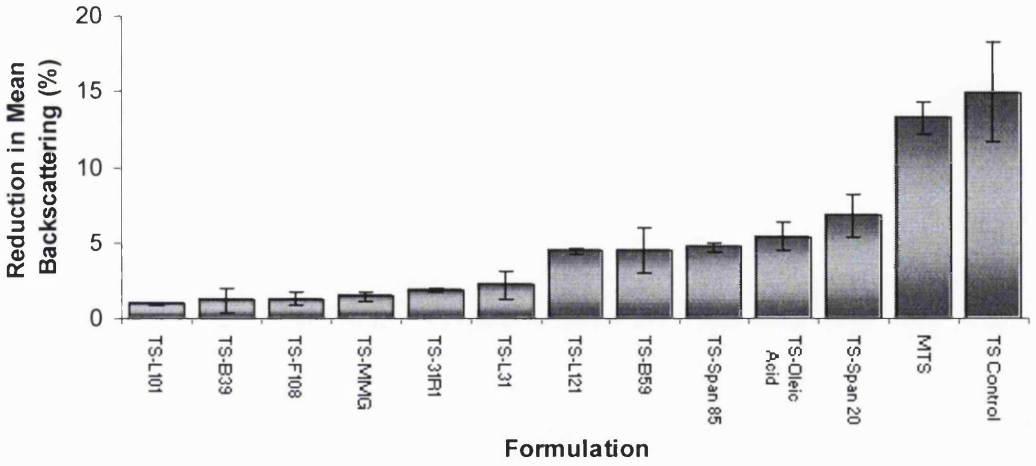

Figure 3.31 Reduction in mean backscattering for all formulations in HFA 227

It is clear from Figures 3.30 and 3.31 that a wide range of suspension performance is produced following surfactant adsorption to the surface of TS. Also of note is that formulation performance can be seen to differ between HFA propellants, confirming the complex nature of these systems and the interdependence of interactions at

several interfaces (e.g. particle/particle, particle/propellant and particle/container surface). There are several independent factors influencing the suspension performance of these formulations. The variation in formulation performance over the range of surfactants employed here, in a similar manner to the variation observed in powder surface energy, suggests surfactant structure is influencing suspension performance. Construction of similar graphs to those observed in Section 3.7 comparing reduction in mean backscattering with both surfactant molecular weight and HLB number once again failed to produce any discernible correlation between suspension performance (in terms of a reduction in mean backscattering) and these elements of surfactant molecular structure. As a result, the plots investigating a possible correlation are not shown. Again the failure to elucidate a link between surfactant structure and suspension performance is unfortunate, as the empirical choice of a surfactant hampers an efficient formulation strategy. Another factor seen to influence suspension performance is the particular HFA propellant in which formulations are suspended. The two HFA propellants used in this work are known to differ slightly in several physicochemical properties, described in Chapter One. Density differences between the two propellants may be responsible for the observed variation in suspension performance. The observation that some formulations suspended in HFA 134a appear to exhibit a more favourable performance in HFA 134a than in HFA 227 may be due to this propellant's density being closer to that of the drug TS.

3.8 SHAKE-PAUSE-FIRE TESTING

3.8.1 EXPERIMENTAL PROTOCOL

3.8.1.1 DOSE COLLECTION

As an alternative method of evaluating suspension performance, selected formulations were analysed by Shake-Pause-Fire (SPF) testing. While the Turbiscan technique investigates suspension performance in the bulk by direct observation through a transparent vessel, the principle of SPF allows analysis of the bulk indirectly, by assaying the contents of a dose fired from a metering valve for drug concentration. It was hoped that data from SPF testing would support those obtained from Turbiscan analysis. Formulations chosen for investigation were a control TS

formulation, in addition to two formulations containing the adsorbed poloxamer surfactants F127 and L121. Suspension samples were prepared in 11.5 ml aluminium canisters using a small-scale industrial filling apparatus. Prior to filling with propellant, 50 µl metering valves were crimped on to the canister neck using a pneumatic crimper. All apparatus have been described in Chapter Two, Section 2.2.5.2.1. Formulations were prepared in HFA 134a, as results from Turbiscan investigations suggested adsorbed surfactant containing formulations to exhibit a more favourable suspension performance in this propellant when compared with HFA 227. Again formulations were prepared at a concentration of 0.2 % w/w to allow comparisons with Turbiscan results to be made. Initial steps in SPF testing involved the actuation of sample canisters according to a dedicated protocol. As such, canisters were placed in an inverted position within plastic actuators, and manually shaken for ten seconds. A waste shot was then fired to ensure no blockage of the metering valve had occurred. Canisters were then held in the inverted position for an ascribed period of time, after which point a priming shot was fired to waste, thereby allowing a sample from the suspension bulk to be collected anew in the chamber of the metering valve. In this way, separation of suspended material over an increasing period of time following shaking could be assessed (T=0, 10, 20 and 60 s). This test shot was then fired onto a filter paper (1.6 µm Whatman GF/A) housed within a glass dose collection apparatus, attached to a vacuum.

3.8.1.2 High performance liquid chromatography assay

A high performance liquid chromatography (HPLC) assay was then employed to assay doses for TS content. A protocol previously devised and validated by AstraZeneca was adopted. As such, filter papers were washed with a phosphate buffer containing 0.05 M of a previously prepared 1.0 M phosphate buffer in purified water (at pH 2.5). All washings were collected in 250 ml volumetric flasks and made up to volume with 0.05 M phosphate buffer. An HPLC assay was then executed using a Hewlett Packard LC106 high performance liquid chromatograph fitted with a thermostatted column compartment and an ultraviolet (UV) detector (Hewlett Packard, US) according to the conditions listed in Table 3.9. Stock and working standard solutions of TS were prepared (nominally 0.1 mg/ml and 0.5 µg/ml respectively) using a sample previously analysed for percentage purity and moisture content. System suitability tests were carried out according to protocol to ensure

acceptable limits for peak resolution, tailing factor, repeatability of injections and repeatability of standards. A system suitability solution containing nominally 0.5 µg/ml TS and 0.15 µg/ml 3,5-dihydroxybenzoic acid in 0.05 M phosphate buffer was prepared. Limits imposed on system suitability may be seen in Table 3.10.

Table 3.9 HPLC conditions imposed on washings from SPF testing

Chromatography Conditions	
Column	Hichrom Kromasil C_{18} column (5 µm packing), 15 cm x 0.46 cm i.d.
Mobile Phase	0.01 M phosphate buffer in 4.5 % ethanol
Blank	0.05 M phosphate buffer
Injection Volume	100 µl
Flow Rate	1.5 ml/min
Column Temperature	45 °C
Detection Wavelength	210 nm
Approximate Run Time	5 min

Table 3.10 System suitability conditions imposed on HPLC assay

System Suitability Criteria	
Blank	Acceptable baseline with no interfering peaks
Peak Resolution	> 2.0
Peak Tailing Factor	< 2.0
Injection Repeatability	Coefficient of variance < 2.0 %
Standard Repeatability	1 ± 0.02

3.8.1.3 CALCULATION OF TERBUTALINE SULPHATE MASS PER ACTUATION

Atlas software (Thermo Labsystems) was used to analyse results from HPLC according to Equation 3.1.

$$TS(\mu g) = \frac{A_{sam}}{A_{std1}} \times \frac{W_{std1} \times (100 - M_{std}) \times P_{std} \times V_{sam}}{5 \times 10^8} \times 1000 \quad \text{(Equation 3.1)}$$

Where A_{std1}: Mean peak area of first TS working standard solution

A_{sam}: Mean peak area of sample

W_{std1}: Weight (mg) of TS reference standard in first TS stock standard solution

M_{std}: Moisture content of TS reference standard (% w/w)

P_{std}: Purity of TS reference standard (% w/w)

V_{sam}: Sample dilution (ml) i.e. 250

3.8.2 RESULTS AND DISCUSSION

Results from SPF testing may be observed in Figure 3.32. An initial interpretation of the results suggest that a comparison of suspension performances for a TS control formulation and that of adsorbed surfactant containing formulations support the results previously obtained from Turbiscan analysis. Formulations examined in this study were prepared in HFA 134a, and therefore over time will tend to sediment. As time following canister shaking elapses, mass of TS per actuation was observed to increase. This is consistent with collection of suspended material at the bottom of the canister, allowing a greater proportion of TS to be collected within the metering valve chamber with each shot fired. While a TS control formulation exhibited a sharp increase in mass of TS per actuation between the 10 and 20 second measurement time points, both surfactant formulations remained constant. This increase in mass of TS per actuation for the control formulation appeared to lose momentum over the remainder of the experiment, and was seen to increase only slightly between 20 and 60 second measurement time points.

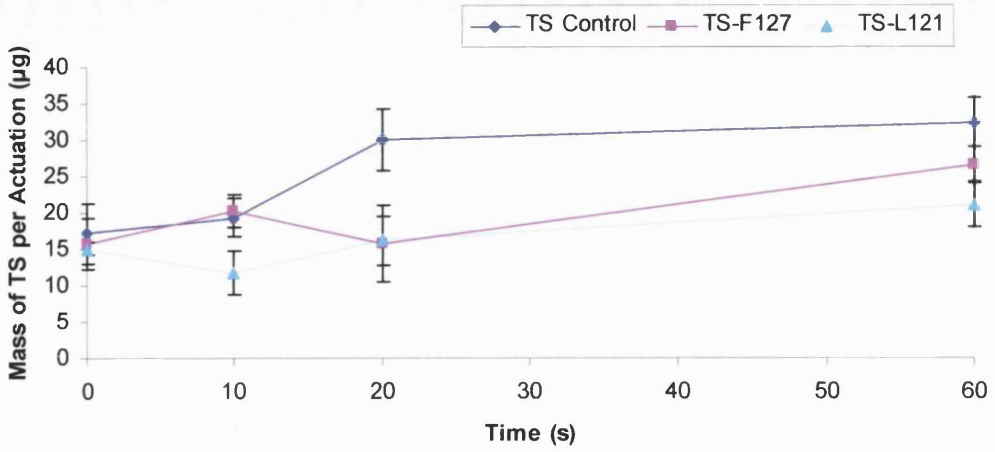

Figure 3.32 Shake-Pause-Fire results for three TS formulations tested

While surfactant formulations did show an overall increase in mass of TS per actuation over the course of the experiment, it was to a lesser extent than the control formulation, and at a slower rate. A comparison of the two adsorbed surfactant containing formulations reveals a greater increase in stability of the TS-L121 formulation, seen as a smaller increase in mass of TS per actuation over 60 seconds. However, error limits are such that this cannot be conclusive. While Turbiscan experiments were carried out over a three minute period, extensive separation of unstable formulations was observed over the first minute of analysis. As such, it is reasonable to compare suspension performance results from both methods of analysis (in HFA 134a only), over a 60 second period. Again however, the protocols followed pertaining to the shaking of dispersions prior to testing differ; with sonication adopted for Turbiscan experiments, and a 10 second manual shaking period for canisters used in SPF testing. While formulations were prepared at identical concentrations, they were contained in different vessels, specifically a glass measurement cell in the case of Turbiscan experiments, and aluminium canisters in the case of SPF testing. It would seem prudent therefore to use results from SPF testing as an additional insight into pMDI suspension performance for the formulations examined, that may only be loosely compared to those obtained over the first minute of investigation for identical formulations in HFA 134a using Turbiscan analysis.

With regard to the possible mechanism of suspension stabilisation at work in the formulations tested, the consensus view is that in non-aqueous systems such as those under investigation here, the possibility of electrostatic interactions contributing to suspension stability may be discounted. Work conducted by Kitahara investigating a relationship between electrostatic repulsive force, zeta potential (ζ) and dielectric constant produced a theory stating that unless suspended particles were large and possessed a substantial ζ, electrostatic stabilisation would be ineffective in non-polar media, thus declaring that steric mechanisms of stabilisation would be the dominant forces at play in such systems (1974). Subsequent work on non-aqueous dispersions of carbon black confirmed the need for a large ζ in order to allow effective electrostatic stabilisation (Pugh et al., 1983). As such, the improvement in suspension performance achieved in this work is likely due to steric repulsive forces between surfactant chains projecting outward from the surface of drug molecules into the HFA propellant. The magnitude of these repulsive forces is known to depend in part on adsorbed layer thickness, serving to increase inter-particle distance thus allowing long range van der Waals repulsive forces to dominate. Unfortunately the extent of surfactant adsorption to TS remains unknown in this work. Previous studies attempting to elucidate the adsorption characteristics of block co-polymer surfactants onto hydrophilic surfaces such as silica have suggested that initial adsorption involves hydrophilic PEO moieties attaching to surfaces through hydrogen bonding as expected. However, in time PPO moieties will also adsorb to the surface (Killman et al., 1988). Considering that the theory of steric stabilisation relies on the projection of part of the polymer molecule away from the surface, the possibility that all of the polymer may eventually adsorb to the surface would throw doubt on the effectiveness of that polymer to increase inter-particle distance. However, it has been further suggested in the literature that block co-polymer surfactants may adsorb to hydrophilic surfaces in a bilayer as PPO moieties from fresh polymers arrive at the particle surface and interact with other PPO chains anchored by PEO adsorption (Van Lent, 1989; Malmsten et al., 1992). Formation of such a bilayer would increase the adsorbed layer thickness, thus giving rise to stabilisation by steric means. There remains the problem of questionable transference of adsorption theories elucidated in aqueous media to non-aqueous systems however and as such the exact mechanism of adsorption and subsequent suspension stabilisation observed in TS-surfactant formulations may only be

speculated upon. Further investigations focussing on these particular systems are required to construct a dedicated theory of surfactant adsorption behaviour and stabilisation mechanisms.

3.9 SUMMARY AND CONCLUSIONS

Work detailed in Part B of this chapter has examined the effect of surfactant adsorption to the surface of TS on pMDI suspension performance in HFA propellants. Some success has been achieved with regard to suspension stabilisation in formulations containing adsorbed surfactant. Although a wide range of suspension performances were observed, all of the surfactant-containing formulations showed some improvement in suspension performance over a TS control formulation in terms of both a reduced separation rate and flocculation. Attempts to discover a relationship between surfactant molecular structure and suspension performance were unsuccessful, as previous attempts to explain powder surface energy in the same terms had also been. The consensus view is that in non-aqueous systems such as those found in pMDI formulations, electrostatic stabilisation does not play a part in reducing suspended particle aggregation. Instead it is understood that surfactants confer stabilisation on these systems through steric mechanisms serving to increase inter-particle distances. Work previously published suggests non-ionic surfactants may adsorb to hydrophilic surfaces in the form of a bilayer although this may only be suggested as a possible adsorption mechanism allowing steric stabilisation in the systems investigated in this work. Results from Parts A and B of this chapter have revealed two distinct formulation characteristics that have altered following surfactant adsorption, those of powder surface energy and suspension performance. The final part of this chapter will investigate a possible relationship between these two characteristics in the hope of gaining a greater understanding of the influence of powder surface energy on pMDI suspension behaviour in HFA propellants.

PART C: CORRELATION BETWEEN SURFACE ENERGY AND pMDI SUSPENSION STABILITY

3.10 INTRODUCTION

The relationship between powder surface energy and pMDI suspension stability has been discussed in Section 3.3.6. A reduction in powder surface energy is desirable as particles for inhalation exist in a pMDI suspension system with highly energetic surfaces by virtue of their very small particle size. Any reduction in surface energy caused by particle manipulation will consequently reduce the tendency for particles to aggregate in order to minimise their total surface free energy. Work already presented in the first two parts of this chapter has reported both a reduction in powder surface energy and an improvement in pMDI suspension performance following adsorption of various non-ionic surfactants to the surface of TS. In the final part of this chapter, attempts to relate these two findings using equations developed to describe the complicated interactions at play at system interfaces will be detailed. This will test the hypothesis that a reduction in surface energy gives rise to an improvement in suspension performance. Further discussion of such equations may be found in Chapter One.

The concept of a surface energy interaction (SEI) in aerosol systems was first discussed by Cline and Dalby (2002). Using theory developed by van Oss describing the interfacial tension of two liquids in terms of three components of interfacial surface energy, namely dispersive, Lewis acid and Lewis base, Cline and Dalby attempted to predict performance of a dry powder inhaler (DPI) based on surface energy results obtained from IGC analysis. In this way, a surface energy interaction between drug and carrier particles was expressed in an equation as an interrelationship between powder surface energy parameters of both phases. The SEI value subsequently obtained was then plotted against fine particle fraction (FPF), an indicator of DPI performance measured by cascade impaction. Results published by Cline and Dalby found a good correlation between a calculated SEI and measured FPF (r^2=0.928). It is hoped that application of this approach to data obtained for TS-surfactant formulations in previous studies may reveal similar correlations linking suspension performance with powder surface energy. In addition to investigating a correlation with SEI values, correlations between suspension performance and

individual components of powder surface energy will also be investigated to determine whether influence of surface energy on suspension performance may be ascribed to one parameter in particular rather than total surface energy.

3.11 EXPERIMENTAL PROTOCOL

3.11.1 CALCULATION OF SURFACE ENERGY INTERACTION USING VAN OSS THEORY

SEI values for all formulations were calculated according to the equation used by Cline and Dalby (2002) based on theory originally developed by van Oss (1994). Rather than relate the SEI value to FPF as was pertinent to a study on DPI performance, here SEI was related to the reduction in mean backscattering (RMB) calculated for each pMDI formulation obtained from Turbiscan analysis. This value had been previously chosen as an indicator of suspension performance. As such, the following equation was used:

$$RMB = 2(\gamma^{D}_{1} \cdot \gamma^{D}_{2})^{1/2} + 2(K_{A1} \cdot K_{D2})^{1/2} + 2(K_{A2} \cdot K_{D1})^{1/2} \quad \text{(Equation 3.2)}$$

where *1*: TS-surfactant formulation

2: HFA propellant

Published values for propellant surface tension were used (Solvay Fluor und Derivate GmBH, Germany). Powder surface energy results obtained from IGC analysis were substituted into the equation appropriately, producing a SEI value in mJ/m^2. Once calculated, SEI values were plotted against RMB to investigate a possible correlation.

3.11.2 CORRELATION BETWEEN pMDI SUSPENSION STABILITY AND POLAR SURFACE ENERGY PARAMETERS

Using values for RMB in addition to values for polar components of surface energy obtained from IGC analysis, the influence of polar surface energy on suspension performance was investigated for all formulations by plotting RMB against K_A, K_D and K_D/K_A values.

3.11.3 DETERMINATION OF MODEL PROPELLANT SURFACE ENERGY PARAMETERS USING SURFACE TENSION MEASUREMENTS

While the volatile propellant systems employed in pMDI suspension formulation are regarded as non-polar in nature, it is accepted that HFA propellants exhibit increased polarity in comparison to CFCs (Rogueda, 2003). This is evident in the higher values for HFA propellant dielectric constant and dipole moment when compared to those of CFC propellants (Chapter One, Table 1.2). Initial calculation of SEI values was based on the assumption of non-polarity of HFA propellants. As such, in order to investigate whether a small polar element of propellant surface energy would affect any SEI values and subsequent correlations with suspension performance, surface energy parameters of the HFA propellants under investigation were necessary. As these are both volatile molecules, existing as gases at room temperature and pressure, standard methods of measuring surface tension cannot be applied. Initial attempts to estimate a solubility parameter for each propellant using the group contribution method of van Krevelen were unsuccessful, as all functional groups expressed in HFA 134a and HFA 227 were classified non-polar (1990). Instead, it was decided to investigate the surface energy parameters of a model propellant 2H, 3H-Decafluoropentane. These were deduced from surface tension measurements using a Dynamic Contact Angle analyser (Cahn Instruments, USA). This technique is fully described in Chapter Two Section 2.2.9. The use of a model propellant allows an approximation of surface energy parameters for HFA 134a and HFA 227 to be calculated, by analysing a material structurally similar to the HFA propellants of interest, which exists in a liquid state at room temperature. Hence surface tension measurements may be carried out under ambient conditions. The surface tension of the model propellant was measured against three surfaces, that of glass, Parafilm, and finally polymethyl methacrylate (PMMA). Preparation of a PMMA surface was carried out by coating glass slides with a 6 % solution of PMMA in toluene as described previously by van Oss et al., (1993). Five surface tension determinations were made for each surface. Surface tension measurements were then used to calculate individual surface energy parameters of the model propellant using a number of equations previously described in Chapter One.

3.11.4 MODIFIED CORRELATIONS USING MODEL PROPELLANT DATA

Using surface energy parameters calculated for the model propellant 2H, 3H-Decafluoropentane, correlations originally investigated between SEI and pMDI suspension performance were modified. As such, surface tension values for HFA 134a and HFA 227 were replaced with dispersive and polar components of model propellant surface energy and SEI values were re-calculated for all formulations. Amended SEI values were then once again plotted against a reduction in mean backscattering for all formulations tested.

3.12 RESULTS AND DISCUSSION

3.12.1 CALCULATED SURFACE ENERGY INTERACTION VALUES AND THEIR CORRELATION WITH SUSPENSION PERFORMANCE

Table 3.11 lists SEI values for all TS-surfactant formulations in both HFA propellants calculated using a modified version of Equation 3.2, adopted by Cline and Dalby (2002). HFA propellants were initially assumed to be non-polar systems in line with convention, and therefore without K_A and K_D components to their surface energy. As such, published values for liquid surface tension of propellants were assumed to consist of dispersive forces only, and these values were substituted for γ^D in Equation 3.2. It was therefore necessary to use an abridged form of Equation 3.2, ignoring the elements describing polar components of surface energy (Equation 3.3).

$$RMB = 2(\gamma^D{}_1 \cdot \gamma^D{}_2)^{1/2} \qquad \text{(Equation 3.3)}$$

Table 3.11 Surface energy interaction values for all TS-surfactant formulations

	SEI in HFA 227 (mJ/m^2)	**SEI in HFA 134a (mJ/m^2)**
Micronised TS	40.64	44.68
TS control	39.55	43.48
TS-F108	33.76	37.10
TS-L31	34.12	37.50
TS-31R1	33.05	36.33
TS-F127	33.58	36.91
TS-B39	34.24	37.64
TS-B59	34.30	37.70
TS-MMG	34.03	37.41
TS-L101	30.93	34.00
TS-L121	30.48	33.51
TS-Span 20	33.80	37.16
TS-Span 85	34.63	38.06
TS-Oleic Acid	33.82	37.18

As expected given that SEI values have been calculated using IGC data, adsorption of surfactant to the surface of TS has reduced the SEI value of both micronised TS and a TS control formulation to varying extents depending on the surfactant present. Considering for a moment the significance of an SEI value, it should describe the interaction at the interface of a suspended drug-surfactant particle and propellant in the pMDI suspension formulations investigated here. As such, a reduction in the magnitude of this interaction following surfactant adsorption would suggest a corresponding reduction in suspension stability. This may be explained in terms of two competing forces where a strong interaction between suspended particle and propellant would surely act against a tendency for particle aggregation. However, results from Turbiscan analysis contradict this theory, as surfactant-containing formulations were found to exhibit some improvement in suspension performance. The reduction of SEI values observed concomitantly with an increase in FPF by Cline and Dalby allowed an explanation of improved formulation performance in terms of a more efficient release of drug from the carrier molecule. However, as described previously, there is more than one interface to consider in a complex pMDI formulation. While a reduction in the interaction between suspended particles and propellant might be thought to reduce the stability of the system, the benefits of a reduced surface energy in terms of particle aggregation may outweigh the supposed

disadvantage. Plots of SEI values versus RMB are shown below, with each group of surfactant formulations plotted independently. The term POEAE refers to the polyoxyethylene alkyl ether surfactants Biodac B39 (B39), Biodac B59 (B59) and Marlipal MG (MMG) while the term "miscellaneous surfactants" refers to Span 20, Span 85 and Oleic Acid.

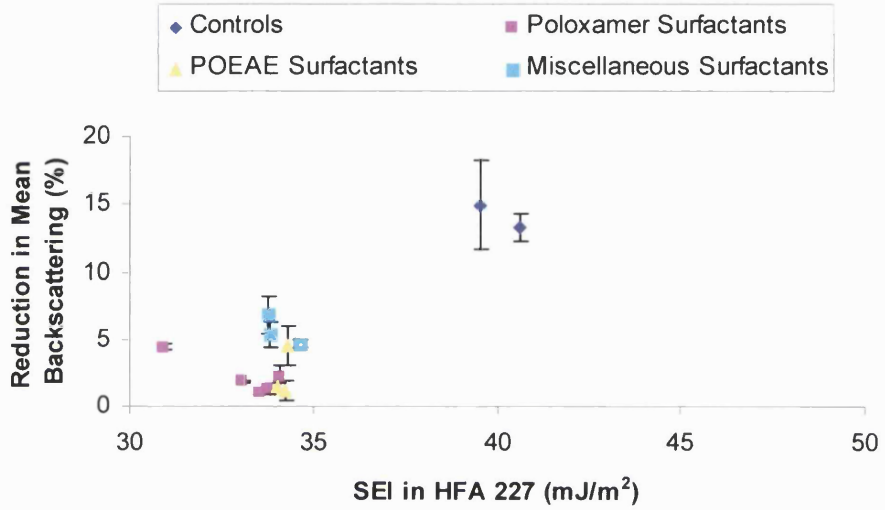

Figure 3.33 Correlation between SEI and RMB (HFA 227)

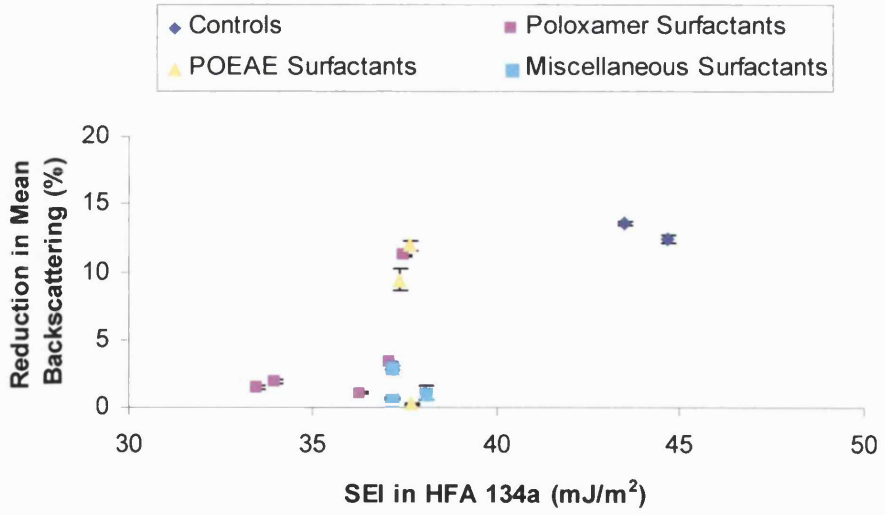

Figure 3.34 Correlation between SEI and RMB (HFA 134a)

Figures 3.33 and 3.34 go some way to confirm a suggested correlation between a reduction in powder surface energy in surfactant-containing formulations and an

improvement in pMDI suspension performance, particularly in the case of formulations suspended in HFA 227. On consideration of individual surfactant groups, it would appear that despite possessing similar SEI values, POEAE surfactants display a range of suspension performances, where a single value for RMB might have been expected. In fact it seems that poloxamer surfactants adhere closest to the correlation of all surfactant groups examined. Only the influence of the dispersive component of surface energy has been considered here, and it is possible that polar components may also influence suspension stability. In light of this possibility, correlations between K_A and K_D with RMB were subsequently investigated.

3.12.2 Correlation between pMDI suspension stability and polar surface energy parameters

Similar to the graphs observed in the previous section, values for polar surface energy components for all formulations obtained from IGC analysis were plotted against RMB taken from Turbiscan measurements. Again surfactants have been plotted in groups.

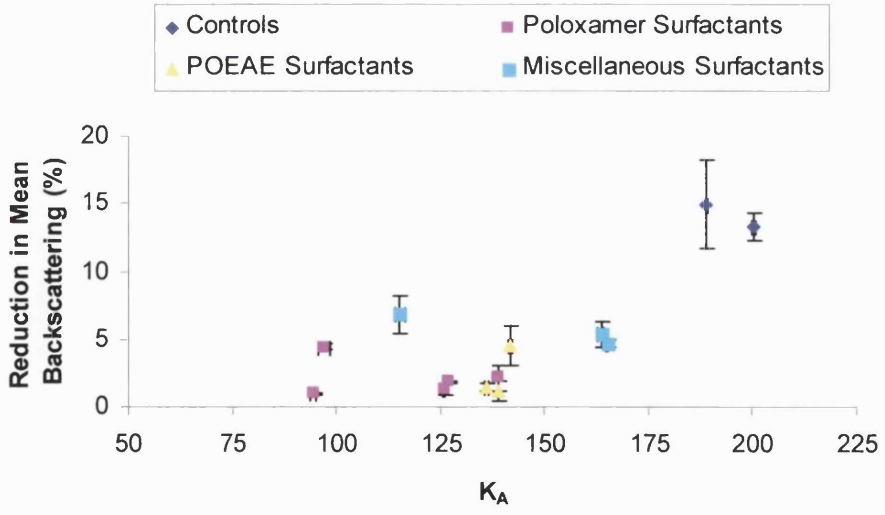

Figure 3.35 Correlation between K_A values of surface energy and RMB (HFA 227)

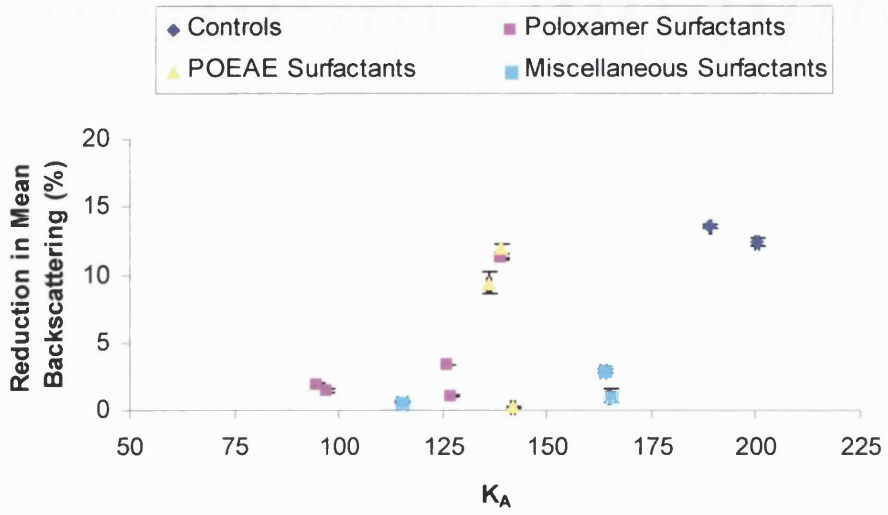

Figure 3.36 Correlation between K_A values of surface energy and RMB (HFA 134a)

The following figures plotting a relationship between K_D, the basic component of powder surface energy, in addition to the K_D/K_A ratio with RMB do not contain data points for formulations containing Span 20, Span 85 and Oleic Acid. A decision to omit K_D values for these formulations from further data analysis was made, due to the return of negative values from IGC analysis.

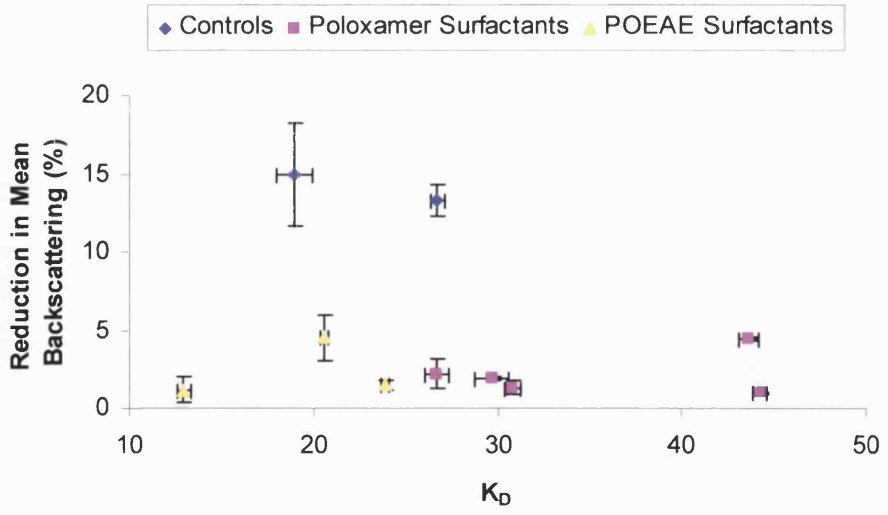

Figure 3.37 Correlation between K_D values of surface energy and RMB (HFA 227)

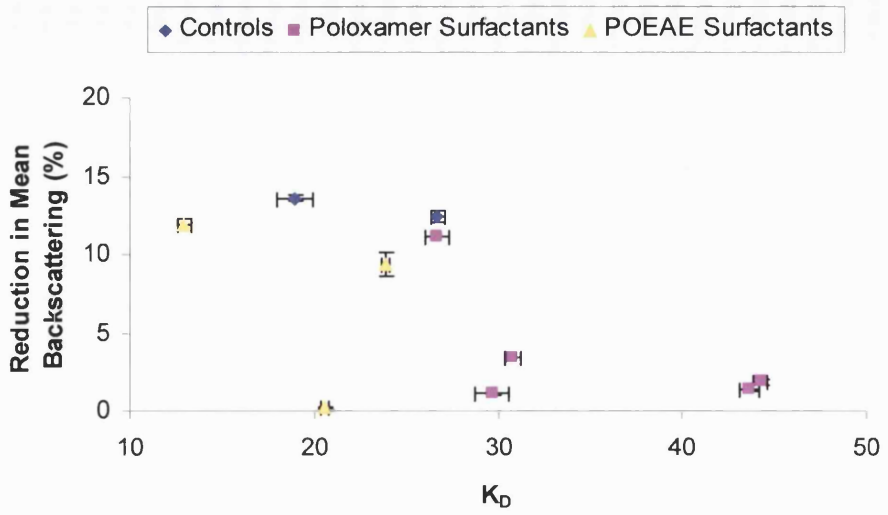

Figure 3.38 Correlation between K_D values of surface energy and RMB (HFA 134a)

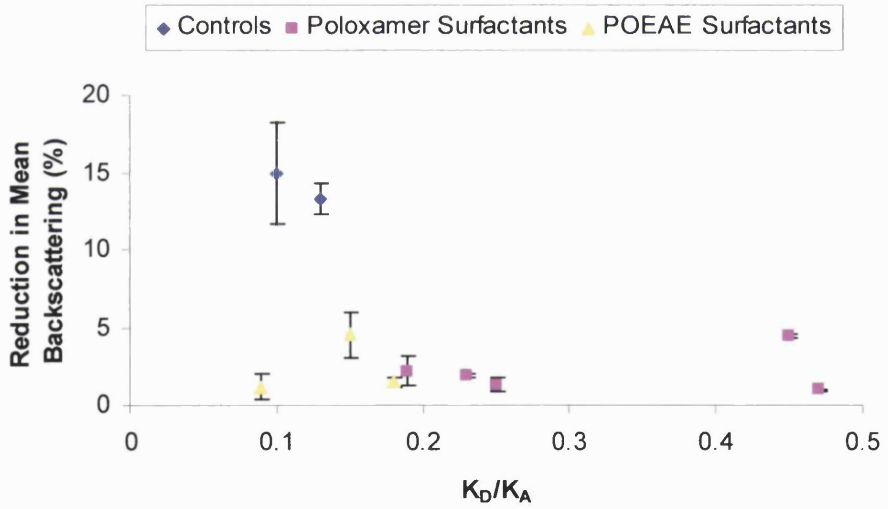

Figure 3.39 Correlation between K_D/K_A ratio and RMB (HFA 227)

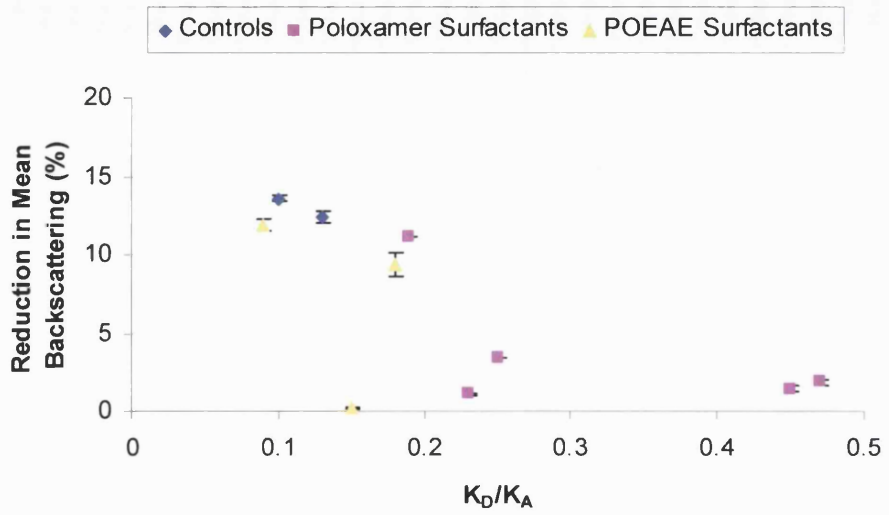

Figure 3.40 Correlation between K_D/K_A ratio and RMB (HFA 134a)

Examination of plots relating polar components of surface energy with suspension performance reveal an additional link between a reduction in K_A values and improved suspension stability, particularly in formulations suspended in HFA 227. Conversely, no discernible relationship between suspension performance and K_D was observed. This confirms initial suspicions that the unpredictable changes in the basic component of surface energy following surfactant adsorption observed in IGC results discounted this particular surface energy parameter from having an influence on suspension performance. As such, the correlation between K_D/K_A ratio and suspension performance displayed in Figures 3.39 and 3.40 is due primarily to the influence of K_A values but has been masked somewhat by the interference of K_D values. It is possible that the reduced magnitude of K_D values with respect to K_A values is the reason why K_D values have apparently not altered according to the same pattern as values following surfactant adsorption.

3.12.3 SURFACE ENERGY PARAMETERS OF MODEL PROPELLANT FROM SURFACE TENSION MEASUREMENTS

Results from surface tension measurements are displayed in Table 3.12.

Table 3.12 Surface tension measurements of model propellant on a range of surfaces

	Surface Tension (dynes/cm ± SD; n=5)
Glass	11.42 (0.31)
Parafilm	8.26 (0.37)
PMMA	12.2 (0.29)

Surface tension measurements listed in Table 3.12 were used to deduce individual surface energy components of the model propellant 2H, 3H-decafluoropentane. Firstly, surface tension measurements with glass, and with Parafilm were substituted into Equation 3.4. Glass is assumed to provide a measurement for total surface energy (γ^{Total}) as a result of measurement on a surface with zero contact angle. In the case of Parafilm, this surface interacts with other materials through dispersive forces alone, and therefore is assumed to provide a measurement for γ^{LW}.

$$\gamma^{Total} = \gamma^{LW} + \gamma^{AB} \qquad \text{(Equation 3.4)}$$

The value of 3.16 mJ/m^2 was subsequently obtained for γ^{AB}. Literature values for surface energy components of PMMA show this surface lacks the ability to interact with other materials through Lewis Acid forces. As such, the γ^{AB} value for this surface is equal to zero, while γ^- is seen to equal 20.4 (van Oss et al., 1993). It follows that any polar interaction of a PMMA surface with the model propellant involved Lewis Base groups on PMMA and corresponding Lewis Acid groups on model propellant. Therefore, the value of 3.16 mJ/m^2 obtained for γ^{AB} of the model propellant reflects an interaction due solely to Lewis Acid forces or γ^+. The value of γ^+ for the model propellant was then calculated according to Equation 3.5, expressing the relationship between γ^{AB} and both γ^- and γ^+. Once this was obtained, values were again substituted into a combination of Equations 3.4 and 3.5 to solve for γ^-. Surface energy parameters of the model propellant deduced from these calculations are listed in Table 3.13.

$$\gamma^{AB} = 2\sqrt{\gamma^{+}\gamma^{-}} \qquad \text{(Equation 3.5)}$$

Table 3.13 Surface energy parameters of model propellant deduced from surface tension measurements. All values expressed in mJ/m^2

γ^{LW}	γ^{+}	γ^{-}
8.26	2.50	1.0

As expected, the model propellant is found to have a small polar component of surface free energy. These values will now be used to amend previously calculated SEI values for all formulations tested.

3.12.4 Modified correlations using model propellant data

Figures 3.41 and 3.42 display plots of modified SEI values (calculated using model propellant surface tension data) against RMB. SEI values describing the interaction between model propellant and TS-surfactant microparticles for each formulation have been used twice, plotted initially against RMB in HFA 227, and subsequently against RMB in HFA 134a. Once again, formulations containing Span 20, Span 85 and Oleic Acid were not considered here due to negative K_D values obtained for these formulations from IGC analysis.

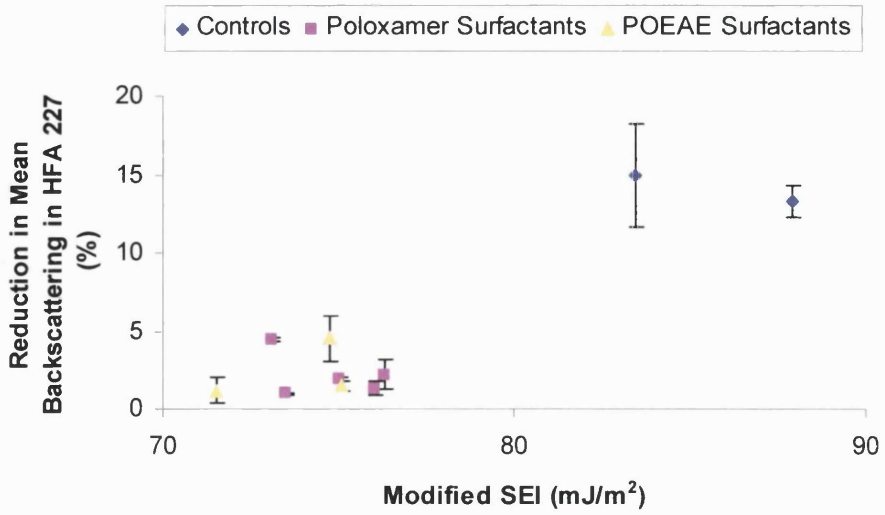

Figure 3.41 Modified SEI plotted against RMB in HFA 227

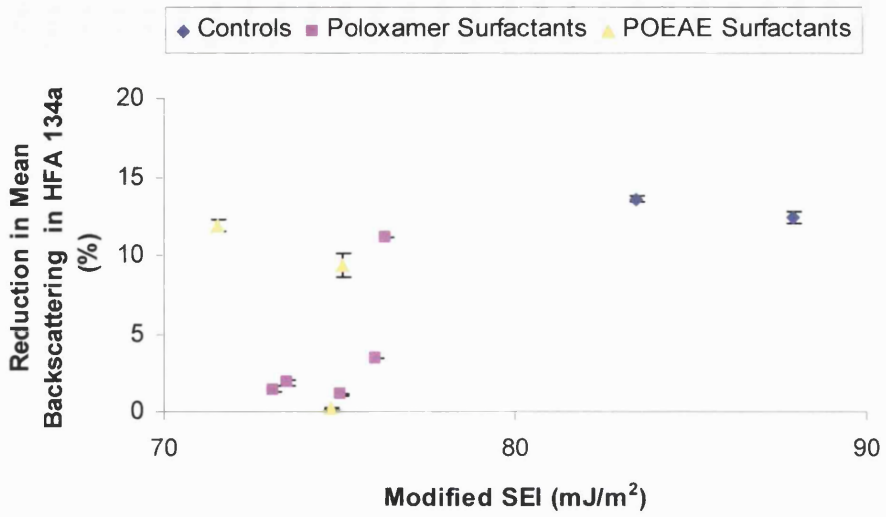

Figure 3.42 Modified SEI plotted against RMB in HFA 134a

These plots represent the first attempt to describe as fully as possible the interaction between propellant and suspended particle, taking into account all components of surface energy. Considering the encouraging findings of previous correlation plots suggesting a relationship between both dispersive component and acidic component of surface energy of TS-surfactant microparticles and corresponding suspension performance, it is disappointing that Figures 3.41 and 3.42 do not show a more convincing correlation. This is particularly disappointing in the case of Figure 3.41, as the model propellant used is known to be a closer model for HFA 227 (Rogueda, 2003). Again however, it is likely that the unpredictable changes to K_D values observed following surfactant adsorption have masked any correlation that may have been otherwise apparent.

3.13 SUMMARY AND CONCLUSIONS

Work described in Part C of this chapter has attempted to elucidate a relationship between powder surface energy and suspension performance in a pMDI suspension formulation in HFA propellants using results obtained in Parts A and B. Applying theory developed by van Oss and an approach previously used by Cline and Dalby, equations expressing the interaction between suspended microparticles and the propellant in which they are suspended have been employed to calculate a SEI value. Plots of this SEI value against RMB revealed a general trend of improved suspension

performance with reduced powder surface energy but failed to produce a good correlation, even once all components of surface energy had been taken into account using model propellant data. It is possible that while application of this theory was successful in DPI formulations, it is less suited to more complex pMDI formulations where interactions at several interfaces contribute to overall formulation stability. In addition to a reduction in dispersive component of surface energy having a favourable effect on suspension performance, a reduction in K_A value was also seen to be linked with a similar improvement from correlation plots. In contrast, no relationship between alteration in K_D values and suspension performance was observed. It has been suggested that the unpredictable changes in K_D caused by surfactant adsorption have masked any correlation that may exist in plots describing the relationship between all components of surface energy and suspension performance. For this reason, it may perhaps be more useful to examine an abridged form of van Oss theory, considering dispersive and acidic components of surface energy only.

3.14 OVERALL SUMMARY AND CONCLUSIONS FOR CHAPTER THREE

Work detailed in this chapter has attempted to construct a comprehensive picture describing the effect of adsorption of surfactants with a low solubility in HFA propellants onto the surface of a hydrophilic drug TS, and the corresponding effect on pMDI suspension formulation performance. Due to the non-aqueous conditions imposed on surfactant adsorption, attempts to elucidate adsorption characteristics of the surfactants have not been successful. Instead, an indirect indication of successful adsorption was taken from the alteration in powder surface energy of surfactant-containing formulations observed from IGC analysis. The reductions in dispersive and acidic components of powder surface energy caused by surfactant adsorption were subsequently linked to an improvement in pMDI suspension performance. This has been explained in terms of a reduced tendency for particle-particle interactions, therefore retarding particle aggregation and phase separation. No relationship between either surface energy changes or suspension stability improvements with surfactant molecular structure was discovered. Application of van Oss theory following work previously published by Cline and Dalby (2002) was only partly successful in revealing a relationship between reduced surface energy and improved suspension performance. While an effective tool in describing DPI formulation

interactions, it has been suggested that this approach is not suited to more complex formulations such as those contained in pMDI suspensions. In conclusion, this chapter has succeeded in showing that low solubility surfactants may indeed significantly alter pMDI suspension characteristics and contrary to conventional belief may be considered as formulation stabilisers in the search for novel surfactants for HFA pMDI suspension formulations.

3.15 FURTHER WORK

Results from this chapter reaffirm the need to understand adsorption characteristics in non-aqueous media. Unfortunately, further investigations in this area were outside the remit of this work, and were therefore not carried out due to time constraints. Moving forward from the findings of this chapter, a change in drug substrate for surfactant adsorption is planned. As such, the following chapter will investigate similar parameters to those described in Chapter Three, but using micronised budesonide as a substrate in place of micronised TS. It is hoped that additional data obtained using a hydrophobic drug may be considered in conjunction with results from this chapter to gain a greater understanding of both low solubility surfactant adsorption and the corresponding effects on pMDI suspension performance.

CHAPTER FOUR

PREPARATION AND CHARACTERISATION OF BUDESONIDE-SURFACTANT MICROPARTICLES

4 PREPARATION AND CHARACTERISATION OF BUDESONIDE – SURFACTANT MICROPARTICLES

PART A: PARTICLE ENGINEERING

4.1 INTRODUCTION

Studies discussed in Chapter Three relate to the effect of surfactant adsorption to the surface of a model hydrophilic drug, micronised TS. The work detailed in the first part of this chapter concerns the effect of using an alternative substrate drug for formulation with surfactant, namely the model hydrophobic micronised drug, budesonide. An identical portfolio of non-ionic surfactants to that used in Chapter Three will be discussed, comprising a range of poloxamer surfactants, polyoxyethylene alkyl ether surfactants and other miscellaneous non-ionics such as Span 20, Span 85 and Oleic Acid. By characterising the budesonide-surfactant formulations, in particular their powder surface energy, it is hoped that any differences in surfactant adsorption or incorporation resulting from the different substrate nature may be identified. Parts B and C of this chapter will discuss pMDI suspension performance, and explore relationships between powder surface energy and pMDI suspension performance, of those surfactant containing budesonide formulations prepared in Part A.

4.2 PRELIMINARY STUDY: PREPARATION OF BUDESONIDE-SURFACTANT MICROPARTICLES USING AN INCUBATION METHOD

The aim of this work was to allow a direct comparison between surfactant-containing microparticle characteristics prepared with substrates TS and budesonide. Preparation of TS-surfactant microparticles had been carried out using an incubation method to facilitate surfactant adsorption on to the surface of the micronised drug. As such, initial attempts to prepare budesonide-surfactant microparticles also followed an incubation method. However, in light of the fact that dichloromethane, chosen as a non-solvent for TS formulations, is a very good solvent for budesonide, it was decided to use purified water in all incubation studies involving budesonide. An initial study examined the feasibility of preparing budesonide-surfactant microparticles according to the adsorption protocol previously described in Chapter Three, and focused on two poloxamer surfactants F127 and F108. In light of

surfactant adsorption taking place in an aqueous environment, the use of a colorimetric assay previously discussed in Chapter Three and originally described by Baleaux was possible to assess the extent of surfactant adsorption to the surface of micronised drug (1972).

4.2.1 EXPERIMENTAL PROTOCOL

4.2.1.1 POLOXAMER SURFACTANT ADSORPTION TO MICRONISED BUDESONIDE

Experimental conditions imposed in the preparation of terbutaline sulphate-surfactant microparticles described in Chapter Three were used here. As such 0.2 g of micronised drug was incubated in two solutions of poloxamer surfactants F127 and F108. Surfactant solutions were prepared at a concentration of 200 mg/L in purified water, and incubated in a shaking water bath (Grant) maintained at a temperature of 25 °C for a period of three hours. Following incubation, surfactant solution was isolated from suspended drug-surfactant microparticles in order to assay for poloxamer content remaining after incubation. Samples were centrifuged at 15,000 rpm for 20 minutes in a Beckman Avanti centrifuge (rotor JA25.50). Drug-surfactant microparticles were harvested following removal of the supernatant and dried in an oven maintained at a temperature of 50 °C for three days (Columbano, 2000).

4.2.1.2 ULTRA VIOLET SPECTROSCOPY ASSAY FOR POLOXAMER ADSORPTION

Calibration curves for F127 and F108 concentration in purified water were constructed. Stock solutions of the surfactants in question were prepared by dissolving a known amount of surfactant in purified water and making up to volume. Serial dilutions were made producing a number of poloxamer solutions of concentrations varying from 20 to 5 mg/L. The supernatant of samples used in adsorption studies described in Section 4.2.1.1 was then isolated by centrifugation and analysed using the standard assay for poloxamers previously detailed in Chapter Three, Section 3.2.3 (Baleaux 1972). As such, 10 ml of the supernatant was diluted to 100 ml with purified water. This was then reacted with a stock standard indicator solution, comprising 1 g iodine (BDH) and 2 g potassium iodide (BDH) dissolved in 100 ml purified water at room temperature. Once produced, the indicator solution may be kept for one week, provided it is protected from light. The absorbance of the

resulting solution was measured at a wavelength of 500 nm in an Ultrospec 2000 UV/Vis spectrophotometer (Pharmacia Biotech, UK). Calibration curves for both F108 and F127 were then constructed.

4.2.1.3 POWDER CHARACTERISATION

Preliminary investigations into the characteristics of drug-surfactant microparticles prepared by incubation were carried out. As such, the particle size of budesonide-surfactant microparticles in addition to that of a budesonide control sample was analysed using laser light scattering in a Malvern Mastersizer S (Malvern, UK) according to the method described in Chapter Two. Unlike TS formulations which were sized in chloroform, the particle size of budesonide-containing formulations was investigated in purified water. Suspension stability of pMDI formulations containing drug-surfactant particles was also investigated. In line with previous pMDI sample preparation, suspensions were prepared in both HFA propellants at a concentration of 0.2 % w/v by a pressure-filling method also described in Chapter Two. Samples were analysed using the Turbiscan apparatus according to the standard scanning protocol adopted throughout this work.

4.2.2 RESULTS AND DISCUSSION

4.2.2.1 POLOXAMER SURFACTANT ADSORPTION TO MICRONISED BUDESONIDE

Calibration curves describing the concentration of the two poloxamer surfactants chosen in purified water were prepared, and are presented in Figures 4.1 and 4.2. The magnitude of standard deviation values was such that they were indistinguishable from mean values on the axes scale employed.

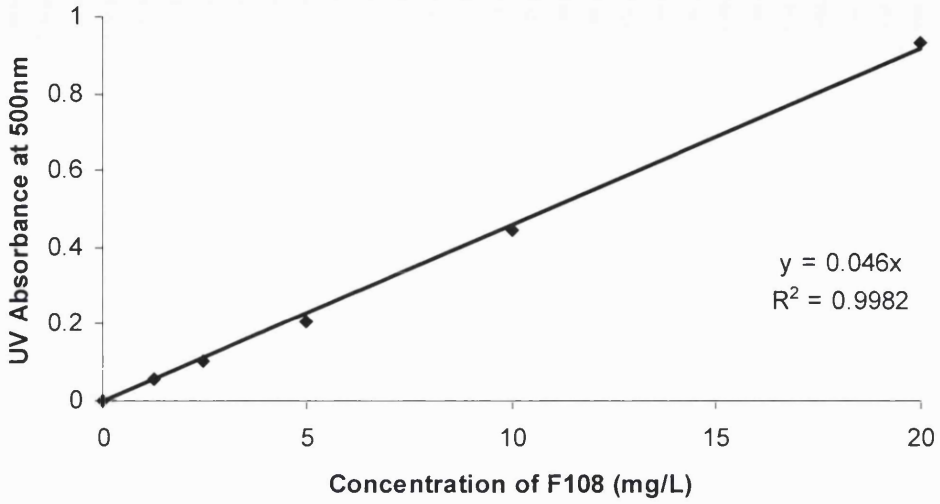

Figure 4.1 Calibration curve for F108 concentration in purified water (n=3)

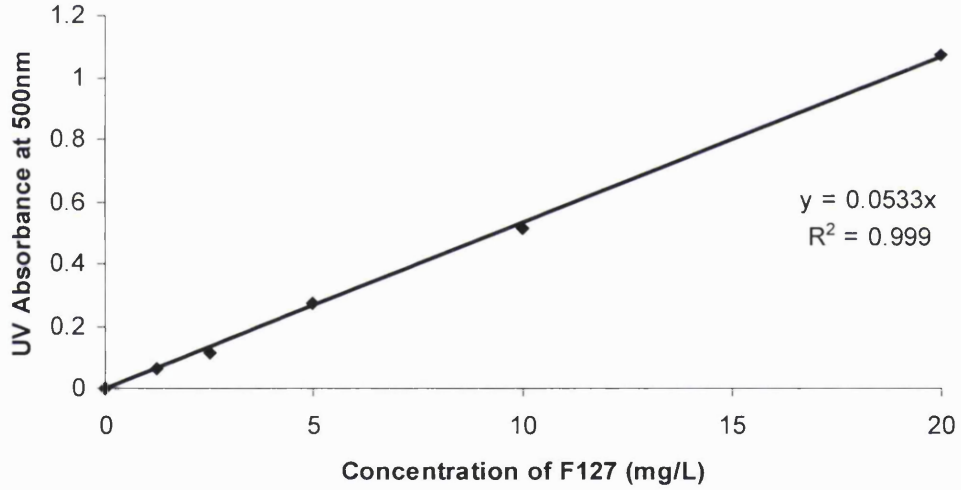

Figure 4.2 Calibration curve for F127 concentration in purified water (n=3)

From these calibration curves, it was possible to calculate the concentration of poloxamer surfactant remaining in the supernatant following incubation with micronised budesonide and centrifugation to remove suspended material. Subsequent calculations allowed an indirect measurement of the amount of surfactant to have adsorbed onto the drug surface during incubation. Amounts of adsorbed surfactant are listed in Table 4.1 expressed in mg/g of micronised drug.

Table 4.1 Amount of surfactant adsorbed to the surface of micronised budesonide from a 200 mg/L solution

	Amount of surfactant adsorbed (mg/g of micronised drug ± SD, n=3)
F108	3.60 (0.65)
F127	6.59 (1.65)

Results observed in Table 4.1 reveal successful adsorption of the two poloxamer surfactants in question on to the surface of micronised budesonide. Adsorbed values appear small, however as discussed in Chapter Three, Section 3.3.2, previously published work has described small amounts of adsorbed surfactant successfully modifying several physicochemical properties of various drug substrates.

4.2.2.2 POWDER CHARACTERISATION

Results from particle size analysis by laser light scattering are listed in Table 4.2.

Table 4.2 Particle size of drug-surfactant microparticles prepared by incubation (B=budesonide)

Formulation	Volume Mean Diameter (μm ± SD, n=5)	Span (co-efficient of spread)
Micronised Drug	3.30 (0.27)	3.98
B-F127	20.80 (1.73)	2.92
B-F108	16.11 (6.60)	4.04

Despite repeated sonication of samples prior to investigation of particle size; drug-surfactant microparticles prepared by incubation appeared to exhibit irreversible aggregation resulting in an overly large particle size distribution when compared to the initial size of micronised material. The use of a vibratory ball mill in an attempt to reduce particle size was not successful in causing a significant size reduction. Furthermore, the disadvantages of applying comminution techniques such as milling to pharmaceutical powder characteristics are well documented (Ward & Schultz, 1995). Shear forces generated during processing may alter the nature of a powder surface, producing small areas of amorphous material. As discussed previously, areas of amorphicity may cause powders to behave unpredictably, as regions of amorphous material exhibit increased uptake of water molecules with associated re-crystallisation.

Suspension performance of pMDI suspension samples containing budesonide formulations prepared by incubation was subsequently examined using the standard Turbiscan scanning protocol adopted throughout this work. Results are not shown here as suspension stability for formulations containing either F127 or F108 was found to be particularly poor when compared to a control budesonide formulation, and efforts then moved to determining a more suitable method of particle engineering. Reasons for this poor performance were ascribed to the significantly larger particle size of surfactant-containing formulations, allowing for a more rapid phase separation under the rules of Stoke's Law. Precisely why a method for surfactant adsorption previously found to be acceptable for the substrate drug

micronised TS appeared contrastingly unsuitable for micronised budesonide is not known at this point. The hydrophobic nature of micronised budesonide may be responsible for an increased powder surface energy. This in turn would go some way to explaining the increased aggregation seen following incubation. Inverse gas chromatography investigation may therefore provide an explanation as to why preparation of drug-surfactant microparticles by incubation appears to have yielded a particle size several magnitudes larger than the parent particle.

In light of the failure to obtain a drug-surfactant microparticle of an appropriate size for inhalation studies by using an incubation method, it was decided to explore an alternative method of particle engineering to facilitate surfactant adsorption to the surface of micronised budesonide.

4.3 PREPARATION OF DRUG-SURFACTANT MICROPARTICLES BY CO-SPRAY DRYING FROM SUSPENSION

The use of spray drying to create pharmaceutical mixtures is well documented and a full description of the technique may be found in Chapter Two, Section 2.2.8. Its speed and simplicity are responsible for the frequent selection of spray drying in formulation studies. As detailed previously, both suspensions and solutions may be spray dried. In this work, it was decided to co-spray dry micronised budesonide suspended in a solution of non-ionic surfactant in purified water. By spray drying a suspension, it was hoped to facilitate surfactant adsorption to the surface of the micronised drug particles rather than incorporation of both the drug and surfactant into a spray dried particle. In addition, it was hoped that the crystalline nature of micronised budesonide would be preserved, as dissolution of the drug would be minimised through the choice of water as a solvent for the surfactant. The choice of purified water as a solvent for surfactants precluded the preparation of co-spray dried formulations using hydrophobic surfactants. As such, only hydrophilic surfactants were used. Identical surfactants used in the preparation of TS-surfactant formulations were employed, constituting a mixture of poloxamer and polyoxyethylene alkyl ether non-ionic surfactants.

4.3.1 EXPERIMENTAL PROTOCOL

4.3.1.1 SPRAY DRYING PARAMETERS

Suspensions of budesonide in surfactant solution were spray dried using a Mini Spray Dryer 191 (Buchi, Switzerland). Parameters are described in Table 4.3. Formulations were magnetically stirred throughout the spray drying process. Initial experiments were carried out in the presence of a surfactant solution of 200 mg/L concentration, in line with the surfactant concentration employed in Chapter Three during preparation of TS-surfactant particles by incubation. However, yield of spray dried product was found to be very low. In an effort to improve yield, surfactant concentration was increased to 600 mg/L in all subsequent spray dry runs described here.

Table 4.3 Spray drying parameters adopted for surfactant adsorption to micronised Budesonide

Spray drying Parameters	
Air Flow	800 L/hr
Aspirator	70 %
Feed Flow Rate	8 %
Inlet Temperature	150 °C
Outlet Temperature	92 – 99 °C
Suspension Conc^{n}	5 % w/w
Surfactant solution Conc^{n}	600 mg/L

4.3.1.2 DRUG-SURFACTANT MICROPARTICLE CHARACTERISATION

Particle size of all formulations collected following co-spray drying was analysed using laser light diffraction in a Malvern Mastersizer S according to the protocol previously described in Chapter Two, Section 2.2.1. In addition to investigating particle size, particle morphology and physical state were also investigated using SEM and PXRD. These techniques have also been previously described in Chapter Two, Sections 2.2.2 and 2.2.3.

4.3.2 RESULTS AND DISCUSSION

4.3.2.1 SPRAY DRIED YIELD

A range of yields was obtained following co-spray drying of micronised budesonide and various hydrophilic non-ionic surfactants (Table 4.4). In the majority of cases, a disappointing yield was obtained. Considering no optimisation of spray drying parameters was undertaken at the outset this is perhaps not unexpected. Despite the obvious inefficiency of the process, the primary concern in this formulation step was preparation of microparticles of an appropriate size for inhalation studies, in addition to retention of drug crystallinity. Results from particle size analysis and PXRD are therefore more relevant than the percentage yield obtained following co-spray drying.

Table 4.4 Yield obtained following co-spray drying of micronised budesonide and a range of hydrophilic non-ionic surfactants (B=budesonide)

Formulation	**Yield (%)**
Micronised Drug	11.71 (0.91)
B-F127	15.81 (2.45)
B-F108	29.73 (1.87)
B-31R1	29.16 (6.69)
B-L31	15.25 (1.65)
B-B39	18.76 (4.07)
B-B59	18.97 (3.12)
B-1216CO3	23.72 (0.57)
B-MMG	23.47 (2.31)

4.3.2.2 PARTICLE SIZE INVESTIGATION BY LASER LIGHT DIFFRACTION

In contrast to that observed following incubation, particle size of budesonide-surfactant microparticles prepared by co-spray drying was found to be closer to the initial particle size of micronised budesonide. Results from particle size analysis are shown in Table 4.5.

Table 4.5 Particle size of budesonide-surfactant microparticles prepared by co-spray drying from suspension

Formulation	Volume Mean Diameter (μm ± SD, n=5)	Span (Coefficient of Spread)
Micronised Drug	3.30 (0.27)	3.98
B-F127	3.54 (0.45)	3.65
B-F108	3.52 (0.13)	4.21
B-31R1	3.67 (0.62)	4.35
B-L31	3.89 (1.04)	3.85
B-B39	4.01 (0.32)	3.20
B-B59	3.76 (0.55)	2.97
B-1216CO3	3.97 (0.21)	3.66
B-1216CO7	4.21 (0.12)	4.03
B-MMG	3.31 (0.18)	3.32

4.3.2.3 PARTICLE MORPHOLOGY INVESTIGATION BY SEM

The morphology of microparticles produced from co-spray drying mixtures of micronised budesonide and various non-ionic surfactants may be observed in Figures 4.3, 4.4, 4.5 and 4.6.

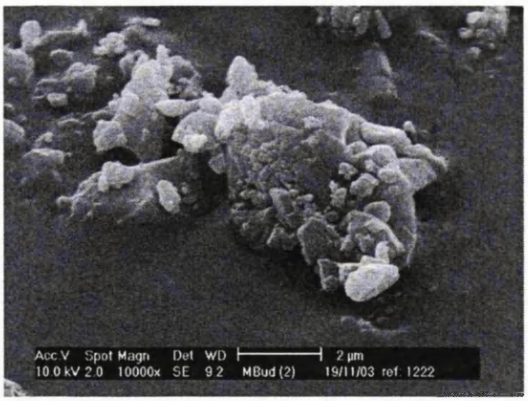

Figure 4.3 Micronised budesonide control

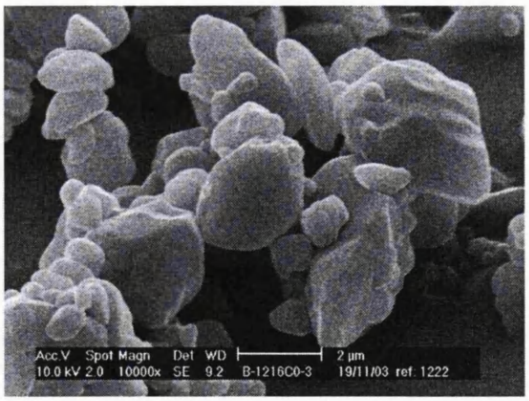

Figure 4.4 Spray dried formulation resulting from a mixture of budesonide and the surfactant 1216CO3

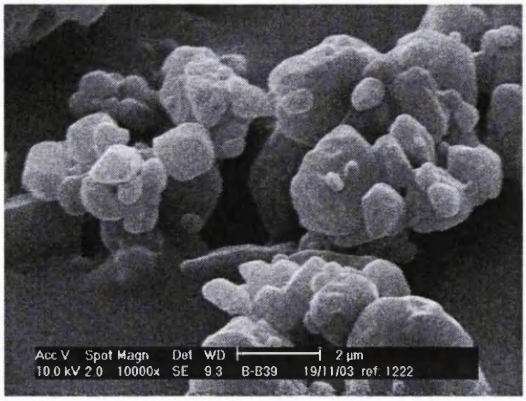

Figure 4.5 Spray dried formulation resulting from a mixture of budesonide and the surfactant B39.

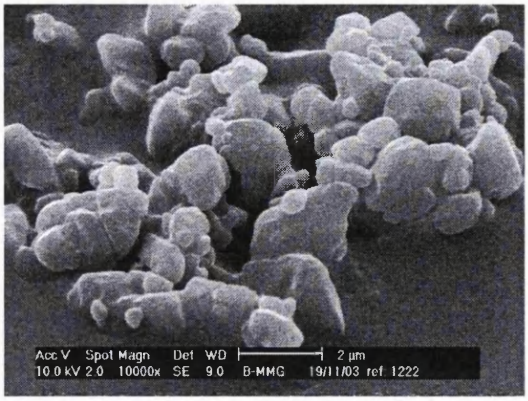

Figure 4.6 Spray dried formulation resulting from a mixture of budesonide and the surfactant Marlipal MG.

Morphology of all surfactant-containing microparticles appeared identical. Images obtained from SEM analysis confirmed results from particle size investigation, showing median microparticle size to be within the desired limits for inhalation formulation. A comparison between surfactant-containing formulations and a budesonide control (seen in Figure 4.3) shows a slight difference in particle aggregation. It would appear that formulations containing surfactant exhibit less aggregation. The application of continuous magnetic stirring to all formulation feeds during spray drying appears to have been more effective in the presence of a surfactant.

4.3.2.4 PHYSICAL STATE INVESTIGATION BY PXRD

An x-ray pattern of micronised budesonide shown in Figure 4.7 displays the crystalline nature of the starting material used in these studies. As previously mentioned, it was hoped that co-spray drying a mixture of drug and surfactant in the form of a suspension rather than a solution would preserve this crystalline structure. This appears to have been successfully achieved and may be observed in the superimposed patterns for two surfactant-containing formulations in Figure 4.7. All spray-dried microparticles containing surfactant exhibited an identical x-ray pattern.

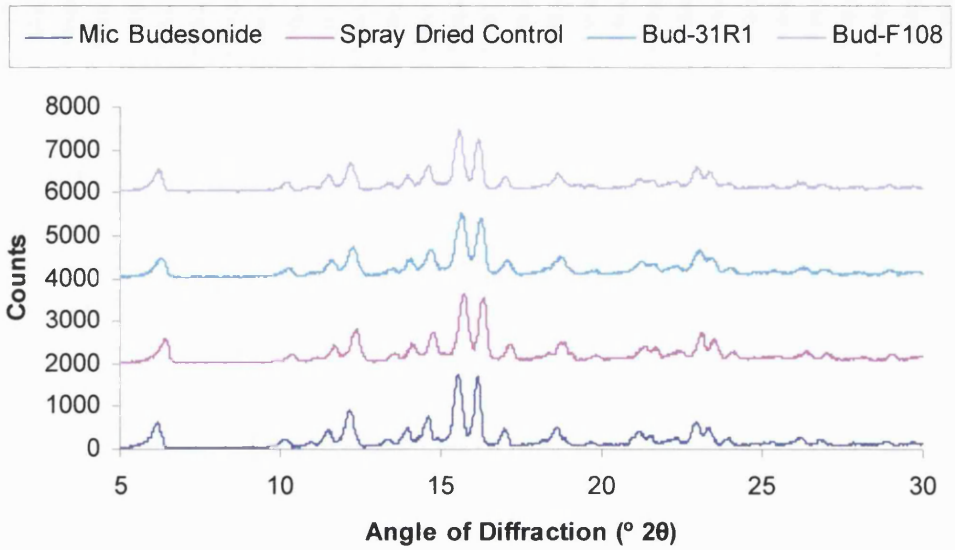

Figure 4.7 PXRD patterns comparing formulations spray-dried from suspension

Preparation of budesonide-surfactant microparticles by co-spray drying has been shown to be preferable to that of an incubation method. The crystalline nature of the micronised drug has been maintained, while producing a formulation of a particle size small enough to be considered for inhalation studies.

4.4 PREPARATION OF DRUG-SURFACTANT MICROPARTICLES BY CO-SPRAY DRYING FROM SOLUTION

The use of purified water to prepare solutions of non-ionic surfactants precluded the adsorption of hydrophobic surfactants onto the surface of micronised budesonide. In order to employ the full range of surfactants used in the previous chapter in studies involving terbutaline sulphate, an alternative method of spray drying was adopted. Solutions of micronised drug in a hydrophobic surfactant solution contained in dichloromethane (DCM) were prepared, and subsequently spray-dried. By spray-drying a solution of micronised drug and surfactant, it was understood that the likelihood of producing an amorphous product was greatly increased. In addition, by incorporating both the drug and surfactant in solution, microparticles formed during the drying process may constitute a solid solution of the two components rather than isolating the surfactant at the drug surface. It was decided that the primary concern for microparticle preparation was particle size, as production of spray dried formulations was carried out in order to prepare pMDI suspension samples, and to

conduct subsequent investigations into suspension performance. Any deviation from the powder characteristics exhibited by formulations prepared by spray drying from suspension would be discovered upon powder characterisation using SEM, PXRD and IGC analysis. However, previous concerns about the efficiency of the spray drying process particularly with respect to yield and therefore cost-effectiveness prompted a decision to initiate spray drying from solution with a factorial design experiment to optimise yield while retaining a particle size appropriate to inhalation studies.

4.4.1 SPRAY DRIED YIELD OPTIMISATION – A FACTORIAL DESIGN EXPERIMENT

4.4.1.1 EXPERIMENTAL PROTOCOL

In complicated systems such as those present during the spray drying process, the interrelationships between experimental variables and subsequent influence on experimental results may be particularly difficult to interpret. Examination of spray drying literature reveals the dependence of spray dried product characteristics on several experimental parameters such as drying temperature, feed flow rate and feed concentration (Maa et al., 1997, Billon et al., 2000 and Elversson et al., 2003). In light of the poor yield obtained in previous spray drying experiments, and in an attempt to investigate the possible interrelationships mentioned above, a factorial type experimental design was devised. By definition, a factorial design experiment allows the testing of each experimental variable at a range of levels by running a series of trials (Bohl, 1990). The advantage of such an experimental design lies in the potential for investigation of possible interactions among variables in addition to the effect of variables on experimental results. By providing the maximum replications of the effect of each variable and each interaction for the given number of experiments, factorial design experiments are also highly efficient (Bohl, 1990). In the present study, it was decided to vary four experimental conditions, those of feed concentration, inlet temperature, feed flow rate and the concentration of surfactant solution used to dissolve micronised budesonide. While these experimental conditions were varied, the parameters of air flow and aspirator level were maintained at 800 L/hr and 75 % respectively. In addition to monitoring yield, particle size and morphology were investigated and recorded in an effort to analyse the relationship between these characteristics and spray drying parameters. One

particular surfactant, the hydrophobic poloxamer surfactant L101, was chosen to spray dry with micronised budesonide for all experiments, with the intention of including the other hydrophobic surfactants once optimal spray drying conditions had been deduced. According to the experimental design adopted, parameters were assigned to a "base" case experiment. Experimental conditions were then varied below and above the base case to give a "low" and a "high" case experiment. Table 4.6 lists experimental variables assigned to each case. Given the decision to vary four experimental conditions, investigation of 3-way, 4-way and higher interactions between experimental variables would have required a total of 81 experiments. However, it is generally accepted that the effect of 3-way and higher interactions is negligible. As a result, only 2-way interactions were investigated. An algorithm shown in Equation 4.1 based on the number of variables was used to reveal the least number of experiments required. A minimum value of 2^k greater than the value calculated in Equation 4.1 then revealed the total number of experiments required to investigate 2-way interactions between the four variables fully, in addition to the effect of these variables on experimental results (Box et al., 1978).

$$N + \frac{N(N-1)}{2} + 1 \qquad \text{(Equation 4.1)}$$

An experimental protocol was then devised, consisting of 16 independent spray-drying experiments and 3 repeats of the base case experiment, resulting in a total of 19 experiments. Repetition of the base case trial throughout the experiment allowed for identification of any inherent experimental error introduced as the experiment progressed. The product of each experiment was investigated in terms of spray dried yield, microparticle size (by laser light scattering as detailed previously) and morphology (by SEM).

Table 4.6 Spray drying parameters adopted for factorial design experiment

	Low	**Base**	**High**
Feed Conc^n (% w/v)	1	3	5
Inlet Temp (°C)	50	60	70
Feed Flow Rate (%)	4	8	12
Surfactant Conc^n (mg/L)	400	600	800

Table 4.7 lists the experimental conditions of the 19 spray drying runs that were carried out in order to fulfil the criteria of a partial factorial design experiment. Columns to the right of the table indicate which parameters have been varied, with "0" representing the base case, "-" the low case and "+" the high case.

Table 4.7 Experiments carried out according to factorial design, showing parameters varied in each case

	Inlet Temp (°C)	**Feed Flow Rate (%)**	**Feed Conc^n (% w/v)**	**Surf Conc^n (mg/L)**				
B C 1	60	8	3	600	0	0	0	0
1	50	4	1	400	-	-	-	-
2	50	4	1	800	-	-	-	+
3	50	4	5	400	-	-	+	-
4	50	12	1	400	-	+	-	-
5	70	4	1	400	+	-	-	-
6	70	4	1	800	+	-	-	+
7	70	4	5	400	+	-	+	-
8	70	12	1	400	+	+	-	-
B C 2	60	8	3	600	0	0	0	0
9	50	12	5	400	-	+	+	-
10	50	12	1	800	-	+	-	+
11	50	4	5	800	-	-	+	+
12	70	12	5	400	+	+	+	-
13	70	12	1	800	+	+	-	+
14	70	4	5	800	+	-	+	+
15	50	12	5	800	-	+	+	+
16	70	12	5	800	+	+	+	+
B C 3	60	8	3	600	0	0	0	0

4.4.1.2 RESULTS AND DISCUSSION

Results from the 19 spray drying runs undertaken as part of the factorial design experiment are displayed in Table 4.8. Three repetitions of the base case experiment allowed estimation of the error inherent in the experimental process. The calculated mean value of spray-dried microparticle size under "base" conditions was found to be 5.41 μm ± 0.24 μm, while that of spray dried yield was 47 % ± 2 %. The calculation of a greater standard deviation of the mean of spray-dried yield is likely due to the fact that recovery of spray-dried product is at best an inexact process, whereas the measurement of microparticle size by laser light scattering is contrastingly precise. Despite the increased error found in the measurement of spray-dried yield, overall variability present in the spray drying process was deemed to be acceptable.

	Inlet Temp (°C)	Pump Rate (%)	Feed Concn (% w/v)	Surf Concn (mg/L)	Yield (%)	Particle Size (μm)	Morphology
Base Case 1	**60**	**8**	**3**	**600**	**47**	**5.67 (2.20)**	**Spherical, aggregates**
Run 1	50	4	1	400	10	5.75 (1.07)	Irregular spheres, aggregates
Run 2	50	4	1	800	10	4.02 (1.89)	Rough surface, aggregates
Run 3	50	4	5	400	22	3.12 (1.84)	Spherical
Run 4	50	12	1	400	29	5.62 (1.23)	Pitted particles, aggregates
Run 5	70	4	1	400	25	6.82 (0.29)	Spherical, few aggregates
Run 6	70	4	1	800	44	4.21 (1.35)	Rough surface, aggregates
Run 7	70	4	5	400	40	7.14 (0.57)	Spherical, few aggregates
Run 8	70	12	1	400	42	7.23 (0.79)	Spherical, aggregates
Base Case 2	**60**	**8**	**3**	**600**	**45**	**5.20 (1.70)**	**Spherical, aggregates**
Run 9	50	12	5	400	50	3.97 (2.01)	Smooth, spherical, few agg.
Run 10	50	12	1	800	42	8.36 (2.54)	Rough, aggregates
Run 11	50	4	5	800	36	8.97 (0.49)	Smooth, spherical
Run 12	70	12	5	400	41	6.13 (1.33)	Smooth, spherical
Run 13	70	12	1	800	31	5.08 (2.30)	Rough, pitted, aggregates
Run 14	70	4	5	800	39	5.64 (0.50)	Mixed, some aggregates
Run 15	50	12	5	800	60	4.70 (1.90)	Spherical, few aggregates
Run 16	70	12	5	800	44	3.80 (0.49)	Spherical, v few aggregates
Base Case 3	**60**	**8**	**3**	**600**	**49**	**5.35 (1.70)**	**Spherical, aggregates**

Table 4.8 Results from spray drying factorial design experiment relating yield, microparticle size and morphology to experimental conditions.

Statistical analysis of the results listed in Table 4.8 was carried out in order to investigate the significance of each experimental parameter on yield, and spray-dried microparticle size. In addition, statistical analysis provided an insight into the presence of any interactions between experimental parameters. Factorial analysis of variance (ANOVA) was performed using a commercially available statistical analysis software package SPSS 12.0 for Windows (SPSS Inc., USA). Significance at a 95 % confidence interval was investigated ($p < 0.05$). Table 4.9 describes the findings from this statistical analysis.

Table 4.9 Statistical significance of results obtained from a spray-drying factorial design experiment

Experimental Factor	Yield P value	Microparticle Size P value
Inlet Temp (A)	0.028 *	0.250
Pump Rate (B)	0.005 **	0.502
Feed Conc^n (C)	0.006 **	0.064
Surf Conc^n (D)	0.028 *	0.407
Inlet Temp/Pump Rate (AxB)	0.007 **	0.133
Inlet Temp/Feed Conc^n (AxC)	0.021 *	0.133
Pump Rate/Feed Conc^n (BxC)	0.744	0.007 **
Inlet Temp/Surf Conc^n (AxD)	0.078	0.004 **
Pump Rate/Surf Conc^n (BxD)	0.168	0.399
Feed Conc^n/Surf Conc^n (CxD)	0.048 *	0.021 *

* $P < 0.05$, ** $P < 0.005$

Examination of Table 4.9 reveals those experimental parameters found to have had a significant effect on either spray-dried yield or spray-dried microparticle size. In the case of spray-dried yield, the effect of all four variables was observed to be significant ($p < 0.05$). In addition, two significant 2-way interactions between inlet temperature and feed concentration; and between feed concentration and surfactant concentration were observed. One highly significant interaction between inlet temperature and pump rate was also discovered ($p < 0.005$). As discussed previously, an interaction indicates the inability of one factor to produce the same effect on an experimental outcome at different levels of a second factor. In the case of spray dried microparticle size data, none of the experimental factors were found to have an individually significant effect. This is contrary to what was expected, as

several studies have shown that both pump rate and feed concentration in particular are known to influence particle size (Paterakis et al., 2002; Esposito et al., 2000; Conte et al., 1994). It is possible that the experimental range of these parameters adopted in this study was not broad enough to produce a similarly broad range of spray dried microparticle sizes. Ideally, a factorial design experiment should be preceded by preliminary experiments to investigate the optimal maximum and minimum value of experimental parameters in order to produce a range of products suitable for statistical analysis. Unfortunately time constraints were such that this was not possible. Despite the lack of significance for all experimental variables on microparticle size, three 2-way interactions were found to be significant – those of pump rate and feed concentration; and inlet temperature and surfactant concentration (both highly significant with a p value of < 0.005); and finally an interaction between feed concentration and surfactant concentration ($p < 0.05$). It is unclear why these 2 way interactions show significance over any individual effect of experimental parameters.

While no statistical analysis of particle morphology results was possible, due to the visual interpretation of morphology using SEM images, it is clear from Table 4.8 that morphology has varied across the range of experimental parameters. Both particle shape and surface were seen to change depending on the experimental conditions. The formation of spherical particles has been shown to depend greatly on the drying rate imposed on a spray dried feed with fast drying rates resulting in the formation of an exterior crust which may subsequently collapse giving rise to irregularly shaped particles (Maa et al., 1997). However, no trend relating morphology to inlet temperature was observed in this study. Again, the range of inlet temperatures chosen for investigation may not have been broad enough to observe such a trend. The presence of irregularly shaped particles in a spray dried product may lead to an increase in particle surface interactions and therefore reduced flow and re-dispersion of powder (Maa et al., 1997). Therefore the production of spherical microparticles was desirable and influenced the choice of optimum spray drying experimental conditions to apply to other formulations containing micronised budesonide.

Analysis of the factorial design experiment as discussed above allowed optimal spray drying conditions to be identified. Taken into consideration were the requirements of a high process yield, the formation of microparticles of a size suitable for inhalation studies, and the desirable morphology of smooth spherically shaped microparticles with little or no aggregation. Optimum parameters are shown in Table 4.10.

Table 4.10 Optimum spray drying parameters applied to preparation of micronised budesonide and hydrophobic surfactant microparticles

Spray drying Parameters	
Air Flow	800 L/hr
Aspirator	75 %
Feed Flow Rate	12 %
Inlet Temperature	70 °C
Outlet Temperature	53-55 °C
Feed Conc^{n}	5 %
Surfactant solution Conc^{n}	800 mg/L

4.4.2 ROLL-OUT TO OTHER HYDROPHOBIC SURFACTANTS

Spray drying parameters optimised in the previous section had been investigated in the presence of a single hydrophobic poloxamer surfactant L101. Subsequent experiments were then carried out, spray drying micronised budesonide in a solution of all remaining hydrophobic surfactants previously examined in Chapter Three, i.e. the poloxamer surfactant L121 in addition to Span 20, Span 85 and Oleic Acid.

4.4.2.1 EXPERIMENTAL PROTOCOL

4.4.2.1.1 SPRAY DRYING PARAMETERS

Spray drying parameters were taken from the previous factorial design experiment and have been listed in Table 4.10.

4.4.2.1.2 DRUG-SURFACTANT MICROPARTICLE CHARACTERISATION

Drug-surfactant microparticles prepared by spray drying from solution were investigated for particle size by laser light scattering, particle morphology by SEM and physical state by PXRD. All methods have been described previously in Chapter Two.

4.4.2.2 RESULTS AND DISCUSSION

4.4.2.2.1 SPRAY DRIED YIELD

Despite choosing experimental conditions to maximise spray dried product yield, the substitution of various alternative surfactants for L101 (that which was used in the original factorial design experiment) reveals a range of yields (Table 4.11) . It seems that the nature of excipient is pivotal to the yield obtained, and therefore optimum conditions for the preparation of a formulation involving one surfactant may not be applied to additional formulations containing alternative surfactants. Yields are listed in Table 4.11.

Table 4.11 Spray dried yield obtained from co-spray drying micronised budesonide with hydrophobic surfactants from solution

Formulation	**Yield (%)**
Micronised Drug	26.62 (1.21)
B-L101	40.23 (2.03)
B-L121	39.99 (2.88)
B-Span 20	29.57 (0.75)
B-Span 85	57.11 (1.38)
B-Oleic Acid	24.98 (0.69)

4.4.2.2.2 PARTICLE SIZE INVESTIGATION BY LASER LIGHT SCATTERING

Microparticle size was observed to be within the preferred limits for inhalation studies. Varying the surfactant spray dried with micronised budesonide caused slight variations in the microparticle size, in addition to the size distribution. However, the magnitude of standard deviations shown in Table 4.12 is such that all formulations may be considered identical in size.

Table 4.12 Particle size of budesonide-surfactant microparticles prepared by co-spray drying from suspension

Formulation	Volume Mean Diameter (μm ± SD, n=5)	Span (Coefficient of Spread)
Micronised Drug	3.48 (0.32)	1.96
B-L101	3.80 (0.49)	3.42
B-L121	3.02 (1.02)	3.25
B-Span 20	4.67 (0.55)	4.21
B-Span 85	3.41 (0.42)	2.05
B-Oleic Acid	4.16 (0.26)	2.97

4.4.2.2.3 PARTICLE MORPHOLOGY INVESTIGATION BY SEM

Particle morphology of drug-surfactant microparticles prepared by co-spray drying from solution were expected to be similar to that of a budesonide-L101 formulation produced under experimental conditions deemed optimal according to the factorial design experiment previously discussed. This was indeed found to be the case, with formulations containing budesonide and hydrophobic surfactants obtained following co-spray drying from solution observed as being spherical in shape, possessing a relatively smooth surface, and being of a size appropriate to inhalation studies. Figures 4.8 and 4.9 display images of particle morphology obtained by SEM.

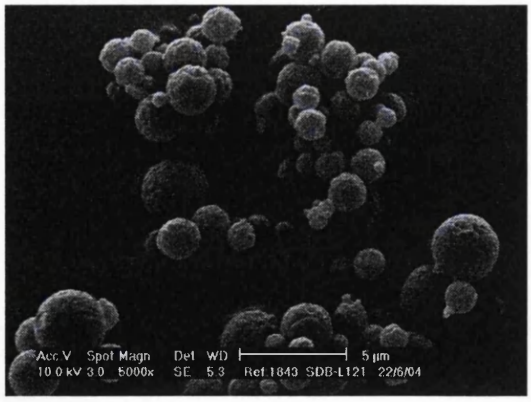

Figure 4.8 Formulation containing budesonide and L121 produced following co-spray drying from solution

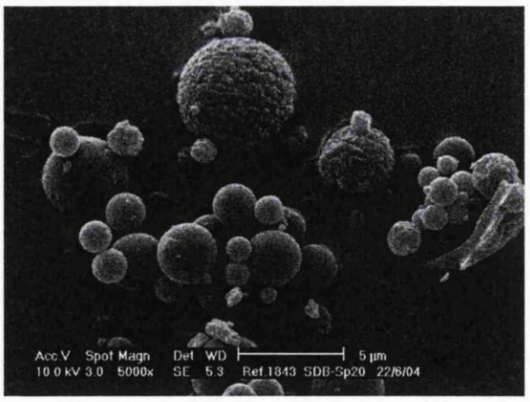

Figure 4.9 Formulation containing budesonide and Span 20 produced following co-spray drying from solution

4.4.2.2.4 PHYSICAL STATE INVESTIGATION BY PXRD

Contrary to formulations prepared by co-spray drying from suspension, x-ray patterns obtained for those produced by co-spray drying from a solution show a significant alteration in the powder physical state, changing from crystalline to amorphous. The recovery of an amorphous product was expected, as preparation of a liquid feed has involved the dissolution of micronised budesonide in DCM. This, coupled with the subsequent drying step that has occurred as part of the spray drying process is sufficient to disrupt the molecular organisation of a powder such that the regular conformation of a crystal lattice deteriorates giving rise to regions of long range disorder or amorphous material (Corrigan et al., 2002; Corrigan et al., 2003). Previously published reports have suggested that manipulation of experimental variables, in particular the addition of certain stabilisers during the spray drying process has been successful in retaining a crystalline product throughout the process (Maa et al., 1997, Corrigan et al., 2004). However while the production of crystalline drug-surfactant microparticles would have been desirable considering the increased instability of amorphous material, time constraints prevented extensive investigations into the optimum experimental conditions necessary for the production of a crystalline product.

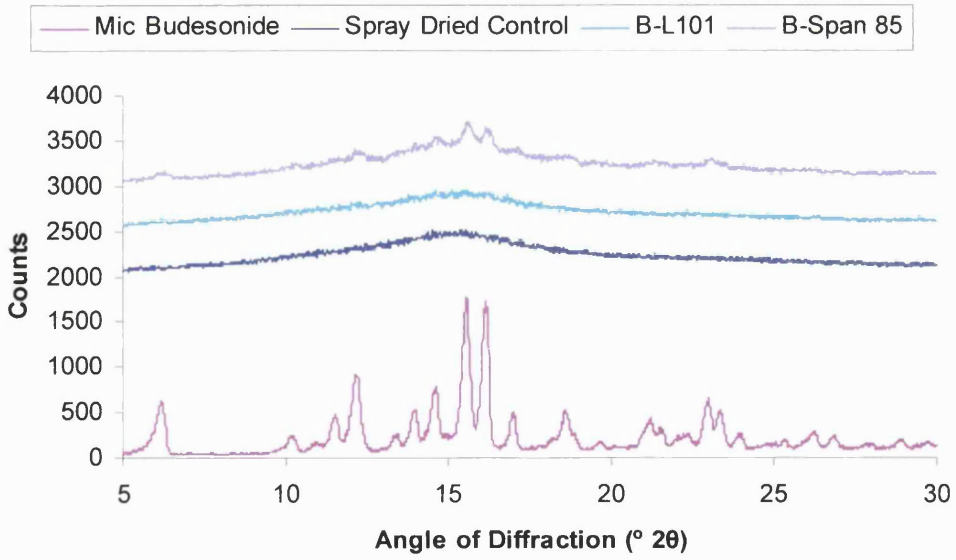

Figure 4.10 PXRD patterns comparing budesonide controls with formulations co-spray dried from solution

Figure 4.10 reveals a difference between the physical state of two surfactant-containing spray dried products. While the x-ray pattern for a formulation containing the poloxamer surfactant L101 appears identical to that of a spray dried control, possessing an entirely amorphous profile, that of a similar formulation containing a different surfactant, Span 85, appears to have some regions of crystallinity. Other formulations prepared by co-spray drying from solution exhibited similar subtle differences in x-ray pattern. Two possible scenarios may explain these observations. Firstly, the presence of different stabilisers in the liquid feed may have altered the drying process and subsequent physical state of the spray dried product. Alternatively, incorporation of a range of stabilisers into the spray dried drug-surfactant particle has given rise to a population of drug-surfactant microparticles possessing a range of glass transition temperature (*T*g) values, *T*g being a temperature unique to amorphous materials. By possessing a lower *T*g, the formulation seen to exhibit small areas of crystallinity in Figure 4.10 would be inherently less stable than the formulation containing budesonide and L101, and may begin to re-crystallise sooner. However, considering all formulations were analysed by PXRD immediately following recovery from the spray drying apparatus, it seems more likely that the first explanation stands, and that in agreement with previously published work, the incorporation of different surfactants has altered the physical state of spray dried product. Analysis of spray dried microparticles by differential scanning calorimetry (DSC) would provide information pertaining to *T*g values, and may illuminate the exact nature of the differences observed between different surfactant containing formulations. This was not carried out in this work, but would be an interesting additional study.

The production of amorphous powders or those containing amorphous regions such as reported here is notable when considering the application of these powders in subsequent inhalation studies. Areas of disorder within a powder are thermodynamically unstable, and will tend to re-crystallise. This will affect how the powder interacts with water, generally manifested in increased uptake of water from the surroundings. As a result, the behaviour of amorphous materials is unpredictable in the long term, indeed often in the short term also, largely dependent on factors such as *T*g and storage temperature (Byrn et al., 1999). Nevertheless, powders produced by spray drying from solution were used in subsequent inhalation studies in

order to assess the effect of varying the surfactant present within the formulation on pMDI suspension performance.

4.5 SURFACE ENERGY ANALYSIS OF CO-SPRAY DRIED FORMULATIONS BY IGC

All formulations produced by co-spray drying micronised budesonide with surfactant both as a suspension in purified water, and as a solution in DCM were subjected to IGC analysis in order to determine powder surface energy. The experimental protocol followed in surface energy investigations was identical to that described previously in Chapter Two. Results from IGC analysis are displayed in Table 4.13.

Table 4.13 Surface energies of budesonide-surfactant microparticles prepared by co-spray drying (B: budesonide)

Formulation	γ^d (mJ/m^2)	K_A	K_D	K_D/K_A
Micronised Drug	59.4 (0.3)	140.7 (0.2)	52.7 (0.7)	0.37
Formulations produced by co-spray drying from suspension				
Control Drug	41.3 (0.2)	142.9 (0.2)	52.5 (1.2)	0.37
B-L31	32.6 (0.1)	129.9 (0.2)	61.2 (0.5)	0.42
B-F108	33.8 (0.4)	122.5 (0.5)	46.3 (0.4)	0.38
B-31R1	33.7 (0.1)	123.4 (0.2)	34.0 (0.2)	0.28
B-MMG	35.1 (0.0)	126.5 (0.2)	61.9 (0.3)	0.49
B-1216CO3	37.1 (0.2)	115.3 (0.3)	26.9 (0.4)	0.23
B-B39	34.7 (0.1)	101.7 (0.6)	114.7 (0.7)	1.13
B-B59	34.7 (0.1)	127.8 (0.1)	66.7 (0.4)	0.52
Formulations produced by co-spray drying from solution				
Control Drug	46.0 (0.6)	117.5 (1.2)	13.7 (0.6)	0.12
B-L101	39.7 (0.8)	102.5 (0.4)	24.6 (0.2)	0.24
B-L121	38.5 (0.7)	98.6 (0.5)	16.0 (0.3)	0.16
B-Span 85	40.8 (0.1)	94.6 (0.8)	16.9 (0.7)	0.18
B-Oleic Acid	37.6 (0.2)	92.7 (0.2)	17.9 (0.7)	0.19

The surface energy of micronised budesonide was found to decrease upon passing through the spray dryer without surfactant present. A similar reduction in surface energy caused by the formulation process was observed in the case of TS in Chapter Three. Table 4.13 shows a higher dispersive component of surface energy (γ^d) in a control produced by spray drying from solution when compared to that obtained

following spray drying from a suspension (γ^d 46.0 mJ/m^2 vs 41.3 mJ/m^2). This was expected, as a PXRD pattern for this control showed a wholly amorphous product, whereas that produced by spray drying from a suspension was observed to be crystalline. In the case of formulations containing surfactant, surface energy was observed to decrease in comparison to controls. Formulations produced by spray drying from a suspension showed slightly lower values of γ^d than those produced by spray drying from a solution. Again, an investigation into the physical state of these products spray dried from solution using PXRD revealed them to be amorphous in nature, which may account for the slightly higher values for the dispersive components. However, while formulations were analysed by PXRD immediately following collection from the spray drying apparatus, the same cannot be said for IGC analysis. Despite storage at 0 % relative humidity (RH) in a desiccator some degree of re-crystallisation may have occurred preventing any conclusive statement about the physical state of formulations at the time of IGC analysis.

Similar to the IGC results obtained for formulations containing TS and an identical range of surfactants in Chapter Three, in addition to a reduction in γ^d, values for the acid component K_A were also reduced in budesonide formulations containing surfactant regardless of whether they were produced by spray drying from a suspension or a solution. Again, this suggests that the overall polarity of the powder surface has been altered, resulting in reduced interactions with any basic groups on neighbouring particles. Changes to K_D values following spray drying with surfactant did not appear to follow any discernible pattern, with values both increasing and decreasing depending on the surfactant within the formulation. Marked changes in K_D values were seen in formulations prepared by spray drying from solution, with the value for micronised budesonide decreasing sharply from 52.7 mJ/m^2 to 13.7 mJ/m^2 following spray drying from DCM with no surfactant present. This significant reduction observed in a control formulation suggested any changes to K_D values were most likely due to the spray drying process rather than the individual surfactant present.

Results from IGC analysis may provide some insight into the location of surfactant molecules in relation to molecules of budesonide following co-spray drying. While spray drying from suspension is likely to have resulted in the formation of a

surfactant coat on the micronised drug particle, spray drying from solution may not. Possible locations of the surfactant molecule in these formulations are either on the drug surface as in those formulations co-spray dried from suspension or incorporated within a drug-surfactant matrix particle formed when a homogenous solution of the two was dried. Given the surface active nature of surfactant molecules, and their tendency to migrate to an interface, it is reasonable to suggest that the former has occurred and that despite spray drying by a different method, the structure of the resulting drug-surfactant particle is essentially the same. Differential scanning calorimetry (DSC) may have been useful in identifying differences in melting points of various formulations. It is possible that two melts would have been observed in a formulation consisting of a layer of surfactant molecules surrounding budesonide. However, it likely that a complete surfactant layer would be necessary to see such an effect and it is not possible to precisely determine the location of the surfactant molecules following co-spray drying. If it is assumed that surfactant molecules were indeed situated at the drug surface following co-spray drying from both suspension and solution, we may examine the possible orientations of the surfactant molecule. Conventional theory would suggest that the hydrophobic PPO moiety of surfactant molecules in question would have a greater affinity for the surface of the hydrophobic budesonide, adsorbing though hydrophobic interactions. This would leave hydrophilic PEO groups projecting outwards, away from the drug surface. However, adsorption of an identical range of surfactants to two very different surfaces – those of a hydrophilic drug TS and those of a hydrophobic drug budesonide have resulted in very similar surface energy values of γ^d and K_A. This would suggest that orientation of surfactants at both drug surfaces is the same despite the marked difference in the nature of the drug surface. As such, the process of co-spray drying surfactants with budesonide appears to have resulted in the reverse orientation of surfactant molecules to that which might have been expected. Further work to investigate the exact orientation of surfactant molecules on the surface of both TS and budesonide would be valuable. Atomic force microscopy (AFM), Fourier Transform Infra-red Spectroscopy (FT-IT), Nuclear Magnetic Resonance (NMR) and Raman Spectroscopy are all possible techniques that may be used to provide a clearer picture of surfactant structure at a surface and in turn provide information relating to molecule orientation following adsorption (Shi et al., 2004; Bjelopavlic et al., 2000).

Similar to work discussed in Chapter Three concerning TS, attempts to characterise the amount of surfactant adsorbed onto the surface of micronised budesonide were unsuccessful. However, the changes in surface energy of budesonide observed here following co-spray drying with various surfactants is indicative of successful surfactant adsorption onto the drug surface.

An attempt to correlate powder surface energy with surfactant molecular weight and hydrophile-lipophile balance (HLB) was not carried out. This decision was based on the similarities in surface energy values of budesonide formulations with previously investigated TS formulations, and the fact that no correlations with surfactant structure were observed in the latter group (Chapter Three, Section 3.3.6).

4.6 SUMMARY AND CONCLUSION

Initial work to facilitate surfactant adsorption to the surface of micronised budesonide using an incubation method similar to that employed in TS studies was unsuccessful, due to the formation of drug-surfactant microparticles too large to be considered for pMDI suspension stability studies. Co-spray drying a suspension of micronised budesonide with a solution of a hydrophilic surfactant in water produced a product of an acceptable size range, however spray dried yield was observed to be low and inconsistent. It was decided therefore when examining co-spray drying of budesonide with hydrophobic surfactants from solution to conduct an initial factorial design experiment using a test poloxamer surfactant L101, in an attempt to optimise spray dryer parameters while maintaining spray dried particle size within desired limits. Results from statistical analysis suggested a broader range of experimental variables would have been preferable in order to fully investigate the effect of various factors on spray dried particle size. However it was possible to identify optimal experimental conditions which were then imposed on further spray drying experiments involving other hydrophobic surfactants. Powder characterisation of products produced by spray drying identified differences between those produced by spray drying from suspension and from solution in terms of physical state. An investigation into powder surface energy revealed a surprising similarity between surface energy values for budesonide-surfactant particles and TS-surfactant particles previously discussed in Chapter Three. This was despite the marked differences in substrate hydrophilicity, in addition to the method of surfactant adsorption.

Conclusions as to the orientation of surfactant molecules on the drug surface were not possible based on the experiments carried out. Overall, results in Part A of this chapter have shown successful adsorption of surfactant onto the surface of micronised budesonide, in addition to a reduction in both the dispersive and acidic components of powder surface energy. Subsequent work in Parts B and C will investigate the effect of surfactant adsorption on suspension stability of a pMDI budesonide formulation and ultimately whether any changes in suspension behaviour may be ascribed to the observed manipulation of powder surface energy.

PART B: pMDI FORMULATION AND SUSPENSION STABILITY TESTING

4.7 INTRODUCTION

In Part B of this chapter the suspension performance of engineered budesonide-surfactant microparticles created by co-spray drying will be discussed. The suspension behaviour of pressurised metered dose inhaler formulations, produced in both HFA propellants, will be analysed and characterised using the optical method Turbiscan.

4.8 EXPERIMENTAL PROTOCOL

Suspension formulations were manufactured by pressure filling in both HFA 134a and HFA 227 according to the protocol detailed in Chapter Three, Section 3.7.1.1. Formulations were manufactured at a concentration of 0.2 % w/v, an identical concentration to that of TS-surfactant containing formulations, to allow direct comparison of results. Turbiscan analysis was conducted according to the same scanning protocol described in Section 3.6.1.3 of Chapter Three, again to allow a direct comparison with results obtained for TS-surfactant containing formulations.

4.9 RESULTS AND DISCUSSION

Results from Turbiscan analysis failed to show any significant improvement in suspension performance following the co-spray drying of surfactant with micronised budesonide. This was in direct contrast to results observed in TS-containing formulations discussed in Chapter Three, where all TS-surfactant formulations exhibited signs of a reduced phase separation in addition to reduced aggregation when compared to control TS formulations. The backscattering signal observed in suspension formulations containing budesonide alone prepared in HFA 134a was observed to decrease over the three minute scanning period, suggestive of an immediate separation of suspended phase from propellant. Contrary to expectation, rather than forming a layer of sediment, the budesonide control formulation appeared to cream. Previous experience with TS indicated that all formulations were likely to sediment in HFA 134a while creaming in HFA 227. A difference in density between TS and budesonide would explain the formation of a creamed layer in Figure 4.11, however the two drugs possess very similar values for density (Table 4.14).

Table 4.14 Density of micronised budesonide and TS, measured by helium pycnometer (AstraZeneca R&D Charnwood inhouse data)

	Density (g/cm^3)
Budesonide	1.322
Terbutaline Sulphate	1.348

Pronounced fluctuation in the signal was also noted indicating extensive aggregation which would undoubtedly contribute to the observed instability, in line with Stoke's Law. Figure 4.11 shows the backscattering signal for such a budesonide control formulation.

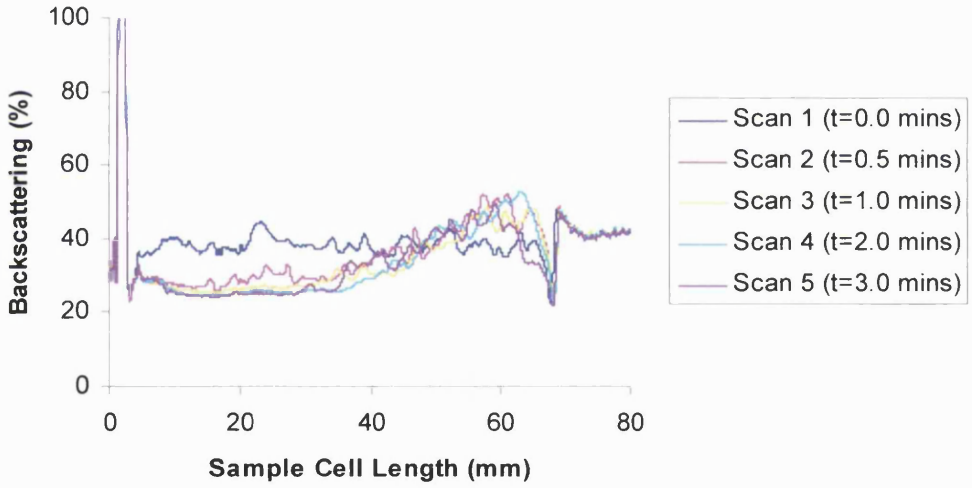

Figure 4.11 Turbiscan trace for formulations containing spray dried budesonide alone in HFA 134a

A small number of surfactant-containing formulations did exhibit slight improvements in suspension performance when compared to that of a control. Examples of these formulations were those containing oleic acid (Figure 4.12) in addition to the hydrophobic poloxamer surfactant L121 (Figure 4.13). It is interesting that both of these formulations were prepared by co-spray drying from a solution in dichloromethane and not from a suspension in purified water. Figure 4.12 shows a turbiscan trace for a formulation containing budesonide and oleic acid. The

backscattering signal appears to decrease to a lesser extent over the three minute scanning period when compared with the trace shown in Figure 4.11. Fluctuation in the backscattering signal is also less pronounced, indicative of reduced aggregation when compared with the control formulation.

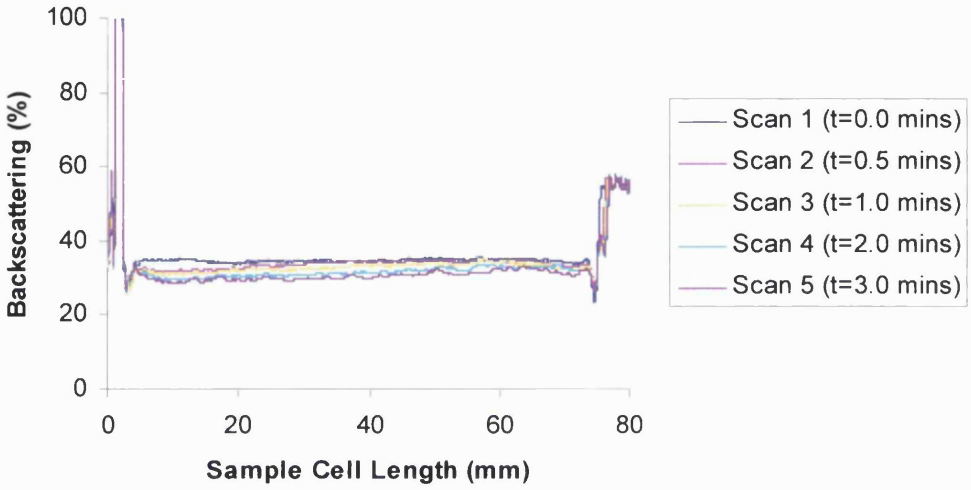

Figure 4.12 Turbiscan trace for a formulation containing budesonide and oleic acid in HFA 134a

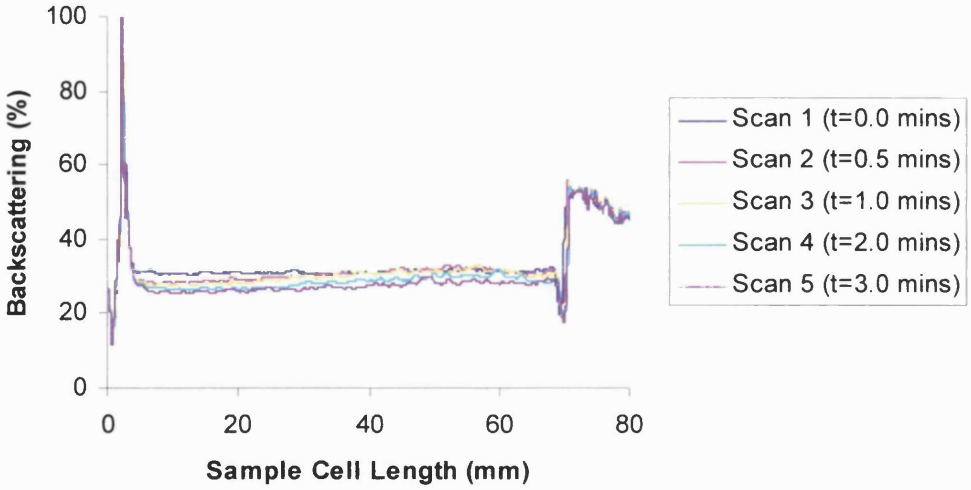

Figure 4.13 Turbiscan trace for a formulation containing budesonide and L121 in HFA 134a

The remaining formulations failed to show any improvement in suspension stability, with backscattering signals suggestive of phase separation and aggregation similar to that observed in a budesonide control. The suspension behaviour of such a formulation is shown in Figure 4.14.

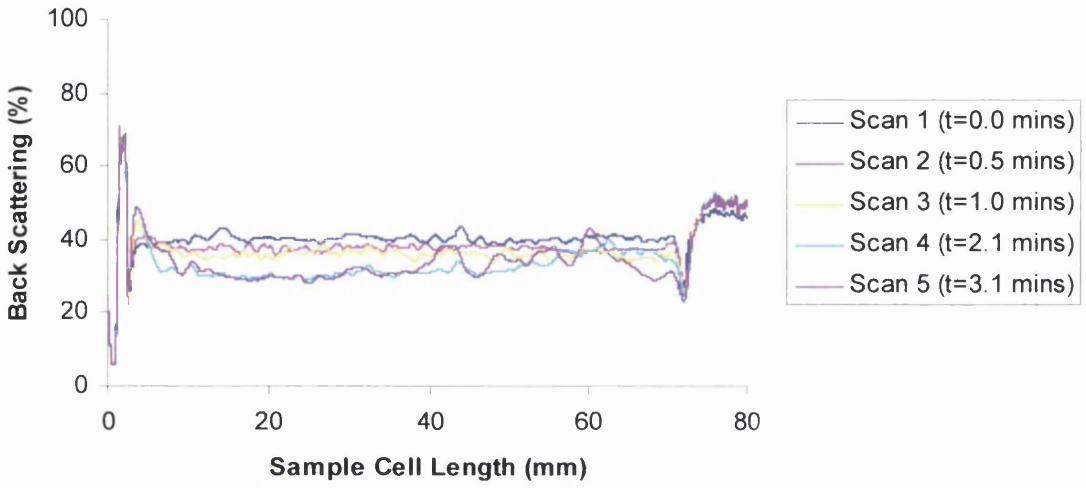

Figure 4.14 Turbiscan trace for a formulation containing budesonide and F108 in HFA 134a

Results obtained from suspension behaviour analysis in HFA 227 were no better than those observed in HFA 134a. A Turbiscan trace of a budesonide control in HFA 227 again showed a very rapid phase separation, commencing immediately following sonication. Figure 4.15 shows a trace for such a control formulation.

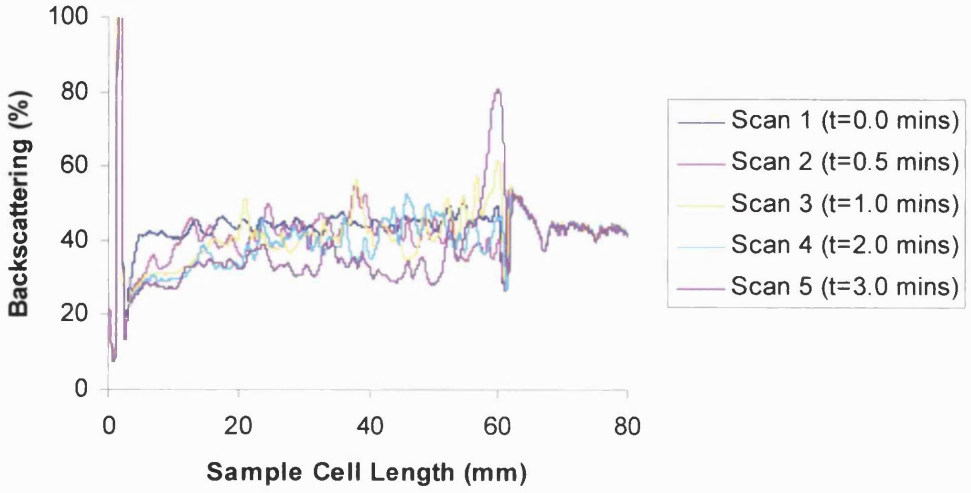

Figure 4.15 Turbiscan trace for a budesonide control formulation in HFA 227

No surfactant-containing formulation was observed to exhibit a backscattering profile indicative of reduced phase separation when compared to a control. Turbiscan traces for all formulations containing surfactant in HFA 227 showed an increase in backscattering signal at the upper region of the suspension over time (similar to that seen in Figure 4.13), consistent with the formation of a creamed layer of suspended material. Visual confirmation of such a layer was obtained on removing the sample cell from the Turbiscan apparatus. However some formulations did exhibit a reduced fluctuation in the backscattering signal, again suggestive of an overall reduction in particle aggregation over the three minute scanning period. Despite this observation, suspension performance in formulations containing surfactant tested in HFA 227 was not overall noticeably improved when compared to budesonide-only controls. It is interesting to note that the pattern of generally increased stability in HFA 134a over HFA 227 observed here was also the pattern observed in suspension stability testing of TS formulations discussed in Chapter Three. The small density difference between these two propellants may explain this observation, with HFA 134a being less dense than HFA 227 (Table 4.15).

Table 4.15 Densities of HFA propellants (Solvay Fluor und Derivate GmBH, Germany)

	Density kg/l
HFA 134a	1.23
HFA 227	1.41

In order to compare the suspension performance of all formulations analysed directly, mean backscattering across a central zone (30-40 mm) of the Turbsican sample cell was calculated for each formulation, in both propellants. As described previously in Chapter Three, a reduction in mean backscattering over the three minute scanning period is suggestive of clarification of a suspension, as light transmitted through the suspension increases. Mean backscattering data were treated in an identical manner to those for TS-containing formulations and further manipulated to construct charts representing the reduction in mean backscattering over time for each formulation. Figure 4.16 represents the reduction in mean backscattering for all formulations analysed in HFA 134a. The limited improvement

in suspension performance following inclusion of surfactant is reflected in this figure, with a control budesonide formulation exhibiting the largest reduction in mean backscattering over the period of analysis. Formulations containing oleic acid and L121 as mentioned above as having displayed backscattering traces suggestive of the greatest improvement in suspension performance when compared with controls are seen in Figure 4.16 to posses the minimum reduction in mean backscattering over time.

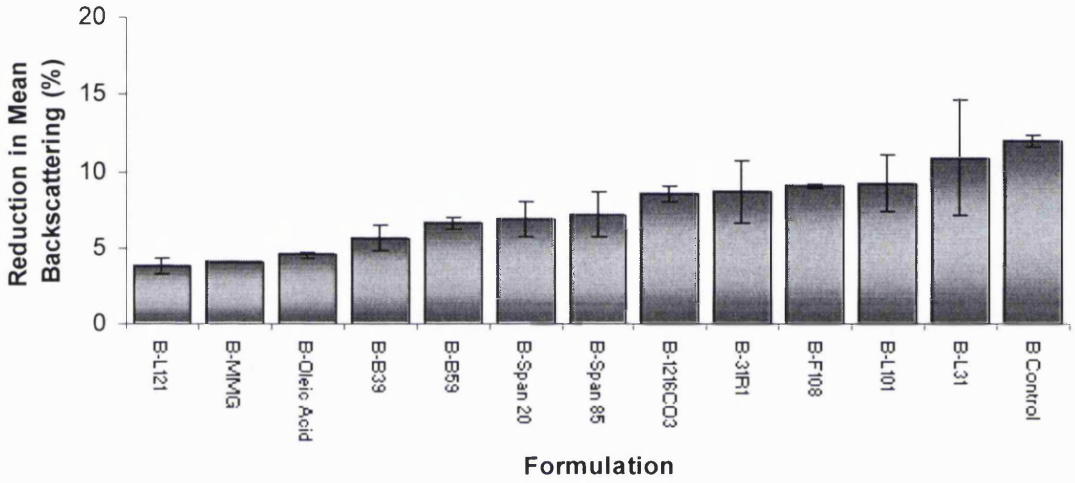

Figure 4.16 Reduction in mean backscattering in HFA 134a (B: budesonide)

On inspection of a similar manipulation of data from Turbiscan analysis of formulations in HFA 227 in Figure 4.17 however, the less favourable performance of such suspensions was confirmed. It is clear that a control budesonide formulation does not exhibit the least stable suspension behaviour over time, with several surfactant-containing formulations possessing a greater reduction in mean backscattering over time suggestive of a more extensive phase separation in these formulations. The large errors observed in Figure 4.17 may be due to the extensive fluctuation in backscattering signal recorded. As such it is difficult to state with certainty that surfactant-containing formulations with reductions in mean backscattering greater than a control budesonide formulation, and as such appearing to the right of the control formulation in Figure 4.17, were in fact indicative of a worsening in suspension performance. Instead, it is more appropriate to state that no

improvement in suspension performance was observed in these formulations (this may not be said for the formulation B-L31 however).

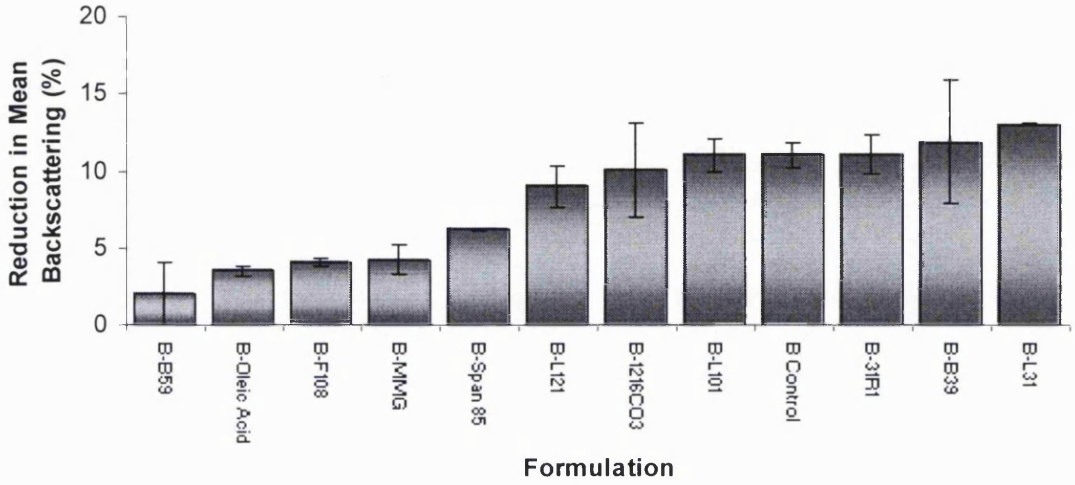

Figure 4.17 Reduction in mean backscattering in HFA 227 (B=budesonide)

Consideration of all suspension performance results for formulations containing budesonide-surfactant microparticles highlights the relatively disappointing effect on suspension stability produced following co-spray drying surfactants with micronised budesonide. The relatively small improvement observed in a small number of formulations suspended in HFA 134a is in contrast to results for TS-containing formulations where in some cases significant improvements in suspension stability over a control formulation were observed in formulations containing surfactant. Reasons for the failure of surfactant adsorption to micronised budesonide to produce the same favourable effects on suspension performance of a pMDI formulation as were observed in TS formulations (when surface energy values were found to be very similar for all formulations regardless of the drug present) may only be speculated upon. The contrasting nature of the drug surfaces in terms of their hydrophilicity and its possible effect on surfactant orientation at the drug surface has already been discussed. The primary source of variation in suspension performance may have arisen in the different methods adopted to facilitate surfactant adsorption to the drug surface, these being an incubation method in the case of TS and co-spray drying in the case of budesonide. One possible factor not represented in results observed to date was the visual observance of adhesion of suspended material to the

wall of the PET containers used in the preparation of pMDI suspension samples. This adhered material did not re-disperse upon sonication and was therefore not transferred to the Turbiscan sample cell prior to suspension stability testing. While extensive adhesion was observed in the case of control budesonide formulations, formulations containing surfactant exhibited a reduced level of adhesion. It is possible that as control formulations analysed by Turbiscan would have possessed slightly less suspended material than surfactant-containing formulations and may therefore have exhibited a more favourable stability profile than otherwise expected due to a reduced concentration. It was decided to investigate these observations further, and these investigations will be fully described in Chapter Six. In any case, it is clear that similar surface energy values are not sufficient to produce suspensions of similar stability and as such the effect of physicochemical characteristics on suspension stability such as density must be considered. Attempts to correlate suspension performance with surface energy to be described in Part C of this chapter will confirm this observation.

Attempts described here to improve suspension performance of a budesonide formulation by co-spray drying micronised drug with surfactant have not succeeded to the same extent as those relating to TS, and alternative methods of stabilising budesonide formulations could therefore be considered. Manipulation of density is a consideration not investigated here, but may produce formulations with improved suspension stability due to the harmonisation of suspended material density with that of propellant density. In addition, several novel formulation methods have been previously described showing improvements in suspension stability including the formation of porous particles (Bowman & Greenleaf, 1999) and the production of a reverse water in fluorocarbon emulsion (Butz et al., 2002). In the case of specific improvements to budesonide suspension performance in HFA propellants, the controlled precipitation of budesonide and excipients in a liquefied HFA 227 system producing a physically stable micro-suspension has also been described (Steckel & Wehle, 2004).

4.10 SUMMARY AND CONCLUSION

Results from suspension stability studies investigating the performance of budesonide-surfactant formulations in HFA propellants were disappointing. Formulations suspended in HFA 134a showed slight improvements over a control formulation, while those suspended in HFA 227 failed to show any conclusive improvement over a control formulation. These results were in contrast to those obtained from similar studies involving TS containing formulations detailed in Chapter Three. This was in spite of the fact that surfactant-containing formulations of both drugs possessed similar surface energy values, lower than that of the control drug, indicating that suspension performance is not influenced by surface energy of suspended material alone and that other factors must be considered. It is possible that the necessary use of alternative methods of particle engineering for budesonide-surfactant microparticles compared with TS-surfactant microparticles contributed to the differences in pMDI suspension behaviour observed. No pattern could be identified among the range of suspension performances attributed to individual surfactants. Just as the performance of different budesonide-surfactant formulations was seen to vary between HFA 227 and HFA 134a, so too did the performance of a surfactant formulation vary depending on whether the drug substrate was budesonide or TS. As such, surfactants that appeared to confer the most favourable stabilising properties on a TS pMDI formulation in Chapter Three did not have the same effect in budesonide pMDI formulations. A greater understanding of surfactant molecule orientation at each drug surface may illuminate the reasons for these inconsistencies. The phenomenon of adhesion of suspended material to the container wall observed in budesonide-containing formulations, and that of reduced adhesion in the presence of surfactant was identified and selected for further investigations, to be described in Chapter Six.

PART C: CORRELATION BETWEEN SURFACE ENERGY AND pMDI SUSPENSION STABILITY

4.11 INTRODUCTION

As previously undertaken in Part C of Chapter Three, attempts to correlate surface energy with pMDI suspension stability will be investigated. However, this is now in light of the findings discussed in Chapter Three, where no strong correlation between the surface energy of TS-surfactant microparticles and the suspension performance of the microparticles in HFA propellants was identified. A general trend linking a reduced dispersive component and acidic component of surface energy with improved pMDI suspension performance was observed and so while previously published work has confirmed the positive influence of a reduction in surface energy on suspension performance, results obtained here would suggest that surface energy is only one of many factors involved in the behaviour of pMDI suspensions.

4.12 EXPERIMENTAL PROTOCOL

Similar to the approach described in Part C of Chapter Three, a surface energy interaction (SEI) describing the relationship between the surface energy components of budesonide-surfactant microparticles and those of HFA propellants were calculated. Surface energy components for the model propellant 2H, 3H-Decafluoropentane determined from contact angle measurements were used in the calculation of SEIs, and therefore SEI values calculated have been designated "modified" SEIs. The calculation of SEIs was carried out using the equation stated in Equation 3.2 (Chapter Three). The relationship between a calculated SEI and reduction in mean backscattering (RMB) was then investigated, plotting SEI against RMB for all surfactant-containing budesonide formulations in both HFA 227 and HFA 134a.

4.13 RESULTS AND DISCUSSION

Calculated SEI values may be seen in Table 4.16. The reduction in the dispersive component of surface energy of a control formulation over that of micronised drug previously discovered in IGC analysis accounts for the difference in SEI value calculated for these two powders. SEI values for the majority of surfactant-containing formulations reveal a deviation from budesonide-alone formulations again

reflecting the more pronounced reduction in surface energy components of these formulations over a control obtained from IGC experiments.

Table 4.16 Modified SEI values calculated using model propellant surface energy data obtained in Chapter Three. (B=budesonide)

Formulation	**Modified SEI (mJ/m^2)**
Micronised Budesonide	64.34
B-Control	59.22
B-F108	54.49
B-L31	56.81
B-31R1	52.35
B-MMG	57.57
B-B59	58.20
B-B39	62.17
B-1216CO3	52.15
B-L101	51.02
B-L121	48.19
B-Span 85	48.88
B-Oleic Acid	48.01

Figures 4.18 and 4.19 show the relationship between SEI and reduction in mean backscattering in HFA 134a and HFA 227 respectively. In a similar manner to the approach taken in Chapter Three, the three main groups of surfactant have been differentiated through the use of a range of markers. The miscellaneous group of surfactants constitutes formulations containing budesonide in addition to either Span 85 or Oleic Acid.

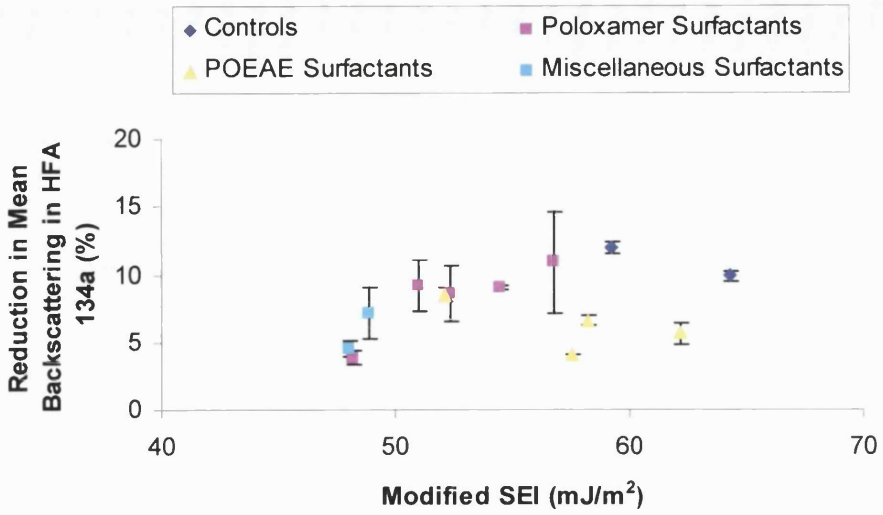

Figure 4.18 Correlation between SEI and RMB (HFA 134a)

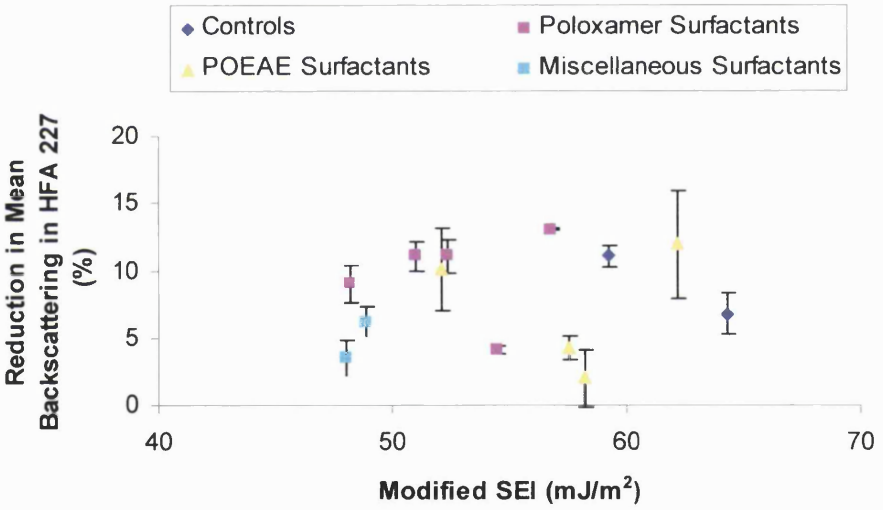

Figure 4.19 Correlation between SEI and RMB (HFA 227)

No overall correlation between SEI and RMB is evident from the Figures 4.18 and 4.19. Analysis of formulation groups in terms of the surfactant type present reveals a possible correlation between SEI and RMB in formulation containing poloxamer surfactants, in HFA 134a. As such, a reduced SEI would appear to be consistent with an improvement in suspension performance. This confirms findings discussed in Chapter Three. No other such surfactant type-specific correlations were identified. It is unknown why a possible correlation was identified in poloxamer surfactant-containing formulations only. The absence of any correlation in formulations

suspended in HFA 227 may be explained by the generally poor performance of all formulations in this propellant. It is important to note that SEI values calculated for all formulations take into account experimentally determined surface energy parameters for a model propellant, and not actual data pertaining to HFA 134a and HFA 227. These data are unavailable at this time.

The possible existence of correlations between individual formulation powder surface energy parameters and suspension performance in both HFA 134a and HFA 227 was investigated, by plotting RMB against individual dispersive energy components (γ^D), acid components (K_A), base components (K_D), and the base/acid ratio (K_D/K_A). The following figures show the relationship between surface energy parameters and suspension performance in HFA 134a only. No correlations were identified in HFA 227, and these plots are not shown. This was once again thought to be attributable to the generally poor suspension performance for all formulations recorded in this propellant.

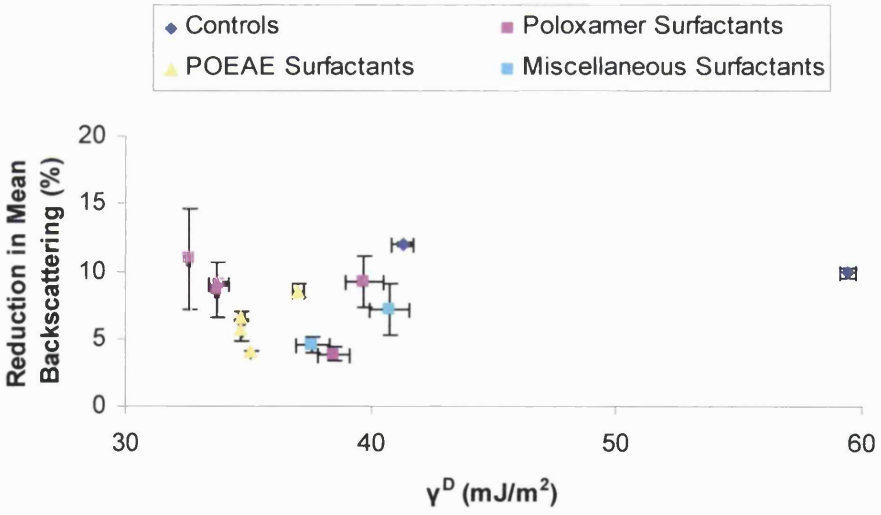

Figure 4.20 Correlation between γ^D values of surface energy and RMB (HFA 134a)

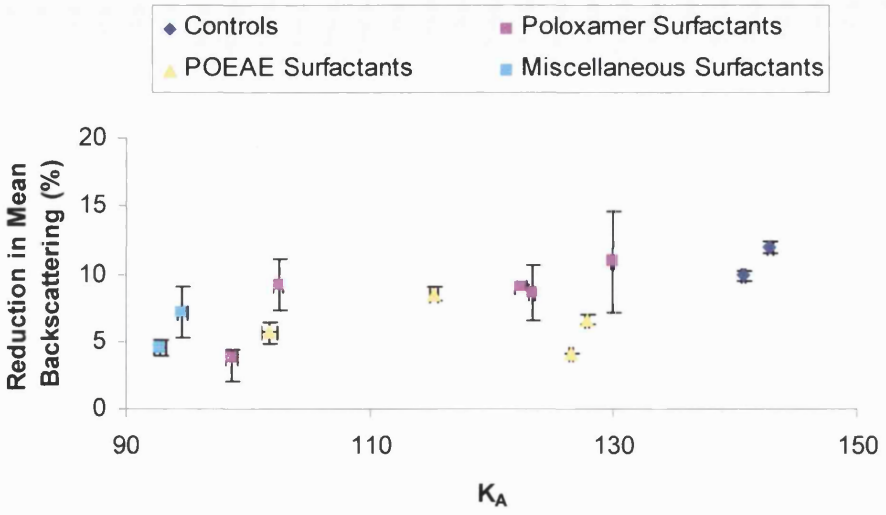

Figure 4.21 Correlation between K_A values of surface energy and RMB (HFA 134a)

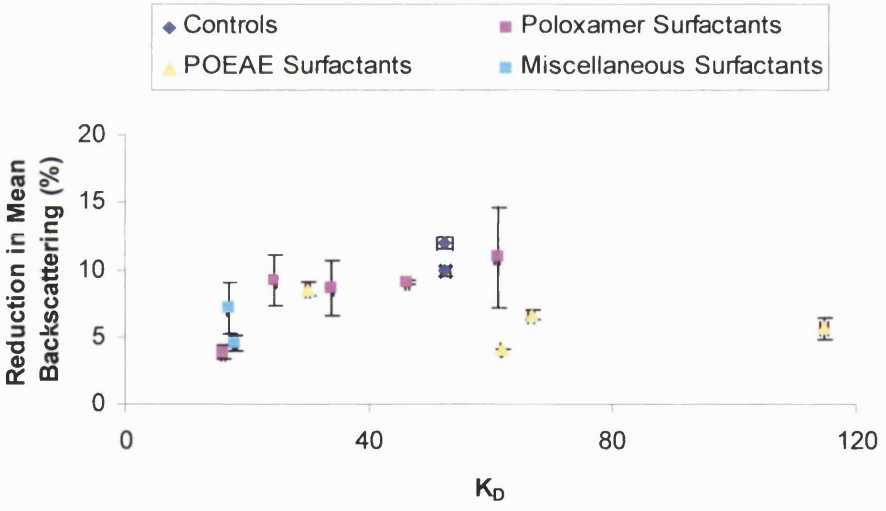

Figure 4.22 Correlation between K_D values of surface energy and RMB (HFA 134a)

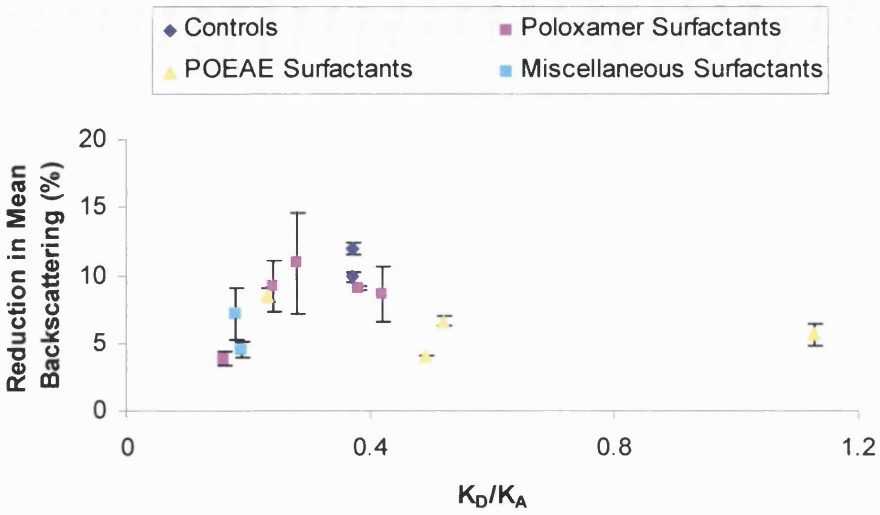

Figure 4.23 Correlation between K_D/K_A values of surface energy and RMB (HFA 134a)

Arguably the only plot revealing a possible correlation is that displaying the relationship between K_A values of surface energy and RMB (Figure 4.21). The possibility of a reduction in the acid component of surface energy having a positive influence on suspension performance was identified in Chapter Three, when examining terbutaline sulphate-surfactant formulations. Results displayed here pertaining to surfactant-containing budesonide formulations would appear to support this theory. An exact mechanism behind this relationship remains unclear. A reduction in overall polarity of a powder surface would contribute to the reduction in dispersive surface energy identified by IGC analysis following the incorporation of a surfactant and so result in a consolidated overall reduction in particle surface energy. Such a reduction in powder surface energy has been previously identified as promoting favourable suspension performance, as suspended material exists in a more stable form, less inclined to aggregate in an effort to reduce surface energy. What is clear from studies conducted in both TS-surfactant and budesonide-surfactant containing formulations, is that while surface energy doubtless contributes to the stability of a suspension of micronised material in volatile propellants, it is merely one of many physicochemical properties at play.

4.14 SUMMARY AND CONCLUSION

Part C of this chapter has attempted to identify a relationship between powder surface energy, and suspension performance in HFA propellants. An identical approach to that in Chapter Three was followed, namely to use van Oss theory and subsequent work by Cline and Dalby to calculate a surface energy interaction value for each formulation, incorporating all three components of surface energy for both the suspended powder and the propellant in a pMDI formulation system. Results from these investigations identified a possible correlation between a reduction in SEI in poloxamer containing formulations, and improved suspension performance, and between a reduction in K_A value and a generalised improvement in suspension performance. No correlations were evident in HFA 227 systems. The lack of any definitive correlation between powder surface energy and suspension performance suggested suspension performance is controlled by more than one, and perhaps several physicochemical properties. Unfortunately, the interrelationship between these properties and their overall affect on pMDI suspension performance is outside the scope of this research.

4.15 OVERALL SUMMARY AND CONCLUSIONS FOR CHAPTER FOUR

The original aim to formulate budesonide with a range of non-ionic surfactants and to investigate the physicochemical characteristics and subsequent performance in pMDI suspensions of budesonide-surfactant formulations has been achieved. Direct measurement of surfactant present in formulations has not been successful; however results from IGC analysis have clearly shown a reduction in surface energy following the incorporation of surfactants by spray drying. Similar to results obtained in Chapter Three, a reduction in both the dispersive and acidic components of surface energy was observed following incorporation of all surfactants. By using budesonide, a hydrophobic substrate, it was hoped that work in this chapter would allow a comparison with TS-surfactant formulation results. In turn it was hoped that a greater understanding of surfactant adsorption to hydrophobic and hydrophilic substrates in terms of molecular orientation would be achieved. However, the similarity in powder surface energy following surfactant incorporation by spray drying (in the case of budesonide formulations), and surfactant adsorption using an incubation method (in the case of TS formulations) prevented any elucidation of the dependence of surfactant orientation at the drug surface on the nature of that surface.

Instead results appeared to indicate that surfactant orientation at the drug surface was identical, regardless of whether the substrate was hydrophilic or hydrophobic. While phase separation of surfactant-containing budesonide formulations was seen to be somewhat improved compared to a control formulation, an additional observation relating to container wall adhesion was made. Formulations containing surfactant exhibited visibly less adhesion of suspended material to the wall of PET containers used in the preparation of pMDI suspension formulations. This phenomenon was identified for further investigation. Finally, investigations into the possible relationship between powder surface energy and pMDI suspension performance failed to identify a definitive correlation, with the exception of a link between a reduction in SEI values for poloxamer surfactant-containing budesonide formulations and suspension stability, and a further link between a general reduction in the acidic component of surface energy and suspension stability. Both of these possible correlations were identified in HFA 134a. The likelihood of pMDI suspension performance relying on an interrelationship of several physicochemical properties other than surface energy alone was concluded.

4.16 FURTHER WORK

Having investigated the formulation of micronised budesonide-surfactant particles for inhalation in some detail, with the aim of using data pertaining to TS-surfactant formulations reported in Chapter Three to understand better the role of surfactant stabilisation and powder surface energy in pMDI suspension stability, future work will explore other aspects of suspension stability particular to those formulations previously prepared. Further work is doubtless necessary to elucidate fully the complex nature of surface energy forces at play in pMDI suspension formulations, and their interaction with other physicochemical properties within the system. Suspension stability data reported thus far for surfactant-containing formulations have been obtained very shortly after pMDI suspension preparation. The next two chapters will describe work aimed at investigating the influence of storage on pMDI suspension performance.

CHAPTER FIVE

STABILITY OF TERBUTALINE SULPHATE – SURFACTANT PMDI FORMULATIONS IN THE PRESENCE OF WATER

5 STABILITY OF TERBUTALINE SULPHATE – SURFACTANT PMDI FORMULATIONS IN THE PRESENCE OF WATER

5.1 INTRODUCTION

Work discussed in Chapter Three described the stabilising influence of a number of surfactants with a low solubility in HFA propellants. Suspension stability of a pMDI formulation containing the hydrophilic drug terbutaline sulphate (TS) in the presence of a range of non-ionic surfactants was seen to improve, with both reduced particle aggregation and phase separation being observed. A number of the surfactants employed in Chapter Three were hydrophobic in nature. One such hydrophobic poloxamer surfactant, L121, was seen to confer stabilising properties on a pMDI formulation in both Turbiscan and Shake-Pause-Fire testing. It was decided to investigate the stabilising effect of adsorption of a hydrophobic surfactant to TS further, by examining the stability of TS pMDI formulations in the presence of small amounts of water over a defined storage period. The aim of this chapter therefore, is to explore whether the adsorption of the hydrophobic surfactant L121 to the surface of TS would consistently confer the stabilising effects observed in Chapter Three despite the presence of increasing amounts of water within the formulation.

The unfavourable effects on both pMDI solution and suspension formulation stability resulting from the presence of small amounts of water within the formulation are well documented (Blondino & Byron, 1998). The level of water contained within a formulation can be critical, and an increase in the initial concentration may result in both physical and chemical degradation. Physical instability can be manifested in increased particle aggregation within suspension formulations in addition to increased adhesion of suspended material to the container. Increased water levels are also known to cause a general decrease in formulation vapour pressure (Atkins et al., 1992). The solubility of drugs within a solution formulation may also be decreased by the presence of water in a pMDI formulation, resulting in physical and chemical instability of drugs susceptible to hydrolysis (Miller, 1990; Johnson, 1992). All negative effects mentioned here have a corresponding effect on the formulation "efficiency" and can cause erratic dosing upon actuation of the device in question. Water is generally accepted to infiltrate pMDI solution and suspension formulations

via ingress through the metering valve. The choice of valve materials in reference to propellant solvency properties is paramount to minimise such ingress. HFA propellants, in addition to possessing altered solvency properties to their predecessors CFC propellants, also possess a higher solvency for water itself. Solubility of water in these propellants is described in Table 5.1. These factors serve to underline the importance of controlling HFA pMDI formulations to prevent any contamination with water.

Table 5.1 Water solubility in HFA and CFC propellants (Solvay Fluor und Derivate GmBH, Germany)

Propellant	**HFA 134a**	**HFA 227**	**CFC 11**	**CFC 12**	**CFC 114**
Water Solubility (ppm)	2200 *(25 °C)*	610 *(25 °C)*	130 *(30 °C)*	120 *(30 °C)*	110 *(30 °C)*

The objectives of the work discussed in this chapter are to use the techniques of both Turbiscan and near infra red spectroscopy (NIRS) to evaluate the performance of pMDI suspension formulations containing TS-L121 microparticles in the presence of increasing amounts of added water, over a storage period of four weeks. It was intended to use Turbiscan to assess suspension performance by examining separation of suspended material from the continuous phase in addition to particle aggregation. The planned use of NIRS was to examine changes in particle size that may occur in formulations containing added moisture, in addition to investigating whether the technique was sensitive enough to qualitatively detect changes in small quantities of water within pMDI suspension formulations contained in transparent PET vials. Such water is expected to be present within the formulation as a solution in the propellant, and therefore free or unbound rather than bound water will be under investigation. It was decided to formulate suspensions in HFA 134a in reference to its increased solubility for water and therefore the greater capacity for water before phase separation.

The use of Turbiscan as an analytical tool to investigate pMDI suspension stability has been extensively discussed previously in Chapters Three and Four, and described in various publications (Rogueda, 2002; Elson et al., 2003). A literature search on

the use of NIRS in the characterisation of pMDI suspension formulation did not yield any previously published work. The principles of NIRS have been described in Chapter Two, Section 2.2.10. NIRS is increasingly used in industry for the purposes of identification and quantification of pharmaceutical samples. It is generally accepted to be particularly suited to relatively pure samples and is not ideally suited to the identification of individual components in a complex system (Jee, 2003). NIRS is increasingly used today in process analytical technology (PAT), whereby quality is built into industrial manufacturing processes through the implementation of analytical control testing on both raw materials and in-process samples. Several advantages may be gained by using NIRS, the primary one being that it is a non-invasive and non-destructive analytical technique, therefore allowing samples to be repeatedly analysed over time. Most relevant to its use in the context of pMDI suspension formulations is that samples may be analysed through their container provided of course that it is transparent. While commercial pMDI canisters are commonly composed of aluminium, the transparent PET vials used throughout this research are suitably transparent. The lack of published work describing the use of NIRS in the characterisation of pMDI formulations may however not be without reason. Potential limitations for using NIRS in this regard may be immediately apparent. As discussed throughout this thesis, pMDI suspension formulations are extremely complex systems comprising at the very least drug, propellant and container, and more commonly propellant blends, multiple surfactants, co-solvents and container coatings. This, combined with the lack of previous research to assign absorbance peaks to functional groups within the system may make spectra difficult to interpret. However, as there remains a need for a non-invasive method of characterisation of these pressurised systems in order to collect data in situ, this work aims to assess the suitability of NIRS for this purpose.

5.2 TURBISCAN ANALYSIS

5.2.1 EXPERIMENTAL PROTOCOL

5.2.1.1 SURFACTANT ADSORPTION AND MICROPARTICLE PREPARATION

Surfactant adsorption to the surface of TS was achieved according to the incubation method previously described in Chapter Three, Section 3.2.2. In summary, 0.2 g of micronised drug was incubated in a dichloromethane solution of surfactant at a concentration of 200 mg/L for 3 hours after which microparticles were recovered by filtration under vacuum. In addition to adsorbing the hydrophobic surfactant L121 to the drug surface, two alternative microparticle formulations were prepared by the same incubation method – one containing the hydrophilic surfactant F127 and the other a TS control formulation. In this way it was hoped to identify any favourable or unfavourable stability conferred on pMDI formulations directly attributable to the hydrophobic nature of the surfactant.

5.2.1.2 PREPARATION OF pMDI HFA SUSPENSION FORMULATIONS

pMDI suspension formulations were prepared according to the pressure filling process previously described in Chapter 2, Section 2.2.5.2. Microparticles from each of the three formulations chosen for investigation (TS control, TS-F127 and TS-L121) were added to PET vials as before. However prior to valve crimping, increasing masses of water at a final concentration of 0.001 % w/w, 0.01 % w/w and 0.1 % w/w were also added to the PET vials using glass capillary tubes. Continuous metered valves were then crimped on to the vials and vials were pressure-filled with HFA 134a to a final concentration of 0.2 % w/w. Samples were stored in the laboratory at approximately 20-25 °C and 55 % RH, and were analysed immediately following preparation, after one week and finally after four weeks.

5.2.1.3 TURBISCAN SCANNING PROTOCOL

Samples were scanned according to the same scanning protocol originally described in Chapter Two, Section 2.2.7.2.

5.2.2 RESULTS AND DISCUSSION

Similar to data treatment described previously in Chapters Three and Four, data obtained from Turbiscan analysis were manipulated to produce a mean backscattering trace for each formulation over the three minute scan period. An identical section of the sample cell length was examined i.e. 30-40 mm, corresponding approximately to the central region of the sample cell. Results from turbiscan analysis of TS-control, TS-F127 and TS-L121 formulations conducted immediately following sample preparation have thus been combined to show the mean backscattering of each formulation over the three minute scan period (Figure 5.1). On initial inspection of TS control formulations at all moisture concentrations, a clear decrease in mean backscattering over the scan period was evident, indicating phase separation and clarification of the suspension over time. This result was consistent with previous analysis of TS control formulations in Chapter Three. In the case of control formulations containing both F-127 (a hydrophilic poloxamer) and L-121 (a hydrophobic poloxamer) with no added moisture however, mean backscattering remained almost constant over the three minute scan period. This confirmed the stabilising influence of adsorption of these surfactants to the drug surface, originally reported and discussed at length in Chapter Three. Figure 5.1 also shows that TS-F127 and TS-L121 formulations containing 0.001 % w/w and 0.01 % w/w added moisture behaved very similarly to the corresponding control formulations containing no added moisture, indicating that the stabilising influence of both surfactants persisted in the presence of small amounts of added moisture. Of particular interest in Figure 5.1 however, are the significantly reduced baseline values of mean backscattering for both TS control and TS-F127 formulations containing 0.1 % w/w added moisture of approximately 24 % when compared to all other formulations examined. Such a reduction in baseline mean backscattering in an evenly dispersed suspension implies that the concentration of suspended material is proportionally lower in the two formulations in question. A visual inspection of formulations prior to analysis by Turbiscan supported this conclusion. As previously discussed in Chapter Three, a formulation must be transferred under pressure from the PET vial in which it is prepared through a continuous valve into the Turbiscan measurement cell. TS-control and TS-F127 samples containing 0.1 % w/w added moisture exhibited extensive particle aggregation immediately post-filling which significantly impaired transfer of the formulations through the continuous valve,

causing a proportion of the suspended material to remain in the PET vial. In contrast, baseline mean backscattering for TS-L121 formulations containing 0.1 % w/w added moisture remained high, within the range of baseline values for other formulations. Therefore results presented here have shown that formulations containing the hydrophobic surfactant L121, in addition to the maximum concentration of added moisture, remained well dispersed and did not exhibit the same particle aggregation. In summary, it may therefore be concluded that the addition of water at a concentration of 0.1 % w/w to pMDI suspension formulations caused an immediately significant aggregation of suspended material and a corresponding increase in particle size in both TS-control and TS-F127 formulations. However, adsorption of a hydrophobic surfactant to the surface of TS conferred persistent stabilising properties on the formulation despite challenging the formulation with 0.1 % w/w added moisture and would therefore appear to have protected the formulation from the instabilities that added moisture may cause when analysed immediately after formulation preparation.

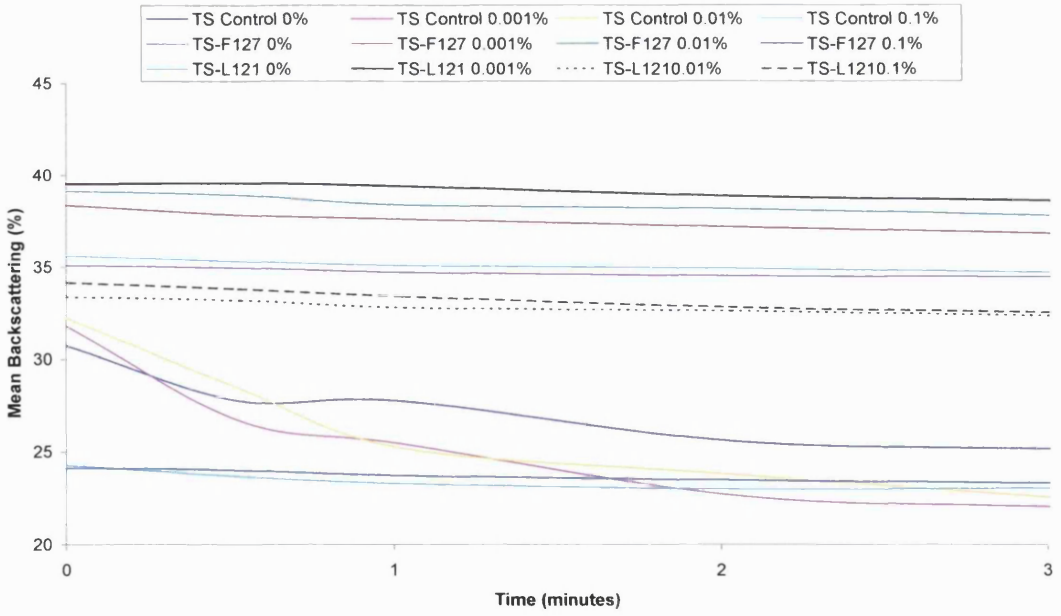

Figure 5.1 Mean backscattering over zone 30-40 mm of the sample cell for all formulations immediately post sample preparation

Similar graphs to that seen in Figure 5.1 are shown in Figures 5.2 and 5.3, presenting the Turbiscan results for all formulations analysed one week and four weeks after

sample preparation respectively. Again, mean backscattering for formulations containing both surfactants was more stable than TS control formulations, the latter showing a clear reduction in mean backscattering over the three minute scan period. In Figure 5.1, a TS-L121 formulation containing 0.1 % w/w added moisture alone was seen to exhibit a favourable suspension performance immediately post sample preparation. However, when analysed one week and four weeks after sample preparation, all three formulations (TS-control, TS-F127 and TS-L121) containing 0.1 % w/w added moisture showed a significantly lower baseline mean backscattering than formulations containing 0.01 % w/w or 0.001 % w/w added moisture, or control formulations. As previously identified in Figure 5.1, it is likely that these observations were the result of impaired transfer of formulations through continuous valves due to an increased particle size caused by the presence of water within the formulation. In fact, formulation suspension behaviour analysed one week and four weeks following sample preparation appears similar, confirming that the destabilising effect of water addition to pMDI suspension formulations is very rapid. Any stabilising influence attributable to the adsorption of a hydrophobic surfactant to the drug surface seen immediately after sample preparation would thus appear to have been short-lived. All masses of water added to pMDI formulations are within the limit of solubility for HFA 134a (Table 5.1). As such, it is not certain why the stabilising effect of F127 observed in pMDI formulations containing 0.001 % w/w and 0.01 % w/w added moisture was not also observed in those containing 0.1 % w/w added moisture. The addition of water to non-aqueous suspensions has previously been shown to impair suspension stability at values above the limit of solubility for water in the continuous phase but to have no negative effect at levels below the limit of solubility (Somasundaran et al., 1998). One reason proposed as a possible cause of the extensive water-induced flocculation observed was a change in the structure of the adsorbed surfactant layer, resulting in the layer becoming more fluid and mobile as water adsorbs at the interface. While it is not certain that such manipulation of the adsorbed surfactant layer was responsible for the suspension instability observed here, it can be concluded that addition of water at a concentration of 0.1 % w/w to formulations caused significant particle aggregation and increased particle size. The adsorption of the hydrophobic surfactant L121 to the drug surface appeared to confer a persistent stabilising effect on a TS formulation

containing 0.1 % w/w added moisture immediately after sample preparation. However, this effect was not apparent one week later.

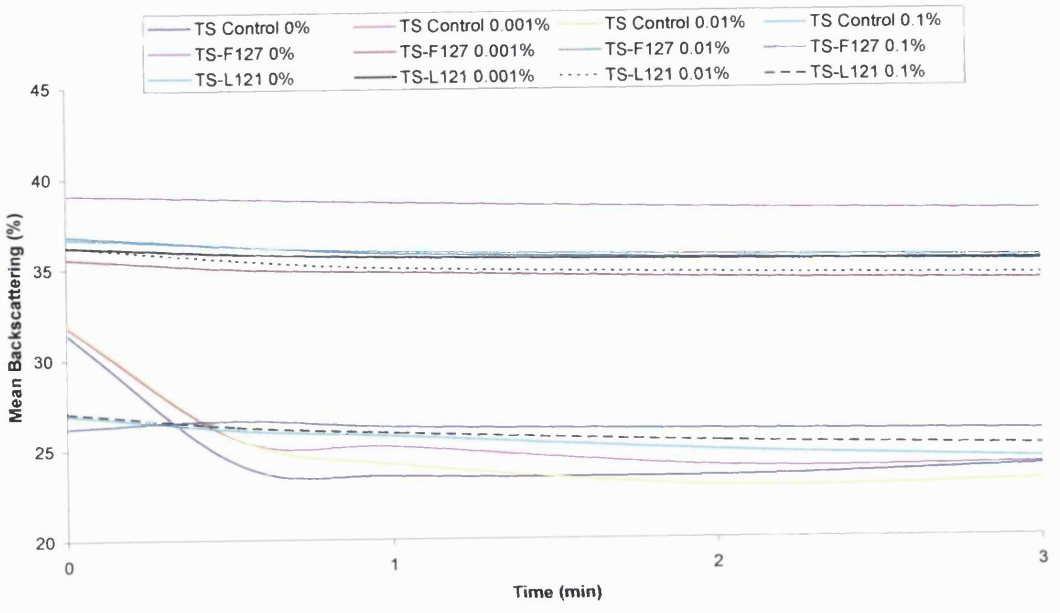

Figure 5.2 Mean backscattering over zone 30-40 mm of the sample cell for all formulations one week post sample preparation

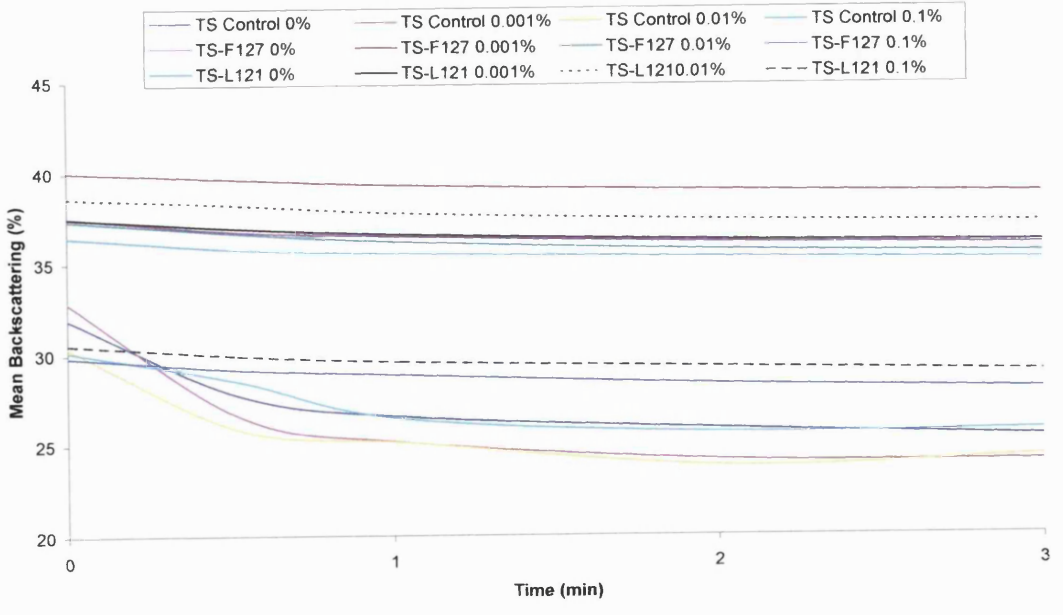

Figure 5.3 Mean backscattering over zone 30-40 mm of the sample cell for all formulations four weeks post sample preparation

5.3 NIRS ANALYSIS

5.3.1 EXPERIMENTAL PROTOCOL

Preparation of pMDI suspension samples, including water addition, was carried out according to the same protocol as described for Turbiscan analysis, observing the same incremental additions of water prior to filling with propellant. Two formulations were considered for NIRS analysis – a TS control formulation, and a formulation containing TS-L121 microparticles. Spectra were recorded for samples at the three time points examined in the previous Turbiscan study, i.e. immediately following sample preparation, one week after preparation, and finally four weeks after preparation. All formulations were manually shaken for one minute prior to scanning. A reference spectrum was obtained using a white reflective ceramic tile standard prior to each scan. Radiation reflected by samples was then measured as a function of wavelength and with respect to reflectance of the standard. Initial experiments investigating variability in spectra obtained for PET vials were carried out. No significant differences were observed in spectra obtained for multiple vials (n=7, data not shown), and as such, the contribution of the sample vial to the spectra of "entire" formulations was deemed to be consistent. In a further attempt to investigate the variability of sample components, spectra of PET vials containing HFA 134a alone (n=4, data not shown) were also recorded. Again no significant differences were observed between samples. Consequently, it was decided that a spectrum for a formulation containing TS alone in HFA 134a (i.e. no surfactant present) with no added moisture would be used as a control at each time point, and the possible influence of the sample vial, or the propellant on sample spectra would no longer be considered.

5.3.2 RESULTS AND DISCUSSION

Spectra of formulations were initially examined for any change in particle size in line with increasing water concentration. While attempts are routinely made to minimise the affect of particle size on NIR spectra, several chemometric approaches have been used to allow the use of NIRS to quantify particle size in pharmaceutical samples (Frake et al., 1998). Its use here for this purpose however, is purely qualitative. Change in particle size is typically observed in a displacement of the baseline apparent absorbance of NIR spectra. This has been explained in terms of a reduction

in light scattering and a deeper penetration of light into the sample. As such, sample reflectance decreases causing the apparent absorbance (log 1/R) to increase (Osborne et al., 1993). Figure 5.4 shows the shift in baseline of spectra obtained for TS-control formulations containing 0, 0.001, 0.01 and 0.1 % w/w added moisture, immediately following sample preparation. Samples were analysed immediately following preparation in order that the mass of added moisture present within formulations was known. Allowing time to elapse after sample preparation may have facilitated the ingress of water into pMDI formulations through the valves, therefore clouding the interpretation of data. An increase in particle size proportional to the increasing water content is clearly evident as the baseline absorbance profile shifts upwards, corresponding to formulations containing increasing amounts of added moisture. A significant increase in baseline absorbance was observed for a formulation containing the maximum value of added moisture (green spectra), in comparison to the increases observed for formulations containing 0.001 % w/w and 0.01 % w/w added moisture. This in turn implies a significant increase in particle size within the formulation, and supports results from Turbiscan analyses confirming that addition of 0.1 % w/w moisture to TS-control formulations initiated extensive aggregation of the suspended phase and a subsequent increase in particle size.

Similar spectra for TS-L121 formulations containing increasing levels of added moisture again show a shift in the baseline in line with mass of water present within the formulation (Figure 5.5). While the greatest baseline shift is again observed in formulations containing 0.1 % w/w added moisture (green spectra), the absorbance remained lower than that seen in Figure 5.4 for a similar concentration of water in a TS-control formulation. Particle size was therefore not seen to increase to the same extent as that observed for TS-control formulations. As such, the stabilising influence of adsorption of the hydrophobic surfactant L-121 to the surface of TS suggested by data from Turbiscan analysis is, to some extent, confirmed by NIRS. This work has also shown NIRS to be a useful tool for the investigation of particle size fluctuation within pMDI systems in situ, a particularly important finding given the difficulties in analysing these complex pressurised systems.

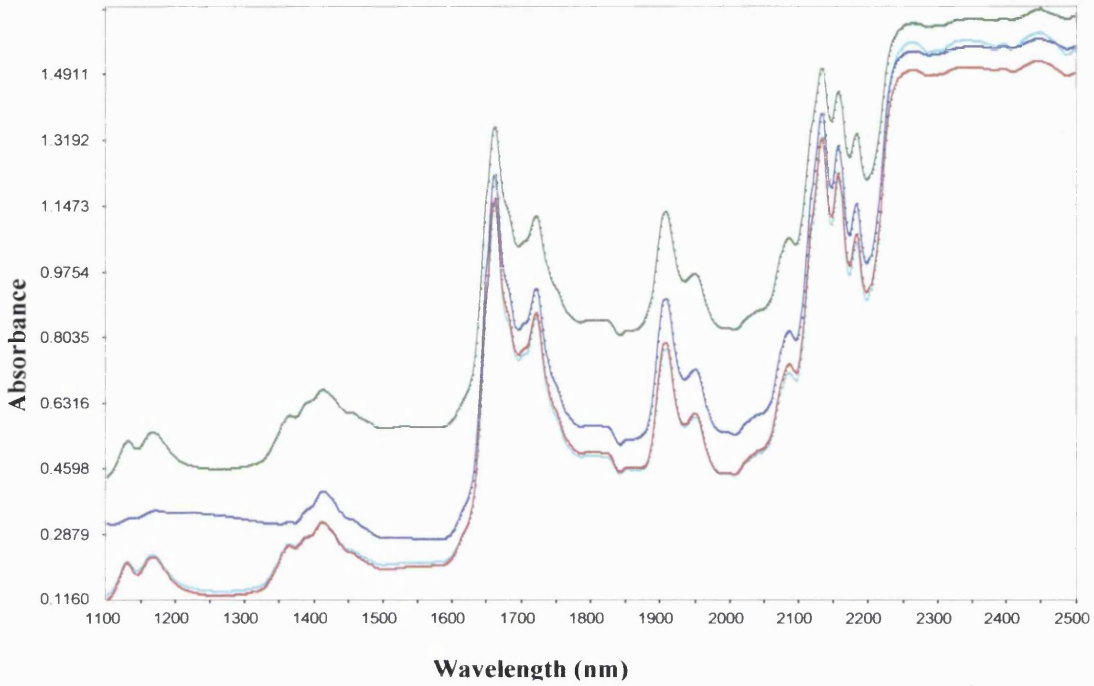

Figure 5.4 Baseline shift in NIR spectra for TS-control formulations containing increasing masses of added moisture. Key: 0 % w/w: red; 0.001 % w/w: light blue; 0.01 % w/w: dark blue; 0.1 % w/w: green

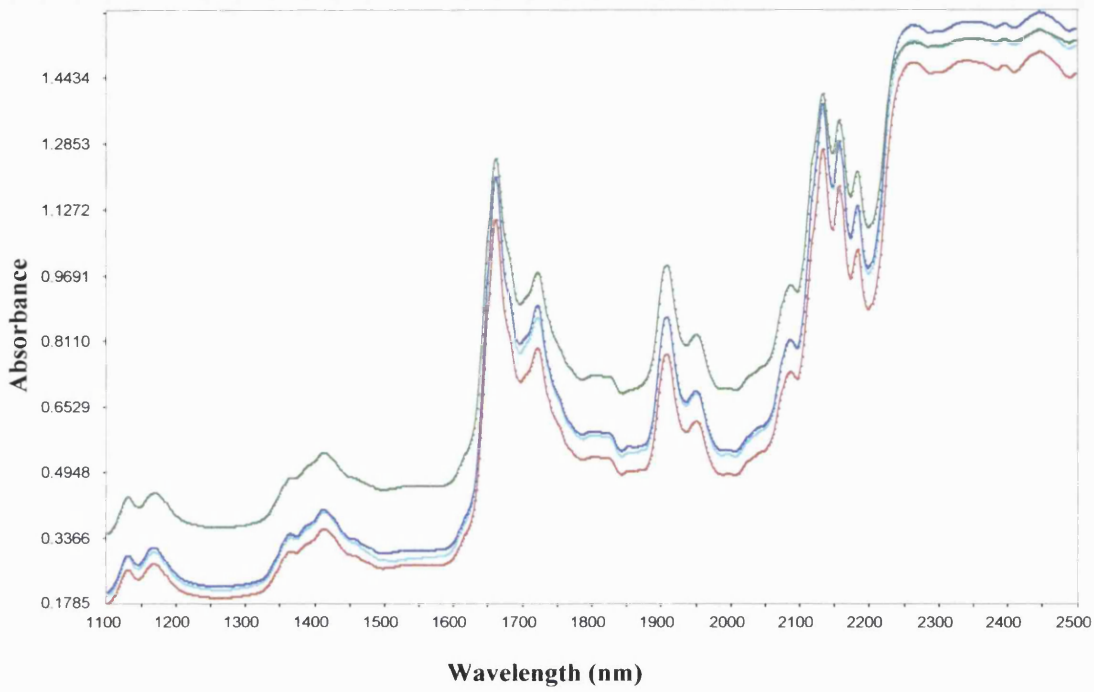

Figure 5.5 Baseline shift in NIR spectra for TS-L121 formulations containing increasing masses of added moisture. Key: 0 % w/w: red; 0.001 % w/w: light blue; 0.01 % w/w: dark blue; 0.1 % w/w: green

The second application of NIRS investigated in this work was its ability to detect small increases in water levels within pMDI systems, such as that which may occur on storage as a result of the ingress of water through the valve. While the effect of particle size was of primary importance in results previously discussed, in order to assess moisture within the pMDI system accurately, the influence of particle size fluctuation on NIR spectra was minimised through mathematical manipulation of data to yield the standard normal variate (SNV) of the second derivative spectra or SNV 2^{nd} Der., (Jee 2003). In this way, peaks appearing in original spectra are inverted while maintaining identical positions and the effect of particle size is minimised. The use of NIRS to investigate water within various systems is well documented. Water typically shows strong absorption bands in two regions of the NIR spectrum, at approximately 1420 and 1920 nm, and while overlapping of absorbance bands is common, those associated with moisture tend to be well resolved. While the quantification of small amounts of water within pharmaceutical

samples has been traditionally carried out using Karl Fischer titration, NIRS has also been shown to be an accurate method for the quantification of water content within pharmaceutical samples. Previously published work successfully used NIRS to quantify water content within a hygroscopic drug powder over the range 0.5 – 11.4 % w/w with a standard error of prediction of 0.11 % w/w (Zhou et al., 1998). However, the work required to construct such accurate quantification methods is considerable and typically requires an accurate reference method (e.g. Karl Fischer) in addition to a large number of spectra from a range of samples in order to produce a suitable calibration set. It is only once this has been prepared that future samples may be measured against the calibration model and their water content predicted. As such, the use of NIRS to investigate changes in water content within pMDI formulations in this work is purely qualitative.

The conventional assignment of absorption bands for water within NIR spectra dictates that two regions in particular apply: 1450 nm corresponding to the first overtone of O-H stretch at 3500 nm, and 1930 corresponding to a combination of the same O-H stretch in addition to an O-H bend at 1645 nm (Osborne et al., 1993). However, the exact position and width of these absorption bands may vary depending on the chemical environment. Initially, analysis of the spectra recorded for TS formulations was focused on the identification of a suitable peak to investigate changes in water content of the pMDI systems considered here. This analysis revealed the absence of a consistent peak in the region of 1450 nm and so attention was focussed on the 1930 nm region. Three peaks were evident in a typical NIR spectrum of TS pMDI formulation samples in this region. Based on a literature search, the most likely peak attributable to free water contained within these systems was that observed at 1908 nm (Bonner & Choi, 1974; Zhou et al., 2003).

Figure 5.6 shows the SNV 2nd Der of a representative NIR spectrum for a TS-control formulation containing no added moisture, taken immediately following sample preparation. The highlighted section of the spectrum in Figure 5.6 focuses on the 1930 nm region of the spectrum. This was then enlarged and the magnified region of the spectrum may be seen in Figure 5.7. The three peaks in the 1930 nm region of the spectrum were clearly evident upon magnification. While the peak at 1908 nm was the only likely candidate for free water, a peak at this wavelength appeared in

"blank" spectra for empty PET vials. The potential for this peak to mask any peak corresponding to water within the pMDI formulations was minimised by subtracting the "blank" spectrum from all subsequent sample spectra. Figure 5.7 therefore shows both the original spectrum, and the corrected spectrum produced following subtraction. The peak assigned to water at 1908 nm, while reduced slightly in intensity, was seen to persist after this correction.

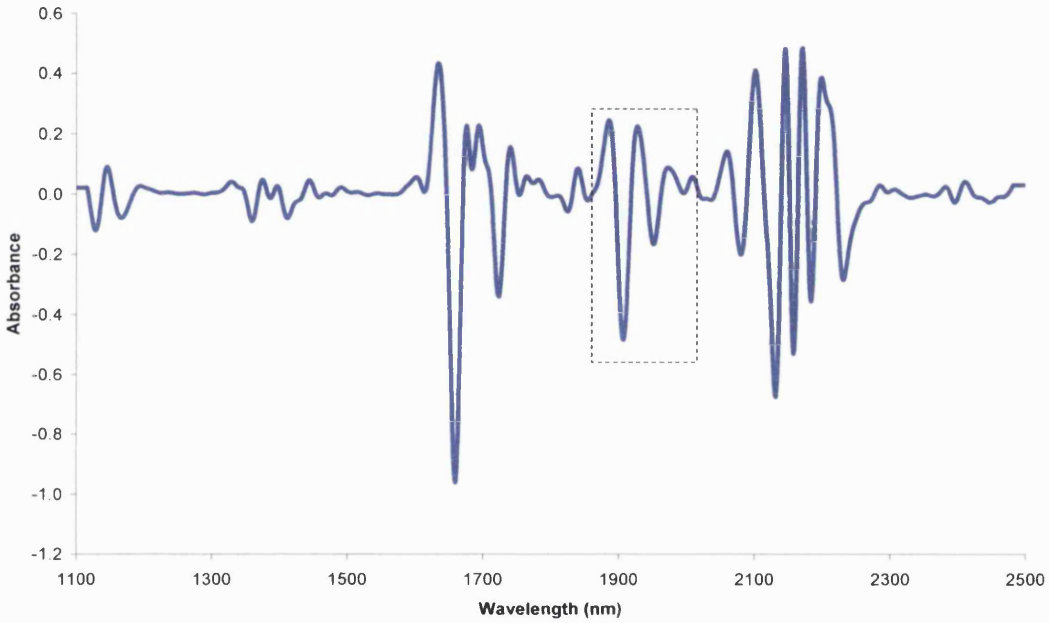

Figure 5.6 SNV 2nd Der of NIR spectra for TS-control formulation in HFA 134a, 0 % w/w added moisture

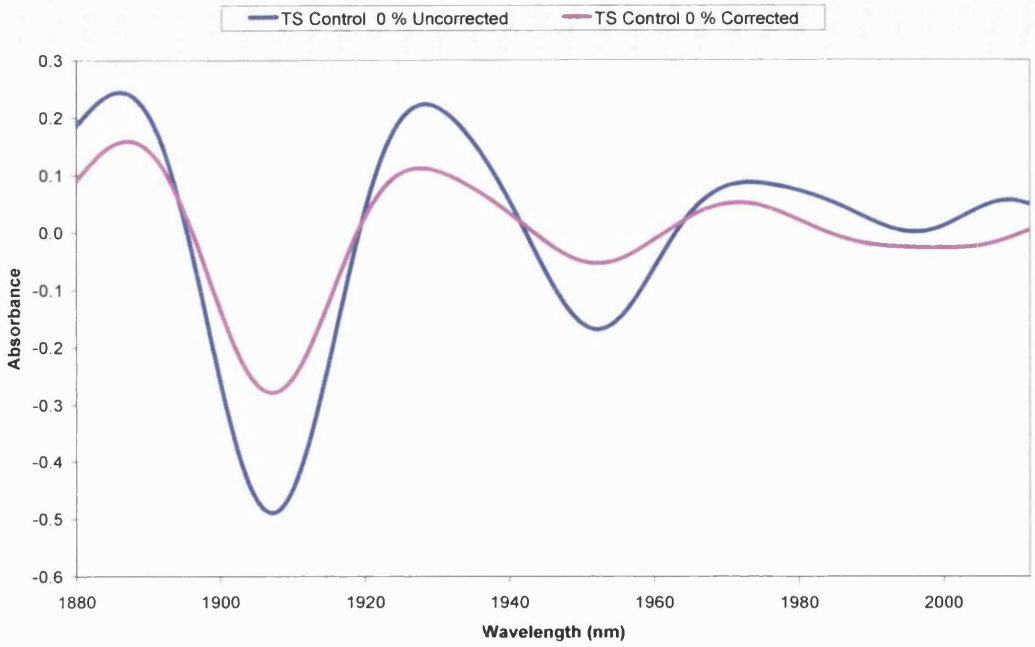

Figure 5.7 SNV 2nd derivative of NIR spectra for TS-control formulation in HFA 134a, 0 % w/w added moisture

Examination of spectra recorded for TS formulations initially aimed to investigate whether NIRS was sensitive enough to detect small changes in water corresponding to the incremental additions of water made to the pMDI suspension formulation samples. Therefore spectra of TS-control formulations containing increasing amounts of added moisture were plotted against one another in the hope that an increase in system water content would be reflected in a corresponding increase in peak intensity at 1908 nm (Figure 5.8).

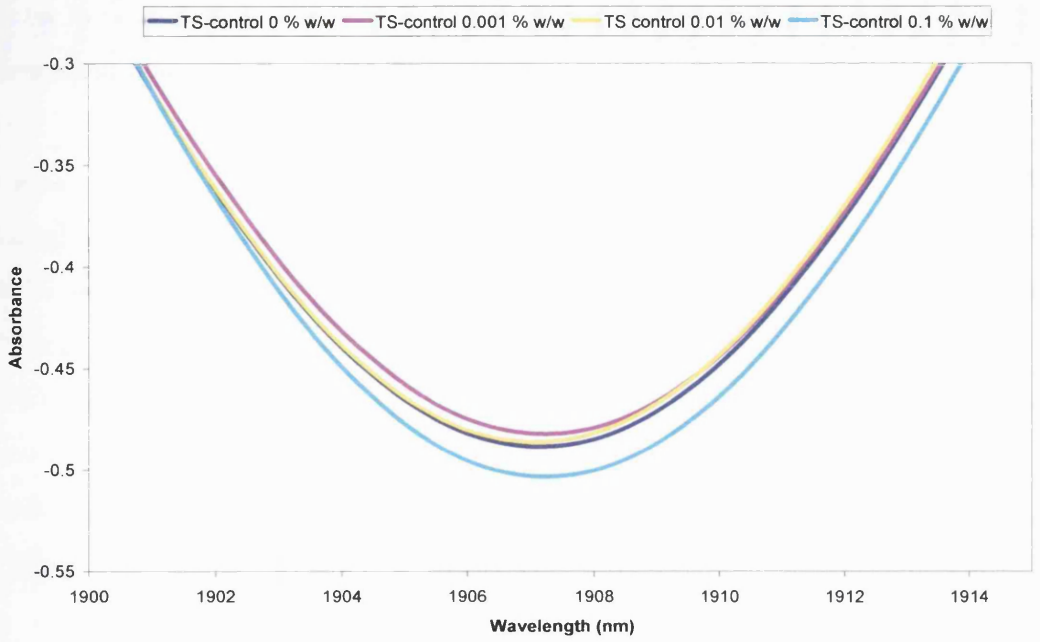

Figure 5.8 TS control formulations containing increasing masses of added water, immediately following sample preparation

The peak at 1908 nm shown in Figure 5.8 was observed to alter in intensity over the range of water concentrations; however the change in intensity was not linear. As a result, other peaks across the NIR spectrum were examined to determine whether a linear response was evident in the behaviour of any further peaks previously discounted. A linear response in peak intensity corresponding to the change in water concentration was not observed in any other peaks. Examination of spectra for TS-L121 pMDI formulations containing increasing masses of added water confirmed that a linear increase in peak intensity corresponding to the incremental additions of water could not be identified (data not shown). As such, it would appear that NIRS was not sensitive enough to detect changes in water concentration within pMDI systems at the levels present in this work. Indeed this is in line with other published work by Stokvold et al., (2002) who identified a limit of detection of water within a freeze-dried product to be 0.08 % w/w. The maximum mass of added water present in this work, at 0.1 % w/w is notably close to the limit of detection recorded by the authors and may serve to confirm the findings discussed here.

A further attempt to identify a use for NIRS in the characterisation of pMDI formulations was then carried out, by investigating the possibility of using NIRS to detect water ingress through a valve over the four week storage period imposed on samples examined here. Given that the technique was shown not to be sensitive enough to detect a linear change in water concentration from 0 % w/w to 0.1 % w/w in TS samples, it was decided to look at the effect of possible water ingress on the TS-control sample containing the maximum mass of added water initially (0.1 % w/w). As such, NIR spectra for the TS-control sample containing 0.1 % added water recorded immediately after sample preparation, one week later and finally four weeks later were plotted against a TS-control formulation containing no added water (Figure 5.9).

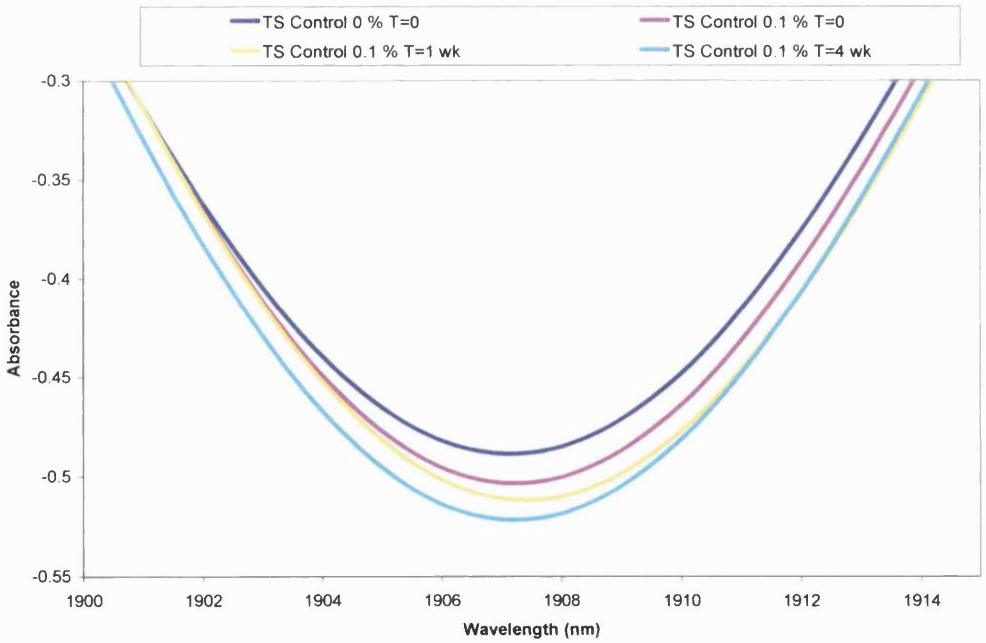

Figure 5.9 TS-control formulations containing 0.1 % w/w added moisture

In contrast to results presented in Figure 5.8, a linear increase in peak intensity at 1908 nm over the four week storage period was observed (Figure 5.9). These data would suggest that ingress of water through the valve did indeed occur, giving rise to a gradual increase in the water present in TS-control formulations over the period of investigation. It is possible that the limit of detection for water within the system was very close indeed to 0.1 % w/w, and subsequent increases in water content were accurately detected. However, given that NIRS was deemed insensitive to the

discreet changes in water content within the pMDI systems examined here in the previous study, this cannot be concluded with any conviction.

Further studies may aim to investigate whether NIRS may be suitable to detect greater quantities of water within pMDI systems. However consideration must be given to the applicability of the study to the levels of water ingress that may be expected to occur in representative pMDI formulations. Consideration should also be given to the type of materials making up the device, and other components of the formulation. Future investigations may benefit from challenging the system with large amounts of water initially, in an attempt to unequivocally identify a peak or peaks within the NIR spectra attributable to the free water contained within the system. Finally, the preparation of a calibration set may also provide sufficient support to enable the use of NIRS in the quantification of water content in pMDI systems.

5.4 SUMMARY AND CONCLUSION

Initial work described in this chapter aimed at investigating whether the adsorption of the hydrophobic surfactant L121 to the surface of TS would confer the same stabilising properties as those shown in Chapter Three, in the presence of an increasing amount of water within the pMDI suspension formulation. The presence of water at a level of 0.1 % w/w was shown to precipitate extensive particle aggregation in TS-control formulations and those containing TS-F127, however such aggregation was not observed in formulations containing TS-L121. Results from Turbiscan analysis therefore confirmed that such a stabilising influence was achieved through the adsorption of L121 to the surface of TS. This effect was however short-lived, and was not evident one week after sample preparation.

The role for NIRS in the characterisation of pMDI formulations was then assessed in subsequent experiments. A good correlation between increasing water content and particle size was observed however, the technique was not found to be adequately sensitive to detect changes in water content within the systems examined. It must therefore be concluded that given the low levels of water likely to be present within pMDI formulations, NIRS is not a viable technique for this purpose.

5.5 FURTHER WORK

Experiments presented and discussed in this chapter have been directed at investigating the effect of storage on pMDI suspension performance, in the presence of increasing masses of water. Results recorded here have advanced an understanding of the behaviour of pMDI suspension formulations initially obtained from the work described in Chapters Three and Four. The final chapter of this thesis will describe further attempts to build on this understanding by examining the behaviour of budesonide pMDI formulations on storage. However, rather than investigate the effect of water on storage, work will instead be focused on the phenomenon of adhesion of the suspended microparticles to the container wall initially identified in Chapter Four. Work will also aim to identify a relationship between adhesion and surface energy.

CHAPTER SIX

ADHESION PHENOMENA IN BUDESONIDE PMDIS

6 ADHESION PHENOMENA IN BUDESONIDE PMDIS

6.1 INTRODUCTION

Work described in Chapter Four detailing the preparation and characterisation of budesonide-surfactant microparticles revealed an unexpected aspect of instability particular to pMDI suspension formulations containing micronised budesonide. Adhesion of suspended material to the wall of PET vials was observed almost immediately after vials had been filled with HFA propellant. In contrast, pMDI formulations containing budesonide co-spray dried with a range of non-ionic surfactants did not show the same tendency for container wall adhesion. Interestingly, adhesion was only observed to occur to the container surface above the suspension meniscus. While the suspension stability of budesonide-containing pMDI formulations has been previously examined in Chapter Four, both in terms of particle aggregation and phase separation using the Turbiscan apparatus, the phenomenon of container wall adhesion warrants dedicated investigation and is therefore the focus of this chapter. The aims of this chapter were therefore to confirm the preliminary visual observations made during the experiment described in Chapter Four, and through further investigation of adhesion phenomena in budesonide suspension pMDI formulations, to reveal the relationship between container wall adhesion and surface energy in suspension pMDI HFA systems.

The adhesion of suspended material to either the container wall or valve components is a well documented potential instability within suspension pMDI systems. In such delivery systems which rely on consistent, accurate dosing with each actuation of the device, adhesion can result in inaccurate dosing, valve blockage and therapeutic failure. The phenomenon of adhesion within these systems can be explained through the concepts of surface area, and surface energy. The optimal particle size range for suspended drug particles within a pMDI formulation has been defined as being between 2-5 μm. By virtue of this very small particle size, drug particles within such systems exist in a state of high surface free energy, which the system seeks to minimise through particle aggregation, or adhesion to the container wall (Parsons et al., 1992). An increase in the extent of adhesion has been observed generally with the advent of alternative pMDI suspension systems comprising HFA propellants rather than their CFC predecessors. It is believed that the primarily electronegative

mantel of the HFA propellants acts to repel material suspended within the continuous phase, and as such adhesion in these systems is driven by repulsive forces rather than an attraction between suspended material and container surface (Vervaet & Byron, 1999). In practice, the interior surface of pMDI containers is commonly coated with a low energy film prior to filling in an attempt to minimise particle adhesion. Materials used commercially include fluorinated ethylene-propylene (FEP) and perflourinated alkoxy (resin) (PFA). However, such processes naturally increase the cost of manufacture and therefore the observation of reduced adhesion in budesonide formulations containing the range of surfactants employed in this thesis certainly warrants further investigation.

Several objectives were defined during the planning of this work. Initial experiments were planned in order to recreate the experimental conditions particular to formulations in Chapter Four in which the original observations of reduced adhesion in budesonide formulations containing surfactants to PET containers were made, in addition to monitoring the adhesion over extended periods of time. Further experiments investigating the adhesion of micronised budesonide alone to varying surfaces were also devised. Finally it was hoped that by using contact angle measurement, surface energy parameters for all surfaces investigated would be deduced, and these data used to elucidate the general relationship between surface energy and container wall adhesion, by way of calculating both surface energy interaction and work of adhesion values.

6.2 EXPERIMENTAL PROTOCOL

6.2.1 ADHESION OF BUDESONIDE-SURFACTANT MICROPARTICLES TO PET VIALS

The first objective of this work was to recreate experimental conditions in Chapter Four in order to confirm the original anecdotal observation of reduced container wall adhesion in budesonide-surfactant pMDI formulations. As such, pMDI suspension formulations were prepared containing a range of budesonide-surfactant microparticles, prepared by co-spray drying from suspension, in both HFA 227 and HFA 134a at a concentration of 0.2 % w/w. Co-spray dried material was identical to that described in Chapter Four. Control formulations containing micronised budesonide alone were also prepared. Vials were stored for a total of four weeks in

the laboratory in an upright position, and samples taken for analysis at 24 hours, 1 week and 4 weeks following preparation. Three vials were prepared for each formulation, for each time point in each of the propellants. Once removed for analysis, each vial was manually shaken to dislodge any loosely adhered microparticles and then photographed. Vials were actuated until empty in the inverted position, at which point a tube cutter (Imperial Eastmann) was used to remove aluminium valves. Vials were then weighed until constant weight (W_1) to ensure evaporation of all remaining propellant. Vials were rinsed with absolute ethanol until all material adhering to the container wall was dissolved. Vials were again dried to a constant weight (W_2). The amount of material adhered to the container wall was subsequently calculated as W_1-W_2. This amount was expressed as a percentage of the initial mass of material present in each vial.

6.2.2 ADHESION OF BUDESONIDE-SURFACTANT MICROPARTICLES TO PET VIALS COATED WITH SURFACTANT

An alternative method of reducing container wall adhesion in PET vials was investigated in order to discover whether the location of surfactant at the drug surface was an essential requirement for reduced adhesion. As such, PET vials were incubated with solutions of identical surfactants to those contained in budesonide-surfactant formulations investigated in Section 6.2.1 and a similar assessment of the extent of adhesion was made. Surfactant solutions of the poloxamer surfactants L31 and F108, reverse poloxamers 10R5 and 31R1 and the polyoxyethylene alkyl ether surfactants B59 and 1216CO3 at a concentration of 1 % w/v in purified water were prepared and filled into empty PET vials and set aside for 2 hours. After this time, vials were emptied and dried in an oven at 50 °C until constant weight. Subsequent pMDI suspension formulations containing micronised budesonide alone were prepared in both HFA propellants at a concentration of 0.2 % w/w. Three vials were prepared for each formulation, in each of the two propellants. Vials were stored for one week in the laboratory after which time the amount of adhered material was calculated according to the same method as that described in Section 6.2.1.

6.2.3 ADHESION OF BUDESONIDE-SURFACTANT MICROPARTICLES TO COATED GLASS VIALS

The adhesion of micronised budesonide to surfaces coated with two commercial coating agents Repelcote (BDH) and Sigmacote (Sigma) in addition to the poloxamer surfactant F108 and the reverse poloxamer surfactant 31R1 was investigated. Repelcote consists of a 2 % solution of dimethyldichlorosilane in octamethylcyclotetrasiloxane, while Sigmacote is a colourless, clear solution of chlorinated organopolysiloxane. The organic nature of the commercial coating agents prohibited their use in PET vials and consequently, 15 ml Purgard glass vials (Schott) were employed in this particular adhesion study. Four coating strategies were used in the current experiment. Vials were pre-coated with Repelcote (group 1), Sigmacote (group 2), Repelcote and a subsequent aqueous solution of F108 (group 3), or finally with an aqueous solution of 31R1 alone (group 4). The two coating strategies in groups 3 and 4 were employed in the hope that the container surface could be engineered in terms of being hydrophilic and hydrophobic respectively by way of designed orientation of the surfactant molecules. Manufacturers' coating instructions were followed for both Repelcote and Sigmacote. Vials coated with Repelcote were filled with the agent and then emptied after a period of between 5 and 10 minutes. Vials were then rinsed with ethanol to remove any excess Repelcote and were left to air-dry. Vials coated with Sigmacote were simply rinsed with the agent and left to air-dry for 5 minutes. Both agents act by reacting with the surface silanol groups of glass to produce a neutral, hydrophobic and microscopically thin film. Vials in group 3 were coated with an aqueous solution of F108 following coating with Repelcote according to the same method described in Section 6.2.2. Similarly, vials in group 4 were coated with an aqueous solution of 31R1 according to the same method. Suspension pMDI formulations containing micronised budesonide alone were then prepared in both HFA propellants at a concentration of 0.2 % w/w. All vials were stored in the laboratory for one week, at which time the amount of adhered material was assessed according to the method described in Section 6.2.1. The majority of vials were stored in an upright position however two additional groups of vials coated with Repelcote and Sigmacote respectively were stored horizontally. A final group of vials were half-coated with Repelcote by immersing vials in the solution in an inverted position such that only the upper half of the vial was in contact with the solution. In this manner it

was hoped to coat the region of the vial not in contact with the pMDI suspension once filled into the vials. In turn, by reducing adhesion above the suspension meniscus, the region where adhesion had been exclusively observed previously, the possibility of adhesion to the section of the container wall in contact with the suspension could be investigated. Again, three vials were prepared for each group, in each of the two propellants.

6.2.4 CONTACT ANGLE MEASUREMENTS TO ELUCIDATE SURFACE ENERGY OF VIAL COATINGS AND PET

In order to investigate the relationship between surface energy and adhesion to the container wall in the budesonide pMDI suspension systems investigated here, surface energies of all container surfaces employed were required. Using the method previously described in Chapter One of van Oss et al (1988), the contact angles of three fully characterised liquids on the solid surfaces in question were determined by the Wilhelmy plate method detailed in Chapter Two, Section 2.2.9 using a Dynamic Contact Analyser (Cahn). Glass cover slips were coated to produce identical surfaces to those described in groups 1-4 in Section 6.2.3 (coated in an identical manner). In addition, sheet PET (Westward Plastics, UK) of 3 mm thickness was cut to create sections of approximately the same size as glass cover slips. The contact angle made by two polar liquids, purified water and ethylene glycol (Sigma), and one non-polar liquid 1-bromonaphthalene (Fisher) on each surface was measured. In the case of PET, the alternative non-polar liquid diiodomethane was employed due to difficulties in measurements using 1-bromonaphthalene. A series of simultaneous equations were then used to calculate surface energy parameters for each of the surfaces under investigation.

6.3 RESULTS AND DISCUSSION

6.3.1 ADHESION OF BUDESONIDE-SURFACTANT MICROPARTICLES TO PET VIALS

Figures 6.1 (HFA 134a) and 6.2 (HFA 227) show results of initial experiments designed to recreate the conditions present in Chapter Four, where the original observations regarding reduced container wall adhesion were made. All formulations containing surfactant were seen to possess a reduced amount of material adhering to the container wall following vial actuation. Control formulations in HFA

134a showed approximately 22 % adherence when sampled after 24 hours in comparison to formulations containing spray dried budesonide with the reverse poloxamer 10R5 and the polyoxyethylene alkyl ether surfactant B59 which both showed approximately 11 % adherence at 24 hours. Adhesion for all formulations containing surfactant remained less than that of the control formulations at all sampled time points. Adhesion at 24 hours appeared to be close to the maximum adhesion value for all formulations examined with the exception of formulations containing 10R5. As such there appeared a small increase in adhesion over the four week period but given the magnitude of error values this increase did not appear significant. This finding would suggest that the adhesion phenomenon occurring in these formulations is very fast in onset, confirming observations made in Chapter Four where adhesion in vials containing micronised budesonide alone was visible almost immediately after filling with propellant.

Results in HFA 227 were in line with those of HFA 134a in that all formulations containing surfactant exhibited reduced adhesion when compared to micronised budesonide control, however the effect appeared more pronounced. Initial adhesion in control formulations was slightly higher than that seen in HFA 134a at approximately 25 %, and the greatest reduction in adhesion was seen in formulations containing the poloxamer surfactant F108 and the polyoxyethylene alkyl ether surfactant 1216CO3 at approximately 9 %. As such, different formulations presented varying orders of performance in terms of reducing adhesion depending on the propellant used. Similar variations have been observed throughout this thesis where orders of suspension stability of a range of formulations have differed between propellants.

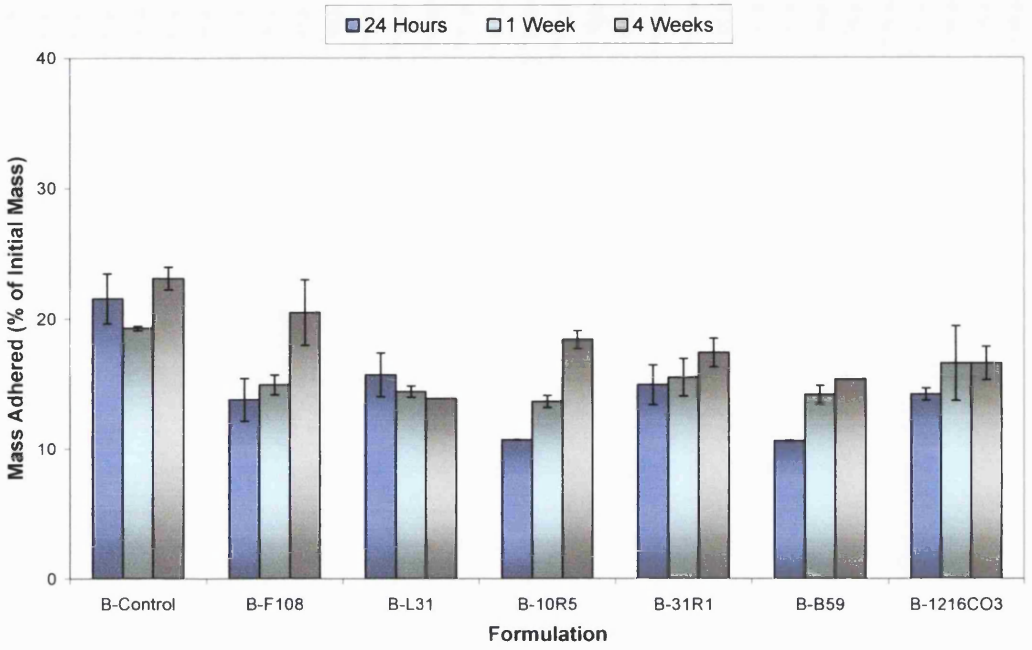

Figure 6.1 Adhesion of budesonide-surfactant microparticles to PET vials in HFA 134a

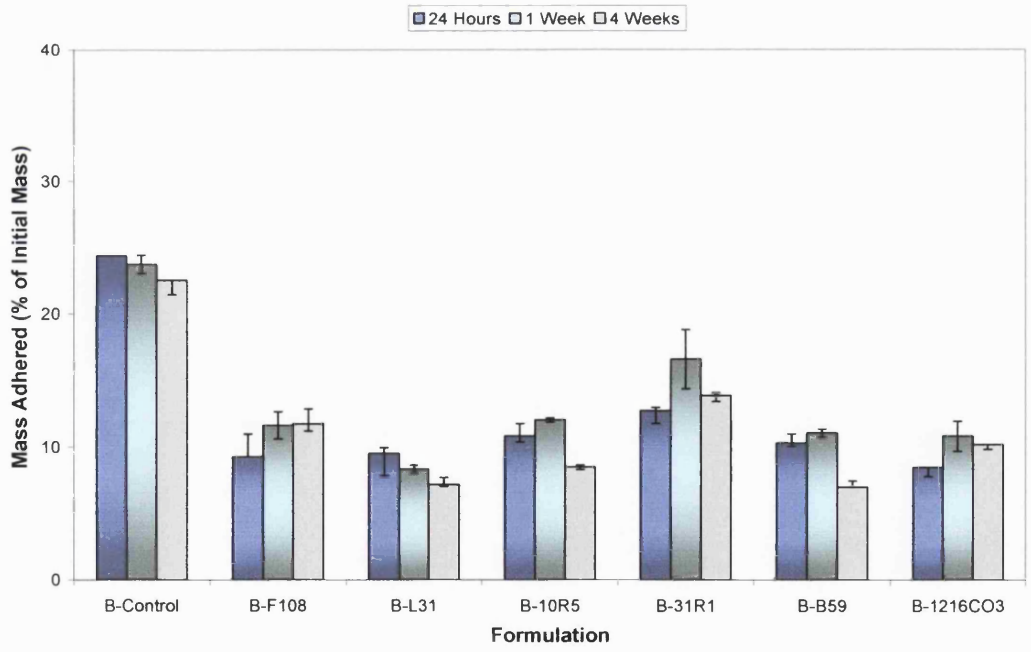

Figure 6.2 Adhesion of budesonide-surfactant microparticles to PET vials in HFA 227

Photographic images shown in Figures 6.3 and 6.4 provide a visual representation of the reduced adhesion observed in HFA 227. Figure 6.3 shows three vials containing micronised budesonide alone following storage at four weeks. Material adhering to the upper half of the PET vials is clearly evident. In contrast, Figure 6.4 shows three vials containing a suspension of budesonide-F108 microparticles again in HFA 227. Very little adhesion is visible. In all formulations investigated, adhesion was observed above the meniscus of the suspension only, in keeping with observations made during experiments described in Chapter Four. Overall, results from this experiment successfully recreated experimental conditions imposed in Chapter Four and confirmed the original anecdotal observation that adhesion to the container wall was reduced in formulations containing surfactant.

Figure 6.3 Adhesion of budesonide to PET in HFA 227 at 4 weeks

Figure 6.4 Adhesion of budesonide-F108 to PET in HFA 227 at 4 weeks

6.3.2 ADHESION OF BUDESONIDE-SURFACTANT MICROPARTICLES TO PET VIALS COATED WITH SURFACTANT

Attempts to coat PET vials with surfactant solutions were unsuccessful in reducing adhesion of micronised budesonide to PET vials. No difference in the mass of material adhered to PET was observed between uncoated control vials and vials coated in any of the surfactants examined, with the adhesion of micronised budesonide in line with the results observed in control formulations described in Figures 6.1 and 6.2. Results are therefore not shown. It was unclear why the coating strategy had not imparted the same protection against adhesion as adsorption of the same surfactant to the surface of the micronised drug. A likely explanation was that the anticipated migration of surfactant molecules to the interface of solution and container wall did not occur, and/or did not result in any subsequent adhesion of the surfactant molecules to the container wall. Alternatively, adhesion may have occurred but was reversible and surfactant molecules were dislodged upon filling the vial with propellant. In any case, it is clear from these experiments that in order to effectively reduce the adhesion of micronised budesonide to the walls of PET containers, surfactant present in the formulation must be located at the drug surface.

6.3.4 ADHESION OF BUDESONIDE-SURFACTANT MICROPARTICLES TO COATED GLASS VIALS

Given that adhesion was observed to occur very rapidly following formulation preparation, it was decided to conduct further experiments over a one week period rather than the four weeks previously employed. Previous results had indicated that the extent of adhesion at this point would be at an approximate maximum. Results of the third approach to container wall adhesion investigation are presented in Figures 6.5 and 6.6 which show the extent of adhesion of micronised budesonide to varying coated glass surfaces when formulated in both HFA 227 and HFA 134a. Uncoated glass was used as a control. Results from this experiment revealed a range of adhesion profiles among the different coatings examined. In both HFA propellants, adhesion was greatest in containers coated with Repelcote. Interestingly, adhesion to the uncoated glass surface was less than to any other surface in HFA 227. In HFA 134a, adhesion to uncoated glass was also low in comparison with other surfaces, with the lowest adhesion reported in containers coated with 31R1. However, standard deviation values are such that adhesion to uncoated glass and to glass coated

with 31R1 is effectively the same in both propellants. Similarly, adhesion to surfaces coated with Repelcote, and with Repelcote and subsequently with F108 is also very similar. This is in agreement with the results of the previous experiment indicating that attempts to coat the interior surface of PET vials with various surfactants was unsuccessful. Adhesion to Sigmacoted-glass was less than that observed to Repelcoted surfaces, with the difference more pronounced in HFA 227. A comparison of the results of this experiment with work previously published by Parsons et al., (1992) revealed an interesting deviation. The work of these authors examined the adhesion of five model micronised particles to coated glass containers in a model propellant. Among the coating agents employed in their work was Repelcote. The energy of adhesion of most of the micronised particles to Repelcoted glass, including that of beclometasone, was less than to uncoated glass; a result which has not been reproduced in the experiment described here. It is unclear as to why the behaviour of budesonide, similar to beclometasone in terms of being a hydrophobic steroid molecule was not consistent with these previously published results. However, surface energy data for beclometasone presented in the work of Parsons et al. reveals a dispersive component of surface energy for beclometasone of 44.0 mJ/m^2, a value lower than that determined experimentally in Chapter Four of this thesis for budesonide (59.4 mJ/m^2). This, in combination with the suspension of formulations in the study by Parsons et al. in a model propellant chosen for its similarity to CFC propellants rather than the newer HFA propellants used here may explain the discrepancies observed.

Adhesion in vials coated only above the meniscus of the suspension was no different to that of other vials and as such results are not shown. Given that the coating strategies employed in the experiment were unsuccessful in reducing the amount of micronised budesonide adhering to the container wall, this particular result was not surprising. Similarly, vials fully coated with Repelcote and Sigmacote, but stored horizontally showed similar adhesion to vials stored in the upright position. In addition, adhesion in these vials was to the upper surface of the prone vial and not to the surface in contact with the suspension. As such, in all vials examined, adhesion occurred only to surfaces not in contact with suspended formulation.

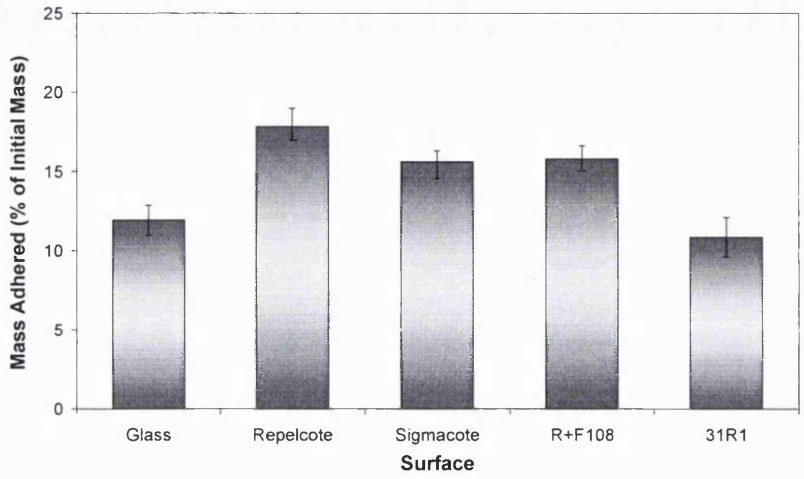

Figure 6.5 Adhesion of micronised budesonide to coated glass surfaces in HFA 134a

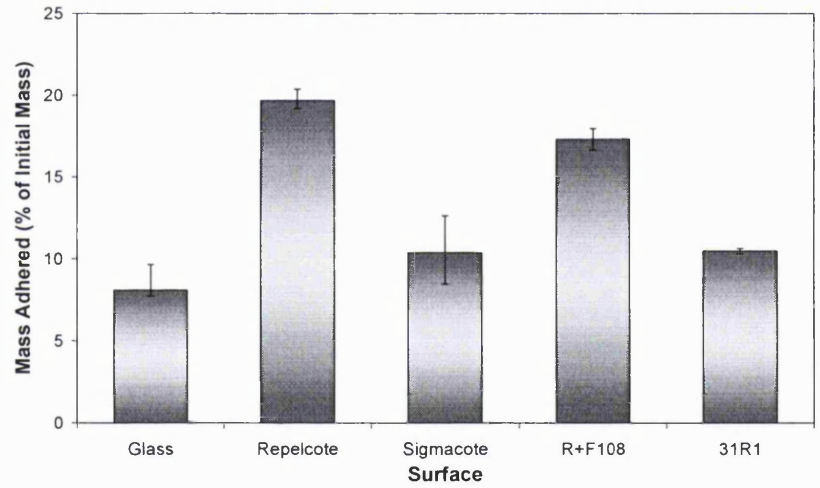

Figure 6.6 Adhesion of micronised budesonide to coated glass surfaces in HFA 227

In terms of the reasons behind the differences in adhesion observed between uncoated and coated glass, the explanation is likely to lie in the hydrophobic nature of budesonide. As previously described, Repelcote and Sigmacote impart a hydrophobic surface to glass which may be attractive to the micronised drug. Explaining the observation that adhesion to the container surface occurred only above the suspension meniscus in all samples investigated is more challenging. It is likely that surface tension is the driving force behind the "creeping" of liquid propellant along the vial wall above the suspension meniscus. Similar to the creeping of supercritical fluids such as nitrogen up the wall of a container and their subsequently evaporation, but to a lesser extent, propellant present in the

formulations under investigation here may advance upwards along the vial wall above the suspension meniscus. Suspended microparticles may be brought upwards along the wall with the propellant, pushed further upwards by microparticles advancing behind them. A combination of the strong affinity of the drug for the container wall and the evaporation of the propellant then produces the irreversible adhesion of microparticles to the container wall. While the theory of surface tension is the more likely, another possible explanation for the observed adhesion may be that of the three phase line tension, a concept first described by Gibbs (1961). Line tension is now a well documented thermodynamic property, and may be defined as the excess free energy associated with a unit length of a three-phase contact line (Rowlinson & Widom, 1984). However published values for both the sign and magnitude of line tension for various combinations of surfaces/interfaces are notably inconsistent (Aveyard et al., 1999). Line tension is in theory considered to be more complex than surface tension given that the latter relates to two bulk phases meeting at a surface, while several bulk phases and sufaces may meet simultaneously at a line (Amirfazli & Neumann, 2004). Aveyard & Clint previously described the de-wetting of small oil lenses positioned on water, and the subsequent expulsion of the lenses into air in the form of oil droplets (1997). Similarly, it is possible that the excess free energy of line tension may have forced some of the liquid propellant towards the container wall and upwards, bringing with it the suspended solid material. Once above the suspension meniscus the propellant would then have evaporated leaving solid material adhered to the container surface. However, while line tension is accepted to affect nanoparticles and possibly micelles, it is not certain whether it would be of a magnitude sufficient to influence microparticles. It is therefore very difficult to explain the puzzling phenomenon of adhesion to the container wall above the suspension meniscus only, and the cause may only be speculated upon.

6.3.5 CONTACT ANGLE MEASUREMENTS TO ELUCIDATE SURFACE ENERGY OF VIAL COATINGS AND PET

Surface tensions for all fully characterised liquids were experimentally determined using the Dynamic Contact Analyzer prior to contact angle measurements, and compared with values referenced in literature to ensure that liquids had not degraded on storage, and were free from any contamination. Table 6.1 shows that

experimentally determined values for surface tension were in good agreement with literature values (presented in the right-most column).

Table 6.1 Surface tension values of liquids used in contact angle measurements

Liquid	Surface Tension ($mN/m^2 \pm SD$)	Surface Tension ($mN/m^2 \pm SD$)*
Purified Water	72.23 (0.26)	72.8
Ethylene glycol	47.56 (0.09)	48.0
1-Bromonaphthalene	43.84 (0.48)	44.4
Diiodomethane	50.06 (0.30)	50.8

* reference values (Jasper, 1972)

Contact angles of these liquids on each of the surfaces under investigation were then measured. Results are displayed in Table 6.2. Attempts to measure the contact angle of 1-bromonaphthalene on PET were unsuccessful and therefore an alternative fully characterised non-polar liquid, diiodomethane, was used.

Table 6.2 Contact angle values of varying surfaces on three characterised liquids

Surface	Contact Angle (°, ± SD)		
	Water	Ethylene Glycol	1-bromonaphthalene
Repelcote	103.32 (0.57)	87.21 (0.41)	66.58 (0.43)
Sigmacote	81.33 (0.47)	67.37 (0.17)	63.19 (0.59)
Repelcote + F108	81.73 (0.15)	75.60 (0.38)	62.21 (0.68)
31R1	65.15 (0.60)	55.14 (0.40)	26.11 (0.11)
PET	75.02 (0.71)	53.94 (0.56)	18.81 (0.47)*

*contact angle measured with diiodomethane

Using the values for contact angles determined experimentally, surface energy components for all surfaces under investigation were then calculated according to the method previously described by van Oss et al., (1988). Similar to the approach used in Chapter Three to determine the surface energy parameters of a model propellant 2H, 3H-decafluoropentane, a series of three of the same equation derived from the complete Young equation were solved simultaneously for each of the three unknown surface energy parameters γ^{LW}, γ^{+} and γ^{-} for each surface under investigation. Equations were solved using the commercially available mathematics software (Maple version 9.5). The equation used is listed in Equation 6.1. Reference values

for the previously mentioned fully characterised liquids were used, and are presented in Table 6.3.

$$(1+Cos\theta)\gamma_L^{TOT} = 2((\gamma_S^{LW}\gamma_L^{LW})^{1/2} + (\gamma_S^{+}\gamma_L^{-})^{1/2} + (\gamma_S^{-}\gamma_L^{+})^{1/2}) \quad \text{(Equation 6.1)}$$

Table 6.3 Reference surface energy parameters of characterised liquids (van Oss et al., 1992)

Test liquids	Surface Energy Parameters (mJ/m^2, ± SD)			
	γ^{LW}	γ^{+}	γ^{-}	γ^{Tot}
Water	21.8	25.5	25.5	72.8
Ethylene glycol	29.0	1.92	47.0	48.0
1-Bromonaphthalene	44.4	0	0	44.0
Diiodomethane	50.8	0	0	50.8

Results from surface energy parameter calculations are shown in Table 6.4. In addition to calculation of individual surface energy parameters as discussed, collective parameters such as γ^{AB} γ^{TOT} and % polarity were also calculated. Values for glass were taken from literature (Boury & Proust, 1993).

Table 6.4 Calculated surface energy parameters of surfaces under investigation

Surface	Surface Energy Parameters (mJ/m^2)					
	γ^{LW}	γ^{+}	γ^{-}	γ^{AB}	γ^{Tot}	% Polarity*
Repelcote	21.48	0.36	9.68	3.72	25.2	14.76
Sigmacote	23.16	0.33	18.21	4.90	28.06	17.46
Repelcote + F108	23.65	0	22.23	-	23.65	-
31R1	39.63	0.07	29.26	2.86	42.49	6.73
PET	48.12	0.19	15.90	3.48	51.6	6.74
Glass**	41	3	45.5	20.5	61.5	33.33

* % Polarity = [(γ^{AB}/ γ^{Tot}) X 100], ** Boury & Proust, 1993

6.3.6 CORRELATIONS BETWEEN SURFACE ENERGY AND ADHESION

Subsequent work attempted to correlate the relationship between container wall surface energy, suspended microparticle surface energy and adhesion. As such, surface energy interaction values for the interaction of each budesonide-surfactant formulation with PET in addition to the interaction of micronised budesonide with

each characterised surface were calculated using data from ICG analysis (Table 6.5). Surface energy interaction (SEI) values were calculated using the equation previously discussed in Chapters Three and Four, displayed here again for convenience (Equation 6.2; Cline & Dalby, 2002):

$$SEI = 2(\gamma^{D}{}_{1} \cdot \gamma^{D}{}_{2})^{1/2} + 2(K_{A1} \cdot K_{D2})^{1/2} + 2(K_{A2} \cdot K_{D1})^{1/2} \quad \text{(Equation 6.2)}$$

Table 6.5 Surface energy parameters of budesonide formulations (IGC data, Chapter Four)

Formulation	Surface Energy Parameters (mJ/m^2, ± SD)					
	γ^{LW} (γ^{d})	γ^{+} (K_A)	γ^{-} (K_D)	γ^{AB}	γ^{Tot}	% P*
Micronised Budesonide	59.4 (0.3)	140.7 (0.2)	52.7 (0.7)	86.1	145.5	48.5
B-L31	32.6 (0.1)	129.9 (0.2)	61.2 (0.5)	89.2	121.8	73.2
B-F108	33.8 (0.4)	122.5 (0.5)	46.3 (0.4)	75.2	109.0	69.0
B-31R1	33.7 (0.1)	123.4 (0.2)	34.0 (0.2)	64.8	98.5	65.8
B-1216CO3	37.1 (0.2)	115.3 (0.3)	26.9 (0.4)	55.7	92.7	60.0
B-B59	34.7 (0.1)	127.8 (0.1)	66.7 (0.4)	92.3	127.1	72.7

* % P = [(γ^{AB}/ γ^{Tot}) X 100]

As an alternative method of assessing the relationship between adhesion and surface energy, work of adhesion (W_a) values between each formulation and the respective surfaces were also calculated, according to Equations 6.3 and 6.4. The work of adhesion between two phases has been described as the combined total surface free energy of both phases, minus the total interfacial energy between the two phases (Equation 6.3, Buckton & Chandaria, 1993). The total interfacial energy between the two phases must be calculated according to Equation 6.4.

$$W_a = \gamma_1^{TOT} + \gamma_2^{TOT} - \gamma_{12}^{TOT} \quad \text{(Equation 6.3)}$$

$$\gamma_{12}^{TOT} = (\sqrt{\gamma_1^{LW}} - \sqrt{\gamma_2^{LW}})^2 + 2(\sqrt{\gamma_1^{+} \cdot \gamma_1^{-}} + \sqrt{\gamma_2^{+} \cdot \gamma_2^{-}} - \sqrt{\gamma_1^{+} \cdot \gamma_2^{-}} - \sqrt{\gamma_1^{-} \cdot \gamma_2^{+}}) \quad \text{(Equation 6.4)}$$

Finally, values for work of cohesion (W_c) between microparticles of all formulations were calculated according to Equation 6.5. Work of cohesion is known to be equivalent to twice the dispersive surface energy of a substance.

$$W_c = 2\gamma^{LW} \qquad \text{(Equation 6.5)}$$

Results for all calculations are presented in Table 6.6 for the interactions between budesonide-surfactant formulations with PET, and in Table 6.7 for those of micronised budesonide with all investigated surfaces. Table 6.6 also contains values for W_c calculated for each budesonide formulation.

Table 6.6 Surface energy interaction, work of adhesion and work of cohesion values for budesonide formulations and PET

Formulation	**SEI (mJ/m^2)**	**W_a (mJ/m^2)**	**W_c (mJ/m^2)**
Micronised Budesonide	207.5	121.7	118.8
B-L31	176.9	87.8	65.2
B- F108	174.9	99.5	67.6
B-31R1	174.2	106.5	67.4
B-1216CO3	174.7	118.9	74.2
B-B59	179.0	86.8	69.4

Table 6.7 Surface energy interaction and work of adhesion values for micronised budesonide and varying surfaces

Solid surfaces	**SEI (mJ/m^2)**	**W_a (mJ/m^2)**
Repelcote	153.7	67.8
Sigmacote	183.5	98.1
Repelcote + F108	186.6	100.7
31R1	228.9	143.1
PET	207.5	121.7
Glass	283.9	194.9

Adhesion was then plotted against both SEI and W_a for all formulations and all surfaces investigated. Figure 6.7 shows the relationship between adhesion of micronised budesonide to the container wall and the interaction between the container surface and suspended microparticles in HFA 134a. Figure 6.8 presents the relationship between adhesion of budesonide-surfactant formulations to PET, and the interaction between each formulation with PET.

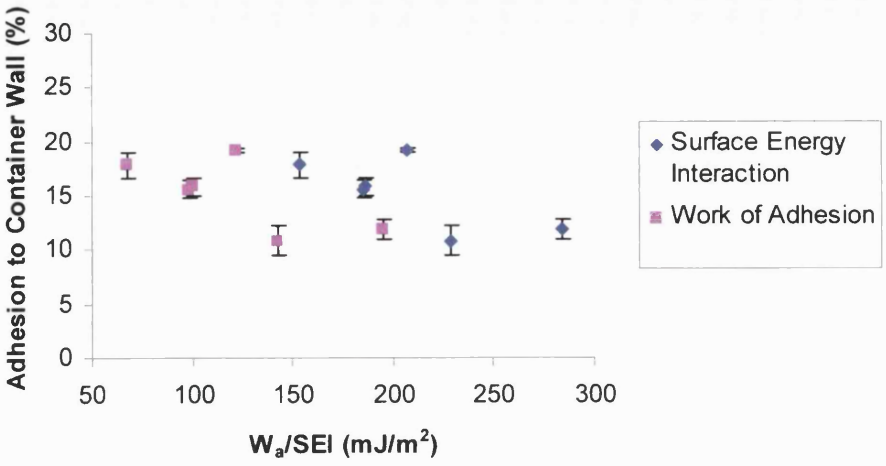

Figure 6.7 Correlation between SEI/W_a and container wall adhesion in HFA 134a for micronised budesonide on coated surfaces

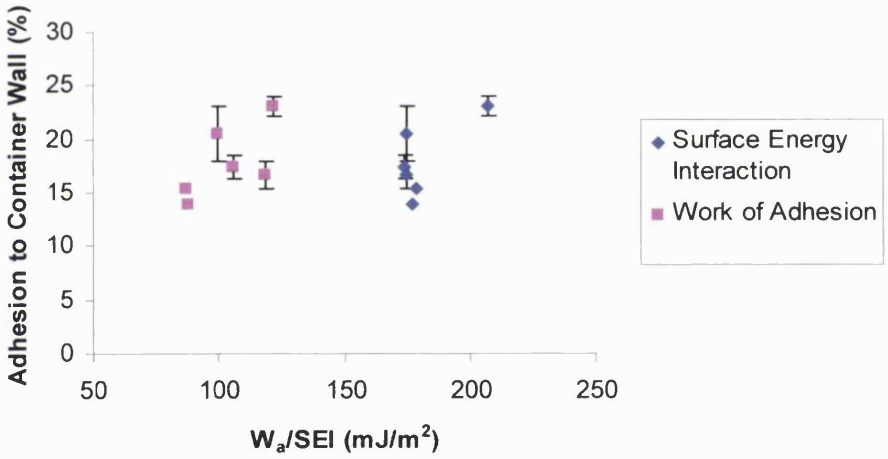

Figure 6.8 Correlation between SEI/W_a and container wall adhesion in HFA 134a for budesonide-surfactant formulations on PET

A similar distribution of values was observed for the relationship between adhesion to the container wall and the interaction between the container surface and suspended microparticles in HFA 227 and therefore these charts are not shown. Given the similarity between the equations used to calculate SEI and W_a values, it is not surprising that both Figure 6.7 and 6.8 show almost identical spreads for each parameter. Interestingly, in the case of all formulations investigated, the work of cohesion between the suspended particles was less than the work of adhesion between the microparticles and container wall, suggesting that there was a stronger

attraction between the microparticles and the container surface than between the suspended particles themselves. While this supports adhesion results for micronised budesonide in PET vials, it is not consistent with other formulations that showed reduced adhesion to the wall of PET vials. The reason for such inconsistency is not immediately clear.

Results presented in Figure 6.8 generally supported previously published results indicating that a lower surface energy is associated with reduced adhesion to container walls. However, the same could not be said for results seen in Figure 6.7 relating to the adhesion of micronised budesonide to the various coated surfaces. A possible explanation for the discrepancy may lie in the different methods used to calculate the surface energy of coated surfaces, and that of micronised budesonide and the various budesonide-surfactant formulations. While the former were determined using contact angle measurement, surface energy of powders had been previously measured using inverse gas chromatography. It is possible that values obtained by a particular method may only be compared to those obtained using the same method and as such, surface energy values determined by contact angle measurement may not be cross-referred to those obtained through ICG analysis.

In addition, errors associated with contact angle measurement are well documented and may also have accounted for the unexpected spreads observed in Figures 6.7 and 6.8. Naturally, any error associated with contact angle measurements presented in this work would have a corresponding effect on surface energy parameter calculation and the subsequent relationship between surface energy and adhesion. The effect of surface roughness on advancing and receding contact angles has been investigated (Zografi & Johnson, 1984). Findings revealed that significant hysteresis of the contact angle was caused by areas of surface roughness exhibited by a range of non-polar pharmaceutical solids investigated. Further work in this area examined errors associated with contact angles measured using the Wilhelmy plate method, as used in this research (Sheridan et al., 1994). Again, surface roughness appeared to have a significant influence on contact angle measurement. Finally, an additional consideration has been raised in work published by Buckton (1993). This work described the potential interference of vapour adsorption to the Wilhelmy plate in contact angle values subsequently measured. While plates used in this research were

used on the day of preparation, it is possible that adsorption of vapour to the plates under investigation did occur, whether they originated from the solvents used in contact angle measurements or from the laboratory atmosphere.

Another possible source of error giving rise to the lack of correlation observed in Figures 6.7 and 6.8 may have the van Oss method of surface energy parameter calculation. The work of van Oss and Good describes the extrapolation of surface energy parameters of an uncharacterised solid using known values for three fully characterised liquids (1988). While the van Oss-Good theory has been widely accepted and applied in surface science, work subsequently published by other researchers challenged the conventional use of this method, proclaiming it inadequate in its current form by examining inconsistencies in values cited in published work and suggesting an alternative method of calculation using matrices (Della Volpe & Siboni, 1997). The authors presented a number of concerns regarding results obtained using the conventional approach. One such concern related to the magnitude of calculated base components of solid surface energy when compared to acid components, the former being systematically greater and thus creating the impression that solids seem significantly more basic than acidic in nature. This observation is certainly borne out in results obtained in this research, where γ^- values calculated for all surfaces under investigation were significantly larger than γ^+ values. The authors also cautioned that results obtained are largely dependent on the three solvents used in the determination of contact angles. Finally, the authors pointed out that equations produced by using the conventional van Oss approach were non-linear and therefore challenging to solve. Rather than using only three solvents for contact angle determination, the authors advocate using a full range of solvents (greater than three) that exhibit the breadth of possible characteristics in terms of polarity (polar, monopole basic, monopole acidic, and non polar). This would give rise to an over-determined linear system of equations describing the three unknowns associated with the solid in question. Therefore it is possible that by only using three characterised liquids in experimental calculations results presented in this chapter were not optimal, thereby hampering subsequent attempts to correlate surface energy with adhesion.

6.4 SUMMARY AND CONCLUSION

The original aim of this chapter was to confirm the preliminary observations made during work discussed in Chapter Four, namely those of reduced container wall adhesion in pMDI formulations containing surfactant co-spray dried with micronised budesonide. In addition, it was hoped that by investigating adhesion phenomena within the budesonide suspension pMDI system further, a greater understanding of the relationship between powder surface energy and adhesion would be gained. Results from initial adhesion investigations successfully confirmed previous observations, showing adhesion of micronised budesonide to PET to be consistently greater than that of any other budesonide-surfactant formulation. Attempts to achieve similar reductions in container wall adhesion by coating PET vials with surfactant were unsuccessful; indicating that in the budesonide pMDI suspension formulations examined here, adsorption of the surfactant to the drug surface was a prerequisite for reduced adhesion. Further investigations into the adhesion of micronised budesonide to various coated glass surfaces also failed to show any significant reduction in adhesion. Unfortunately, attempts to correlate powder surface energy with the extent of adhesion recorded in experiments using PET vials and other coated surfaces were not as successful as originally anticipated. Several explanations for this have been proposed, including the use of more than one experimental method to determine surface energy in addition to limitations of the conventional use of the van Oss-Good method of calculating solid surface energy parameters.

6.5 FURTHER WORK

Alternative methods of measuring adhesion of micronised powder may of course be pursued in an effort to better understand the relationship between powder surface energy and adhesion. Several papers have been published describing the use of atomic force microscopy (AFM) to this end (Ashayer et al., 2004; Jones et al., 2003; Zhou et al., 2003). While the majority of the research has focussed on powders in isolation, one group have presented work examining the drug particulate interactions in a pMDI system, using a model propellant. Their use of AFM to examine interparticulate forces allowed prediction of the extent of adhesion that might occur in a pMDI canister (Young et al., 2003).

CHAPTER SEVEN

CONCLUSIONS

7 CONCLUSIONS

The many advantages of the pMDI device such as portability and low cost outweigh the challenge of coordinating device actuation with inspiration experienced by some patients and serve to maintain its enduring popularity as a device for the pulmonary delivery of several drugs for respiratory conditions. The necessary phase-out of CFC propellants and their replacement with HFA propellants has re-awakened the interest in the formulation science and device design of preparations hitherto accepted as optimal formulations. The altered solvency properties of HFA propellants when compared to their predecessors have further complicated re-formulation attempts as surfactants conventionally used in CFC formulations have a low or negligible solubility in the replacement propellants. While traditional formulation strategies have required surfactants to be soluble in propellant in order to successfully confer stabilising properties on a pMDI suspension formulation, the work of various authors has suggested that this is not in fact essential. The role of surface energy in the stability of pMDI suspension formulations is also not well understood, and therefore in light of the many unanswered questions surrounding the performance of pMDI suspension formulations the aims of this thesis were:

- To explore the use of alternative surfactants possessing a low solubility in HFA propellants as stabilising agents in pMDI HFA suspension formulations.

- To further elucidate the relationship between powder surface energy and suspension performance of pMDI suspension formulations in HFA propellants by modifying powder surface energy of the model hydrophilic drug terbutaline sulphate and the model hydrophobic drug budesonide through the adsorption of alternative surfactants to the drug surface.

Work in Chapter Three focused on the investigation of surface modification of a model hydrophilic drug, terbutaline sulphate (TS) achieved by adsorbing a range of non-ionic surfactants to the surface of the micronised drug using an incubation method, and the subsequent effects of surfactant adsorption on the performance of pMDI suspension formulations prepared in both HFA 134a and HFA 227. Part A of this chapter reported results from adsorption experiments and subsequent work

carried out in order to characterise surfactant-TS microparticles. Surfactants used in this work were demonstrated to have a low solubility in HFA propellants, with the upper limit of solubility reported as < 0.08 % w/v, significantly lower than that observed in traditional CFC formulations. While no change in microparticle size, morphology or physical form were identified following surfactant adsorption, a decrease in both the dispersive and acidic component of microparticle surface energy was revealed by IGC analysis of TS-surfactant microparticles. A reduction in the polarity of the drug surface was therefore reported. The reduction in powder surface energy was in turn suggestive of an increase in suspension stability of future pMDI suspension formulations containing TS-surfactant microparticles. A relationship between surfactant structure (both in terms of molecular weight and HLB number) and powder surface energy was not observed. This was unfortunate as the empirical choice of surfactant currently followed in the development of novel pMDI formulations is inefficient.

Part B of Chapter Three investigated the effect of surface modification of TS microparticles following surfactant adsorption on the performance of pMDI suspension formulations prepared in both HFA propellants. A comparison of two optical methods for assessing pMDI suspension stability assessed the merits of Optical Suspension Characterisation (OSCAR) and Turbiscan apparatus using one TS-surfactant microparticle formulation in addition to a TS control formulation. While consistent results were observed with both methods, Turbiscan was found to be the method of choice for assessing pMDI suspension performance in reference to the fact that data pertaining to the entire sample was obtained in addition to the facility for objectively comparing several formulations through the calculation of mean backscattering over a defined zone of the sample cell length. Turbiscan was then used to investigate the suspension performance of all TS-surfactant pMDI formulations in both propellants. Direct comparisons between formulations were made possible through the calculation of the reduction in mean backscattering for each formulation over the three minute scan period. A range of suspension performances were observed, depending on the particular surfactant present in the formulation. All surfactant-containing formulations showed an increase in suspension stability over control formulations in both propellants, reported as a reduction in phase separation and particle aggregation. Behaviour of formulations

was not consistent between propellants however, and a greater increase in suspension stability of TS-surfactant formulations was observed in HFA 134a. Results from Shake-Pause-Fire testing, an alternative method of assessing pMDI suspension performance, confirmed the findings of Turbiscan analyses and demonstrated an increase in pMDI suspension stability of formulations containing poloxamer surfactants in HFA 134a over control TS formulations. The mechanism of suspension stabilisation conferred by surfactant adsorption was believed to be steric in nature, given that the presence of electrostatic forces in the predominantly non-polar nature of HFA propellants could be ruled out. Therefore surfactant adsorption was believed to have increased the interparticle distances within the formulation, allowing long range van der Waals repulsive forces to retard particle aggregation and phase separation. A discussion on the possible orientation of surfactant molecules at the drug surface was hampered by the lack of knowledge surrounding adsorption in non-aqueous systems, identifying an area for further investigation in order to better understand pMDI formulations.

The final part of Chapter Three investigated the existence of a possible correlation between the reduction in powder surface energy identified following surfactant adsorption reported in Part A and the improvement in suspension performance reported in Part B. A general trend linking a reduction in both the dispersive and acidic components of microparticle surface energy with improved suspension performance was identified, however results suggested that surface energy is not the only parameter affecting the overall behaviour of pMDI suspension formulations. Chapter Three therefore served to demonstrate that adsorption of various non-ionic surfactants to the surface of TS had successfully reduced both the dispersive and acidic components of microparticle surface energy, and in turn had conferred stabilising properties of suspensions of these microparticles in HFA propellants. Furthermore, work in Chapter Three confirmed that surfactants possessing a low solubility in HFA propellants may indeed be considered as formulation stabilisers.

Work in Chapter Four progressed to examine the effect of surfactant adsorption to the alternative substrate drug micronised budesonide. By using a hydrophobic drug, it was hoped that comparisons between adsorption studies in TS and budesonide would reveal whether the nature of the adsorbate influenced surfactant adsorption

and the consequent performance of surfactant-drug pMDI suspension formulations in HFA propellants. An initial attempt to facilitate surfactant adsorption using an incubation method similar to that reported in Chapter Three produced drug-surfactant microparticles exhibiting extensive aggregation causing an overly large particle size distribution. Budesonide-surfactant microparticles prepared using an incubation method were therefore not suitable for inhalation studies. As an alternative method of facilitating surfactant adsorption, suspensions of micronised budesonide were co-spray dried with an aqueous solution of surfactant. The particle size of drug-surfactant microparticles recovered from the spray drying process was found to be very close to the size of the micronised material, and microparticles retained their crystalline structure. Therefore it was concluded that co-spray drying from suspension was the preferred method of adsorption of hydrophilic surfactants to the surface of micronised budesonide.

A factorial design experiment was subsequently carried out to optimise spray dried yield and particle size before applying the optimal parameters to further experiments, co-spray drying micronised budesonide with non-aqueous solutions of hydrophobic surfactants. Results of this experiment suggested that preliminary experiments to estimate the optimal range of each variable examined would have been useful in order to better identify both the influence of individual parameters on the experimental variables under investigation in addition to the interactions between spray drying parameters. Spray drying parameters adopted from this study when applied to spray drying experiments using alternative hydrophobic surfactants to the poloxamer L101 used in the factorial design experiment were no longer found to be optimal in terms of process yield. As such, it was clear that ideal conditions for the preparation of a formulation involving one surfactant could not be widely applied to formulations containing alternative surfactants, and that the nature of the excipient present in the spray drying mixture was pivotal to the process yield. IGC analysis of all budesonide-surfactant formulations prepared by co-spray drying from both suspension and solution revealed a similar decrease in the dispersive and acidic components of powder surface energy when compared to control formulations to that observed in Chapter Three for TS-surfactant microparticles. Microparticles prepared by spray drying from solution possessed surface energy values slightly higher than those prepared by co-spray drying from suspension. This was concluded to be linked

to the amorphous nature of microparticles co-spray dried from solution confirmed by PXRD analysis. Budesonide-surfactant microparticles generally possessed surface energy values similar to those of TS-surfactant microparticles, suggesting that the orientation of surfactant molecules at the surface of both drugs was identical. This was contrary to expectations given the very different nature of the drug substances in terms of hydrophilicity. Further work was therefore required in order to elucidate the exact nature of surfactant organisation at the microparticle surface.

Part B of Chapter Four investigated the suspension performance of all pMDI suspension formulations containing budesonide-surfactant microparticles, the preparation and characterisation of which was discussed in Part A. Results from Turbiscan analysis failed to show any significant improvement in suspension performance of surfactant-containing formulations over control formulations. This was in direct contrast to results reported in Chapter Three relating to TS-surfactant microparticles in suspension. Again, a general increase in suspension stability was observed in budesonide-surfactant formulations in HFA 134a relative to those in HFA 227. Extensive adhesion to the wall of PET vials used in the preparation of pMDI suspension formulations was observed in formulations without surfactant suggesting that incorporation of surfactant into budesonide formulations reduced the extent of container wall adhesion. This phenomenon was therefore selected for further investigation and was the subject of the final chapter of this thesis. In conclusion, it was proposed that the inferior performance of budesonide-surfactant pMDI suspension formulations compared to equivalent TS-surfactant formulations despite them possessing similar values for powder surface energy was in part due to the alternative method of microparticle preparation. In addition, results from Part B of Chapter Four clearly indicated that the effect of other physicochemical characteristics of pMDI suspension formulations such as density must be considered when attempting to understand suspension performance in HFA propellants. Attempts to correlate microparticle surface energy and suspension performance in Part C of Chapter Four revealed a possible correlation between SEI and a reduction in mean backscattering for formulations containing poloxamer surfactants in HFA 134a. Results confirmed that while surface energy of suspended particles doubtless contributes to the stability of suspensions in HFA propellants, it is merely one of the many physicochemical properties at play.

Work in Chapter Five built on results reported in Chapter Three, where adsorption of several non-ionic surfactants to the surface of TS had succeeded in conferring increased stability on corresponding pMDI suspension formulations in HFA propellants. While the stability of suspension formulations in Chapter Three was assessed immediately after sample preparation, work in Chapter Five aimed to investigate the stability of such formulations on storage over a four week period. Furthermore, an investigation into the effects of surfactant adsorption on suspension stability in the presence of water added to formulations during sample preparation was proposed. In addition to assessing suspension performance using Turbiscan, near infra-red spectroscopy (NIRS) was also investigated as a potential technique for the investigation of pMDI suspension systems.

Results from Turbiscan analysis revealed the persistent stabilising effect of adsorbing both a hydrophilic surfactant F127 and a hydrophobic surfactant L121 to TS in the presence of 0.001 % and 0.01 % w/w added moisture. However, suspension stability in the presence of the maximum mass of added moisture, 0.1 % w/w, was only observed in TS-L121 formulations. An identical concentration of water in TS-Control and TS-F127 formulations was seen to cause rapid and significant particle aggregation. Results therefore indicated that the adsorption of a hydrophobic surfactant to the surface of a hydrophilic drug had successfully protected the drug against moisture-induced particle aggregation and phase separation. While this protective effect was reported immediately following sample preparation, it was not evident one week later. Results from NIRS analysis were in general agreement with those from Turbiscan, identifying a large increase in particle size in TS-Control formulations containing the maximum amount of added moisture while particle size increase in formulations containing the adsorbed hydrophobic surfactant L121 was less exaggerated. NIRS was found to be a useful tool for the in-situ investigation of particle size fluctuation within pMDI suspension systems, however was not sensitive enough to detect the changes in water concentration within the pMDI suspension formulations examined. This was believed to be related to the use of a maximum water concentration close to the limit of detection for NIRS. It was therefore concluded that given the low levels of water likely to be present within pMDI formulations, NIRS was not a viable technique for the detection of changes in water concentration.

The final chapter of this thesis investigated the effects of surfactant adsorption to micronised budesonide on the storage of budesonide pMDI suspension formulations prepared in HFA propellants. Investigations focused on the specific phenomenon of the adhesion of suspended microparticles to the container wall originally observed during the execution of work presented in Chapter Four. The effect of surfactant adsorption on container wall adhesion was examined by measuring the amount of suspended material adhered to the wall of PET vials in a number of budesonide-surfactant pMDI suspension formulations over a four week period. Results showed that surfactant adsorption was linked to reduced adhesion to PET vials when compared with control formulations. Adhesion was shown to be rapid in onset, reaching an approximate maximum in the first week of storage. The location of surfactant at the drug surface was found to be essential in order for the reduced adhesion to occur. Various coating strategies were subsequently assessed for their ability to reduce the adhesion of micronised budesonide to the container wall, but were unsuccessful. In all cases, adhesion of suspended material was only observed on surfaces not in contact with the suspension. Surface tension was proposed as the cause of this biased adhesion, responsible for the "creeping" of propellant molecules along the container wall above the suspension meniscus bringing associated suspended microparticles with them.

Work in Chapter Six also aimed to explore the relationship between surface energy and adhesion to the container wall. Using contact angle measurements on the container surfaces investigated, individual surface energy components for each surface were calculated using van Oss theory. In a similar manner to surface energy correlations presented in Chapters Three and Four, SEIs were then calculated for the interactions between suspended microparticles and the container surfaces under investigation. Attempts to correlate the adhesion of suspended material with either SEI values or work of adhesion (W_a) values were not as successful as expected. Several reasons for this were suggested; including the consideration of surface energy values determined using the two different methods of contact angle measurement and inverse gas chromatography, the inherent potential for error in contact angle measurements and finally the limitations of the van Oss method employed to calculate surface energy components from contact angle measurements.

Overall, the work of this thesis has succeeded in confirming that surfactants possessing a low solubility in HFA propellants may indeed be considered as potential stabilisers in novel suspension pMDI formulations. Successful surface modification of both a hydrophilic and a hydrophobic drug has been achieved through adsorption of such surfactants to the drug surface, resulting in corresponding modifications in suspension performance when formulated in HFA propellants. In addition to facilitating reduced phase separation and particle aggregation within these systems over short periods of investigation, surfactant adsorption has also been linked with an increase in suspension stability over an extended storage period. This has been observed as a limited protection against the destabilising effects of water present in pMDI suspension formulations in the case of TS-surfactant formulations, and a reduction in the adhesion of suspended material to the container wall in the case of budesonide-surfactant formulations. A greater understanding of the role played by surface energy in the performance of pMDI suspension formulations in HFA propellants has been achieved, with a reduction in both the dispersive and acidic components of powder surface energy being linked to improved suspension stability. Further work pertinent to each Chapter has been identified with the intention of consolidating work presented in this thesis, in addition to advancing the understanding of these complex pharmaceutical systems.

REFERENCES

Aerosol Consensus Statement, 1999. Chest, 100, 1106-1109.

British National Formulary 49, 2005. British Medical Association; Royal Pharmaceutical Society of Great Britain.

Ahuja,S., Ashman,J., 1991. Terbutaline sulfate. Analytical Profiles of Drug Substances and Excipients, 19, 601-625.

Alexandridis,P., Holzwarth,J.F., Hatton,T.A., 1994. Micellization of poly(ethylene oxide)-poly(propylene oxide)-poly(ethylene oxide) triblock copolymers in aqueous solutions: Thermodynamics of copolymer association. Macromolecules, 27, 2414-2425.

Ali, S., 2000. Adsorption of poloxamer surfactants onto model hydrophobic surfaces in suspension systems. Ph.D. Thesis, University of London.

Amirfazli,A., Neumann,A.W., 2004. Status of the three-phase line tension. Advances in Colloid and Interface Science, 110, 121-141.

Ashayer,R., Luckham,P.F., Manimaaran,S., Rogueda,P., 2004. Investigation of the molecular interactions in a pMDI formulation by atomic force microscopy. European Journal of Pharmaceutical Sciences, 21, 533-543.

Atkins,P.J., Barker,N.P., Mathisen,D., 1992. The design and development of inhalation drug delivery systems. In: Hickey,A.J. (Ed.), Pharmaceutical Inhalation Aerosol Technology. Marcel Dekker, New York.

Aveyard,R., Clint J.H., Nees,D., Paunov,V., 1999. Size-dependent lens angles for small oil lenses on water. Colloids and Surfaces A: Physicochemical Engineering Aspects, 146, 95-111.

Baker,J.A., Berg,J.C., 1988. Investigation of the adsorption configuration of POE and its co-polymers with PPO on model polystyrene latex dispersions. Langmuir, 4, 1055-1061.

Baleaux, 1972. Chimie Analytique - Dosage colorimetrique d'agents de surface non-ioniques polyoxyethylenes a l'aide d'une solution iodo-ioduree. C. R. Academie de Science, C, 1617-1619.

Baumgarten,C.R., Dorrow,P., Weber,H., Gebhardt,R., Kettner,J., Sykes,A.P., 2000. Equivalence of as-required salbutamol propelled by propellants 11 and 12 or HFA 134a in mild to moderate asthmatics. Respiratory Medicine, 94, S17-S21.

Berthod,A., Tomer,S., Dorsey,J.G., 2001. Polyoxyethylene alkyl ether nonionic surfactant: physicochemical properties and use for cholesterol determination in food. Talanta, 55, 69-83.

Billon,A., Bataille,B., Cassanas,G., Jacob,M., 2000. Development of spray-dried acetominophen microparticles using experimental designs. International Journal of Pharmaceutics, 203, 159-168.

Bjelopavlic,M., Singh,P.K., El-Shall,H., Moudgil,B.M., 2000. Role of surface molecular architecture and energetics of hydrogen bonding sites in adsorption of polymers and surfactants. Journal of Colloid and Interface Science, 226, 159-165.

Blondino,F.E., Byron,P.R., 1998. Surfactant dissolution and water solubilization in chlorine-free liquified gas propellants. Drug Development and Industrial Pharmacy, 24, 935-945.

Bohl.,A.H., 1990. Computer Aided Formulation: A manual for implementation. VCH, New York.

Bonner,O.D., Choi,Y.S., 1974. Hydrogen bonding of water in organic solvents. Journal of Physical Chemistry, 78, 1723-1727.

Boury,F.K., Proust,J.E., 1993. Modification of the surface free energy components of a polymer by adsorption of poly(oxyethylene)-poly(oxypropylene) block co-polymers. In: Mittal,K.L. (Ed.), Contact Angle, Wettability and Adhesion. VSP, Utrecht.

Box,G., Hunter,W., Hunter,J.S., 1978. Statistics for Experimenters. John Wiley & Sons, New York.

Boyter,A., Currie,J., Dagg,K., Groundland,F., Hudson,S., 2000. Asthma. Pharmaceutical Journal, 264, 546-556.

Brindley, A., 1999. The chlorofluorocarbon to hydrofluoroalkane transition: The effect on pressurised metered dose inhaler suspension stability. Journal of Allergy and Clinical Immunology 104[6], S221-S226.

Buckton,G., Chandaria,B., 1993. Consideration of adhesion to modified container walls, by use of surface energy and polarity data, and Lewis acid-Lewis base interactions. International Journal of Pharmaceutics, 94, 223-229.

Buckton,G., 1993. Assessment of the wettability of pharmaceutical powders. Journal of Adhesion Science and Technology, 7, 205-219.

Buckton,G., Armstrong,J.K., Chowdhry,B.Z., Leharne,S., Beezer,A.E., 1994. The use of high sensitivity differential scanning calorimetry to characterise dilute aqueous dispersions of surfactants II. Further studies on polyoxyethylene alkyl ethers. International Journal of Pharmaceutics, 110, 179-187.

Buckton,G., 1995a. Interfacial Phenomena in Drug Delivery and Targeting, 1st Ed. Churchill, Harwood.

Buckton,G., 1995b. Surface characterisation: understanding sources of variability in the production and use of pharmaceuticals. Journal of Pharmacy and Pharmacology, 47, 265-275.

Byrn,S.R., 1999. Solid-State Chemistry of Drugs, 2nd Ed. Academic Press, London.

Byron,P.R., 1992. Towards the rational formulation of metered dose inhalers. Journal of Biopharmaceutical Sciences, 33, 001-009.

Byron, P. R., Miller, N. C., Blondino, F. E., and Ward, G. H., 1994. Some aspects of alternative propellant solvency. In: Byron, P. R., Dalby, R., and Farr, S. J. (Eds.), Respiratory Drug Delivery IV. Interpharm Press, Buffalo Grove IL, 231-242.

Carthew, D., 1999. Physico-chemical properties of poloxamer surfactants related to their adsorption. Ph.D. Thesis, University of London.

Carthew,D.L., Buckton,G., Parsons,G.E., Poole,S., 1995. The influence of a phase transition in poly(oxyethylene)/poly(oxypropylene)/poly(oxyethylene) surfactants on adsorption behaviour from dilute aqueous solution. Pharmaceutical Sciences, 1, 3-5.

Carthew,D.L., Buckton,G., Parsons,G.E., Poole,S., 1997. The influence of a phase transition in poly(oxyethylene)/poly(oxypropylene)/poly(oxyethylene) block co-polymer surfactants on the properties of material adsorbed from dilute aqueous solution. Journal of Adhesion, 63, 89-98.

Carveth,H.J., Kanner,R.E., 1999. Optimizing deposition of aerosolized drug in the lung: a review. Respiratory Care, 3(1), http://www.medscape.com/viewarticle/408738

Chehimi,M.M., Pigois-Landureau,E., 1994. Determination of acid-base properties of solid materials by inverse gas chromatography at infinite dilution. Journal of Materials Chemistry, 4, 741-745.

Cline,D., Dalby,R., 2002. Predicting the quality of powders for inhalation from surface energy and area. Pharmaceutical Research, 19, 1274-1277.

Columbano, A., 2000. Modification of microparticle surfaces by use of alkylpolyglycoside surfactants. Ph.D. Thesis, University of London.

Conte,U., Conti,B., Giunchedi,P., Magi,L., 1994. Spray dried polylactide microsphere preparation: Influence of the technological parameters. Drug Development and Industrial Pharmacy, 20, 235-258.

Corrigan,D.O., Corrigan,O.I., Healy,A.M., 2004. Predicting the physical state of spray dried composites: salbutamol sulphate/lactose and salbutamol sulphate/polyethylene glycol co-spray dried systems. International Journal of Pharmaceutics, 273, 171-182.

Dalby,R., Suman,J., 2003. Inhalation therapy: technological milestones in asthma treatment. Advanced Drug Delivery Reviews, 55, 779-791.

Dalby,R.N., Hickey,A.J., Tiano,S.L., 1996. Medical Devices for the Delivery of Therapeutic Aerosols to the Lungs. In: Hickey,A.J. (Ed.), Inhalation Aerosols: Physical and Biological Basis for Therapy. M. Dekker, New York, 441-467.

De Boer,J.H., 1968. The Dynamic Character of Adsorption. 2nd Ed., Clarendon Press, Oxford.

Della Volpe,C., Siboni,S., 1997. Some reflections on acid-base solid surface free energy theories. Journal of Colloid and Interface Science, 195, 121-136.

DeYoung, L., 1998. The AeroDose multidose inhaler: device design and delivery characteristics. In: Dalby, R., Byron, P. R., and Farr, S. J. (Eds.), Respiratory Drug Delivery VI. Interpharm Press, Buffalo Grove IL, 91-96.

Dickinson,P.A., Seville,P.C., McHale,H., Perkins,N.C., Taylor,G., 2000. An investigation of the solubility of various compounds in the hydrofluoroalkane propellants and possible model liquid propellants. Journal of Aerosol Medicine, 13, 179-186.

Ding, J. Y. Blyth K. S., Zimlich, W. C., McVeety, B. D., and Placke, M. E., 2002. Delivery of a chemotherapeutics agent for cancer treatment for cancer treatment via nebulization. In: Dalby, R., Byron, P. R., Peart, J., and Farr, S. J. (Eds.), Respiratory Drug Delivery VIII. David Horwood, Tucson, 359-362.

Donnell,D., 2001. Optimizing drug delivery to the lung: Design of a CFC-free corticosteroid metered-dose aerosol system. Drug Development and Industrial Pharmacy, 27, 111-118.

Drago,R.S., Vogel,G.C., Needham,T.E., 1971. A four-parameter equation for predicting enthalpies of adduct formation. Journal of American Chemistry Society, 93, 6014-6026.

Elson, K. Bland J. Marlow M., 2003. Optimisation of the suspension stability of a hydrofluoroalkane metered dose inhaler formulation using three different characterisation techniques. Drug Delivery to the Lung XIV, Aerosol Society, Bristol, 228-231.

Elversson,J., Millqvist-Fureby,A., Alderborn,G., Elofsson,U., 2003. Droplet and particle size relationship and shell thickness of inhalable lactose particles during spray drying. Journal of Pharmaceutical Sciences, 92, 900-910.

Elworth,P.H., Patel,M.S., 1982. Demonstration of maximum solubilization in a polyoxyethylene alkyl ether series of non-ionic surfactants. Journal of Pharmacy and Pharmacology, 34, 543-546.

Esposito,E., Roncarati,R., Cortesi,R., Cervellati,F., Nastruzzi,C., 2000. Production of eudragit microparticles by spray-drying technique: influence of experimental parameters on morphological and dimensional characteristics. Pharmaceutical Development and Technology, 5, 267-278.

Fell,J., 2002. Surface and Interfacial Phenomena. In: Aulton,M.E. (Ed.), Pharmaceutics: The Science of Dosage Form Design, 2nd Ed. Churchill Livingstone, London, 59-69.

Florence,A.T., Attwood,D., 1998. Physicochemical Principles of Pharmacy, 3rd Ed. Macmillan Press, London.

Fowkes,F.M., 1963. Additivity of intermolecular forces at interfaces I. Determination of the contribution to surface and interfacial tensions of the dispersion forces in various liquids. Journal of Physical Chemistry, 67, 2538-2541.

Fowkes,F.M., 1964. Attractive forces at interfaces. Industrial Engineering and Chemistry, 56, 40-52.

Frake,P., Gill,I., Rudd,D.R., Luscombe,C.N., Waterhouse,J., Jayasooriya,U.A., 1998. Near-infrared mass median particle size determination of lactose monohydrate, evaluating several chemometric approaches. Analyst, 123, 2043-2046.

Gibbs,J.W., 1961. The scientific papers of JW Gibbs. Dover, New York.

Gibbs,K.P., Portlock,J.C., 2002. Asthma and COAD. In: Walker,R., Edwards,C. (Eds.), Clinical Pharmacy and Therapeutics, 3rd Ed. Churchill Livingstone.

Gonda,I., 1990. Aerosols for delivery of therapeutics and diagnostic agents to the respiratory tract. Critical Reviews in Therapeutic Drug Carrier Systems, 6, 273-303.

Good,R.J., 1993. Contact angle, wetting and adhesion: a critical review. In: Mittal,K.L. (Ed.), Contact Angle, Wettability and Adhesion. VSP, Utrecht, 3-36.

Govind, N. Price A. Brindley A. Spary S. Colthorpe P., 2000. Correlation of two methods for assessing pMDI suspension stability. In: Byron, P. R., Dalby, R., Farr, S. J. and Peart J. (Eds.), Respiratory Drug Delivery VII. Serentec Press, Raleigh NC, 337-340.

Grimsey,I., Feeley,J., York,P., 2002. Analysis of surface energy of pharmaceutical powders. Journal of Pharmaceutical Sciences, 91, 571-583.

Gupta,P.K., Adjei,A.L., 1997. Non-ozone depleting propellants. In: Adjei,A.L., Gupta,P.K. (Eds.), Inhalation Delivery of Therapeutic Peptides and Proteins. Marcel Dekker, New York.

Gutmann,V., 1978. The Donor-Acceptor Approach to Molecular Interactions. Plenum, New York.

Hallworth,G.W., 1987. The formulation and evaluation of pressurised metered dose inhalers. In: Ganderton,D., Jones,T. (Eds.), Drug Delivery to the Respiratory Tract. Ellis Horwood, Chicester, 87-118.

Hickey,A.J., Evans,R.M., 1996. In: Hickey,A.J. (Ed.), Aerosol Generation from Propellant-Driven Metered Dose Inhalers. M. Dekker, New York, 116-125.

Hickey,A.J., Dunbar,C.A., 1997. A new millenium for inhaler technology. Pharmaceutical Technology, 116-125.

Hofland,H.E.J., Bouwstra,J.A., Verhoef,J., Junginger,H.E., 1989. Niosomes: A study of structure, stability, drug release and toxicological aspects. Proceedings of the Symposium on the Controlled Release of Bioactive Materials, 16, 136-137.

International Pharmaceutical Aerosol Consortium, 1997. Ensuring patient care. The role of the HFC MDI.

International Pharmaceutical Aerosol Consortium, 2005. Information on Medical Uses of HFCs.

Jee,R.D., 2003. Near Infra Red Spectroscopy. In: Moffat,A.C., Osselton,M.D., Widdop,B. (Eds.), Clarke's Analysis of Drugs and Poisons, Vol. 1, 3rd Ed. Pharmaceutical Press, UK, 346-357.

Jinks, P. A., 1995. A rapid technique for characterisation of the suspension dynamics of metered dose inhaler formulations. Drug Delivery to the Lungs VI. The Aerosol Society, Bristol, 10-13.

Johnson,K., 1996. Interfacial phenomena and phase behaviour in metered dose inhaler formulations. In: Hickey,A.J. (Ed.), Inhalation Aerosols: Physical and Biological Basis for Therapy. Marcel Dekker, New York, 385-411.

Jones,R., Pollock,H.M., Geldart,D., Verlinden,A., 2003. Inter-particle forces in cohesive powders studied by AFM: effects of relative humidity, particle size and wall adhesion. Powder Technology, 132, 196-210.

June,D., 1997. Achieving the change: challenges and successes in the formulation of CFC-free MDIs. European Respiratory Review, 7, 32-34.

Kayes,J.B., Rawlins,D.A., 1979. Adsorption characteristics of certain polyoxyethylene-polyoxypropylene block co-polymers on polystyrene latex. Colloid and Polymer Science, 257, 622-629.

Keller,M., 1999. Innovations and perspectives of metered dose inhalers in pulmonary drug delivery. International Journal of Pharmaceutics, 186, 81-90.

Killman,E., Maier,H., Baker,J.A., 1988. Hydrodynamic layer thickness of various adsorbed polymers on precipitated silica and polystyrene latex. Colloids and Surfaces, 31, 51-71.

Kitahara,A., 1974. Zeta potential in non-aqeous media and its effect on dispersion stability. Program of Organic Coatings, 2, 81-98.

Kunka,R., Andrews,S., Pimazonni,M., Callejas,S., Ziviani,L., Squassante,L., Daley-Yates,P.T., 2000. Dose proportionality of fluticasone proprionate from hydrofluoroalkane pressurized metered dose inhalers (pMDIs) and comparability with chlorofluorocarbon pMDIs. Respiratory Medicine, 94, S10-S16.

Linse,P., 1993. Phase behaviour of poly(ethylene oxide)-poly(propylene oxide) block co-polymers in aqueous solution. Journal of Physical Chemistry, 97, 13896-13902.

Maa,Y., Costantino,H., Nguyen,P., Hsu,C., 1997. The effect of operating and formulation variables on the morphology of spray-dried protein particles. Pharmaceutical Development and Technology, 2, 213-223.

Malmsten,M., Linse,P., Cosgrove,I., 1992. Adsorption of PEO-PPO-PEO block co-polymers at silica. Macromolecules, 25, 2474-2481.

Martini,F., 2002. Fundamentals of Anatomy and Physiology. 6th Ed., Prentice Hall, New Jersey.

Martonen,T.Y., 1996. Deposition mechanics of pharmaceutical particles in human airways. In: Hickey,A.J. (Ed.), Inhalation Aerosols: Physical and Biological Basis for Therapy. M. Dekker, New York, 3-23.

Masters,K., 2002. Spray Drying in Practice. SprayDryConsult International ApS, Denmark.

McDonald,K.J., Martin,G., 2000. Transition to CFC-free metered dose inhalers - into the new millennium. International Journal of Pharmaceutics, 201, 89-107.

Meakin, B. J., Lewis, D. A., Ganderton, D., and Brambilla, G., 2000. Countering challenges posed by mimicry of CFC performance using HFA systems. In: Byron, P. R., Dalby, R., Farr, S. J. and Peart J. (Eds.), Respiratory Drug Delivery VII. Serentec Press, Raleigh NC, 99-107.

Mengual,O., Meunier,G., Cayre,I., Peuch,K., Snabre,P., 1999. Turbiscan MA 2000: Multiple light scattering measurement for concentrated emulsion and suspension instability analysis. Talanta, 50, 445-456.

Miller, N. C., 1990. The effect of water in inhalation suspension aerosol formulations. In: Byron, P.R. (Ed.), Respiratory Drug Delivery. CRC Press, Boca Raton, FL, 249-257.

Mitchell,D.J., Tiddy,G.J.T., Waring,L., Bostock,T., McDonald,M.P., 1983. Phase behaviour of polyoxyethylene surfactants with water. Journal of Chemical Society Faraday Trans, 79, 975-1000.

Mohammed,H.A.H., Fell,J.T., 1982. Contact angles of powder mixtures consisting of spherical particles. International Journal of Pharmaceutics, 11, 149-154.

Montreal Protocol on Substances that Deplete the Ozone Layer, 1989. Liason Office of the United Nations Environmental Program, New York.

Myers,D., 1988. Surfactant science and technology. VCH, New York.

Neumann,A.W., Good,R.J., Hope,C.J., Sejpal,M., 1974. An equation of state approach to determine surface tension of low-energy solids from contact angle. Journal of Colloid and Interface Science, 42, 291-304.

Osborne,B.G., Fearn,T., Hindle,P.H., 1993. Practical NIR Spectroscopy with Applications in Food and Beverage Industry Analysis. 2nd Ed., Longman, Harlow, UK.

Papirer,E., Balard,H., 1999. Inverse Gas Chromatography: A method for the evaluation of the interaction potential of solid surfaces. In: Pefferkorn,E. (Ed.), Interfacial Phenomena in Chromatography. Marcel Dekker, New York, 146-171.

Parsons,G.E., Buckton,G., Chatham,S.M., 1992. The use of surface energy and polarity determinations to predict physical stability of non-polar, non-aqueous suspensions. International Journal of Pharmaceutics, 83, 163-170.

Paterakis,P.G., Korakianiti,E.S., Dallas,P.P., Rekkas,D.M., 2002. Evaluation and simultaneous optimization of some pellet characteristics using a 3^3 factorial design and the desirability function. International Journal of Pharmaceutics, 248, 51-60.

Phillips,E.M., Byron,P.R., 1994. Surfactant promoted crystal growth of micronised methylprednisolone in trichloromonofluoromethane. International Journal of Pharmaceutics, 110, 9-19.

Polli,G.P., Grim,W.M., Bacher,F.A., Yunker,M.H., 1969. Influence of formulation on aerosol particle size. Journal of Pharmaceutical Sciences, 58, 484-486.

Pugh,R.J., Matsunaga,T., Fowkes,F.M., 1983. The dispersibility and stability of carbon black in media of low dielectric constant. I: Electrostatic and steric contributions to colloidal stability. Colloids and Surfaces, 7, 183-207.

Ranucci,J., Dixit,S., Bray,R.N., Goldman,D., 1990. Controlled flocculation in metered dose inhalers. Pharmaceutical Technology, 14, 68-74.

Riddle,F.L., Fowkes,F.M., 1989. Spectral shifts in acid-base chemistry: van der Waals contributions to acceptor numbers. Journal of American Chemistry Society, 112, 3259-3264.

Riker Laboratories Incorporated, 1990. Medicinal aerosol formulations. PCT/GB90/01454[WO 91/04011].

Rogueda, P., 2002. Particle Interactions in HFA formulations: experiment, theory and practice. In: Dalby, R., Byron, P. R., Farr, S. J. and Peart J. (Eds.), Respiratory Drug Delivery VIII. Serentec Press, Raleigh NC, 215-221.

Rogueda,P.G., 2003. HPFP, a model propellant for pMDIs. Drug Development and Industrial Pharmacy, 29, 39-49.

Rowlinson,J.S., Widom,B., 1984. Molecular theory of capillarity. Oxford Science Publications, Oxford.

Rudt,S., Muller,R.H., 1993. In vitro phagocytosis assay of nano and microparticles by chemiluminescence II. Effect of surface modification by coating of particles with poloxamer on the phagocytic uptake. Journal of Controlled Release, 25, 51-59.

Saleki-Gerhardt,A.A.C.Z.G., 1994. Assessment of disorder in crystalline solids. International Journal of Pharmaceutics, 101, 237-247.

Sanders,P., Washington,N., Frier,M., Wilson,C.G., Feely,L.C., Washington,C., 1997. The deposition of solution-based and suspension-based aerosols from metered dose inhalers in healthy subjects and asthmatic patients. Pharmaceutical Sciences, 7, 300-306.

Schultz, R. K., Dupont, R. L., and Ledoux, K. A., 1994. Issues surrounding metered dose valve technology: past, present and future perspectives. In: Byron P.R. (Ed.), Respiratory Drug Delivery IV, 221-220.

Sheridan,P.L., Buckton,G., Storey,D.E., 1994. The extent of errors associated with contact angles II. Factors affecting data obtained using a Wilhelmy plate technique for powders. International Journal of Pharmaceutics, 109, 155-171.

Shi,H., Zhang,S., Steitz,R., Chen,J., Uredat,S., Findenegg,G.H., 2004. Surface coatings of PEO-PPO-PEO block copolymers on native and polystyrene-coated silicon wafers. Colloids and Surfaces A: Physicochemical Engineering Aspects, 246, 81-89.

Smith,I.J., 1995. The challenge of reformulation. Journal of Aerosol Medicine, 8, S19-S27.

Smyth,H.D.C., 2003. The influence of formulation variables on the performance of alternative propellant-driven metered dose inhalers. Advanced Drug Delivery Reviews, 55, 807-828.

Soine,W.H., Blondino,F.E., Byron,P.R., 1992. Chemical stability in pressurised metered dose inhalers formulated as solutions. Journal of Biopharmaceutical Sciences, 3, 41-47.

Somasundaran,P., Yu,X., Krishnakumar,S., 1998. Role of conformation and orientation of surfactant and polymers in controlling flocculation and dispersion of aqueous and non-aqueous suspensions. Colloids and Surfaces A: Physicochemical Engineering Aspects, 133, 125-133.

Steckel,H., Wehle,S., 2004. A novel formulation technique for metered dose inhaler (MDI) suspensions. International Journal of Pharmaceutics, 284, 75-82.

Stefely, J. S., Duan, D. C., Myrdal, P. B., Ross, D. L., Schultz, D. W., and Leach, C. L., 2000. Design and utility of a novel class of biocompatible excipients for HFA-based MDIs. In: Byron P.R (Ed.), Respiratory Drug Delivery. Interpharm Press, Philadelphia, 83-90.

Stokvold,A., Drystad,K., Libnau,F.O., 2002. Sensitive NIRS measurement of increased moisture in stored hygroscopic freeze dried product. Journal of Pharmaceutical and Biomedical Analysis, 28, 867-873.

Ticehurst,M.D., Rowe,R.C., York,P., 1994. Determination of the surface properties of two batches of salbutamol sulphate by inverse gas chromatography. International Journal of Pharmaceutics, 111, 241-249.

Tiwari,D., Goldmann,D., Dixit,S., Malik,W.A., Madan,P.L., 1998. Compatibility evaluation of metered dose inhalers with tetrafluoroethane (P134a), a non-CFC propellant. Drug Development and Industrial Pharmacy, 24, 345-352.

Van Krevelen,D.W., 1990. Properties of Polymers: Their Correlation with Chemical Structure; their Numerical Estimation and Prediction from Additive Group Contribution. 3rd Ed., Elsevier, Amsterdam.

Van Lent,B., Scheutjens,M.H.M., 1989. Influence of association on adsorption properties of block co-polymers. Macromolecules, 22, 1931-1937.

van Oss,C.J., Chaudhury,M.K., Good,R.J., 1987. Monopolar surfaces. Advances in Colloid and Interface Science, 28, 35-64.

van Oss,C.J., Good,R.J., Chaudhury,M.K., 1988. Additive and nonadditive surface tension components and the interpretation of contact angles. Langmuir, 4, 884-891.

van Oss,C.J., Giese,R.F., Li,Z., Murphy,K., Norris,J., Chaudhury,M.K., Good,R.J., 1992. Determination of contact angles and pore sizes of porous media by column and thin layer wicking. Journal of Adhesion Science and Technology, 6, 413-428.

van Oss,C.J., Giese,R.F., Wentzek,R., Norris,J., Chuvilin,E.M., 1993. Surface tension parameters of ice obtained from contact angle data and from positive and negative particle adhesion to advancing freezing fronts. In: Mittal,K.L. (Ed.), Contact Angle, Wettability and Adhesion. VSP, Utrecht, 677-690.

van Oss,C.J., 1994. Interfacial Forces in Aqueous Media. Marcel Dekker, New York.

Vervaet,C., Byron,P.R., 1999. Drug-surfactant propellant interactions in HFA-formulations. International Journal of Pharmaceutics, 186, 13-30.

Ward,G.H., Schultz,R.K., 1995. Process induced crystallinity changes in albuterol sulfate and its effect of powder physical stability. Pharmaceutical Research, 12, 773-779.

Wendel,S., Celik,M., 1997. An overview of spray-drying applications. Pharmaceutical Technology, 124-156.

Williams, G. and Tcherevatchenkoff, 1997. Moisture transport into CFC-free metered dose inhalers. Drug Delivery to the Lung VIII. The Aerosol Society, Bristol, 91-94.

Williams,R.O., Liu,J., 1998. Influence of formulation additives on the vapour pressure of hydrofluoroalkane propellants. International Journal of Pharmaceutics, 166, 99-103.

Wu,S., 1971. Calculation of interfacial tension in polymer systems. Journal of Polymer Science, 34, 19-30.

Wu,S., 1979. Surface tension of solids: An equation of state analysis. Journal of Colloid and Interface Science, 71, 605-609.

Young,P., Price,R., Lewis,D., Edge,S., Traini,D., 2003. Under pressure: predicting pressurized metered dose inhaler interactions using the atomic force microscope. Journal of Colloid and Interface Science, 262, 298-302.

Zhou,G.X., Ge,Z., Dorwart,J., Izzo,B., Kurkura,J., Bicker,G., Wyvratt,J., 2003. Determination and differentiation of surface and bound water in drug substances by near infrared spectroscopy. Journal of Pharmaceutical Sciences, 92, 1058-1065.

Zhou,H., Gotzinger,M., Peukert,W., 2003. The influence of particle charge and roughness on particle-substrate adhesion. Powder Technology, 135, 82-91.

Zhou,X., Hines,P., Borer,M., 1998. Moisture determination in hygroscopic drug substances by near infrared spectroscopy. Journal of Pharmaceutical and Biomedical Analysis, 17, 219-225.

Zografi,G., Johnson,B.A., 1984. Effect of surface roughness on advancing and receding contact angles. International Journal of Pharmaceutics, 22, 159-176.